UNIVERSITY OF CALIFORNIA,
IRVINE

Renewable Distributed and Centralized Generation Dynamic's Impact on Transmission and Storage Upgrades to Achieve Carbon Neutrality

THESIS

Submitted in partial satisfaction of the requirements for the degree of

MASTER OF SCIENCE

In Mechanical and Aerospace Engineering

By

Clinton Thai

Thesis Committee:
Professor Jacob Brouwer, Chair
Professor Scott Samuelsen
Professor Jaeho Lee

2019

DEDICATION

I dedicate this thesis to my parents for their unconditional love and support.

TABLE OF CONTENTS

LIST OF FIGURES

LIST OF TABLES

ACKNOWLEDGEMENTS

Of all educators in my life, I have yet to meet one more inspirational and empowering than my advisor, Professor Jack Brouwer. His patience and support know no bound. I am deeply indebted to him who continues to demonstrate nothing but excellence as a mentor, leader, and friend. To Professor Scott Samuelsen, the director of the Advanced Power and Energy Program (APEP), I would like to offer my gratitude for seeing promise in me and providing an environment in which I have grown professionally and personally.

In addition, I would like to acknowledge my seniors and the staff at APEP who facilitate my learning. I would be erred to think this work is from my effort alone. At last, I would not be where I am today without the unconditional support of my beloved Tracy.

ABSTRACT OF THESIS

Renewable Distributed and Centralized Generation Dynamic's Impact on Transmission and Storage Upgrades to Achieve Carbon Neutrality

By

Clinton Thai

Master of Science in Mechanical and Aerospace Engineering
University of California, Irvine, 2019
Professor Jack Brouwer, Chair

Decarbonizing the power generation sector will indisputably need massive amounts of generation resources and infrastructure upgrades. University of California (UC) campuses throughout the state are considered, each with their own geographical and technological characteristics. The maximum photovoltaic (PV) potential for each campus is identified, an integration strategy evaluated, and the remaining off-campus resources identified to justify a claim of 100% clean electricity. The limited on-campus photovoltaic solar potential and emissions from natural gas fueled plants, where present, require additional projects to generate renewable electricity certifications and carbon offsets. Achieving carbon neutrality for scope 1 and 2 emissions requires accounting for campus fleets and independent heat generation, both of which are relatively minor relative to combined heat and power production.

Entities like the UC that desire to achieve carbon neutrality may generate demand for hydrogen as a clean fuel, instigating large amounts of centralized solar PV plants cited in remote areas. A generalized case comparing the transmission of large amounts of renewable energy as hydrogen in pipelines is compared to the traditional pathway of electricity delivery through power lines. For scenarios in which minimal energy storage is

necessary, the electric pathway yields a lower system cost. However, if the state reaches high renewable penetration levels, power from storage must be available for more hours of the year. In this case, the lower cost of storage from geological hydrogen storage and the innate storage capability of pipelines suggest a lower system cost for hydrogen production and delivery despite the lower pathway efficiency.

1. Introduction

Climate change in 2019 needs no introduction. While many can agree it is an existential threat, there are countless ways to tackling the challenge at hand. Davis et al. [1] suggest that terawatt scale carbon-free energy must be deployed within decades in order to keep the planet's temperature from increasing two degrees Celsius. The authors suggest that in order to do so, greater efforts are necessary every step of the way—from public support to research to demonstration projects and to commercialization. At the end of 2018, the world has been able to increase renewable generator capacity so that it makes up a third of global generation capacity [2]. Similarly, California as a state produces about 35% of electricity from renewable sources [3]. Though this might seem like we are enroute towards a completely renewable future, arriving to this point has not required large energy storage capacity deployments. Only in recent years have we seen global installations totaling gigawatt-hours (GWh) per year [4] with most of the storage capacity installed as lithium-ion battery energy storage systems (BESS). Many studies address the challenges of approaching even higher levels of renewable energy penetration—namely long-term storage capacity, diversification of technology types, flexible operation, and system reliability [5] [6] [7] [8] [9].

The dynamics of renewable energy production not only require storage but can pose challenges to existing infrastructure. Matching load with an increasing amount of generation resources may be challenging. Curtailment can occur due to existing transmission capacity constraints [10]. With only limited amount of storage resources available, curtailment is likely to occur more and more often. The curtailment is

proportional to additional renewable capacity installments, cutting into renewable developer profit margins and consequently slowing deployment. Electrification of heating loads and transport is a popular stance and much work has been done analyzing the implications on the greater system as a whole [11] [12] [13], but others believe that hydrogen as an energy carrier may have some benefits. Balancing the integration of centralized and distributed generation and storage resources into the transmission system and understanding hydrogen's potential role in it all will be required to achieve a renewable future. Goals and corresponding objectives are established to explore the hypothesis that central generation and storage resources are necessary for a carbon free future and some advantages of hydrogen usage as an energy carrier are quantified.

1.1. Goals

The goals of this thesis are to:

1. Identify a means for each UC campus to achieve 100% clean electricity considering each campuses' existing generation resources and load dynamics.
2. Investigate a generalized case for the associated efficiency and cost of transmitting centrally generated energy as hydrogen or electricity.

1.2. Objectives

The following objectives are established, acting as the guideline for achieving these goals:

1. Identify each of the University of California campuses' power generation resources and establish an annual electrical load profile.

2. Develop an image-analysis model to quantify the suitability and quantity for both rooftop and over parking lot PV installations, establishing inputs for storage integration scenarios.

3. Evaluate the storage dynamics and cost of storing on-campus PV with power-to-gas energy storage, lithium-ion based battery systems, and hybrids of the two in order to identify progress toward 100% clean electricity and the consequential off-campus resource requirements.

4. Establish a generalized case of transmitting utility-scale centrally generated PV solar electricity as hydrogen in pipelines or as electricity through power lines.

5. Establish metrics to investigate the levelized costs for transporting energy throughout society as well as for electric end-uses considering the need for storage arising from mismatched demand and renewable generation profiles.

2. Background

2.1. Thermodynamics of Renewable Energy, Power Generation, and Energy Storage

The first law of thermodynamics states that energy is conserved and cannot be created or destroyed. As such, most of society today has been able to utilize fossil fuels which are dense hydrocarbons resulting from the decomposition from biomass over thousands of years. Due to the large production timescale of these valuable fuels, the rapid usage from industrialization, and geopolitical availability and tensions, many turn to renewable energy alternatives. Solar PV electricity is the primary technology of discussion in this work. Solar PV is able to utilize the photons in the radiation from the Sun and convert this thermal energy into electricity using semiconductors. This process is largely steady-state and does not require any additional moving parts, making it a very attractive power generation solution that can be placed on top of any building rooftop or when elevated, acting as a parking shade canopy. The other current major renewable generation technology is wind powered turbines. This technology operates by utilizing the conservation of momentum—transferring the kinetic energy found in air to wind turbine blades which are connected to a motor to generate electricity. Due to the moving blades and typically blade placement at higher heights supported by a large tower-like base, this type of power generation technology is not easily deployed in urban and suburban environments.

Electricity is the flow of electrons moving instantaneously, therefore, typically generators must adapt their electricity production level in response to changing loads. For natural gas power plants, this typically results in a slowing of an electric motor. For

renewable generators previously mentioned, this poses to be a challenge due to their mechanism for power generation. To circumvent this issue, energy storage can be implemented. Electrochemical energy storage is a common method of storing electricity. The two storage technologies addressed in this work are lithium-ion batteries and hydrogen which consists of splitting water to produce hydrogen and oxygen by driving a current. The reverse process produces water and electricity. Because electricity has a lower level of entropy than heat, energy will typically desire to be in a heat form than electric due to the second law of thermodynamics. Similarly, the relatively lower entropy of the chemical species results in some self-discharge of a battery (conversion of electrochemical potential to heat). This occurs in even greater amounts when being charging or discharging a battery. Similar is true for electrolysis and producing power with a fuel cell, with each technology having different amounts of energy loss known as inefficiencies, though stored hydrogen is innate and would only lose energy if the chemical were to physically leaked out of the storage medium.

2.2. Global and California State of Renewable Generation

In 2015, California Governor Edmund G. Brown Jr. issued an executive order to reduce the state's greenhouse gas (GHG) emissions to be 40 percent less than 1990 levels [14] and 50% electricity retail sales to be from renewable generation by 2030 [15]. In 2016, California Senate President pro Tempore Kevin de León introduced Senate Bill 100 which sets California to aim for 100% clean energy by 2045 [16]. In 2018, Google and Apple already purchased 100% renewable energy [17]. RE100 maintains a list of over 200 world-

renowned companies with target goals to achieve 100% renewable electricity-- nearly 60 of them have goals by 2020 and another 40 by 2025 [18].

As the world grows more conscious of the negative impact of using fossil fuels as a power source, countries around the globe have been implementing more non-hydro renewable energy. The leaders for installing solar are China, Japan, the U.S., and Germany with 131, 49, 43 and 42 gigawatt (GW) of peak capacity, respectively [19]. China, the U.S., and Germany are the leaders for installing wind energy with respective peak capacities of 164, 87, and 56 GW [19]. These recent installations are a result of policy support and of decreasing technology prices [20] that make them competitive with fossil fuel based power generation [19]. Hydropower has always had a competitive price tag [21] which is no surprise why it has a global capacity of 1.1 terawatt (TW)—roughly 10% more than all other renewable technologies combined [19]. The implementation of renewable generation is driven by both economic appeal as well as policy. The United Nations put clean and affordable energy on their 2015 Sustainable Development Goals [22]. Germany has specifically adopted one of the most ambitious set of renewable goals: 65% renewable power consumption in 2030 and 80% in 2050 [23]. Similarly, China aims for 15% power consumption from renewables in 2020 [24] and 35% by 2030 [25].

The global pressures and ambition of California as a state are reflected in electricity generated from renewable sources that has improved from 21.90% in 2015 to 31.36% in 2018 [3]. Due to the intermittent nature of solar and wind farms and high market penetration of these resources, large-scale energy storage systems (ESS) are becoming necessary in order to provide power at times of low generation [26]. The U.S. Department

of Energy (DOE) Global Energy Storage Database shows that 95% of electrical energy storage system capacity (ESSC) in the world is 95% pumped hydro energy storage (PHES) as of 2015 [27]. Because of the geographic demands of PHES (elevation change, suitable and non-environmentally damaging geography for dam construction and flooding to produce both upper and lower lakes, etc.), the U.S. has ceased PHES growth in the previous decades and faces pressure to increase ESSC by alternative means to complement growing renewable sources. In addition, Shaner et al. conducted a geophysical analysis considering the effects of energy storage when increasing the generation capacity of solar and wind and finds that 12 hours of storage for an aggregated area the size of California could increase reliability around 15-20% [28]. Long-term energy storage enables higher levels of renewable electricity generation [29] and makes power-to-gas (P2G) an attractive technology because of its ability to use natural gas infrastructure and act as both a transmission and distribution resource as well as a large-scale energy storage system [30],[31].

2.3. Central versus Distributed Generation

The past decade has seen major distributed PV deployment supported by net energy metering programs and incentives. At the time of this writing in 2019, California Distributed Generation Statistics reports 8.4 GW of distributed PV peak capacity [32]. As a means of comparison, CAISO reports 12.5 GW of central PV capacity [33]. The California Energy Commission (CEC) has mandated that all new homes must install enough PV to produce as much electricity as they are projected to consume [34]. This fundamentally exacerbates the mismatch between energy supply and demand known as the "duck curve"

and discussed in more detail in the next section. In terms of distributed resources, this additional solar is expected to increase the economic value of distributed wind [35]. Because solar depresses mid-day prices with abundant generation, peak load is shifted to the evening when solar ramps down. Wind, which is more consistently available throughout the day and night is projected to see increases in economic value as part of its generation occurs during the peak load timeframe [35]. If significant adoption of distributed battery systems are deployed, such as Tesla's Powerwall [36], this may mitigate the effects previously discussed. Distributed storage systems have the potential of shifting daytime electricity production to evening electricity demands and the remaining load seen by utilities would be akin to previous years—allowing the possibility for more PV solar installations at the central level either for RPS compliance or due to economic appeal. This is proposed as a possibility, as the aggregate of distributed PV owners and utility-level central PV owners may only act in such a way if incentives, infrastructure capabilities and policy were aligned with their interests.

In order to complement renewable energy, the characteristics of the infrastructure in which they will be implemented in must be understood. Centralized renewable energy projects have different challenges than distributed projects. Typically, distributed resources are constrained by space whereas centralized resources must address the transmission and distribution of energy to loads. Centralized resources have several more storage options as it may utilize geographical features and may not be as constrained by space (i.e., in a rural rather than urban setting).

Regarding the potential to use hydrogen as a major energy storage and energy carrying option, an older 2004 report concludes that non-hydrogen storage options have efficiencies over 75% while hydrogen storage options are in the 40% range [37]. In addition, Schaber et al. suggest this 40% efficiency incurs an additional penalty as it requires central generation and pipeline delivery. A case study done in 2002 considers the economics associated with transmitting 4,000 megawatt (MW) of wind power over 1,000 miles via high voltage direct current (HVDC) and hydrogen pipeline and addresses the value of the hydrogen pipeline line pack as it has a storage capacity of 120 GWh, but does not consider an equivalent storage system for the HVDC case. Poullikkas identifies lithium-ion and sodium-sulfur batteries as having high energy density and efficiencies for large capacities, but high production costs [38]. Dunn et al. identify storage technologies for grid use [39], but the literature regarding transmission implemented electrical energy storage is sparse.

2.4. The "Duck Curve"

2.4.1. Renewables and the Curve

The California electric load served by renewable generation sources has rapidly grown from 4% in 2008 to 19% in 2013 and most recently 29% in 2017 [40]. Although it may seem like progress to the 2030 and 2045 goal seem on track, the high penetration of renewable generation has created new challenges for the electricity infrastructure and market. The rapid installation of renewable energy has put California at risk for over-generation [41]. This occurs because solar generation peaks midday and in some times of the year there is more supply than demand. In addition, there is a steep ramp in the amount of power that must be met with flexible generators, typically thermal plants, especially when the solar begins to ramp down every evening. Figure 1 [42] displays this midday dip in net load and corresponding evening peak in net load for various years are commonly referred to as the "duck curve" because its overall shape resembles a duck.

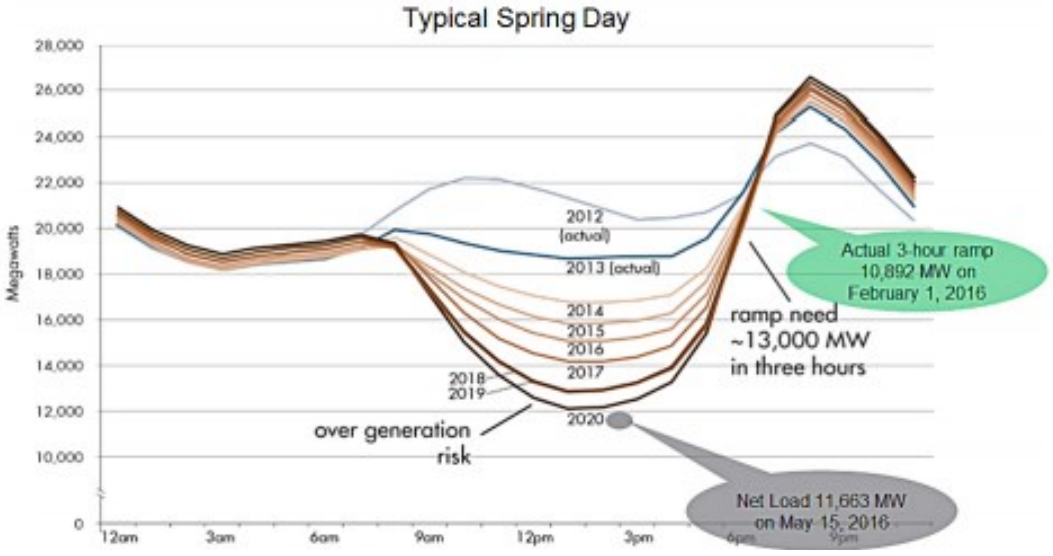

Figure 1 – Illustration of net load of the CAISO system over a typical day in spring. The curves are the remaining load that controllable generation resources must meet to balance the mismatch between electrical supply and demand.

This duck curve must be addressed to allow high renewable penetration [41]. Basic economic theory suggests a dip in demand results in a drop-in electricity prices as well, lessening the economic investment appeal of installing new solar generation. This has forced renewable generators to curtail the excess electricity, essentially discarding operational profits and adds increasing responsibility and operational costs for non-renewable flexible generators. In addition, the load profile changes throughout the year in California. Higher demands in the summer time when air conditioner systems are run is coincident with peak solar generation. Spring and fall seasons tend to succumb to midday over-generation due to similar solar production in the absence of massive air conditioning loads. On the other hand, winter faces under-generation as there is much less solar potential throughout the day and non-renewable sources must meet the remaining load in lieu. This is exacerbated with the major energy demands necessary for heating loads in the wintertime. The system operators rely on reserve capacities to make up the difference when supply is lacking. These include spinning reserves and non-spinning reserves. Spinning reserves are generators that are already connected to the system and producing power while capable of ramping up their output whereas non-spinning reserves start from offline [43]. An unusually-hotter summer in combination with below average PHES levels (which acts as much of the reserves) could induce a state of emergency [44].

2.4.2. Solutions to the Curve

Increasing renewable power generation levels must consider the capabilities of the entire electricity grid, so the literature has an abundance of feasibility and viability studies (e.g., [45], [46]). Heard et al. conduct a 2017 review of 100% renewable generated

electricity systems feasibility studies and critiques common limitations in literature such as: (1) assuming decreases in primary energy demand, (2) limited temporal resolution for reliability studies, (3) lack of consideration for renewable source variability, and (4) lack of consideration for complementing transmission and distribution systems [47]. These studies certainly have challenges they must overcome but addressing the duck curve to approach those theoretical levels is the present issue addressed in this thesis. Some suggest that the demand can be adjusted to account for the increase in supply. The aggregate implementation of storage systems can serve as new system demand to balance the excess supply. Shaner et al. conduct a geophysical analysis on the availability of solar and wind in the U.S. and finds that 12 hours of storage for an aggregated area the size of California could increase reliability around 15-20% [28]. However, the same study expects a sharp rise in costs as the electricity demand met by renewables approaches 80% due to low utilization of a large system [28]. Tarroja et al. evaluate the similarities between the ever-growing electric vehicle fleet batteries in California and stationary energy storage systems serving the grid [48]. They find that higher BEV penetration levels result in lower renewable penetration levels because of the increased need to charge the vehicles; however, for the considered lower BEV penetration level the collection of vehicles can act closely to an ideal energy storage case. Muratori and Rizzoni [49] find that multiple group time of use (TOU) residential electricity prices and smart appliances (such as PEV chargers) can reduce the overall perkiness of the aggregated demand-- measured by the frequency the demand was higher than the average demand. Both Tarroja et al. [48] and Muratori and Rizzoni [49] highlight the challenge of coordinating BEV charging behavior, but another

work by Wang et al. [50] suggest that excess electricity can power electrolyzers to produce hydrogen gas to fuel FCEVs. In addition to avoiding the temporal challenges, Wang et al. quantify the potential ramp mitigation and load leveling capabilities from oversizing the electrolyzers. Guandalini et al. consider a P2G power plant that utilizes gas turbines to increase wind generation capacity [51]. The energy aspect is reasonable considering the losses from curtailment and the economic profitability depends upon the cost of electricity and natural gas, but the gas turbine is fueled by natural gas and only a low volume of hydrogen, so primary energy demand and emissions increase. Long-term energy storage is necessary for high levels of renewable electricity generation [29] which makes P2G an attractive technology because of its ability to scale power and energy capacities independently and because it can potentially use existing natural gas infrastructure and act as large-scale energy storage and transmission and distribution [31]. Doroshenko et al. [52] briefly propose that installing new solar panels with sub-optimal tilt orientations can mitigate thermal plant ramping demands and renewable curtailment. Though this is a creative solution to over-generation and steep ramps, an economic analysis must be conducted to understand the viability. Howlader et al. [53] consider a specific case where implementing storage reduces the ramp requirements of thermal generators consequently reducing their operational costs 9%.

2.5. CAISO Electricity Markets

2.5.1. Participants

A load serving entity (LSE) in the California Independent System Operator (CAISO) definitions business practice manual, is defined as any electrical corporation, electric service provider (ESP), or a community choice aggregator serving retail loads in California

Public Utilities Commission (CPUC) jurisdiction [54]. In California, the largest electrical corporations are the investor-owned utilities: Southern California Edison (SCE), Pacific Gas and Electric (PG&E), San Diego Gas and Electric (SDG&E). The other two large corporations are the municipal-owned utilities: Sacramento Municipal Utility District (SMUD) and Los Angeles Department of Water & Power (LADWP). A complete list of all load serving entities can be found on the CEC website.

Because the larger entities, the investor-owned utilities (IOUs), own most of the transmission and distribution infrastructure in California, smaller load serving entities typically pay a transportation fee to use existing IOU lines. While each IOU also owns a great deal of generation resources (mostly renewable and one nuclear plant, since they were forced to sell all other generation resources during the utility restructuring (deregulation) of the 1990s), some third-party developers can build additional projects, such as solar farms, and contract energy delivery with the smaller load serving entities or sell energy into the wholesale market. All utilities must comply with the California renewable portfolio, having an adequate amount of renewable generation. While compliance is mandatory, some load serving entities aim for higher levels of renewables in their mixture. In the current work, it is only necessary to understand that implementing generation resources (e.g., built by solar developers) to satisfy consumers (e.g., LSEs serving end-users) has consequences on the necessary transmission infrastructure (owned by IOUs). Each party has respective interests and orchestrating progress toward a renewable future is largely driven by policy or renewable plus storage technologies reaching price parity with non-renewable dispatchable options.

2.5.2. Energy, Ancillary Services, Congestion Revenue Rights Markets

The implementation of energy storage systems has been tricky because of the infrastructure of the market. The wholesale generators invest in technology they believe to be profitable based upon the anticipated prices they will receive for energy and ancillary services, but often times the benefits extend to the consumer and transmission system operators. Due to renewable pressures and policies, such as CPUC goal for 1.325 GW of energy storage [55], novel implementation feasibility and viability of energy storage systems studies continue to spawn. The most common analysis for economic viability of ESS is energy arbitrage. Bradbury et al. evaluate the potential return on investment for 14 ESS technologies in 7 U.S. wholesale electricity markets and finds that compressed air energy storage (CAES), PHES, and zero emissions batteries research activity (ZEBRA) batteries, which are based on a molten salt, have the most potential, though the authors admit the analysis makes optimistic assumptions [56]. However, with the collection of economically competitive PHES and CAES sites actualized, energy storage capacity additions since 2003 have been mostly battery energy storage systems (over 80% of which are Li-ion based) [57]. For a comprehensive review of ESS technology characteristics and applications the reader is referred to Luo et al. [58] and Zakeri and Syri [59].

Despite this, the energy arbitrage value of Lithium-ion BESS for four U.S. wholesale electricity markets is evaluated when considering degradation [60]. Walawalkar et al. consider the revenue of both energy arbitrage and regulatory services for a sodium-sulfur battery and flywheel system in NYISO market [61]. Optimization problems for ESS sizing and operation are common in the production sector and consumer side [62], [63],[64]. Le

et al. [65] consider CAES ESS complementing 14 wind generation sites and identifies an increase in energy sales, net stability, and decrease in grid generation cost of 1.7%-8%, 8.3%-18.3% (13 of 14 sites) and 1.7%-9.9% (10 of 14 sites) respectively. Kamal and Hassan propose a hybrid storage system that utilizes both P2G and an electrical battery as a solution for meeting load demand and ancillary services [66]. Tebibel and Labed optimizes the sizing of an electrolyzer and storage to meet the hydrogen-natural fuel mix demand rather than an electrical load [67]. Dusonchet et al. propose continuous charging and discharging at the daily minimum and maximum prices based on the day-ahead market prices [68]. Shcherbakova et al. optimize charging and discharging operation based on difference between daily maximum and minimum electricity prices in South Korea for NaS and Li-ion ESS [69]. Zucker and Hinchliffe find that the capital investment of storage is the biggest obstacle and even if target prices are met in Germany and Italy, the optimal design will be less than 5 hours of discharge and should be limited to 40% of the PV's capacity [70]. Sioshansi et al. highlight the drop off value of having ESS with increasing hours of storage. In addition, they find that perfect foresight of market prices in the PJM market compared to the predicted price if a 1 GW affected the price, still retains 90% of its profit in this particular case [71]. This predicted price is based on a linear price-load relationship and suggests that because PJM load growth has driven the difference reduction between the responsive and unaffected price. Dufo-Lopéz et al. solve for the energy storage selling price for the storage system to be profitable in Spain [72]. They conclude that the battery storage case is far more suitable than the hydrogen storage case because of its superior roundtrip efficiency and costs, even when considering optimistic future scenarios. This

study, however, sizes the systems to have matching power outputs, whereas the value for P2G systems may be the ability to have varying energy to power ratios and realize other revenue streams.

Parra and Patel [73] simulate alkaline and PEM P2G systems participating in the Swiss low carbon gas, heat, oxygen, frequency, and wholesale electricity markets and found the alkaline system can achieve an internal rate of return of 35.1%. Mukherjee et al. consider P2G storage system that provides ancillary services and sells hydrogen gas and finds that the payback period is reduced nearly 60% compared to if the system does not provide ancillary services [74]. This study also highlights the marginal change in payback period for not participating in the ancillary services market when there is a high emission offset target (driven by carbon tax credits). It is also interesting to note, the emission offset target for the system is non-monotonic with payback period because of the IESO ancillary service requirements affecting technical performance and limitations.

2.5.3. Techno-economic Analyses

An older 2013 storage review [75] highlights the challenge of balancing specific-case engineering models with broader-scale network models. In other words, the external validity of engineering models is low due to the case-specific assumptions, while the network models are often complex to model justly to retain internal validity. These engineering models as well as the economic analyses often utilize a fixed average efficiency, but do not capture the technological dynamic differences and how it may affect their economic viability. The feasibility of storage technologies to serve the grid is determined by whether the technical requirements can be met (e.g., CAISO [43]) and the

viability based on market. Awad et al. [76] propose five principles to consider when making an economic assessment of transmission upgrades. This study highlights the importance of identifying consumer, generator, and transmission system owner benefits, representing the entire network, market-based pricing, and sensitivity of unknowns, value in extreme emergencies, and the coordination dynamics between all grid resources. Though accounting for all these factors may increase the complexity of an analysis, it better represents the net societal benefit of the system and how it may other feedback factors.

The technological aspects of ESS must be considered as they affect the ability to operating potential. Naumann et al. [77] conduct a sensitivity analysis for the return on investment in residential li-ion ESS considering ageing characteristics and when to replace them. Zhu et al. [78] conduct a simulation study to see how the spinning reserve market (an ancillary service) may affect the energy market. Hobbs and Rijkers [79] proposes a way to model market price dynamics when a generator with enough market power can single-handedly affect prices. Sandia National Laboratories published an energy storage market benefit report that identifies 17 applications along with lower and upper revenue bounds [80]. It thoroughly describes the typical characteristics (i.e., energy and power capacities) and how the economic value is typically estimated for the technology's lifetime. EPRI has published a similar white paper [81] several months after the Sandia report highlighting existing technologies and their potential for 21 energy storage applications. Feldman et al. [82] address a novel point of projecting prices when considering combined technologies, such as CSP and solar PV to thermal energy storage and lithium-ion electric energy storage.

2.6. Energy Storage

Energy storage is necessary for implementation of renewable power generators. Applications for energy storage are considerable at both the distributed and centralized level. Plenty of review papers have been published comparing the different types of energy storage technologies [83] [84] [39] [58]. Choi and Aurbach [84] highlights how different rechargeable battery chemistries have advanced in terms of energy density and how lithium-ion batteries are at the forefront today. This paper further reinforces the advantages of the need of small footprint batteries for information technology and transportation needs but does not address stationary energy storage needs. Sufyan et al. [85] review the applications of energy storage technologies when integrated in the grid. With peak shaving, home energy management, power fluctuations, T&D upgrade deferrals, frequency regulation, low voltage ride through, minimize losses through supporting components, reliability, reserve, demand response, and charging electric vehicles.

2.6.1. Battery Energy Storage Systems

Many more papers consider integrated strategies for battery energy storage systems. Bahramirad et al. [86] conduct study of generalized ESS for lowering the cost of a microgrid. By modeling natural gas power plants and a wind generator, they attempt to find a balance between the ESS investment cost and a microgrid's operating costs to find a global minimum. This is done with the addition of Monte Carlo simulated outages to account for reliability. Carpinelli et al. [87] look at sizing the battery for the application of reducing end user bills based on time-of-use pricing. Different technologies were considered as well as load variations and in general, higher variation required larger

amounts of storage capacity. This would be an example of behind the meter application or adoption. They found the sizing strongly depended on the time-of-use rates, so we know if policy can be developed to incentivize distributed ESS, then the amount of the amount of energy storage capacity at the central level will decrease. Ju and Wang [88] conduct a similar analysis to reduce a microgrid's energy bill. An additional novelty of this study is that they consider the difference in operation if the cost of the battery's degradation from cycling is accounted for. This and many studies typically compare performance between using an hour-ahead price schedule compared to the spot market price. Zarezadeh et al. [89] consider a probabilistic approach to sizing a solar plus battery system. This study finds that the optimal sizing to reduce energy bill for residential application is dependent on the electricity rate structure. When the price to buy and sell is the same the sizing of the battery and PV amount are independent. This idea can probably be extrapolated to the utility-scale level and wholesale market as well. Current centralized PV farm may see poor wholesale prices not due to a saturation on the grid but due to local transmission constraints since the CAISO price map shows wholesale prices with a wide range of prices even during peak PV generation [90]. Lu et al. [91] consider implementing a battery at a substation to help provide energy during the peak load and smooth the load curve in general—quantified by the difference between daily max and minimum load.

2.6.2. Hydrogen as Energy Storage and Carrier

The concept of power-to-gas as an energy storage system has also gained traction [92] [93] [94] [95]. Though many of these focus on synthetic or also known as renewable natural gas, the concept for renewable hydrogen would be the same. Ma et al. [94] review

power-to-gas geological storage for hydrogen and renewable natural gas. In this paper, several demonstration projects are listed across Europe and Japan and suggest underground gas storage is an effective solution to seasonal peaking in addition to safety and reliability benefits. Opportunities to implement underground storage arises from evaluating wind and solar technical feasibility maps. Buchholz et al. [96] conduct an economic analysis of using hydrogen to produce synthetic natural gas to be stored in pipelines and used for a lignite power plant. By doing this they found they could decrease power plant fluctuation and save on operating and maintenance costs. Though this may not be completely renewable, this is a potential intermediate step in which renewable hydrogen production in the short-term has economic value. Frank et al. [97] evaluate power-to-gas, including methanation, system efficiencies based on start-up events. Likewise, Saint-Jean et al. [98] consider solid-oxide fuel cells for electrolysis.

Other technologies such as flow batteries and lead acid batteries exist as well. May et al. [99] conduct a review of lithium-ion and lead-acid battery construction and degradation mechanisms finding that the latter technology relatively better reliability, sustainability, safety, and costs and lacking in energy and power density. The author attributes this to recent advances in lead-acid technology including the implementation of a hybrid storage system utilizing supercapacitors. In general, the author advocates for lead-acid for stationary energy storage since limitations and recycling processes are well established and power and energy density should not be a constraint for static installations. The amount that can be recovered from lithium ion batteries is relatively low compared to the amount of lead in lead-acid batteries [85].

2.7. Summary

Much of literature tends to analyze short-term energy storage solutions and only few analyses exist at high renewable electric supply levels. In addition, existing work tends to fail to compare energy storage solutions for high renewable penetration scenarios from a system perspective and from market participants simultaneously. This work focuses on an integrated infrastructure that is based on high electrification and complemented by lithium-ion batteries or an equally integrated infrastructure based on using hydrogen as an energy carrier. This type of work has already been done for the California state context by Colbertaldo et al. [100]. In this work, the authors considered the necessary renewable generation and complementary storage capacities in order for the state to achieve 100% renewable electricity and find that a P2G energy storage system achieves significantly lower system costs than a BESS solution. However, this work] only considers the generation capacities and does not address the question of energy transmission. This thesis aims to understand the balance between distributed and centralized resources, highlighting the consequences from implementing energy storage at both levels.

3. Approach

In this approach section one task is defined and described for each of the previously established objectives.

Task 1: *Identify each of the University of California campuses' power generation resources and establish an annual electrical load profile.*

Some UC campuses have gas turbine based power plants fueled by natural gas to produce electricity and heat. Public documentation of power plant capacity will be used as a guideline. Historical generation and demand profiles provided by campus facility managers is ideal, otherwise a statistical regression model based on weather data derived from cooperating campuses' profiles is utilized. Assumptions for minimum and maximum electrical output based on gas turbine configuration are made if not evident from historical operation.

Task 2: *Develop an image-analysis model to quantify the suitability and quantity for both rooftop and over parking lot PV installations, establishing inputs for storage integration scenarios.*

Newer campus buildings are designed to accommodate rooftop PV whereas older buildings may not necessary be as suitable. In addition, unique building architecture may pose as a challenge for determining the suitability of PV installations. Images from Google's Project Sunroof tool is used as the basis for this image analysis model. Parking lot areas are calculated using online geographic analysis tools whilst considering non-parking structure lots are candidate areas for future campus building developments.

Task 3: *Evaluate the storage dynamics and cost of storing on-campus PV with power-to-gas energy storage, lithium-ion based battery systems, and hybrids of the two in order to identify progress toward 100% clean electricity and consequential off-campus resource requirements.*

By defining the operational limits of existing power generation resources, modeling additional PV installations, and inputting annual load dynamics Moments of excess generation and residual load are identified. Lithium-ion is often seen at the forefront of energy storage technologies due to their low cost and high roundtrip efficiency. On the other hand, hydrogen is a flexible fuel and energy carrier. A case in which there is only battery storage, a case with only power-to-gas storage, and two hybrid cases are considered—each prioritizing charging one technology before the other.

Task 4: *Establish a generalized case of transmitting utility-scale centrally generated PV solar electricity as hydrogen in pipelines or electricity through power lines.*

A point to point model for transmission is considered. Although the utility infrastructure operates on a nodal and deeply interconnected system, this pathway represents the backbone of intrastate energy transport. Considering the typical state solar profile and representative load profile, Storage needs at the utility-scale level for the modeled PV capacity are identified.

Task 5: *Establish metrics to investigate the levelized costs for transporting energy around society as well as for electric end-use considering the need for storage arising from mismatched demand and generation profiles.*

Levelized cost of electricity represents the cost per transmitted unit of energy for electric generated from central PV then transmitted to a city-gate before being distributed on a sub-transmission level. When storage is necessary, the costs from implementing storage are also included. Levelized cost of transmission only represents the transmission movers and mediums and excludes the cost of generation and re-electrification in the hydrogen pathway.

4. Results: University of California Case Study

4.1. Scope Justification

In this work, we have considered the UC campuses largely due to the availability of data, range of population density, and range of building types. When considering the balance between distributed and centralized generation resources, California is often seen as an area with the highest potential for distributed solar installations due to the relatively higher technical potential seen in NREL solar resource maps [101]. As this work investigates the interactions between centralized and distributed resources, one must first establish the necessity of centralized generation resources. If the higher solar distributed potential in California is insufficient to meet a decarbonized future, the implication is that communities in the remainder of the United States will struggle to do likewise. This is especially true for colder climates which see larger peaks due to heating demands in winter coincident with less seasonal PV generation potential as previously detailed in Section 2.3. When considering other campuses outside of the UC system in California, such as the California State University (CSU) system, we assume that the UC system energy campus usage is more generalizable to typical distributed loads. Figure 2 depicts seven of the newer multistory buildings at University of California, Irvine and illustrates the range of building type usages from the facilities inventory system at UCI [102]. The largest building usage types are offices, labs, and the "other" category which aggregates various retail usages.

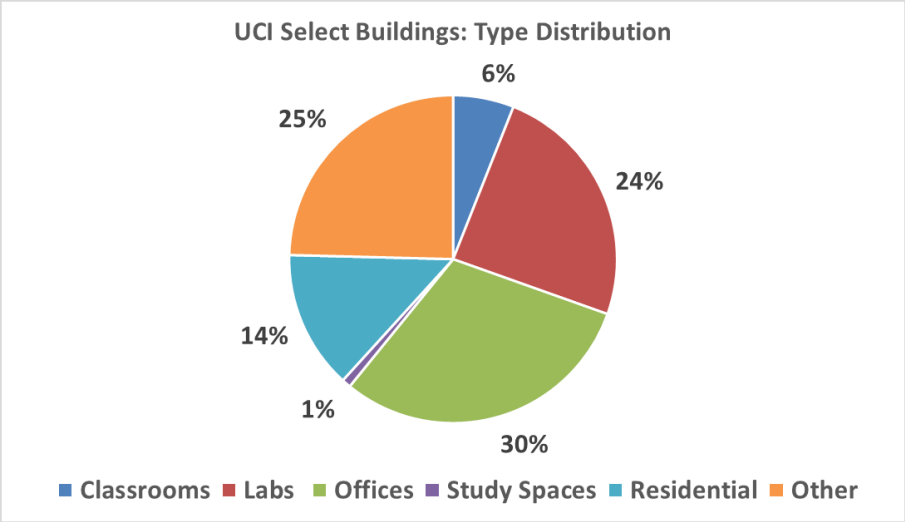

Figure 2 – UCI building usage type distribution. Data derived from the facilities inventory system at UCI [99].

The slice for residential would be smaller at CSU campuses due to their slightly higher percentage of commuting students and staff. Despite this, campuses from both systems represent a large range of campuses in rural to urban settings as well as age. Enrollment in both systems are both expected to grow at similarly steady rates [103], so the advantage of greater building usage diversity is seen as a benefit. The internal availability of data for this work and higher populous per campus suggest a more concise analysis whilst maintaining generalizability integrity for the UC case.

4.2. On-site Solar Potential

The University of California system includes ten university campuses: Berkeley (UCB), San Francisco (UCSF), Davis (UCD), Los Angeles (UCLA), Riverside (UCR), San Diego (UCSD), Santa Cruz (UCSC), Santa Barbara (UCSB), Irvine (UCI), and Merced (UCM). Due to co-location ambiguity this report omits some off-main campus medical centers, the University of California Office of the President (UCOP) offices, as well as the UC Agriculture

& Natural Resources (UCANR) which are all smaller loads. The ten main campuses larger UC campuses make up roughly 90% of the entire UC system electric load, have varying existing power generation resources, and a larger number of buildings subject to rooftop PV installations. Large remote medical centers namely UCD Medical Center (UCDMC) and UCI Medical Center (UCIMC) are accounted for—capturing close to 99% of the UC's electric load. Latter results list these two medical centers apart from the main campuses as they are geographically located away from the main campuses. For sake of brevity, the medical centers are also referred to as "campuses". Efforts toward identifying system-wide solar capacity and providing inputs for energy storage will be strongly dependent on these existing campuses. UCD and UCM have a slight advantage over the other campuses due to their location away from major cities. The availability of land allows them to develop large-scale solar PV farms short distances away from main campus buildings. This analysis does not consider the capacity gained from remote developments and aims to identify PV panel capacity on top of main campus buildings and on-campus parking areas. The considered buildings were chosen according those included in each campuses' online map. Parking structure are referred to as buildings and usage of "parking lots" implies ground level parking areas.

Google's Project Sunroof (PS) is an online tool that can identify the available rooftop area and consequently the number and orientation of the solar panels for a given building or select aggregates. Though a powerful tool, it is 1) unable to capture PV capacity in parking lots and 2) only has aggregated totals for state, counties, cities, or zip codes. Each UC campus, with the exception of UCSC, spans multiple zip codes disallowing the use of

aggregated zip code totals from the PS tool. An attempt to reverse engineer the PS tool to allow identification of PV panel capacity and the orientation-dependent annual energy production for the desired control volume was made. The PS tool utilizes Google's satellite imagery and NREL weather station data to estimate the energy received from direct normal irradiance and diffuse horizontal irradiance for any given area of an urban (or rural) environment. Irradiance, which is strongly proportional to electricity production, is composed of these two components and can be thought to be the following equation.

$$Irradiance_{GHI} = I_{Direct,Normal} + I_{Diffuse,Horizontal} \qquad Eq.(1)$$

The result is a heat map displaying the potential performance for each rooftop. Screenshots of these maps are used as inputs for the image analysis model. Figure 3 is an example of one the areas used for UCI.

Figure 3 - Google Project Sunroof map for zip code 92617. Most of the UCI campus is included in addition to off-campus housing and adjacent commercial buildings.

The brightest rooftops in the PS maps represent the most optimal sites for PV panels. Darker colors occur due to shading from nearby trees, buildings, or rooftop obstacles such as rooftop vents. In California, south-facing solar panels have the highest annual energy. Similarly, north-facing panels receive the least. This is reflected in PS maps, as the north facing rooftops are typically darker than the south facing rooftops. Using MATLAB, the colored PS maps are converted into gray-scale, where each pixel is represented by a numerical value from 0 (black pixel) to 255 (white pixel). An image that is 1000 pixels in width and 500 pixels in length is represented by a 500 x 1000 matrix. Plotting the frequency of each numerical value results in a representation of how bright the rooftop

areas of buildings in the input image are.

A parabolic increase compared to a linear increase at the lower tail of numerical values could be interpreted as an area with proportionally fewer obstacles and rooftops with a higher level of available choice space for solar panels. The darker areas are assumed to be north-facing equivalent panels and the brightest areas are south-facing equivalent panels. By doing so one can assign the pixels with lower end numerical values to be north-facing panels, followed by west-facing, east-facing, flat, and south-facing for the highest values. For each campus nearby zip codes are selected for which PS has a predicted orientation and number of panels. The irradiance is similar due to the geographical proximity of the reference zip code and the target campus volume is assumed. With the PS predicted number of panels and the hierarchy of orientation-based technical potential, upper and lower bounds are assigned to have the numerical value distribution reflect the PS orientation type distribution. The total number of PS module installations is divided by the total number of pixels within the range of all the bins resulting in a "module per pixel" (MPP) ratio (e.g., 0.43 MPP). These threshold values and MPP are held constant and used to categorize the orientation and number of panels in the target area. Figure 4 illustrates the inputs and outputs of the model and Table 1 lists typical numerical bin thresholds to tune the model.

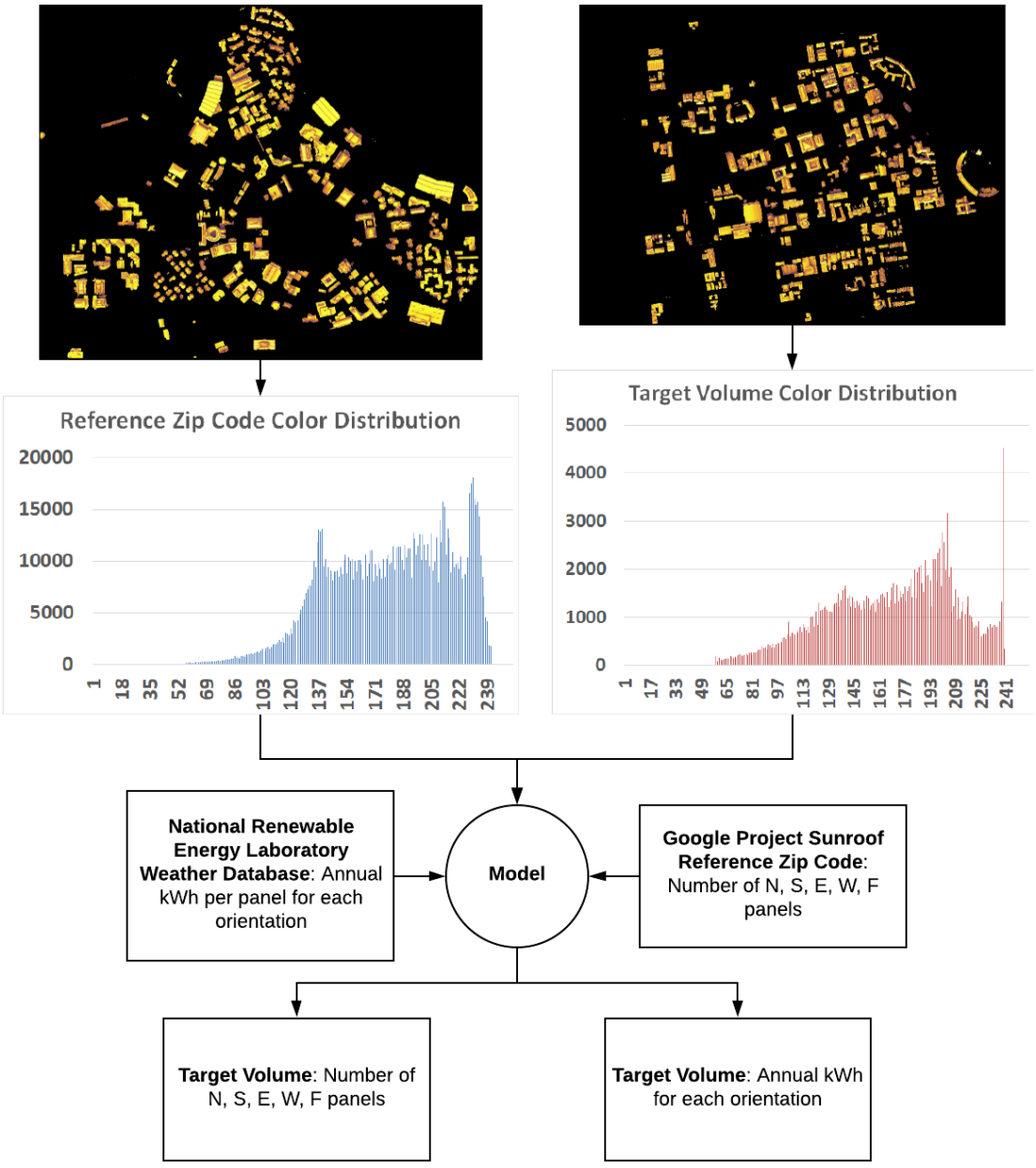

Figure 4 - Concept of the model. A nearby reference zip code image and GPS results are used to predict a target area's rooftop capacity.

Table 1 Sample bin bounds in attempt to match distribution of pixels with PS prediction.

Orientation	Lower Bound	Upper Bound	Percentage of installations from GPS	Percentage of pixels in this bin
N	131	135	2.60%	2.51%
S	205	255	13.08%	14.61%
E	135	144	6.59%	6.34%
W	144	217	12.10%	11.30%
F	217	205	65.63%	65.24%

The PS tool assumes that only areas that are within 75% of the local optimum rooftops are considered to be within technical potential eligibility. This is deemed equivalent to the lower bound for the north-orientated panels and is calculated by iteratively testing values to minimize the reference zip code set MPP standard deviation. As the lower bound increases to higher values, the number of pixels decreases whilst the predicted PS modules is kept constant. Consequently, the range of MPP across the 9 reference zip codes grows. The lower bound value resulting in lowest MPP standard deviation acts as a global minimum threshold and results in the least error across the campuses. Figure 5 illustrates the standard deviation with different global minimum threshold values.

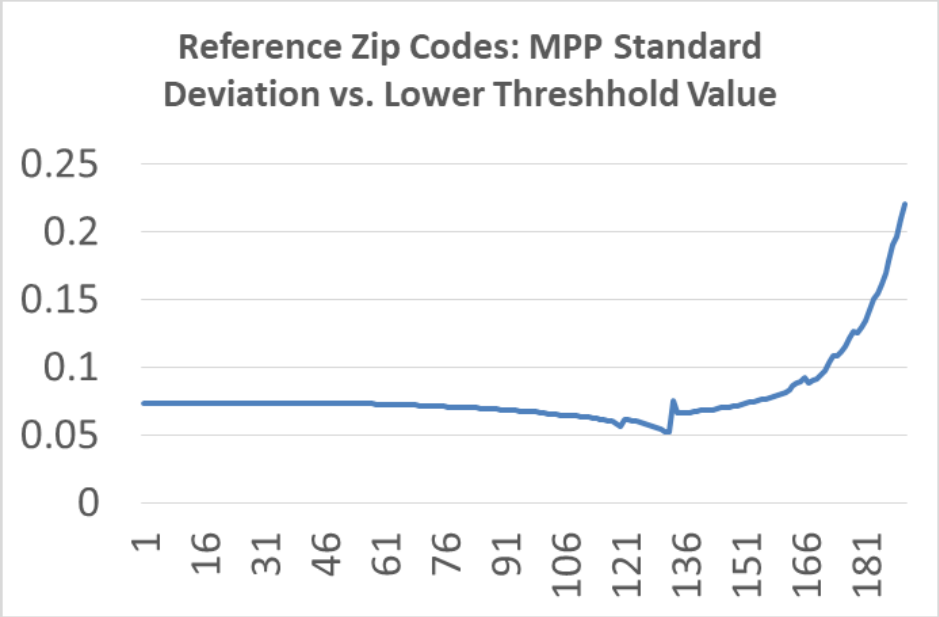

Figure 5 – Lower threshold value determines the level of brightness at which pixels should no longer be considered noise and eligible for solar panel installations. Local minimums occur due to relatively lower standard deviations across multiple zip codes, but the global minimum represents the lowest deviation for the entire set.

4.2.1. Validation

PS predictions for another known zip code can be used as the target volume to validate this methodology. Like how the reference zip code is selected for each campus, a contiguous zip code is selected. For the sake of clarity, the set of zip codes that will be used as reference for the campus predictions is labeled as "zip code 1" and the set of zip codes used to validate this methodology are labeled "zip code 2". These set of zip codes and resulting MPP ratio are tabulated in Table 2.

Table 2 - Reference and Validation Zip Codes. Error for zip code 1 is minimized in the model. The range of error in predicting the set of validation zip codes vary from -15% to 32% from PS predictions. Nearest campus is in parentheses next to reference zip codes.

Zip code 1	MPP Ratio	Zip code 2	MPP Ratio	Zip code 1 : Error from PS Prediction	Zip code 2: Error from PS Prediction
94704 (UCB)	0.353	94720	0.880	0.02%	-5.15%
90025 (UCLA)	0.361	90024	0.490	0.84%	31.60%
92122 (UCSD)	0.453	92161	0.800	0.80%	-15.06%
92507 (UCR)	0.469	92553	0.530	0.15%	11.03%
92617 (UCI)	0.398	92612	0.160	0.06%	0.72%
93117 (UCSB)	0.509	93111	0.008	0.12%	9.68%
95064 (UCSC)	0.299	95060	0.950	0.01%	-8.85%
95348 (UCM)	0.525	95341	0.755	0.26%	-11.30%
95616 (UCD)	0.392	95618	0.760	0.01%	-1.81%

Note that the error for zip code 1 is low because the model attempts to select values so that the pixel distribution matches the PS prediction. Several measurements are made in order to explore the reason for the predictive error. The error could be due to geographical differences (i.e., average latitude or elevation of buildings in zip code) or building characteristics (i.e., size of building or obstacles on rooftops). Buildings between 70 and 500 pixels categorized as small, greater than this range are considered large, and less than counted as noise. A statistical evaluation is conducted, and it is found that the error response is 41% likely due to a factor outside of the four considered and 84% confident the latitude is the sole cause if not due to outside factors. A summary of the factors and resulting p-values are tabulated in Table 3.

Table 3 - List of diagnostics for exploring reasons for model errors. The difference in latitude between reference and validation zip codes yields the lowest p-value implying highest significance.

Nearby Campus	Zip code 2: Error from PS	MPP ratio Difference	Average Latitude Difference	Average Elevation Difference (km)	Difference of Small Building percentages
UCB	-5.15%	0.527	0.0047389	-0.002	0.264
UCLA	31.60%	0.129	0.0200848	0.038	0.060
UCSD	-15.06%	0.347	0.0250129	0.007	0.338
UCR	11.03%	0.061	-0.061227	0.176	0.067
UCI	0.72%	-0.238	0.0225866	-0.033	-0.118
UCSB	9.68%	-0.502	0.0032471	-0.01	0.039
UCSC	-8.85%	0.651	-0.009162	-0.082	0.135
UCM	-11.30%	0.230	-0.054668	-0.001	0.002
UCD	-1.81%	0.368	-0.005758	-0.004	0.023
	All 4 Factors	MPP	Latitude	Elevation	Building Size
p-value	0.4122	0.8513	0.1612	0.2727	0.2823

Because MPP is strongly dependent on obstacles and angles of building rooftops, it would be dangerous to assume the reference zip code has similar rooftops to the validation set or even the campus. This is akin to predicting solar capacity on commercial buildings from the MPP in a heavily residential reference image. In other words, the MPP for the reference zip code is not very valid for another zip code—reflected in the highest p-value among the diagnostics. This is resolved by assuming an MPP that would be characteristic of UC campus buildings. For each campus, the PS available rooftop area for approximately 50 buildings is recorded and divided by the number of pixels in their images. The resulting MPP are summarized in Table 4.

Table 4 - Identifying partial campus MPP.

UCB	0.476
UCLA	0.527
UCSD	0.497
UCR	0.502
UCI	0.427
UCSB	0.504
UCSC	0.493
UCM	0.604
UCD	0.555
Std Error	0.017
AVG	0.509

Table 5 tabulates several buildings and their MPP values to illustrate the range of buildings. Parking structures are typically open and yield the highest MPP values. Office spaces and classroom dominated buildings follow. Buildings with some lab spaces that require venting or rooftop equipment result in the lowest MPP values, as expected.

*Table 5 - Representative buildings on the UCI campus with MPP values. The MPP are more dependent on rooftop geometry than brightness (i.e., solar irradiance). Building images not to scale. * denotes existing solar panels that PS considers an obstacle, resulting in slightly lower MPP.*

Student Center Parking Structure (0.893)	Anteater Parking Structure (0.852)	Social Science Parking Structure (0.835)	Mesa Visitor Parking Structure (0.761)
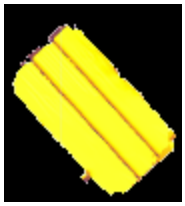	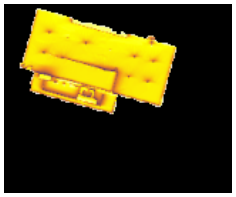	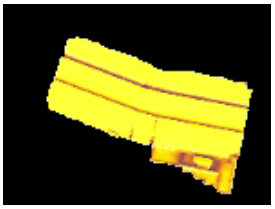	
Campus Village Community Center (0.721)	Engineering Hall (0.645)	Steinhaus Hall (0.609)	Phineas Banning Alumni House (0.595)
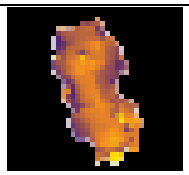	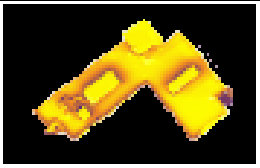		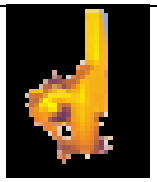
Biological Sciences 3* (0.419)	Social and Behavior Sciences Gateway (0.544)	UNEX Continuining Education (0.650)	Donald Bren Hall (0.611)
	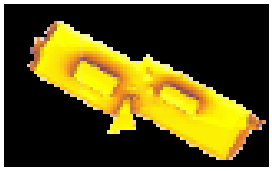		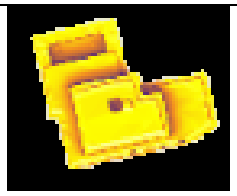
Humanities Gateway (0.507)	Aldrich Hall (0.493)	Natural Sciences II* (0.420)	Fredrick Reines Hall (0.354)
		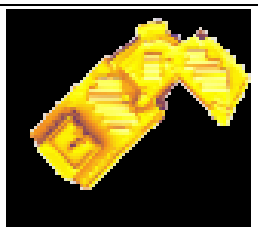	

The Association of Energy Engineers (AEE) has reported that the PV arrays at three of the UCI parking structures totals to 2.57 MW whereas UCI Sustainability reports 3.2 MW. This discrepancy may be due to AEE reporting the peak power in alternating current (AC) whereas the latter number may be in nameplate direct current (DC). Using this current method it is estimated that a total capacity of 2.82 MW in DC, which would be in agreement of the AEE estimate, assuming a DC-AC power conversion efficiency of 91%. The model also assumes panels installed flush whereas the actual installations have some tilt which would allow an increase of number of panels, suggesting it is a conservative estimate for actual installations. Some existing installations are tabulated as validation for the modeled MPP values in Table 6.

Table 6 - Recent PV panel deployment comparison. Panels are assumed to be 250 W, with an area of 1.637 square meters, and 3 modules per panel. Panel area and building area are found with Daft Logic's area calculator.

Campus	Building or Parking Lot	Approximate Panel Area (m2)	Building Footprint (m2)	Fraction Panel Area of Rooftop	MPP Equivalent
Berkeley	Sproul Complex	502	1862	0.27	0.279
Berkeley	Kleeberger Field House	1129	2091	0.54	0.558
Berkeley	Jacobs Hall	400	666	0.60	0.620
San Diego	MESOM Laboratory	400	1186	0.34	0.348
Santa Barbara	Multi-Activity Center	753	2456	0.31	0.317
Riverside	Lot 30	28153	50303	0.56	0.578

When considering the campus cross sections, individual UCI buildings, and analysis of recent PV deployments the following MPP values in Table 7 are suggested to predict PV building rooftop potential.

Table 7 - MPP values used to predict PV building rooftop potential on all UC campuses

Pessimistic Case	0.390
Standard Error Lower Bound	0.478
Average Case	0.495
Standard Error Upper Bound	0.512
Optimistic Case	0.600

4.2.2. Parking Lot PV Solar Potential

Parking lot areas are calculated with Daft Logic's area calculator in conjunction with Zonum Solution's KML compiler. A measuring wheel was used to validate Daft Logic's calculator. When physically measuring the anteater parking structure dimensions, there is an error of less than 1 percentage point. The parking lot area calculated with the Daft Logic tool is presented in Figure 6.

Figure 6 - UCI parking lot area considered. Daft Logic's Google Maps area calculator tool used in conjunction with Zonum Solution's KML compiler.

UC Riverside's Lot 30 panels currently only cover about 56%, leaving room between panels and not shading the area between parking spots. This is aligned with this assumption that open parking lots is likely to maintain 50% of PV potential when developed into a building or parking structure. . Though UCI's parking structure rooftop arrays cover the entire parking area footprint and still have some overhang, parking structures make up a minority of buildings and does not strongly influence the assumed building MPP. Note the parking structure rooftops are treated differently than the considered ground-level parking. Dividing the total parking lot area by the panel area would assume they are parallel with the floor, whereas in reality, they would most likely be tilted toward the south to maximize electricity production and shade. It is assumed that the reduction in panels due

to spacing between subarrays and shading from building construction is offset by the increase of capacity when installing tilted panels resulting in a 50% of PV potential if the entire lot were to be entirely shaded by PV panels.

A secondary case is considered where the future development of campuses is considered. Based on historical trends and campus planning, parking lots tend to become sites for new buildings. While converted parking lot area is designated for new buildings, the designated area the amount of landscaping surrounding the building footprint tends to vary. Though it would be fair to assume new buildings tend to have a 0.6 MPP ratio, there is much uncertainty of how building shading, landscaping, and other unforeseen developments may reduce PV technical potential. In many cases, as much as two-thirds of a parking lot is allocated to new building development. In other cases, the entirety of parking lots is converted to multi-level parking structures to accommodate campus needs. It is estimated that these parking lot areas are only able to maintain 50% of PV potential after all factors are considered.

The total PV solar potential that determined in this study for each of the campuses is presented in Figure 7 and Figure 8. In each case the results present the sum of each campus building total and parking lot total. Error bars arise from the building potential predictions, so that campuses with higher PV installation contribution from buildings have larger ranges of maximum potential PV installed. For example, Merced has a high contribution from parking lots resulting in a small range. If one were to reduce the amount of panels in all parking lots to be closer to Riverside's Lot 30 (56%), the second case results would be fairly close.

The results of Figure 7 present the maximum capacity of PV that can be installed on each of the UC campuses. A more realistic analysis of the transition of existing parking lots (into buildings, landscape, and a parking structure which becomes the primary site for PV installation) is presented in the total PV capacity results in Figure 8.

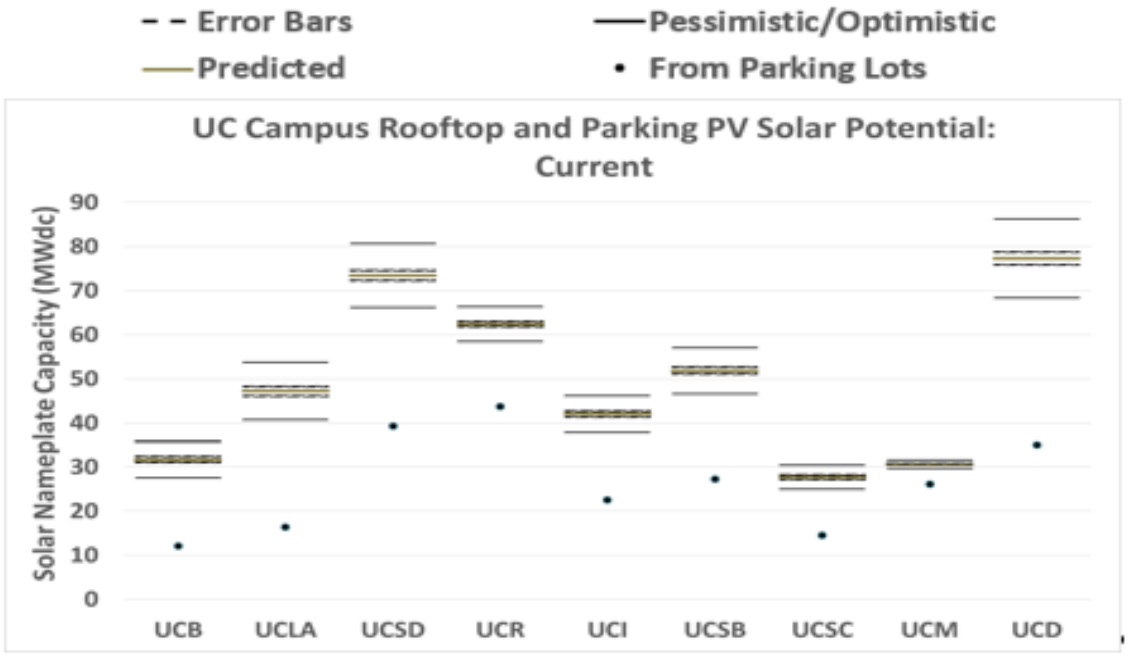

Figure 7 - Summary of on-site UC PV potential. Graphs representing current total (maximum) technical potential.

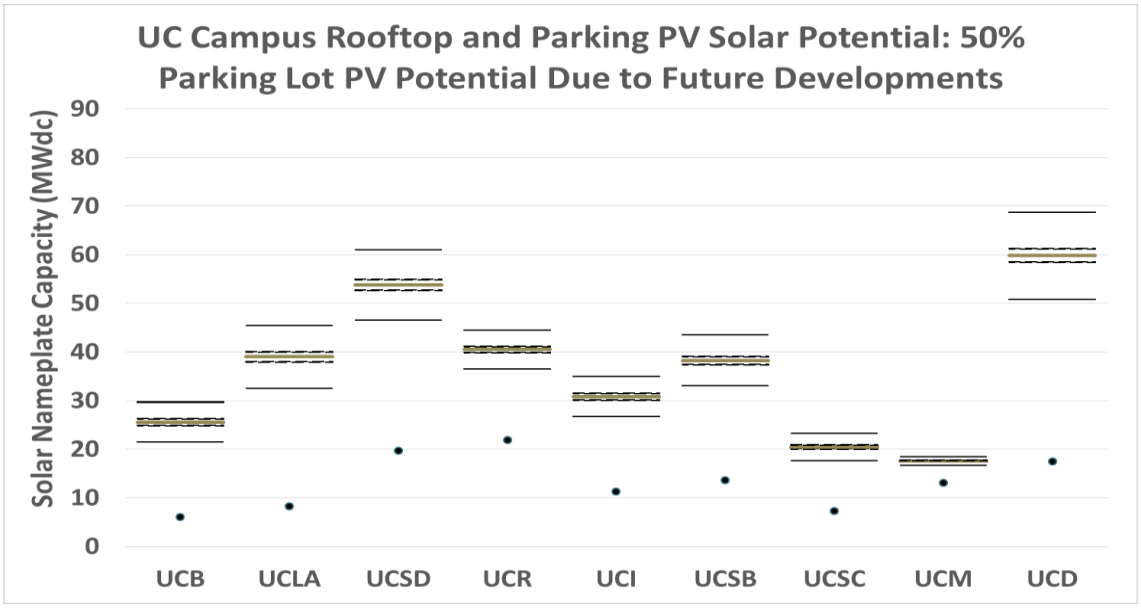

Figure 8 - Summary of on-site UC PV potential. Results represent total potential when anticipating the conversion of existing parking lots into buildings, landscape, and a parking structure (whose top floor becomes the primary site for PV installation).

4.3. Upper and Lower PV Installation Cases

The UCOP has established various policy goals in parallel with the carbon neutrality initiative. One of these goals suggests replacing 40% of natural gas combustion with biogas, allowing me to suggest that electricity produced by cogeneration plants on each campus is arguably 40% renewable electricity. For campuses with natural gas fueled power plants (i.e., UCB, UCI, UCSD, UCLA, UCSC, UCDMC, UCSF), this is a significant jump in renewable energy supply percentage. Though some natural gas is used for independent heating (e.g., duct burners and boilers) rather than cogeneration, it is assumed that significant majority of natural gas consumption amongst the campuses is utilized for cogeneration dictated by electrical demands.

The upper bound of off-campus PV installations corresponds with the scenario in which each campus halts additional distributed PV installations, but is still able to execute the biogas policy. The lower bound of off-campus PV installations corresponds with the scenario in which each campus deploys a high level of distributed PV installations in addition to implementing the biogas policy. The high-level of distributed PV installations considers future campus developments and halves PV potential in those areas corresponding with case 2 in the previous task. Figure 9 summarizes the capacity of installations for the lower bound case.

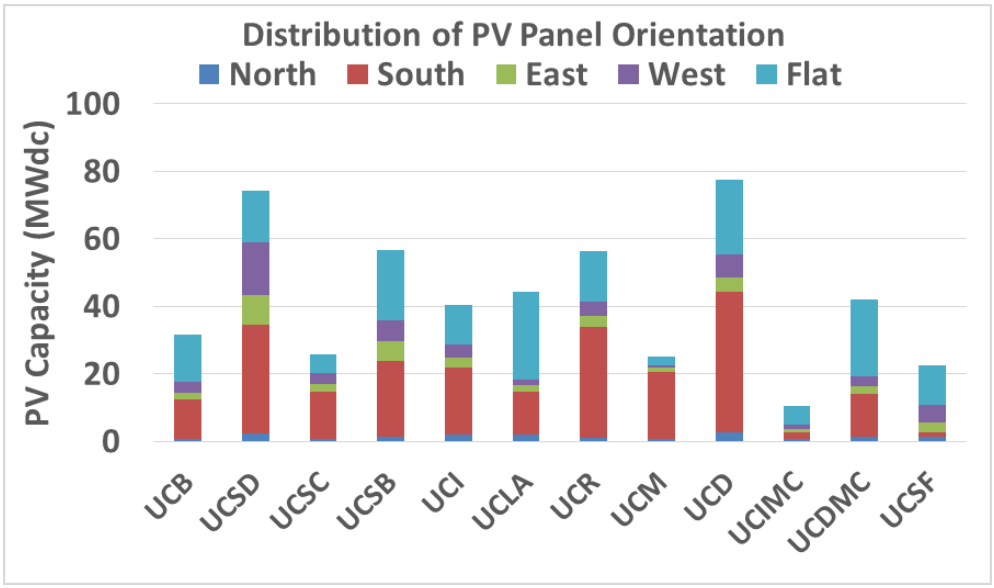

Figure 9 - Distribution of orientation for rooftop and parking lot PV solar arrays. All parking lot PV is considered to be south-facing. These capacities represent the practical maximum previously identified. The orientations are differentiated by their generation dynamics and annual production.

The orientation of each panel is relevant because the exposure to direct sunlight changes throughout the day. When the angle of the sun is aligned with the normal line of from the PV panel plane, the greatest amount of electricity can be produced. While diffuse light also plays a role in PV electricity production, the greatest portion is typically from the normal irradiance component. As such, the orientation allows us to account for some slight generation dynamics rather than assuming all PV panels produce electricity coincidentally.

From this point on, we detail the approach to obtaining the solar generation profile, electrical load profile, and how existing generation resources for applicable campuses are dispatched. We also detail how energy storage components are sized and integrated into a single model. Figure 10 is a visualization of logic the model uses in order to dispatch generation and storage resources. Each component is a zero-dimensional model with

average efficiencies ensuring the amount of electricity from generation resources or storage after any inefficiencies is equal to demand at all hourly simulated time steps.

4.3.1. On-site PV Integration Strategy

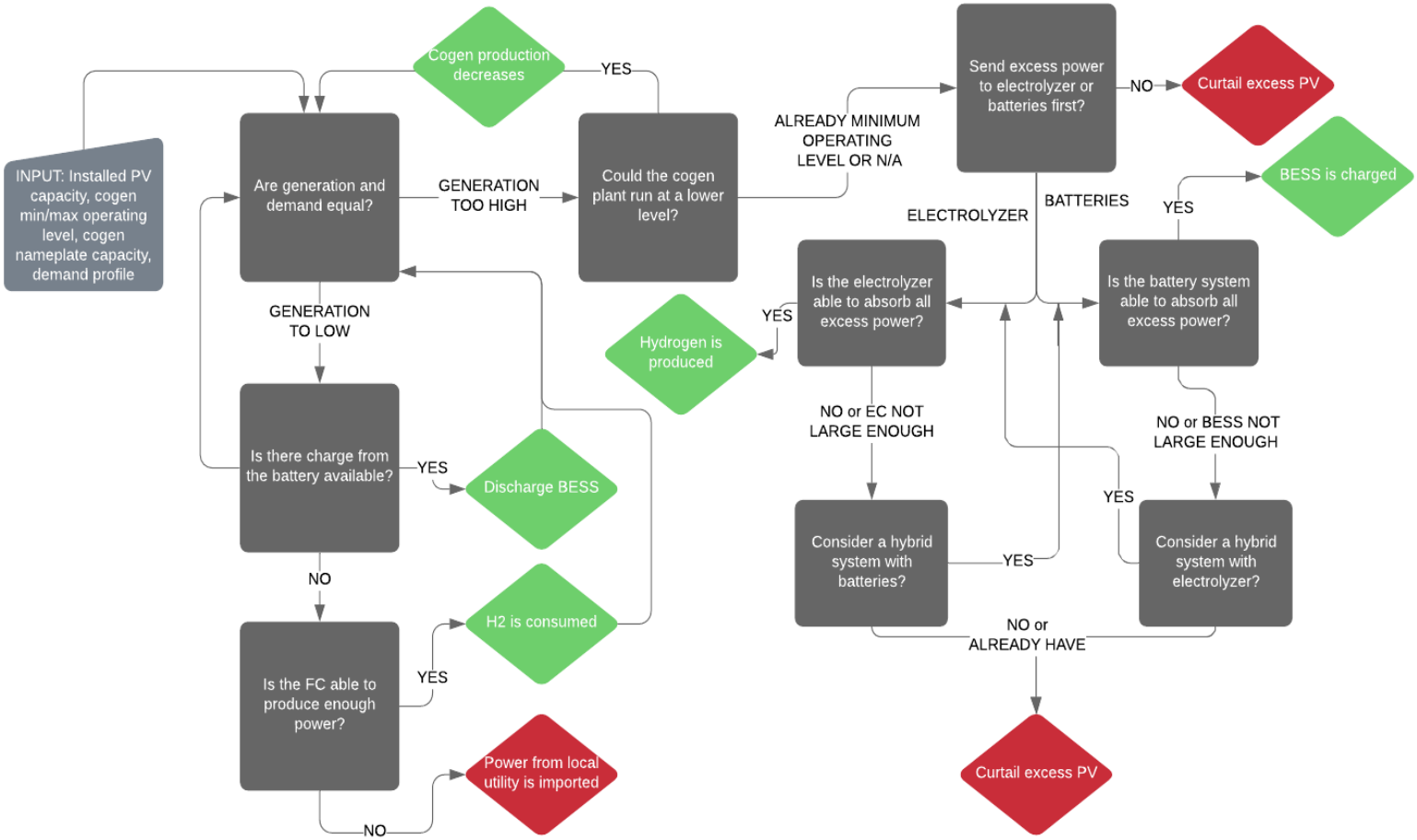

Figure 10 – Visualization of the logic based heuristics of implementing storage on each campus. Existing cogeneration power plants attempt to meet load or accommodate additional PV generation by operating at lower loads. Excess power may be sent to storage and residual loads are met by power from s torage.

4.3.1.1. Solar Profile

2018 Historical PV generation has been provided for UCB, UCSD, and UCD. For every other campus NREL's typical meteorological year (TMY) data are derived from decades of National Solar Radiation Data Base archives is utilized. TMY datasets report representative irradiance levels per area that are scaled to match the provided 2017 total annual production from solar for each campus by the UCOP. Table 8 lists the nearest weather stations' datasets that were used for each campus.

Table 8 – Summary of source of solar profile data used for each campus.

Campus	TMY3 Weather Station
UCB	Provided Data Used
UCD	Provided Data Used
UCDMC	SACRAMENTO EXECUTIVE ARPT
UCI	SANTA ANA JOHN WAYNE AP
UCIMC	SANTA ANA JOHN WAYNE AP
UCLA	SANTA MONICA MUNI
UCLAMC	SANTA MONICA MUNI
UCM	MERCED/MACREADY FLD
UCOP	OAKLAND METROPOLITAN ARPT
UCR	RIVERSIDE MUNI
UCSB	SANTA BARBARA MUNICIPAL AP
UCSC	SAN JOSE INTL AP
UCSD	Provided Data Used
UCSDMC	SAN DIEGO MIRAMAR NAS
UCSF	OAKLAND METROPOLITAN ARPT C2
UCSFMC	OAKLAND METROPOLITAN ARPT C2

Because irradiance data are given for horizontal surfaces, the TMY profiles are treated to reflect slightly different generation dynamics each orientation has. In other

words, west-facing PV panels typically generate slightly more as the sun sets than an east-facing panel would. Generation profile from east facing is shifted one hour earlier and west is shifted one hour later. All profiles are scaled to the predicted annual electric production per orientation listed in Table 9. The numbers are given in units of kilowatt-hours (kWh).

Table 9 – Summary of annual production per panel sin specific orientation.

Solar Panel Annual Electricity Production per Panel (kWh)					
Campus	North	South	East	West	Flat
UCB	491	518	486	456	441
UCD	511	556	501	484	447
UCDMC	511	556	501	484	447
UCI	521	556	512	494	456
UCIMC	521	556	512	494	456
UCLA	517	556	508	491	453
UCLAMC	517	556	508	491	453
UCM	531	556	521	504	465
UCOP	491	518	486	456	441
UCR	539	556	529	511	471
UCSB	531	568	517	500	469
UCSC	482	517	473	460	434
UCSD	512	546	503	489	456
UCSDMC	512	546	503	489	456
UCSF	491	518	486	456	441
UCSFMC	491	518	486	456	441

4.3.1.2. Demand Profile

2018 Historical electrical demand data has been provided for UCB, UCSD, UCD, UCI, and UCSB. For UCB, UCSD, UCD, and UCSB, an analysis of variance is conducted and found that the dry bulb temperature, relative humidity, and illuminance levels (from TMY3 dataset) have statistically significant impact on demand. This matches intuition as

much of electrical load is likely heating, ventilation, and air conditioning, and reflects the diurnal nature of campus activity. The average of each model coefficient is taken and utilized for the other campuses to predict the load profile. Profiles are then scaled to 2017 annual electrical consumption tabulated in the appendix.

4.3.1.3. Combined Heat and Power Generation (Cogen) Plant

Gas turbines typically have a minimum operating level before efficiency drops significantly and emission levels are no longer compliant, also known as minimum emissions-compliant load. This is typically somewhere around 70% of nameplate. Because UCSD has a 2-1 configuration (two gas turbines, one steam turbine), it is possible that operation of only one gas turbine is sufficient. This would translate to the minimum operating load to be around 25% of their 33 MW nameplate capacity. In another example, UCI's cogeneration plant is 1-1, so the gas turbine operating at its minimum load results in a plant minimum operating load of around 50%. For each cogeneration campus an attempt to identify the cogeneration configuration and gas turbine size to calculate the minimum operating load in the model is made. In the data provided by UCSD the highest load was only 88% of nameplate whilst still having imports. If data are available, it is utilized with the historical maximum operating level as the maximum in the dispatch model, otherwise it is assumed the power plant can be operated up to 99% of nameplate. It is assumed CHP operations are dependent on electrical loads and heating loads are essentially parallel and near sufficient. Figure 11 illustrates an example of how resources are dispatched to meet the load dynamics. The yellow bars represent the solar that comes online and the grey bars surrounding it is the cogeneration plant electricity production. Note that despite the

cogeneration operating at minimum load when solar peaks, there is excess electricity going to storage or being curtailed. The green and lighter red represent the discharge of energy from storage and when all generation resources are insufficient for meeting load, electricity must be imported from the grid (represented by purple).

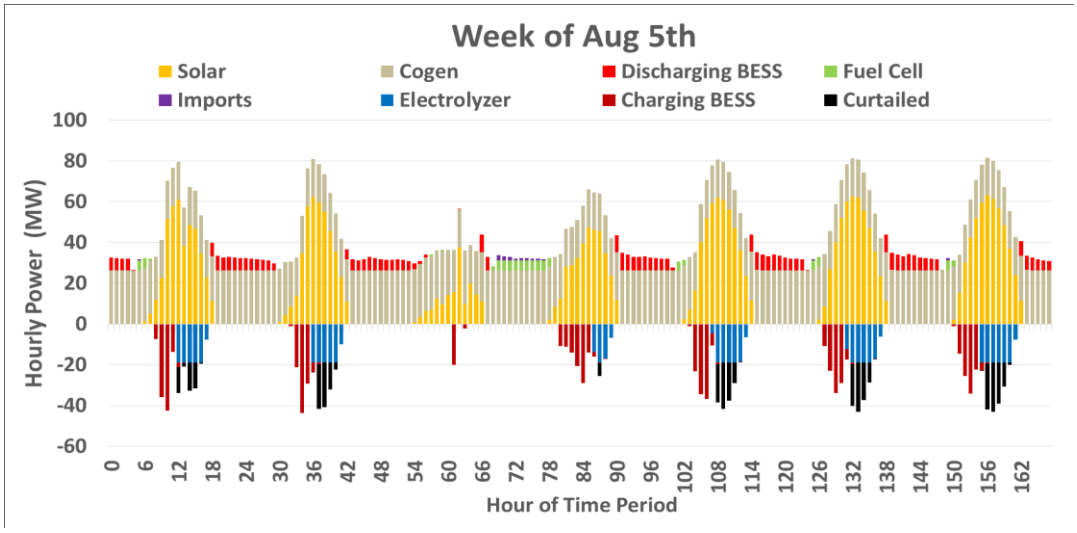

Figure 11 – Sample of energy dispatch to meet campus electrical load. A week is provided to illustrate the daily shifting of the BESS whereas the fuel cell operates to complement meeting the evening load. Days without much solar require power from P2G to continue enabling the cogeneration plant to operate at minimum load.

Prior to the biogas implementation in cogeneration plants, most renewable energy supply (RES) comes from the existing PV installations as well as the fraction from imports that is renewable. Some campuses have direct access electricity, a somewhat exclusive option to purchase electricity from a third-party electric service provider. Direct access electricity can be 100% renewable offering the consumers the ability to purchase electricity and the associated renewable energy certificates (RECs) as a bundle. Alternatively, RECs can be purchased as standalone commodities. Because RECs are retired for a megawatt-hour (MWh) of electricity consumed, 100 RECs must be retired for 100

MWh of imported electricity, rather than 66 RECs for 100 MWh of electricity from an IOU (assuming 34% IOU RES).

Note the following discussion is regarding the frozen PV installation versus the practical maximum identified previously. The prior is referred to as the low PV case and the latter as the high PV case for clarity. Both cases are considered possible 2025 cases and both have increased RES% from the time of this writing. The campuses are organized into the four following categories based upon similar results and infrastructure: no-cogeneration campuses, no storage needed campuses, accommodating cogeneration campuses, and high P2G potential campuses. The carbon neutrality goal for 2025 includes reducing the emissions from campus transportation fleets as well.

We have only considered on-site power generation and electricity imports. Imported electricity would have to be 100 percent renewable or enough RECs to make the claim of reaching the 2025 electricity goal, but still falls short of the carbon neutrality goal because since the imported natural gas for dedicated heating demands nor the fleet emissions on these campuses is not accounted for.

4.3.1.4. Energy Storage Component Capacity Factors and Sizes

An energy dispatch model as described illustrated in Figure 10 is developed which considers the limitations of cogeneration plant operations alongside PV solar and storage. Cogeneration plant operations are modeled to be online year-round and prioritized over energy from storage for meeting loads. Energy from storage is only dispatched when the cogeneration plant is inadequate for meeting total electric load. For the maximum solar installation case, cogeneration production is turned down to within minimum operating

load constraints (typically 50% of rated power) before any solar is curtailed. Any excess power not going toward load is sent to storage. A case in which a battery energy storage system (BESS) is prioritized over an electrolyzer and vice-versa is considered. In both cases, the BESS is prioritized for discharge due to its limitations with storage capacity and self-discharge, but also because of a higher roundtrip efficiency. The fuel cell, electrolyzer, and BESS capacities are sized so that a moderate capacity factor roughly the average of the extreme high and low values is achieved. . A high capacity factor typically results in a high level of curtailment resulting in a low utilization of solar PV production. On the other hand, a low capacity factor typically results in a high energy storage costs that are not utilized to its potential. The moderate capacity factor case is considered to be the average of these two extremes and consequently deemed an economically practical case regarding storage implementation. Our selected capacity values are summarized in Table 10 and sizes in Table 11 below. A visualization of each components' capacity factor is provided alongside levelized cost results in Figure 14 and Figure 15 of the later Section 4.2.3.

Table 10 – Summary of energy storage component capacity factors for simulated scenarios.

Campus	Scenario	Fuel Cell CF	Electrolyzer CF	BESS CF		Campus	Scenario	Fuel Cell CF	Electrolyzer CF	BESS CF
UCSD	Hybrid EC>BESS, Max PV	49	16	21		UCR	Hybrid EC>BESS, Max PV	69	19	19
UCSD	Hybrid BESS>EC, Max PV	30	6	22		UCR	Hybrid BESS>EC, Max PV	62	7	28
UCSD	BESS Only, Max PV	N/A	N/A	14		UCR	BESS Only, Max PV	N/A	N/A	22
UCSD	P2G Only, Max PV	46	12	N/A		UCR	P2G Only, Max PV	70	14	N/A
UCSC	Hybrid EC>BESS, Max PV	15	35	17		UCM	Hybrid EC>BESS, Max PV	50	24	19
UCSC	Hybrid BESS>EC, Max PV	10	15	30		UCM	Hybrid BESS>EC, Max PV	19	13	36
UCSC	BESS Only, Max PV	N/A	N/A	15		UCM	BESS Only, Max PV	N/A	N/A	18
UCSC	P2G Only, Max PV	42	19	N/A		UCM	P2G Only, Max PV	57	18	N/A
UCI	Biogas w/ Max PV	N/A	N/A	N/A		UCSB	Hybrid EC>BESS, Max PV	62	23	19
UCB	Biogas w/ Max PV	N/A	N/A	N/A		UCSB	Hybrid BESS>EC, Max PV	40	7	32
UCLA	Biogas w/ Max PV	N/A	N/A	N/A		UCSB	BESS Only, Max PV	N/A	N/A	25
UCSF	Biogas w/ Max PV	N/A	N/A	N/A		UCSB	P2G Only, Max PV	63	17	N/A
UCDMC	Biogas w/ Max PV	N/A	N/A	N/A		UCIMC	Hybrid EC>BESS, Max PV	88	8	7
UCD	Hybrid EC>BESS, Max PV	76	17	19		UCIMC	Hybrid BESS>EC, Max PV	88	3	18
UCD	Hybrid BESS>EC, Max PV	73	6	25		UCIMC	BESS Only, Max PV	N/A	N/A	22
UCD	BESS Only, Max PV	N/A	N/A	20		UCIMC	P2G Only, Max PV	89	6	N/A
UCD	P2G Only, Max PV	77	12	N/A						

Table 11 - Summary of energy storage component sizes for simulated scenarios.

Campus	Scenario	Fuel Cell (MW)	Electrolyzer (MW)	BESS (MW)		Campus	Scenario	Fuel Cell (MW)	Electrolyzer (MW)	BESS (MW)
UCSD	Hybrid EC>BESS, Max PV	0.979	8.963	2.900		UCR	Hybrid EC>BESS, Max PV	1.767	13.567	5.750
UCSD	Hybrid BESS>EC, Max PV	0.805	14.684	10.393		UCR	Hybrid BESS>EC, Max PV	0.725	14.311	14.625
UCSD	BESS Only, Max PV	N/A	N/A	19.706		UCR	BESS Only, Max PV	N/A	N/A	26.234
UCSD	P2G Only, Max PV	2.395	19.706	N/A		UCR	P2G Only, Max PV	2.377	26.234	N/A
UCSC	Hybrid EC>BESS, Max PV	1.975	1.965	10.656		UCM	Hybrid EC>BESS, Max PV	2.445	10.965	2.871
UCSC	Hybrid BESS>EC, Max PV	1.500	5.768	6.968		UCM	Hybrid BESS>EC, Max PV	2.500	7.799	7.429
UCSC	BESS Only, Max PV	N/A	N/A	14.619		UCM	BESS Only, Max PV	N/A	N/A	16.847
UCSC	P2G Only, Max PV	2.450	14.619	N/A		UCM	P2G Only, Max PV	2.540	16.847	N/A
UCI	Biogas w/ Max PV	N/A	N/A	N/A		UCSB	Hybrid EC>BESS, Max PV	3.305	19.072	5.110
UCB	Biogas w/ Max PV	N/A	N/A	N/A		UCSB	Hybrid BESS>EC, Max PV	1.675	19.618	19.072
UCLA	Biogas w/ Max PV	N/A	N/A	N/A		UCSB	BESS Only, Max PV	N/A	N/A	31.485
UCSF	Biogas w/ Max PV	N/A	N/A	N/A		UCSB	P2G Only, Max PV	3.940	31.485	N/A
UCDMC	Biogas w/ Max PV	N/A	N/A	N/A		UCIMC	Hybrid EC>BESS, Max PV	0.020	0.890	0.736
UCD	Hybrid EC>BESS, Max PV	1.435	13.673	7.431		UCIMC	Hybrid BESS>EC, Max PV	0.007	1.648	0.505
UCD	Hybrid BESS>EC, Max PV	0.630	15.954	15.440		UCIMC	BESS Only, Max PV	N/A	N/A	0.216
UCD	BESS Only, Max PV	N/A	N/A	29.423		UCIMC	P2G Only, Max PV	0.030	1.370	N/A
UCD	P2G Only, Max PV	2.155	29.423	N/A						

Figure 12 reflects the renewable energy supply percentage (RES%) if there is zero direct-access (DA) electricity and instead we consider 33% of the imported electricity is renewable aligned with current state renewable penetration levels. It is known that campuses have existing DA agreements with bundled RECs that enable some campuses to claim the imported electricity is 100%. While many debate the basis for claiming 100% clean electricity and carbon neutrality with tradeable commodities is not universally a replicable and scalable option, for this analysis, it is suggested the redemption of RECs and carbon offsets from a third party or owning the off-campus projects do not influence the results of this work. We are interested in the limitations of meeting on-campus demands with on-campus resources. Figure 12 illustrates how much load for each campus is being met by existing cogeneration power plants, solar PV, energy from storage, and imported electricity for the four types of control strategy aside from the reference cases. The secondary axis corresponding with the black points are a visualization of RES%. The economics of and much of the latter discussion is in reference to these simulated cases.

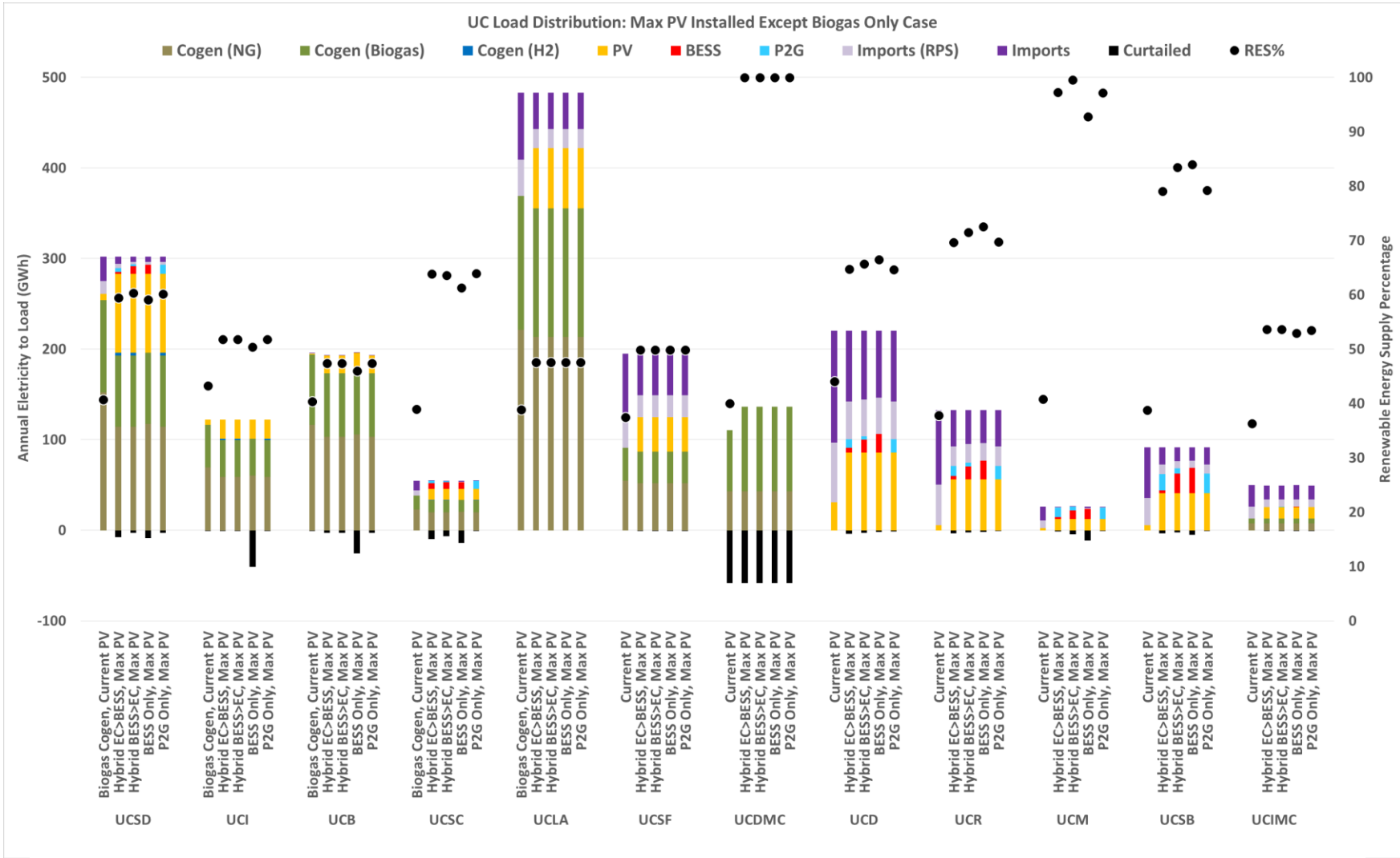

Figure 12 – Summary of energy dispatch for all campuses considered. The primary axis corresponds to the stacked columns that illustrate the energy magnitude that each resource meets. The secondary axis corresponds to the points, which illustrate the renewable energy supply percentage in each case.

4.3.2. Four Integration Archetypes

4.3.2.1. No-cogeneration Campuses: UCD, UCR, UCM, UCSB

Each of these campuses do not have cogeneration on site and have historically depended on imported electricity to meet demand. Though there is already some solar generation on each campus, it is only a fraction of the high PV case. It is found that currently, PV on each campus meets roughly 14, 4, 9, and 6 percent of total load for UCD, UCR, UCM, UCSB, respectively. The high PV case increases these numbers to 39, 42, 48 and 44 percent of load, before considering storage. For these campuses, these figures are equivalent to their RES percentage (if one were to exclude the renewable attributes of imported electricity). If one were to curtail all excess electricity, this would amount to roughly 25, 34, 64, and 52 percent of PV generated electricity going to waste. By implementing storage, the RES% increases up to 48, 58, 99, and 75. The difference between these two sets of RES% levels represents how much excess electricity can be shifted. UCD and UCR can utilize most of the solar PV immediately and require storage for some additional daily shifting. On the other hand, UCM and UCSB have so much PV installed that there is enough excess for both daily and some seasonal shifting. Because of this it is seen that UCM can achieve 95 percent RES and UCSB follows at around 85 percent.

In the P2G storage only case, 26%, 35%, and 53% of PV generation is sent to storage for UCD, UCR, UCSB, respectively. For the BESS only case, these same numbers are 25%, 34%, and 47%. Comparing these 6 scenarios, the RES% is 1, 3, and 5 percentage points higher for the BESS case. In addition, BESS only case yields lower average levelized cost of

renewable even when at the lowest hydrogen storage capacity price. Note these campuses are all of the "no-cogeneration campus" archetype established.

The only campus in this category which has slightly different results is UCM. For UCM, the P2G only case results in a RES% close to 96 whereas the battery only case yields 89. For these cases 68% and 40% of PV generated is sent to P2G and BESS only associated with a 185-255 $/MWh cost range for P2G and 128 $/MWh for the battery case. Though this represents a cost premium, the battery only case curtails 28% of PV generated whereas the P2G case has less than 0.5% of generation curtailed. The costs associated with the battery capacity necessary to match such high RES% is not explored, but the hybrid scenario which prioritizes charging the BESS results in an average renewable levelized cost of electricity (LCOE) of 131-175 $/MWh and achieves 99.3 RES%. Across all campuses and scenarios, this scenario is unique, as it nearly achieves 100% clean electricity endogenously (UCDMC cases are debatable due to the exporting nature of the campus power plant).

4.3.2.2. No Storage Needed Campuses: UCLA, UCSF, UCIMC

We found that these campuses have enormous loads compared to their footprint, very characteristic of being in an urban setting. Despite UCLA and UCSF having cogeneration plants, it is found that these plants only met 66 and 36 percent, respectively, of total load (including their contiguous medical campuses). If one were to displace 40% of the natural gas used with biogas this would translate to roughly 26 and 14% of load being met with the renewable portion of cogeneration. The high PV case provides an additional 14 and 1 percent of load for UCLA and UCSF, respectively, increasing total RES% to 40 and 15 percent, respectively. UCIMC has a baseload molten carbonate fuel cell which provides

roughly 20% of campus load. Because it currently operates on natural gas, one can only consider its generation as much renewable as the natural gas infrastructure is. If it is assumed that 40% of its natural gas usage is biogas derived, this suggests roughly 8% of UCIMC's load being met by renewables. Installing solar increases this figure to 13%. Electricity is being imported in every hour of the year for all three campuses, so there is never excess electricity to store.

4.3.2.3. Accommodating Cogeneration Campuses: UCSD, UCSC

Both UCSD and UCSC campuses have cogeneration plants. In this category, the solar panels generate excess electricity and often require the cogeneration plant to operate at a lower power output level. Doing so may be result in an inability to meet instantaneous heating demands, however, thermal energy storage is typically less constraining than electrical storage. At UCSC there are many hours where the gas turbine power is reduced to minimum operating load during peak solar generation. As a result, the baseload cogeneration plant capacity factor drops to about 88% from a theoretical 100% (ignoring maintenance periods). In addition, the production of hydrogen allows a slightly lower carbon footprint by injecting hydrogen gas upstream of the cogeneration turbines. This would increase the 40% renewable cogeneration from biogas to 41.7% with the addition of renewable hydrogen. With about 61% of load being met by the UCSC gas turbine, mix of fuel translates to about 25% campus RES%. The high level of PV contributes another 21% compared to 1% from the low PV case. Similarly, for UCSD, the cogeneration plant meets 65% of total electrical demand translating to 27 RES% from the renewable

gases use. On-campus solar contributes 28% from the high PV case compared to 2% in the low PV case.

We see some curtailment because peak solar generation may still produce some excess if the power plant is turned off completely. However, on-campus solar alone is not adequate to meet load on either campus. If no storage existed, 65% of UCSC PV generation would be curtailed and 20% for UCSD. Modeling some storage, it is seen that this excess electricity can be captured and provide an additional 4 percent RES for UCSD and 17 percent RES for UCSC—putting the UCSD's total RES% at 60 and UCSC's at 63.

For these campuses, the favorite storage technology as apparent as those in the no-cogeneration campuses. The UCSD P2G only case results in 59% RES with a 191-198 $/MWh LCOE cost range. The battery only case results in 58% RES% with 187 $/MWh. Considering some of the hydrogen is used in the UCSD cogeneration, the overall RES% would be slightly higher yet the levelized cost of electricity met by a fuel cell is within 6% of the battery only case's LCOE. Due to the ability to use hydrogen in the existing cogeneration plant, less electricity is also curtailed in the P2G only case compared to the BESS only case—2% versus 8%. For UCSC, the P2G only case reaches 64% RES with a cost range of 202-256 $/MWh and the BESS only case reaches 60% RES with 185 $/MWh. Here, a hybrid strategy favoring charging the BESS first would reach 63.4% RES with a LCOE range of 171-224 $/MWh. This is the only campus where a hybrid scenario would result in a lower LCOE than a battery only scenario—though dependent on the lowest hydrogen storage cost assumption.

4.3.2.4. High P2G Potential Campuses: UCI, UCB, UCDMC

UCI, UCB, and UCDMC all have cogeneration plants on campus. Those in this category have plants capable of meeting nearly the entirety of the electrical demand. The primary distinguishable characteristic between this category and the prior one is that these campuses rarely need to import any electricity, UCDMC is designed to constantly export. Consequently, there is little reason for energy storage to be installed. Deploying PV to increase renewable generation comes at the cost of reducing cogeneration output, similar to the accommodating campus category. Even at minimum cogeneration operating load, large amounts of curtailment would occur in the high PV case. UCI has already had challenges reducing cogeneration output to handle even the current modest PV generation levels to comply with the existing non-export (inadvertent export only) agreement. Frankly speaking, additional PV is not desired on these campuses to meet electrical loads but offers the opportunity for distributed hydrogen production to target the reduction of scope 1 and scope 2 emissions. Since the electrical load can be entirely met with cogeneration, a 40% biogas blend would achieve a 40 percent RES. Injecting hydrogen would increase this number another 1.7%. There is no significant additional contribution to RES% from solar since it is sent to an electrolyzer and rather than directly used for power generation.

We have considered the amount of hydrogen that can be produced by dedicating PV to hydrogen production. As a flexible fuel, this hydrogen could go toward supplying fuel to hydrogen fueling stations or injected into the natural gas pipeline for the generation of carbon offsets. These carbon offsets would go toward negating the emissions from the

non-renewable portion of cogeneration plants that other cogeneration campuses have not been able to address without off-campus projects.

As a quick thought experiment, UCI has a hydrogen station that in the past year on average has dispensed around 200 kilograms of hydrogen per day and is in process of developing a newer hydrogen station with a design capacity of 1000 kilograms per day. A 10 MW electrolyzer at about 30% capacity factor can produce half a million kilograms of hydrogen throughout the year translating into 1350 kilograms per day even after injecting hydrogen into the cogeneration plant year-round. Without robust hydrogen delivery infrastructure, the local production of hydrogen translates into trucking vehicle miles travelled and associated emissions. The capacity factors vary for each campus depending upon the cogeneration plants' ability to meet existing electrical loads. In general, larger electrolyzers see less opportunity to fully utilize installed capacity—only operating near its nameplate capacity when annual peak solar occurs. On the smaller size end, capacity factors start no higher than 30% corresponding with PV's capacity factor. Increasing the electrolyzer's capacity factor would require the intentional overproduction of electricity from the cogeneration plant or importing renewable electricity from off-campus outside of the PV generation window. Note Table 10 from earlier on tabulates the modeled capacity factors for all campuses not in the "high P2G potential" category. Figure 13 illustrates the possibility of hydrogen production at varying capacity factors.

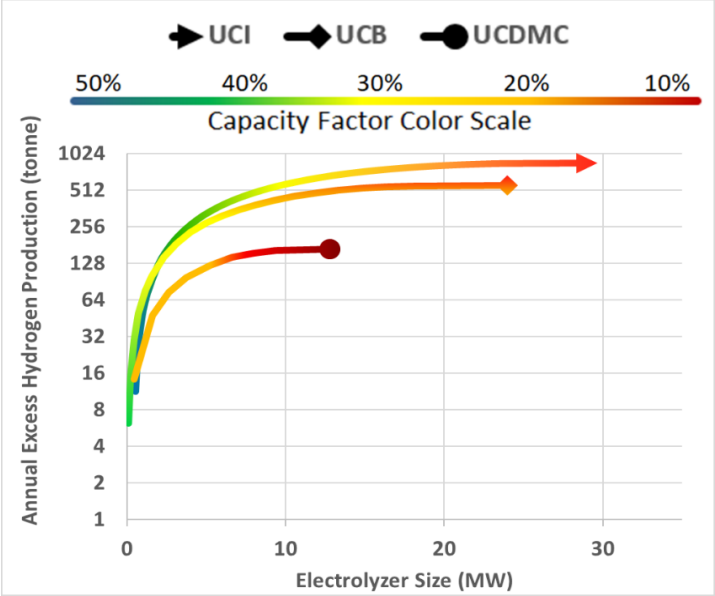

Figure 13 - Annual excess hydrogen production compared to electrolyzer size. The color scale provides the rough capacity factor for each installation scenario. Only campuses with high P2G potential are included.

4.3.3. Levelized Cost Analysis

The ultimate goal is to increase RES% and to ideally do so in a cost-effective way. The average levelized cost of implementing solar with storage is calculated for each of the considered scenarios and compared it with the average levelized cost of renewable electricity from biogas via cogen plant and existing PV installations. The first column in each of the campuses with cogeneration assume that electricity produced from biogas in cogeneration plants is 100% renewable. Even at the low-end cost of biogas, direct PV solar is cheaper on a levelized cost basis. Note that this is only true if the PV can be directly used by load and not sent to storage. Electricity that comes from storage, or serves load indirectly, has an associated for this additional step reflected by the blue and red columns in Figure 14. The levelized cost of renewable electricity being used directly and indirectly is consolidated in Figure 15 as an average levelized cost of electricity

The blue and red columns stacked on top of the PV represent the additional cost to store the excess electricity. Only campuses that implement storage are presented (i.e., high P2G potential and no storage campuses are represented by the biogas and solar columns alone). With near-term costs, each electron that must be stored and then meet load at a later time than generated is clearly more expensive than the biogas case. However, one should consider the higher PV capacity that is enabled by implementing some level of storage. For example, if 80% of PV is generated and used directly and only 20% is sent to the storage, the average cost from direct and indirectly used PV electricity could result in a competitive price. Figure 15 summarizes this illustration across the scenarios. While some analysis show that overbuilding PV even more and curtailing excess generation instead of utilizing storage may be cheaper, this is a debatable control strategy that may face challenges with the integrity of reaching net-zero carbon electricity, may have costs not considered, and also limits the amount of RES% that the campus can achieve without external resources. Figure 14 alone does not capture the value of approaching the 100% carbon neutral electricity goal and only serves to illustrate a comparison between theoretical approaches. In other words, though biogas may be cheaper for initial renewable energy supply gains—it is severely limited by the mixture of biogas in natural gas usages and does not achieve the higher RES% possible with more PV and energy storage

.

a)

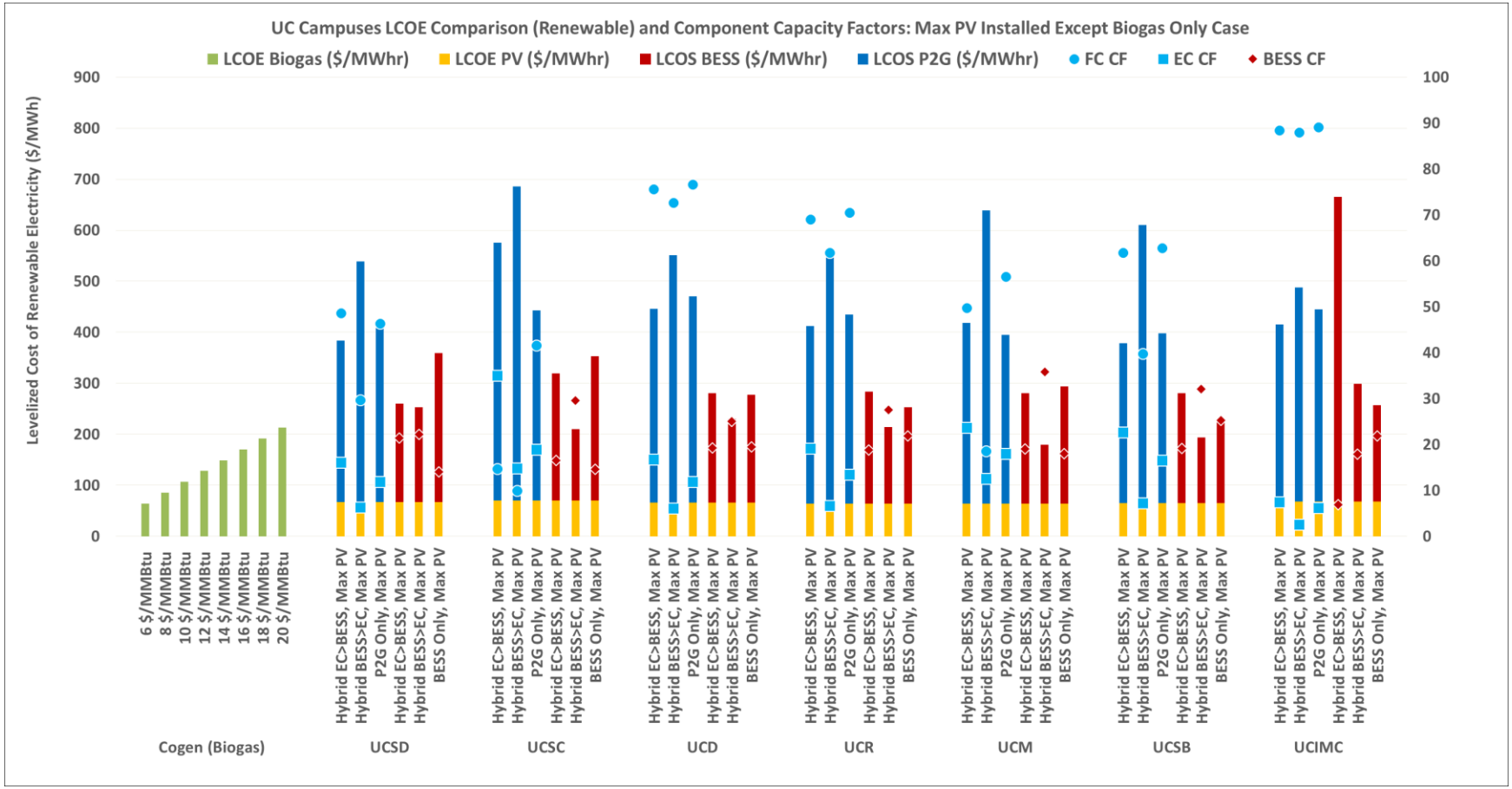
UC Campuses LCOE Comparison (Renewable) and Component Capacity Factors: Max PV Installed Except Biogas Only Case
LCOE Biogas ($/MWhr)
LCOE PV ($/MWhr)
LCOS BESS ($/MWhr)
LCOS P2G ($/MWhr)
FC CF
EC CF
BESS CF
Levelized Cost of Renewable Electricity ($/MWh)
900
800
700
600
500
400
300
200
100
0
100
90
80
70
60
50
40
30
20
10
0
6 $/MMBtu
8 $/MMBtu
10 $/MMBtu
12 $/MMBtu
14 $/MMBtu
16 $/MMBtu
18 $/MMBtu
20 $/MMBtu
Hybrid EC>BESS, Max PV
Hybrid BESS>EC, Max PV
P2G Only, Max PV
Hybrid EC>BESS, Max PV
Hybrid BESS>EC, Max PV
BESS Only, Max PV
Cogen (Biogas)
UCSD
UCSC
UCD
UCR
UCM
UCSB
UCIMC

b)

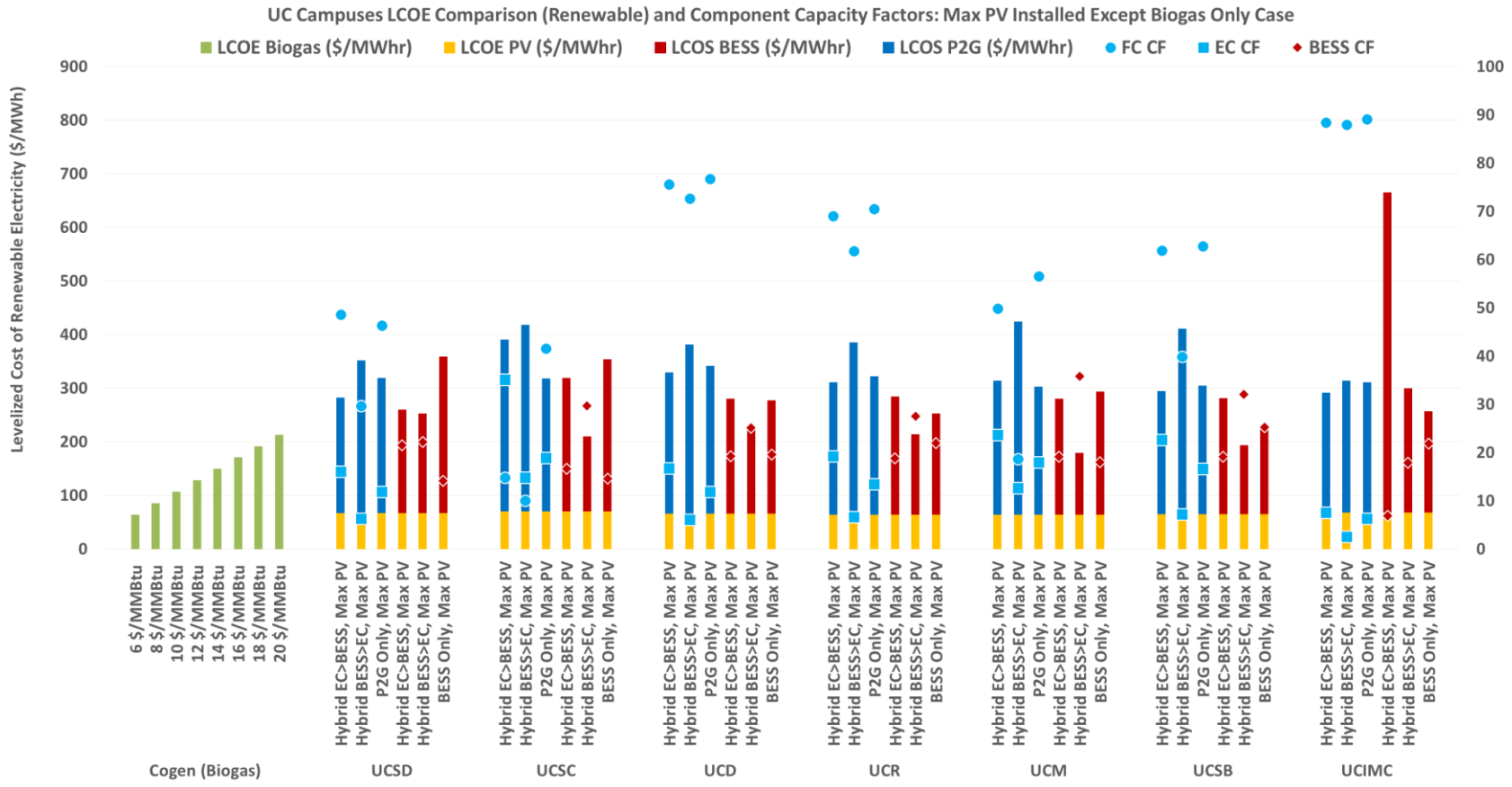
UC Campuses LCOE Comparison (Renewable) and Component Capacity Factors: Max PV Installed Except Biogas Only Case
LCOE Biogas ($/MWhr)
LCOE PV ($/MWhr)
LCOS BESS ($/MWhr)
LCOS P2G ($/MWhr)
FC CF
EC CF
BESS CF
Levelized Cost of Renewable Electricity ($/MWh)
900
800
700
600
500
400
300
200
100
0
100
90
80
70
60
50
40
30
20
10
0
6 $/MMBtu
8 $/MMBtu
10 $/MMBtu
12 $/MMBtu
14 $/MMBtu
16 $/MMBtu
18 $/MMBtu
20 $/MMBtu
Hybrid EC>BESS, Max PV
Hybrid BESS>EC, Max PV
P2G Only, Max PV
Hybrid EC>BESS, Max PV
Hybrid BESS>EC, Max PV
BESS Only, Max PV
Cogen (Biogas)
UCSD
UCSC
UCD
UCR
UCM
UCSB
UCIMC

c)

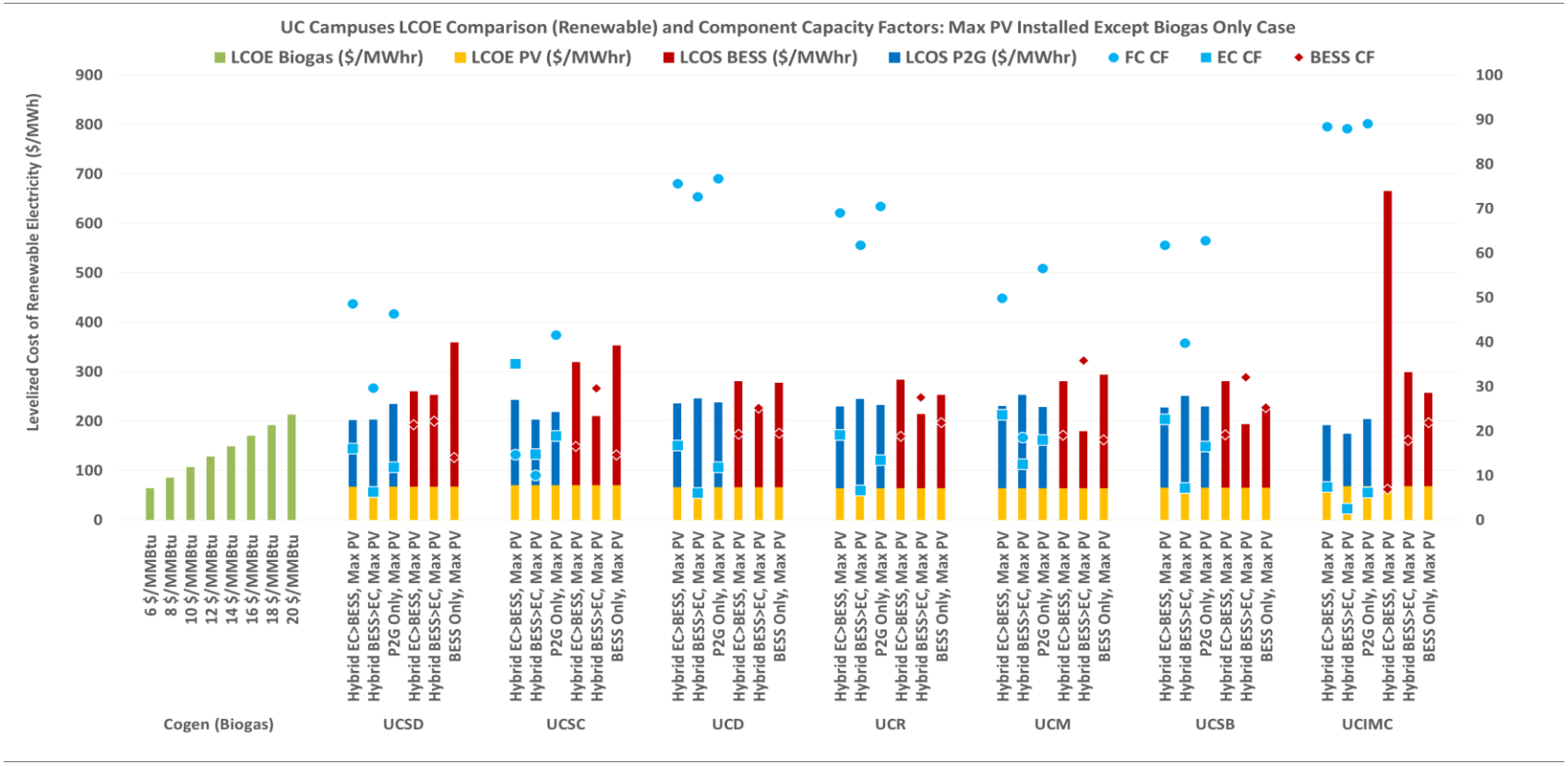

Figure 14 – Comparing the LCOE of biogas in gas turbines versus solar complemented by storage. The yellow column represents the cost from the solar portion and often time does not require storage. The pathway for both P2G and BESS pathways are presented separately for the same hybrid control scenario. Sensitivity to P2G storage component cost is presented in a) as 8 $/kWh b) as 4 $/kWh and c) as 0.8 $/kWh.

Figure 15 is essentially the average cost of renewable electricity for each campus and scenario. The fraction of electricity produced from renewable biogas and injected hydrogen in the cogeneration plant is deemed renewable alongside any PV used directly, and PV sent to the BESS and electrolyzer that meets load later. The results vary quite significantly but some similar trends exist across the board. The first seven campuses are campuses with natural gas powered cogeneration plants and the latter five do not. For this set of figures, the biogas fuel cost is assumed to be 8 $/MMBtu. The first column for each campus is if no additional PV panels were installed and serves as the upper bound for off-campus resources needed and the remaining columns represent the different storage strategies (if applicable) when the maximum amount of PV previously identified in Section 4.2 is deployed.

UCI, UCB, and UCDMC, the high P2G potential campuses, all see higher LCOE because the additional PV installations are not necessary for meeting load. It is either used for producing hydrogen for other applications (e.g. transportation) or curtailed—either way it is not converted back to power and results in a low amount of renewable electricity meeting the electrical load. This is largely due to the cogeneration plants being unable to operate at level lower than the minimum operating load and the energy from storage would be insufficient if the cogeneration plant were completely shut down. UCLA and UCSF have major generation deficits, previously imported massive amounts of electricity, so any PV installed is able to be used directly. Direct PV is cheaper than electricity produced from biogas so the average LCOE is lower than the biogas implementation only case.

For the campuses without cogeneration plants, the base case is the current amount of PV deployed. The biogas only implementation case (for campuses with cogeneration plants) and current PV level case (for campuses without cogeneration plant) both achieve much lower RES%. These base cases require very minimal new investments and consequently look to be the cheaper option but they do not actualize the on-campus potential to achieve higher RES%. Off-campus resources have additional associated fees due to the nature of transmitting electricity. This cost is explored in Chapter 5.

Up to this point we have not discussed the average LCOE resulting from implementing energy storage. In general, the BESS only case seems to be the cheapest method. In almost all cases, any electricity generated from PV if stored can be used in the same day. This leaves only a few opportunities to shift energy to a future week. The P2G energy storage system is only able to achieve the current LCOE by sizing the fuel cell fairly small and operating it year round at a fairly steady level. Its ability to do this allows itto be utilized at times the BESS would be fully charged and not be able to accept additional electricity or emptied and unable to discharge any more. In both the P2G storage only cases and BESS only cases, the same amount of excess electricity is available, but the P2G only case is able to curtail slightly less. The BESS has higher roundtrip efficiency than the P2G storage system, but in many cases they achieve similar RES%. The reader is referred back to Figure 12 to note the RES% for the P2G only case is only higher than the BESS only case for UCM. Only for these two cases did we find that the P2G storage system's ability to seasonally shift results in more renewable electricity delivered outweighing the higher

roundtrip efficiency from the BESS only case. Each campus with storage can achieve below 15 cents per kWh, which is comparable to some retail electricity rates the campuses pay today. Figure 14 alone does not capture the value of approaching the 100% carbon neutral electricity goal and only serves to illustrate a comparison between theoretical approaches. In other words, though biogas may be cheaper for initial renewable energy supply gains—it is severely limited by the mixture of biogas in natural gas usages and does not achieve the higher RES% possible with more PV and energy storage.

a)

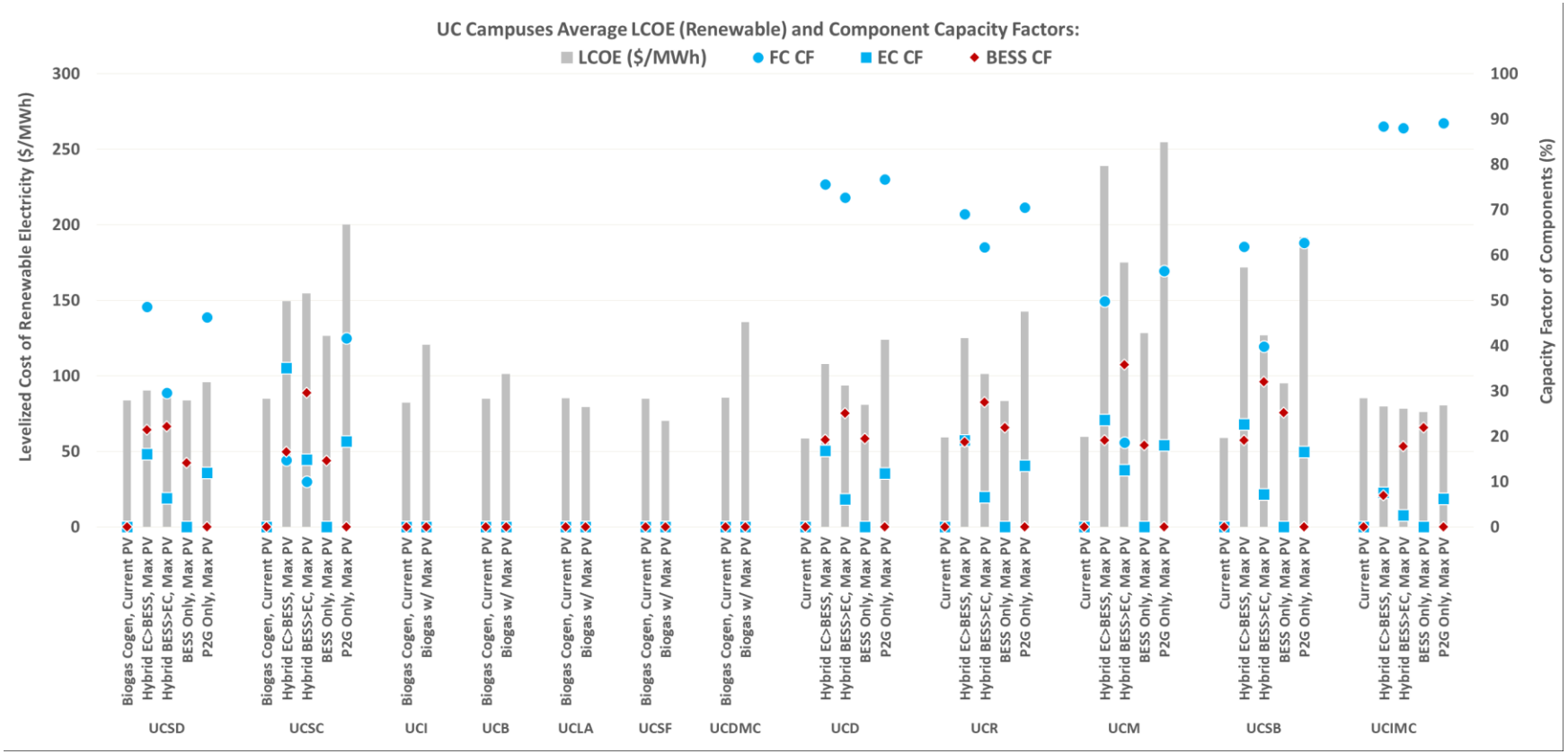
UC Campuses Average LCOE (Renewable) and Component Capacity Factors:
LCOE ($/MWh)
FC CF
EC CF
BESS CF
Levelized Cost of Renewable Electricity ($/MWh)
Capacity Factor of Components (%)
0
50
100
150
200
250
300
0
10
20
30
40
50
60
70
80
90
100
Biogas Cogen, Current PV
Hybrid EC>BESS, Max PV
Hybrid BESS>EC, Max PV
BESS Only, Max PV
P2G Only, Max PV
Biogas w/ Max PV
Current PV
UCSD
UCSC
UCI
UCB
UCLA
UCSF
UCDMC
UCD
UCR
UCM
UCSB
UCIMC

b)

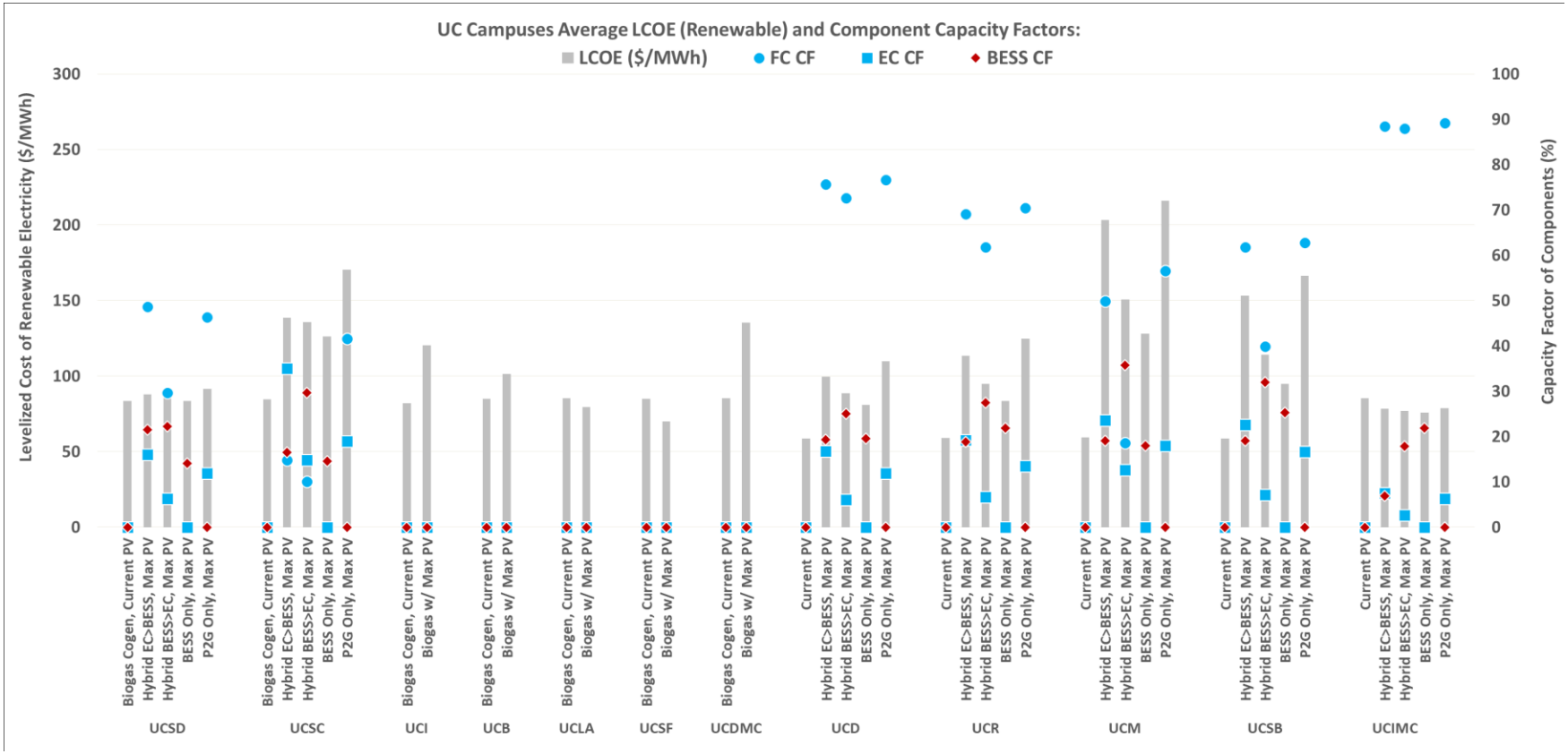
UC Campuses Average LCOE (Renewable) and Component Capacity Factors:
LCOE ($/MWh)
FC CF
EC CF
BESS CF
Levelized Cost of Renewable Electricity ($/MWh)
Capacity Factor of Components (%)
0
50
100
150
200
250
300
0
10
20
30
40
50
60
70
80
90
100
Biogas Cogen, Current PV
Hybrid EC>BESS, Max PV
Hybrid BESS>EC, Max PV
BESS Only, Max PV
P2G Only, Max PV
Biogas w/ Max PV
Current PV
UCSD
UCSC
UCI
UCB
UCLA
UCSF
UCDMC
UCD
UCR
UCM
UCSB
UCIMC

c)

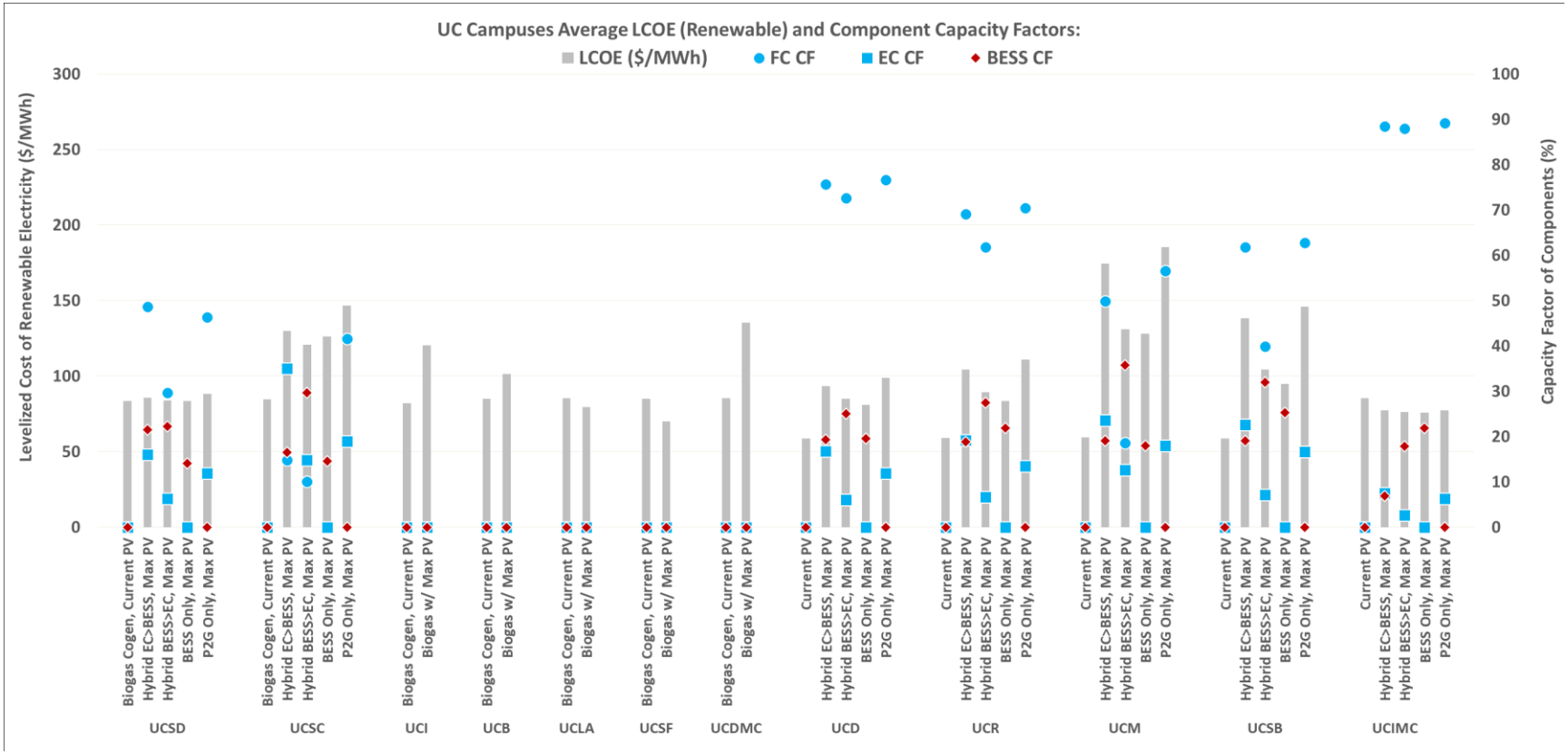

Figure 15 – Average cost of renewable in each scenario is presented. These graphs provide an average cost when considering the cost of directly used solar and costs when coming from storage. Capacity factor of major components are represented as points on the secondary axis. In general, higher capacity factors result in lower LCOS pathways and consequently lower average renewable LCOE cost. Sensitivity to P2G storage component cost is presented in a) as 8 $/kWh b) as 4 $/kWh and c) as 0.8 $/kWh.

Another idea to consider is that biogas prices moving into the future could be volatile with forecasted supply and demand. A Duke University study considers the supply and demand within the United States. Replacing 40% of the UC's natural gas consumption represents a significant portion of supply in California and the future year to year prices for biogas is not guaranteed. On the other hand, installed assets build equity, provide research opportunities, and hedge future costs. P2G components and battery costs will only decrease and poses to be an economic option moving forward. Below is the resulting graph if biogas costs were to double from 8 to 16 $/MMBtu whilst maintaining the higher storage cost of 8 $/kWh.

Figure 16 illustrates the change in levelized cost resulting from a high and low cost of storing hydrogen. For clarity's sake, the levelized cost of storage (LCOS) represents the cost associated with storing excess electricity and accounts for converting hydrogen back to electricity in the P2G case. Moving forward there is no established tariff for injecting hydrogen into the gas system and so a range of storage costs is considered for discussion sake. The higher cost of storage is modeled after the storage systems found in light duty fuel cell electric vehicles. The 8 $/kWh figure the ultimate DOE goal for light duty vehicle onboard hydrogen storage with 10 $/kWh being their 2020 goal. These onboard storage cylinders currently range from 5000 to 10000 pound per square inch (psi) so it is expected some cheaper storage system costs if stationary storage does not have the same high storage pressures due to a relaxed mobile constraint. The 4 $/kWh is based on a PG&E daily customer access charge in conjunction with an energy-basis transportation fee. The

0.80 $/kWh is derived from a negotiated firm storage service tariff on an energy basis assuming the cost from the inventory is equal to the injection and withdrawal rates. Both the 4 and 0.80 $/kWh were calculated by considering tariff rates and applying a factor of 30 to offset the lifespan assumption—converting a capital expenditure into an annual fee. The middle and lower hydrogen costs could potentially be representative of a fully integrated hydrogen renewable gas grid system. In other words, this is a considerable case in which a future tariff structure exists in which an entity can sell and redeem hydrogen or renewable gas credits. This is similar to direct access electricity in which the consumer pays a transportation fee for the usage of transmission infrastructure to a third party separate from the negotiated payment to the generator.

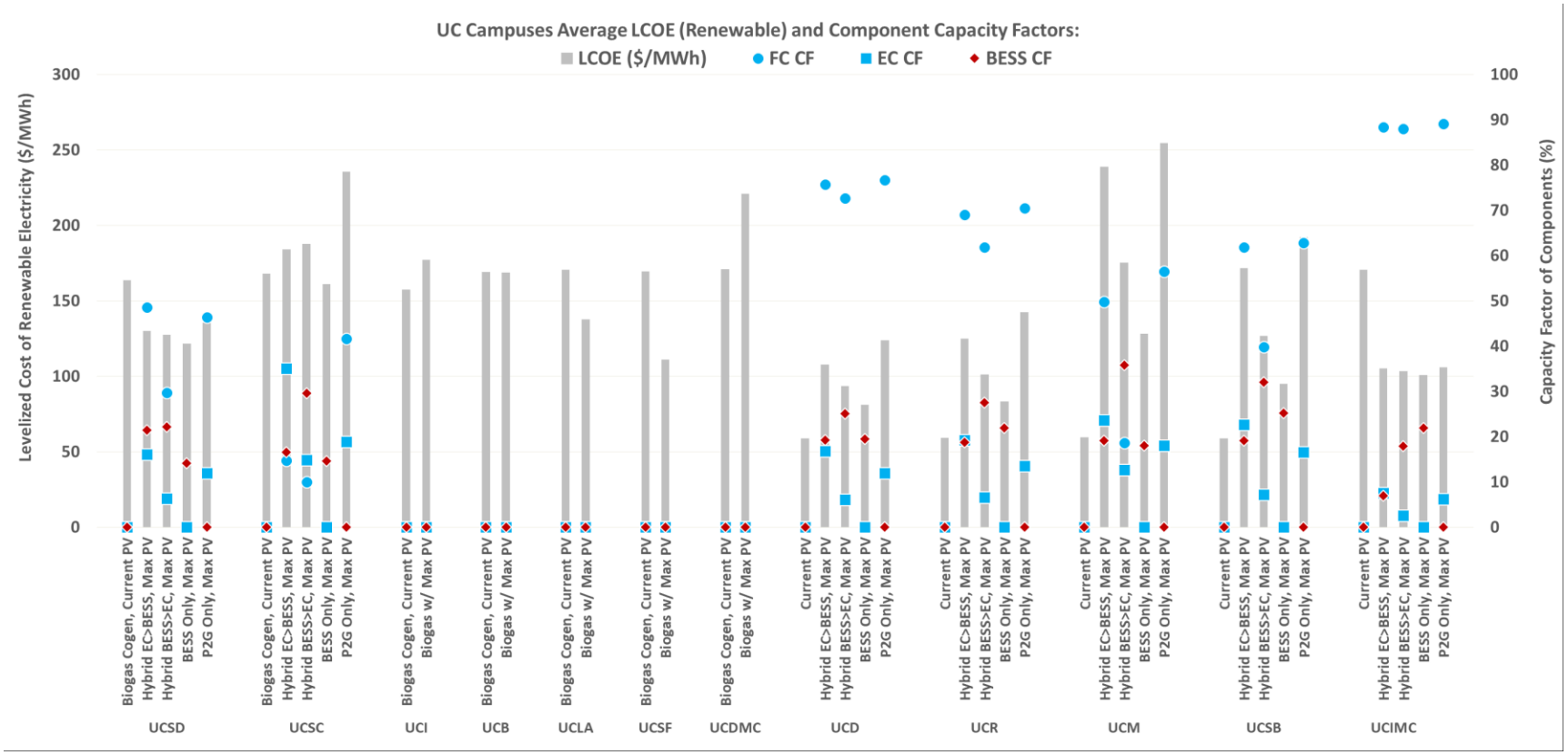

Figure 16 – Update graph of Figure 15a when changing biogas cost to 16 $/MMBtu from the base case of 8 $/MMBtu.

Note that the amount of hydrogen produced by the electrolyzer depends on the range of viable sizes as seen in Figure 13. This analysis has opted to select a value from the middle of the range. The lower capacity factor large component size results represent zero curtailment and consequently high levelized costs whilst the high capacity factor small component size end results in minimal, yet economical, installations resulting in minor impact to RES% with high levels of curtailment. The LCOS will be strongly dependent on how often the battery is utilized—this is true for the accommodating, high P2G, and the no-cogeneration campuses.

The BESS is nearly entirely dependent on the battery component whereas the spread from cost in the P2G pathway has some contribution from the electrolyzer, fuel cell, and the storage medium. LCOS versus the component capacity factors is plotted for all the campuses and control strategies. In Figure 17, each electrolyzer point has a corresponding fuel cell point in which they both have the same LCOS. If the P2G storage component cost is modeled at 2 $/kWh, the LCOS for each campus and control strategy falls into a band spanning 175 to 300 $/MWh comparable to the range that the BESS LCOS fits in. Figure 15c shows the storage component as 0.8 $/kWh which allows me to interpret the contribution to the levelized cost if one were to nearly eliminate the storage component.

Another issue to balance is the degradation mechanism of fuel cells, electrolyzers, and batteries. For batteries, their degradation is dependent upon calendar time, cycling, depth of discharge and temperature. The BESS system operates similarly in all of these considered scenarios, operating with a capacity factor of up to 35% in the BESS only

scenarios and as low as 15% in the hybrid cases. In all cases it operates fairly similarly—attempting to fully charge and discharge once a day and often does so due to the limitations of joint power and energy capacity. As such it is assumed the BESS has a lifespan of 10 years. On the other hand, the electrolyzer has a larger capacity factor range of 5% to 45% and operates more on some days than others. The fuel cell installations range from 10% to 90% capacity factor and have a much more diverse profile of operation. In addition to PEM technology operating at low temperatures, the lifespan is modeled based solely on operation hours rather than calendar time to reasonably consolidate the capital recovery cost from the range of capacity factors. A 10 years lifespan is assumed for the BESS system, 60 thousand operation hours for the fuel cell and electrolyzer, and 30 years for the hydrogen storage component.

Utilizing storage decreases the levelized cost of storing energy as the energy throughput to storage increases. Figure 17 plots the LCOS for both the BESS case along with three P2G cases, each with a different storage component cost. Though the fuel cell and electrolyzer sizes may vary, their capacity factors are averaged to simplify the number of points on the graph. The downward trend in LCOS is evident at higher capacity factors. Note that the storage assets could participate in additional revenue streams such as resource adequacy to increase capacity factor and internal rate of return, but this is left to future work. Figure 17 illustrates that at cheap enough hydrogen storage, the P2G storage pathway could achieve comparable if not lower costs for storing excess power.

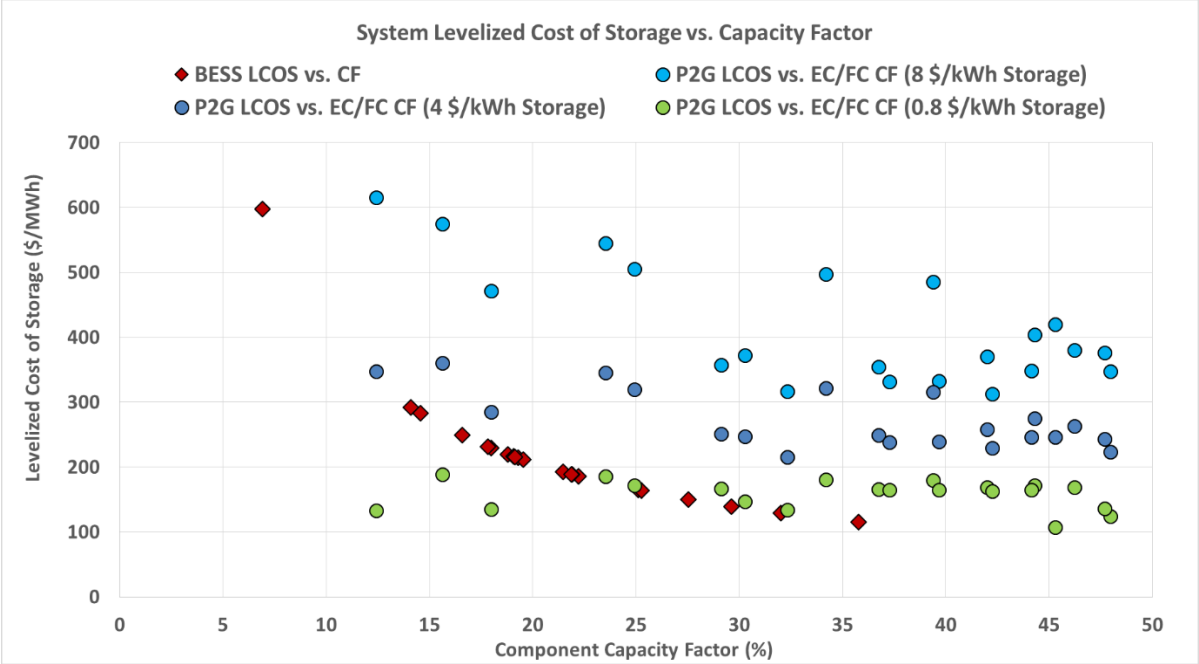

Figure 17 - Plot of levelized cost of storing excess electricity compared to the capacity factor of components. The P2G case is simplified by averaging the electrolyzer and fuel cell capacity factor. Sensitivity to changing cost of hydrogen storage component is presented as series in different colors.

4.3.3.1. Levelized Cost Sensitivity Analysis for System Reliability

The hybrid scenario is better than each technology type alone only for UCM. This is because UCM is the only campus with enough excess PV electricity to fulfill daily shifting needs and still have enough for longer term energy shifting. Every other campus only has enough excess PV for daily shifting. Given the higher roundtrip efficiency, the BESS pathway contributes the most to a higher RES% via daily energy shifting. This analysis does not consider the other possible advantages and value propositions the fuel cell, electrolyzer, and batteries may fulfill. For example, if fuel cells were already implemented on campuses as a backup generator, the levelized cost to implement only the electrolyzer and storage could very well be on parity with the BESS scenario. In addition, we have largely

discounted the heat loads that each campus has. High-temperature fuel cells pose a major value proposition in being able to meet heating loads via cogeneration. These other considerations could very well close the already small LCOE gap seen in Figure 15b and Figure 15c. This work only considers BESS and P2G technologies for energy storage complementing distributed PV.

For example, there may come a time when campuses are required to have sufficient storage on campus and the grid electricity is at a high level of renewable penetration. If many other consumers in the state depend on utility scale renewables, the aggregate of distributed storage resources may be necessary to alleviate transmission and utility scale storage assets. California has already faced similar troubles in 2019 with PG&E shutting off power to over a hundred thousand customers for safety reasons [104]. A 7-day timeframe with very low solar production is selected and suggests that imports may not be available due to an emergency shutdown. We consider a sensitivity analysis that requires that the campus must have sufficient electricity generation resources or energy from storage to meet the electrical load in this timeframe. Figure 18 illustrates the remaining load that must be met by energy storage. Note that this is after any existing natural gas powered generators and available PV is dispatched. For the one day reliability case we arbitrarily take the first day of the week and the two week reliability case is a repetition of the one week profile. UCI, UCB, and UCDMC are able to completely meet load without any additional energy storage and would appear on Figure 18 as a line at zero residual load. It is assumed sufficient fuel cells already exist as backup generators for the

campuses, so there is no additional cost incurred from fuel cells. Additionally, in the BESS case, the corresponding power rating resulting from the necessary energy storage capacity is sufficient for peak residual loads in the considered time period.

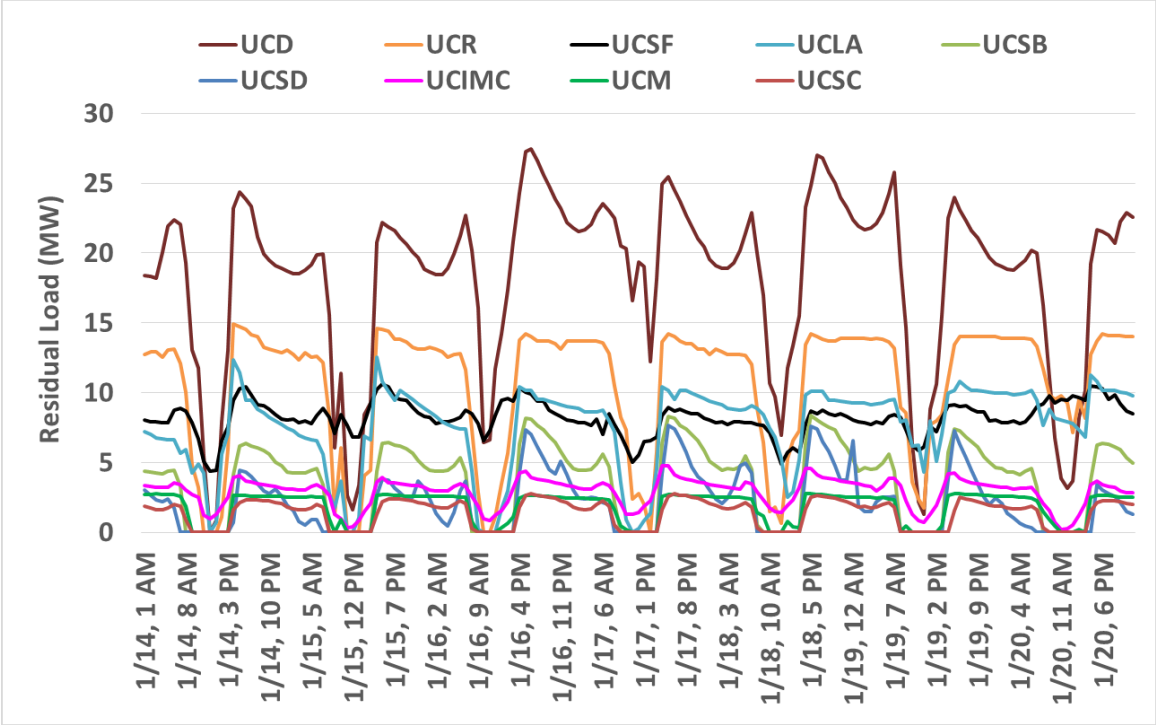

Figure 18 – Identified residual load during a week of low solar production across the campuses. Residual load already accounts for existing generation resources and it is suggested the remaining load must be met by additional on-campus energy storage.

We have already considered a fairly ideal case in assuming that both BESS and P2G energy storage systems are notified enough time in advance to store enough energy in anticipation of low renewable production. If forecast for low production is not perfect, it would be necessary for campuses to maintain this magnitude of energy stored throughout the year at least throughout the winter season. Note that the penalty of self-discharge for a lithium-ion based energy storage system is not captured here. If the need for this amount

of energy reserve must be maintained year-round, more energy would need to be sent to offset the self-discharge in the BESS.

This reliability constraint effectively adds the amount of energy storage capacity necessary on each campus. Consequently, much of the otherwise curtailed energy in the base cases would most likely be able to be captured, but this does not significantly alter the throughput. Figure 19 illustrates the additional amount of electricity that must be sent to storage to satisfy the reliability constraint compared to without.

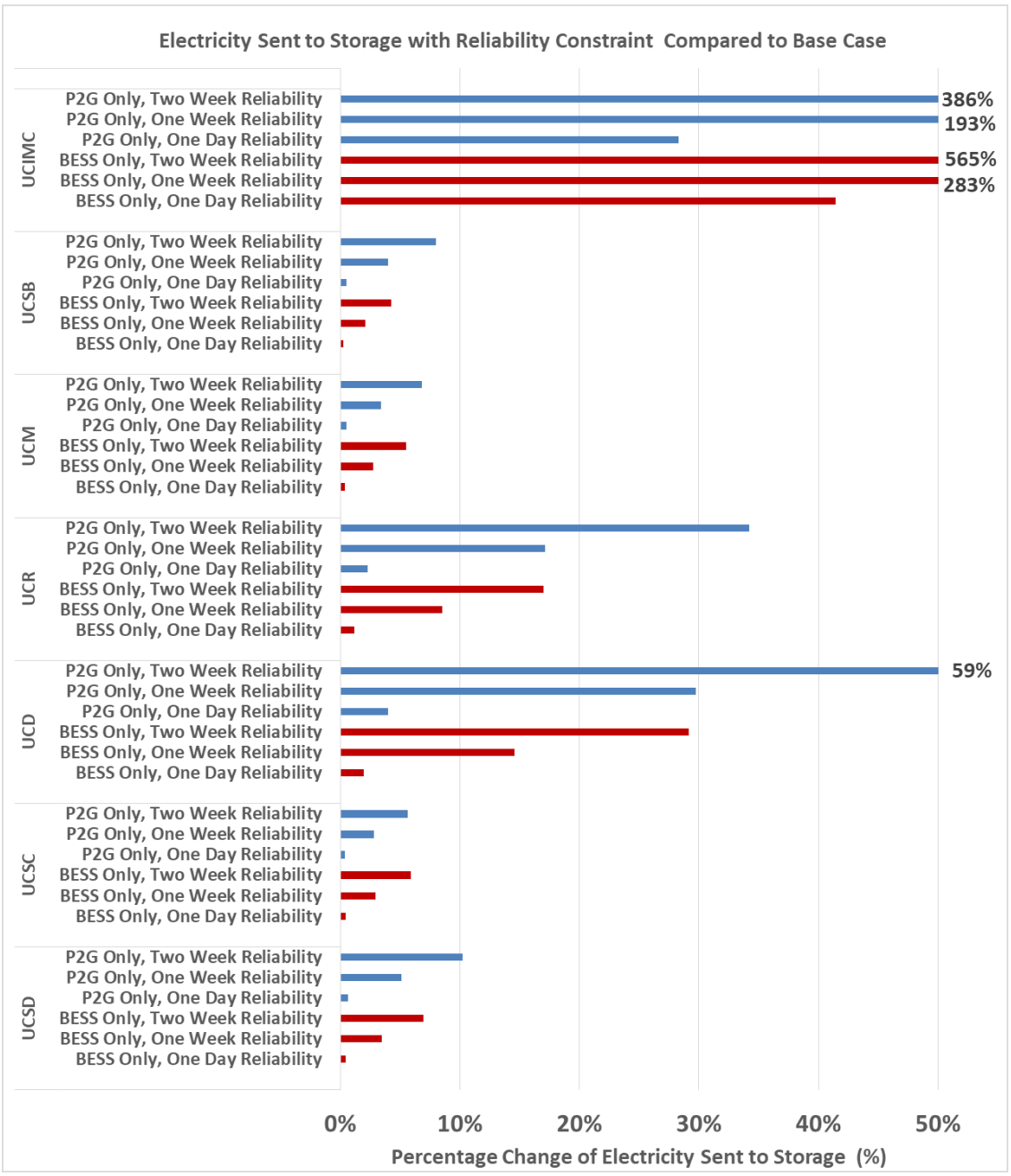

Figure 19 – Additional electricity sent to storage from reliability constraints as a percentage of original amount.

In all cases more energy must be sent to the P2G storage system than BESS due to lower roundtrip efficiency. We see a lesser percentage in the UCSC and UCIMC case because there is significant amount of electricity sent to the electrolyzers to produce

enough hydrogen to inject in their existing natural gas powered generators in the base cases. Figure 20 and Figure 21 are similar graphs to Figure 14 and Figure 15, respectively. Note the addition of energy storage capacity in the P2G case is quite cheap. Increasing the electrolyzer sizes are not necessary as they are able to produce additional hydrogen with imported electricity outside of peak solar times if given enough time prior to the reliability period. The increase in BESS sizes is inevitable in order to satisfy the reliability constraint. This results in a larger battery than what would have resulted in the lowest CF in the base cases. As such, the high capital cost outpaces the amount of throughput the energy storage system serves. UCIMC, which already had comparable P2G only and BESS only average LCOE, sees P2G only case achieve lower LCOE when only a single day of reliability is needed. In some cases the P2G only system achieves lower costs than the BESS only system when one week of reliability is needed. In all cases P2G only sees lower LCOE when two weeks of reliability are needed.

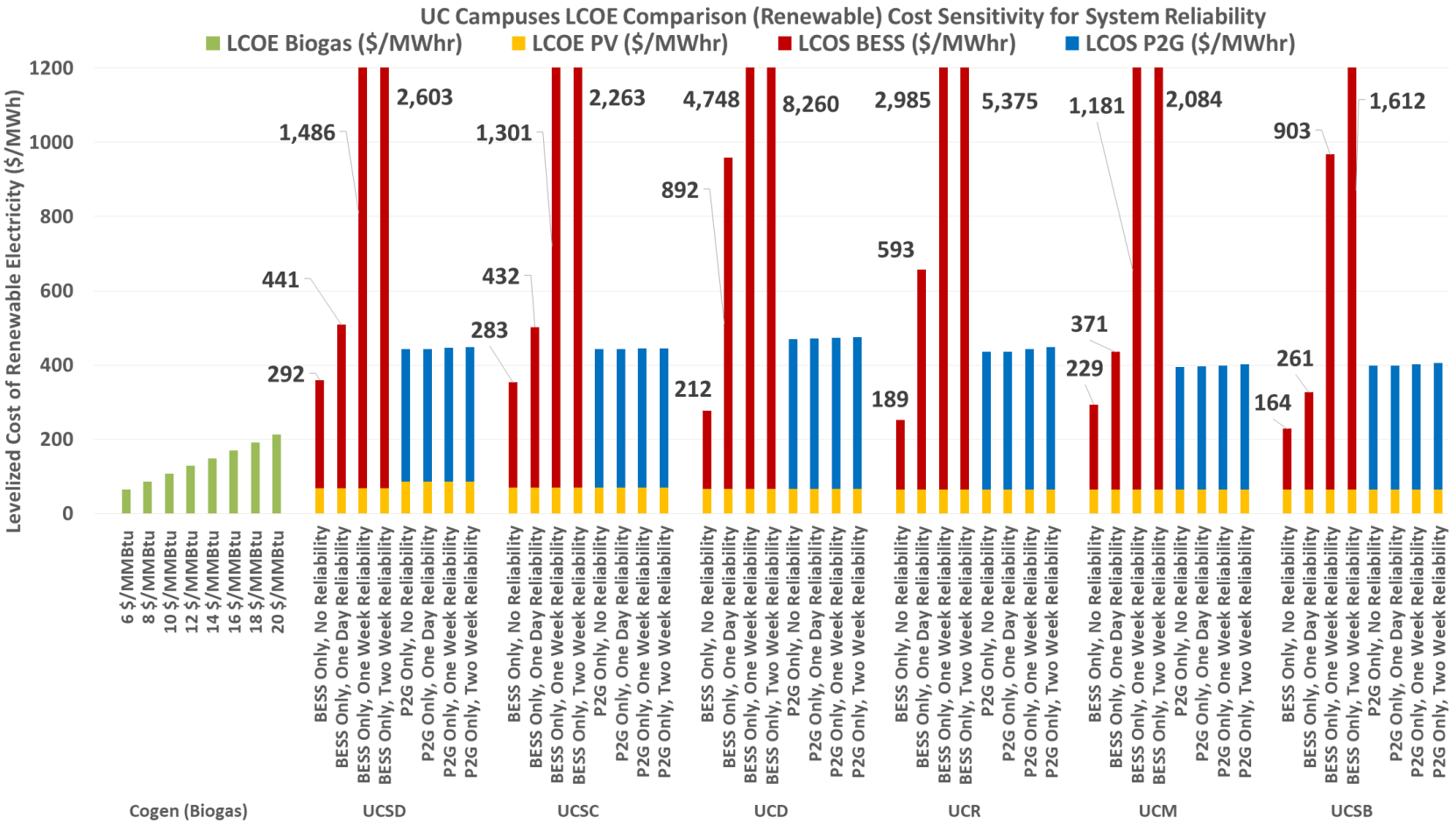

Figure 20 – Levelized cost of storing electricity. This assumes that the storage systems are able to sufficiently charge prior to the reliability period and that the imported electricity has 100% renewable attributes.

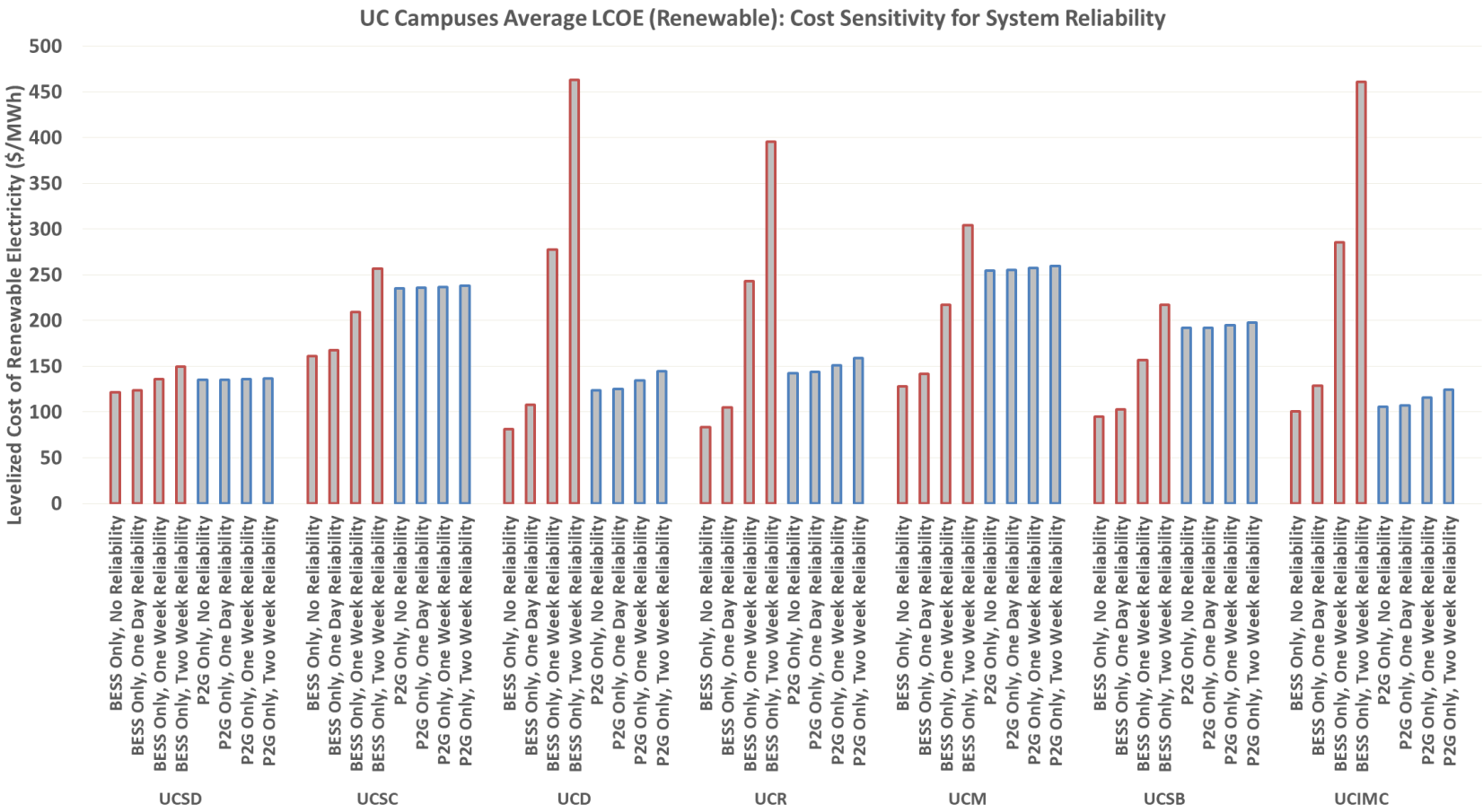

Figure 21 –An update on Figure 15 when implementing the reliability constraint. BESS only cases are outlined in red and P2G only cases are outlined in blue. The increase in LCOE occurs from the need to install greater energy storage capacity with out proportionally increasing throughput.

4.3.4. Energy Storage Capacity and Dynamics

From this point on, we refer back to the base cases analysis which excludes the reliability constraint. The amount of electricity sent to storage throughout the year and the rate at which it is consumed plays a major role in the sizing storage components—battery in the electric case and the hydrogen storage (whether it be cylinders or the capacity allotted from the gas grid). Figure 22 illustrates the capacity of energy storage needed for the two technologies across the considered scenarios. In addition, the difference in average renewable LCOE (the metric shown in Figure 15) is also displayed on the secondary axis. There are two major points that should be discussed from this: the amount of storage capacity for hydrogen is orders of magnitude higher than battery and the reduction in LCOE is not the same across the if the cost of the storage component of hydrogen decreases.

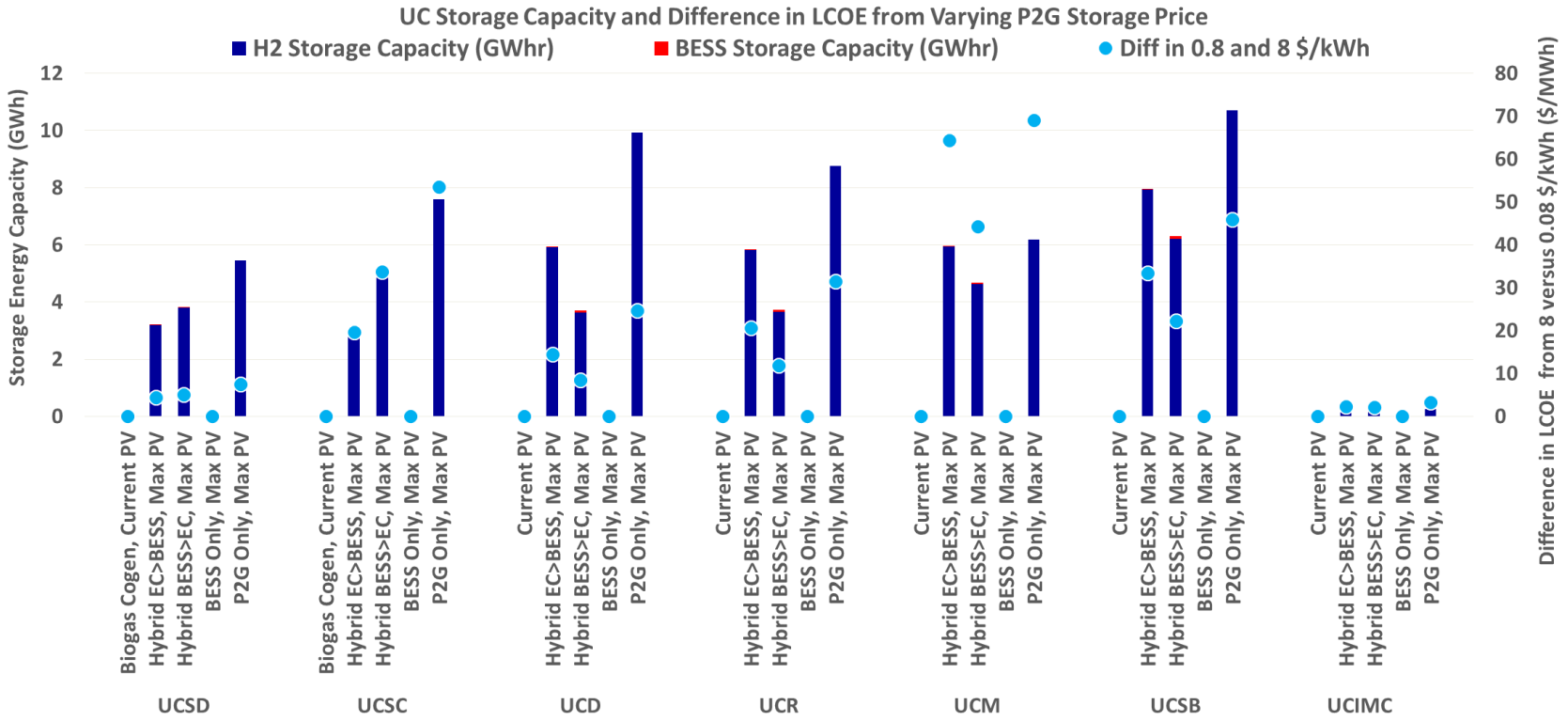

Figure 22 - Summary of storage capacity simulated. Large hydrogen storage capacity is necessary for seasonal shifting despite having daily cycling from cogeneration (where applicable) and fuel cell usage. BESS capacity is orders of magnitude lower due to the daily shifting characteristics allowing reasonable capacity factors at relatively lower storage capacities. Difference between low and high cost of hydrogen storage component on LCOE is presented on the secondary axis to illustrate larger storage capacity does not inherently imply higher levelized costs. Storage scenarios that have more cycling are more resilient to higher storage component capital costs.

The explanations for both points fundamentally stem from the concept of daily energy shifting versus seasonal. Because hydrogen does not suffer from self-discharge that the BESS, it can handle seasonal shifting and achieves a lower LCOE by having larger storage capacity and a small fuel cell rather than small storage capacity with a large fuel cell. Though the two pathways might have similar throughput in the hybrid cases, the levelized costs can be comparable because the cost of storage capacity in the hydrogen pathway is two orders of magnitude lower than in the electric case. Much of the LCOS from the P2G pathways can still be associated to the fuel cell and electrolyzer costs and seen on the secondary axis of Figure 22. We established the hybrid scenarios with the attempt to illustrate the resulting cost differences when attempting to balance the perks of the higher roundtrip efficiency from battery storage systems and the lower cost of energy capacity from hydrogen storage systems. The higher roundtrip efficiency suggests prioritizing charging and discharging the battery system first, effectively moving PV generated electricity efficiently from say noon to the evening. Additional power sent to generate hydrogen can be used (in gas turbines or fuel cells) at times even after the battery has been completely depleted at a lower efficiency but also lower cost, especially considering the seasonal aspect. As a result, the BESS cycles daily— fully charging and discharging each day whereas the hydrogen storage is charging every day, more on average during spring and summer, and discharging every night, more on average during winter and fall.

Figure 23 shows the annual state of charge for both technologies. Note that UCSD has a cogeneration plant that utilizes hydrogen injection and sees much more daily

fluctuations in hydrogen storage. As such, there is more hydrogen throughput per unit of storage capacity compared to UCSB and UCSC. Though UCSC also has a natural gas cogeneration plant, it does not provide as significant a fraction of power as that of UCSD. UCSB, which has no cogeneration plant, experiences fluctuating results from uses of the fuel cell when solar does not completely satisfy the load. These hydrogen storage levels are also supported in the trend of battery storage levels. In the middle of the year UCSC and UCSD have higher frequencies of higher state of charge—suggesting an abundance of energy to be sent to storage whereas the start and end of the year suggest the inverse. Different campuses have slightly different characteristics due to electricity demands and generation resources, but the seasonal trend exists across the board.

a)

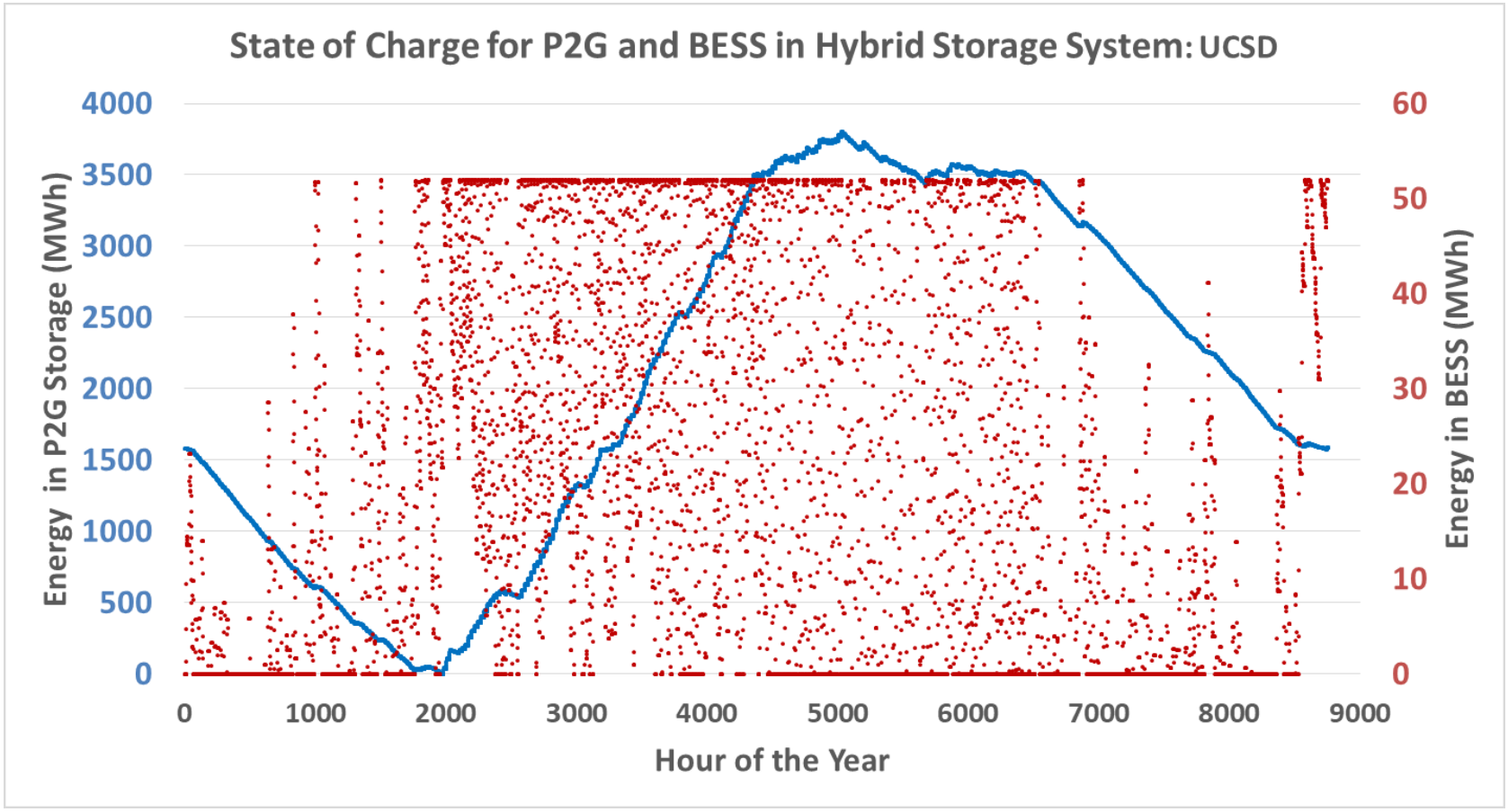
State of Charge for P2G and BESS in Hybrid Storage System: UCSD
Energy in P2G Storage (MWh)
Energy in BESS (MWh)
Hour of the Year
4000
3500
3000
2500
2000
1500
1000
500
0
60
50
40
30
20
10
0
0
1000
2000
3000
4000
5000
6000
7000
8000
9000

b)

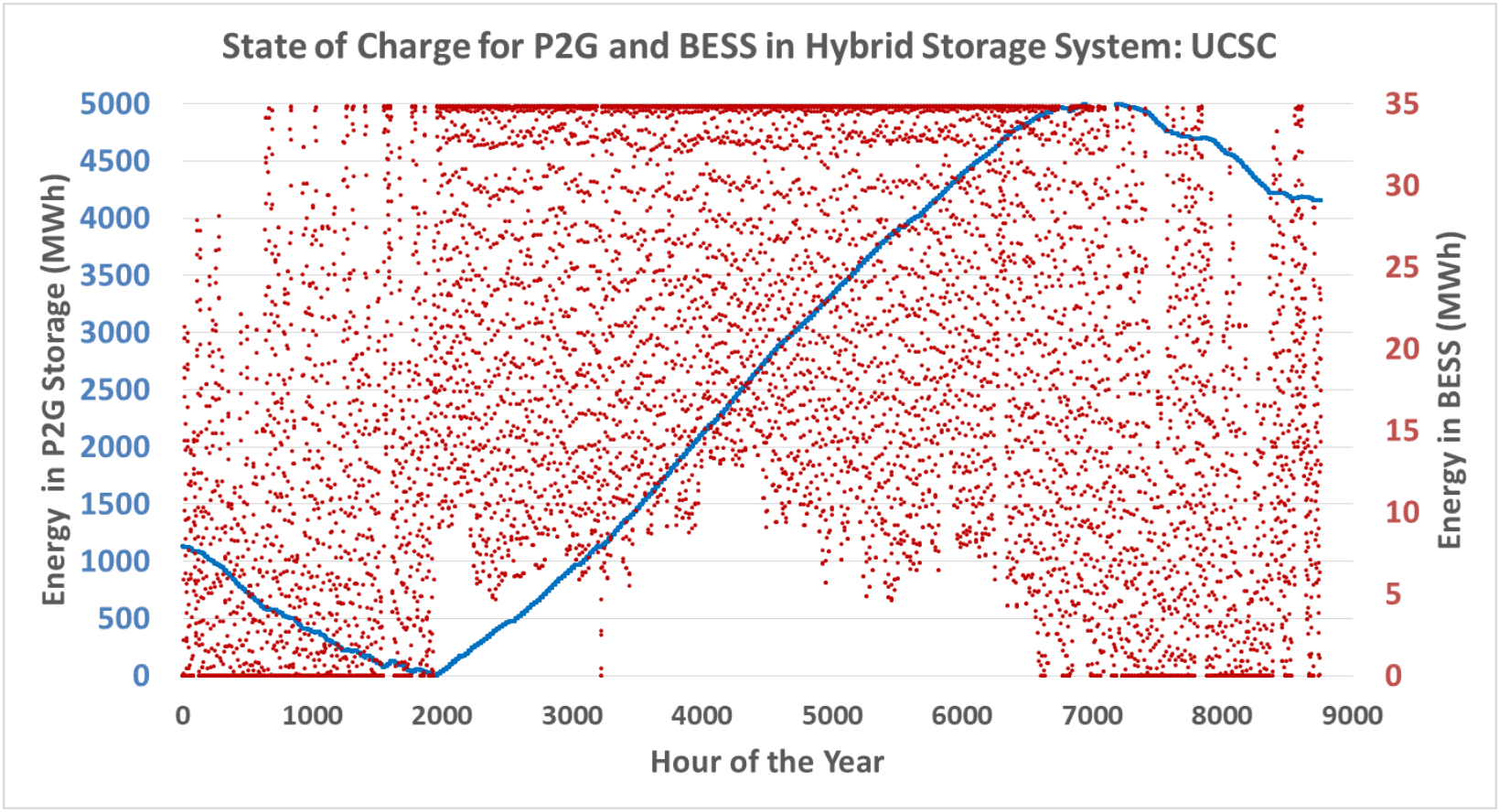
State of Charge for P2G and BESS in Hybrid Storage System: UCSC
Energy in P2G Storage (MWh)
5000
4500
4000
3500
3000
2500
2000
1500
1000
500
0
Energy in BESS (MWh)
35
30
25
20
15
10
5
0
0
1000
2000
3000
4000
5000
6000
7000
8000
9000
Hour of the Year

c)

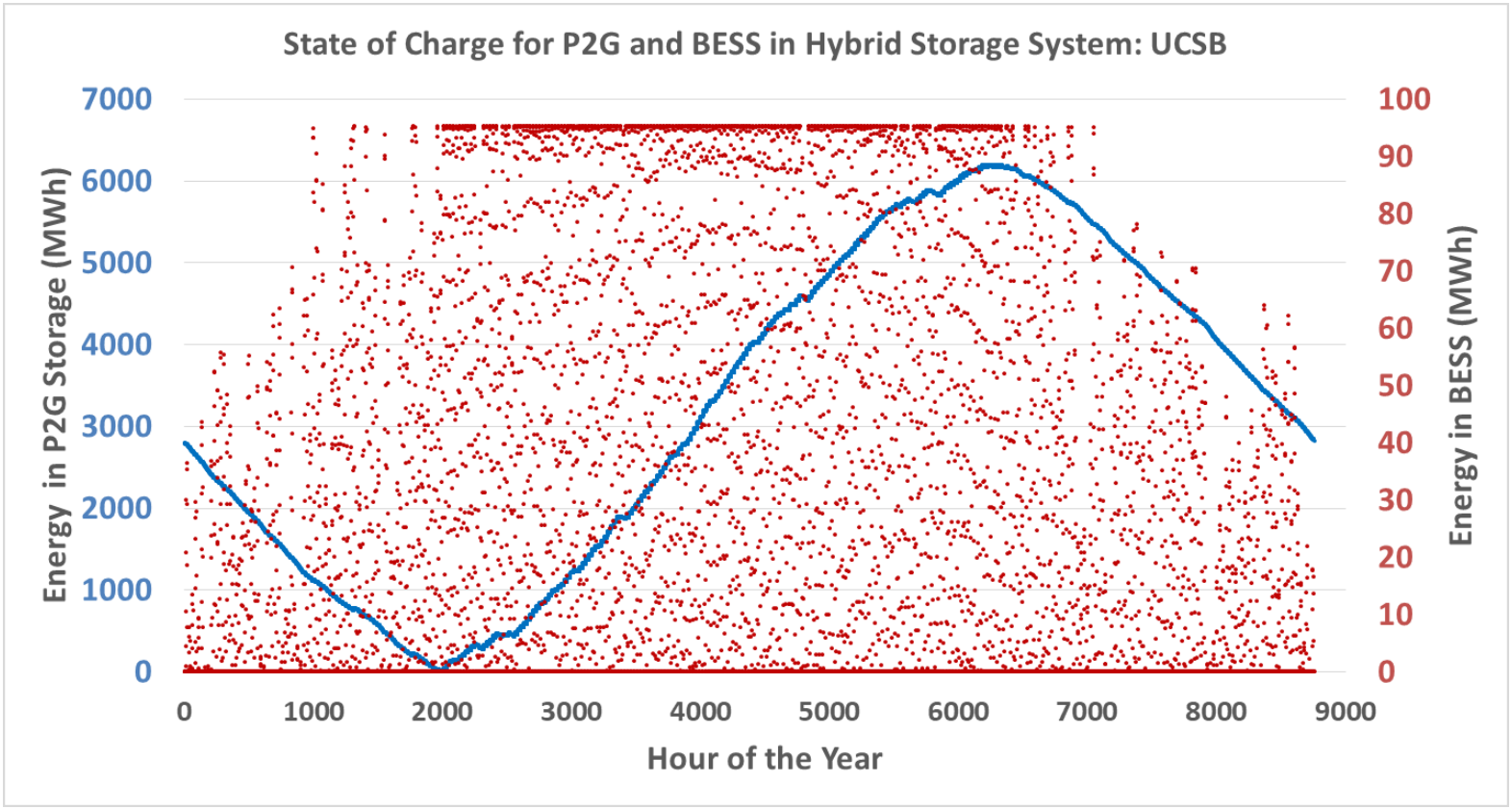

Figure 23 – Storage levels throughout a simulated year for a) UCSD b) UCSC and c) UCSB. Primary axis corresponding with the blue line represents the hydrogen storage levels. The secondary axis corresponding with red points represent battery storage levels. Note hydrogen is often discharged daily as well as seasonal whereas the battery system is cycled daily due to the prioritized charge and discharge control strategy.

Campuses with cogeneration plants require far less energy storage due to most of the campus electrical loads being met by on-site generation. However, this is a trade-off because these cogeneration plants are fueled by natural gas and have on-site emissions from combustion despite the origins of a renewable fraction of the fuel mixture. There is some debate regarding whether combustion from renewable biogas should be considered renewable electricity. In this analysis, it is deemed to be renewable electricity, but the emissions are not discounted. Carbon offsets are necessary to achieve the UCOP's carbon neutrality goal for scope 1 and scope 2 emissions. The opposite trend is seen in campuses without cogeneration plants— high amounts of RECs and zero for carbon offsets. If one were to consider the emissions from natural gas usage solely for heat demand, some carbon offsets would also arise.

In this section all campuses are normalized by their annual electric load to aid in visualizing the differences between the high and low cases. In these graphs, the differences between the high and low case RECs represent the contribution between current PV installations and the high potential case identified. More PV installations on-site displaces imports for campuses without cogeneration plants. The differences between the high and low-case carbon offsets show the impact on cogeneration production reducing as a result of installing the high PV case handling electric loads. Accommodating campuses, such as UCSD, see the largest difference in carbon offsets due to the amount of time that the cogeneration plant must be operated at minimum load to avoid over-generation. These results are illustrated in Figure 24.

a)

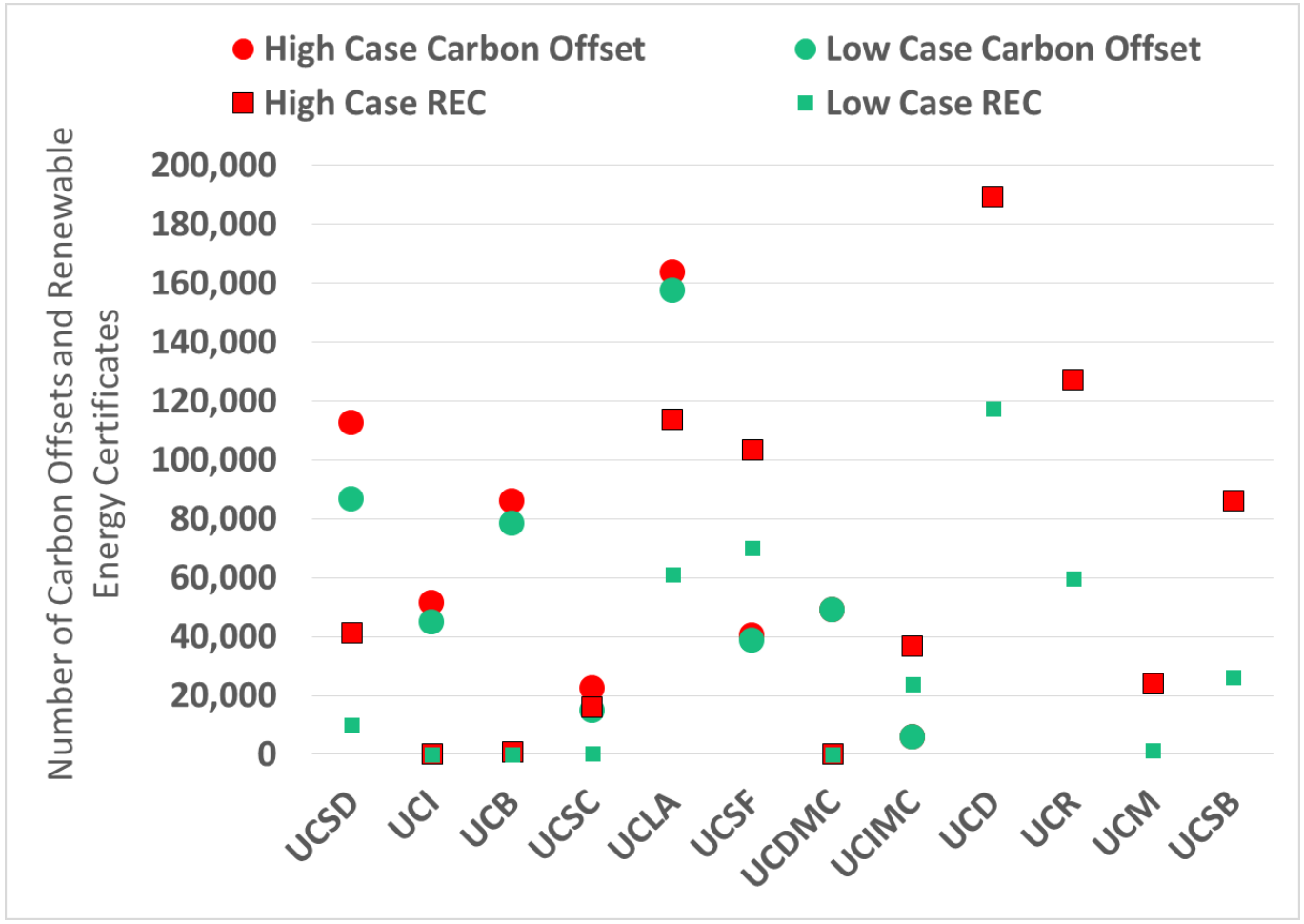
High Case Carbon Offset
Low Case Carbon Offset
High Case REC
Low Case REC
Number of Carbon Offsets and Renewable Energy Certificates
200,000
180,000
160,000
140,000
120,000
100,000
80,000
60,000
40,000
20,000
0
UCSD
UCI
UCB
UCSC
UCLA
UCSF
UCDMC
UCIMC
UCD
UCR
UCM
UCSB

b)

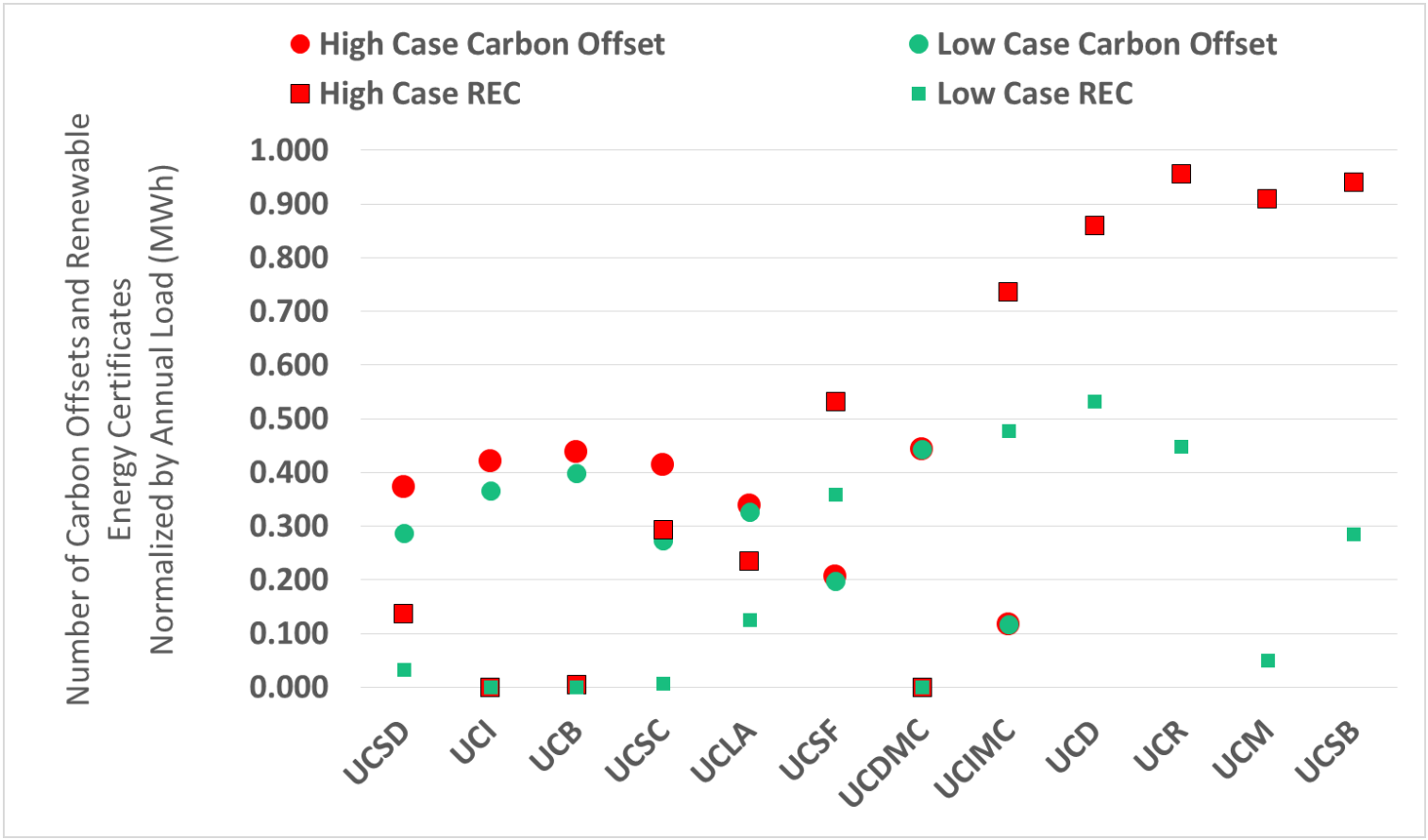

Figure 24 – Summary of a) renewable energy certificates needed to ensure 100% renewable imported electricity and carbon offsets to negate any on-site emissions from power production as well as b) normalized by load to visualize relativity. Red points represent lower on-campus installations resulting in higher off-campus resources and green points the inverse.

Because carbon offsets can be generated in several ways and new pathways can be developed, central level PV to produce electrolytic hydrogen is considered to displace natural gas and generate offsets. It is assumed hydrogen will be used in fuel cells so that the carbon intensity of producing and consuming hydrogen is zero, or a reduction of 0.0827 MTCOe/MMBtu. By doing this the amount of off-site PV for generating offsets and RECs is consolidated to gain some insight of the magnitude of off-campus resources.This figure is calculated assuming these central PV plants would be solely dedicated to generating these commodities regardless of market dynamics that would be accounted for in optimal operation (i.e., only using peak PV generation to produce electrolytic hydrogen instead of all generation). Using the statewide 2018 generation profile from CAISO, about 27.8 terawatt-hours (TWh) are produced from 11.8 GW of nameplate solar. If this profile is scaled down, 316 and 158 MW of utility-scale PV is needed to generate enough RECs for the high and low installation cases, respectively. Similarly, by assuming an 89% inverter efficiency and 74% electrolyzer efficiency, it is found that 1144 and 1024 MW of solar dedicated to producing enough hydrogen are required to generate offset credits. Implementing the biogas only policy would result in a total of 1459 MW of utility-scale PV whereas installing a high amount of distributed PV could bring this value down to 1182 MW. Though this analysis is done on an energy basis and only considers power generation, neither scenario can be recommended without considering the operation of energy storage at both the off-campus sites and on-campus sites. Both contexts have additional potential revenue streams and the higher energy production per nameplate will be better

at the central level at the cost of additional transmission and distribution system interactions. A higher detail campus case study is left to future work.

5. Off-campus Resources Transmission Scenario

This chapter serves to provide a comparison for transmission pathways with emphasis upon understanding the impact of implementing a storage & transmission system for renewable power delivery in two modes. The goal is to estimate the investment economics and efficiency when centralized and remote renewable power generation meets a realistic load, often times requiring storage and always requiring transmission. The equivalent annual cost (EAC) and levelized cost of electricity for each mode are calculated as comparative metrics. The effect of varying transmission lengths and generation capacities is analyzed to explore how the costs look to tackle the economic feasibility of a fully electrified renewable future. The impact on society is measurable by the magnitude of how end-use electricity costs could change in cases where energy storage appears increasingly necessary.

Fundamentally, transmission of electricity results in the potential losses due to the conducting wire heating up and some of the electricity is loss when converted to heat. This is a consequence of the second law of thermodynamics. When transmitting hydrogen, some additional power is needed to compress the gas and create a significant enough pressure differential to move gas downstream. The losses associated with transmission hydrogen are primarily leakage, similar to stationary energy storage. To consider the tradeoff between costs and these different efficiencies, we establish a scenario with representative component sizes and dynamics.

We consider a basic point to point model for transmission with storage. Traditional electric pathways paired with a Li-ion battery system are considered for an electric case and a comparable hydrogen pathway is presented with underground geological storage. Underground storage is modeled after depleted natural gas and oil fields and pipeline storage is not initially considered. This assumption acts is inconsequential to the hydrogen pathway analyses since the pipeline line pack is innate and saves the need from implementing some underground storage, simplifying the initial analysis then explored thereafter. Major contributors to energy losses and cost are considered and characterized by information found in literature and existing analysis tools. For context, the range of distances considered is illustrated in Figure 25.

Figure 25 - Geographical representation of transmission distance centered on Los Angeles, California.

We define the demand end as a sub-transmission station representing the city-gate of a large city or county and the generation point as a theoretical solar PV farm some distance away. If Los Angeles city is the delivery point, a 100-mile case is representative of PV site located in Riverside County, a high solar resource area, a 500-mile case would representative of transmitting energy from New Mexico state (also high-level solar resource) and a 900-mile case is the distance of electricity imports from the Pacific Northwest region as well as a little distance short of natural gas imported from the state East side of Texas. Modeling the longer distances reflects the possible consequences of interstate exchanges: western states sending excess solar to the east during peak generation and wind being sent from the east to the west as time passes during the day.

This becomes more likely as California and other states continues to construct new solar and wind farms to meet intrastate renewable generation goals [105]. For both electric and hydrogen pathways, a minimum of two substations are considered in the pathway: transmission and sub-transmission—one effectively at the start of the bulk transmission lines or pipeline and one at the other end. Transformers (XFMR) on each end are modeled. In the cases where the single-circuit transmission line's capacity is insufficient, as many needed in parallel is added each with its own corresponding power transformers. In the 500 kilovolt (kV) transmission case, two transformers at each substation are modeled since this voltage level transformation is typically done in two steps.

Because pipeline pressure drop is a function of length and throughput, one can install compressor stations in series to recover pipeline pressure or installing parallel pipelines to lower mass flow rate and consequently pressure drop in each line. A constraint is set to have additional compressor substations every 150 miles and additional pipelines are installed thereafter if necessary. For all cases considered, the most downstream substation to double as a storage facility. The electric case will utilize a group of battery energy storage systems whereas the hydrogen case utilizes underground geological storage.

We expect the amount of energy directly used to be dependent on the amount of renewable energy supply. In other words, if the aggregate of instantaneous solar generated electricity is less than the load, storage is not utilized. If the transmitted renewable energy is more than sufficient to meet the demand load, then the surplus will

be sent to storage. The amount of energy sent to storage is dictated by the demand and available energy after transmission.

We use CAISO's aggregated generation and demand data in Southern California, both available on an hourly resolution and scale the annual generation data to match the input generation capacity-- identifying the peak transmission loads, throughput, and ultimately component power ratings [90]. The annual demand profile [106] is scaled down so that the baseline case of 100-mile transmission only requires a single pipeline or single circuit power line resulting. The initial analysis is conducted with an annual peak load of 483 MW and the solar capacity is varied with storage to meet load. 24" and 36" pipeline diameters are considered for the hydrogen transmission and 230 and 500 kV high voltage alternating current (HVAC) for the electric pathway. Higher transmission levels (i.e., 765 kV HVAC and 42" pipelines) are not considered in this analysis due to the sparsity of projects in the region and lack of data, though they may be more appropriate for extreme transmission distances.

5.1. Transmission Endpoints

At the generation site, despite the inverter topology (i.e., central or string), the output voltage is typically for PV power plants is in the 6-36 kV range before being converted to higher voltages for transmission [107]. This is consistent with other literature: An existing PV farm in India uses a 380/33KV AC transformer and a proposed farm in Libya would utilize 400/11KV for this step [20,21]. If electricity is delivered locally, these voltage levels (11-33 kV) are sufficient, however, for long distance transmission electricity this

medium voltage level electricity is routed to a nearby transmission substation where it is converted to high voltage levels for long distance transmission. In California, 115 and 230 kV are the most common intrastate transmission levels and 500 kV is commonly used for interstate exchanges [110].

In the hydrogen case, a boost converter is necessary to convert panel output voltage to achieve maximum power feeding into the electrolyzer. The electrolyzer 435 pound per square inch absolute (psia) outlet pressure is analogous to the medium voltage levels preceding long distance transmission. For clarity sake, the transformer in the electric case is referred to as a generation transformer. In the electrical case, inverters and generation transformer losses are considered at the generation site and for the hydrogen case, the losses from the boost converter and electrolyzer are considered with the electrolyzer pressure outlet being sufficient enough to deliver the hydrogen gas to the transmission compressor station. Distances to transmission substations vary and are small relative to actual transmission distances so the electrolyzer outlet pressure and generation transformer voltage levels are assumed to be high enough to deliver the energy to the transmission station with insignificant cost and losses.

As the transmission lines approach consumers, voltage levels are typically converted back to medium voltage levels for sub-transmission at the city gate. Most transmission lines in Southern California outside of major cities are single-circuit 230 kV and upon entering the city, are converted to sub-transmission level of 66 kV [111]. Despite the frequency of single-circuit power lines, the double-circuit lines are selected as an

economical solution to the anticipated transmission capacity constraints. Double-circuit 500 kV case is considered as well and expected to be aptly representative for the longer transmission lengths. Based on existing substations, the sub-transmission substations will have 230/66 kV transformers [23,24]. An additional 500/230 kV transformer is considered in series for the 500 kV case. The electric energy storage system typically has its own power conditioning system and controller which are assumed to be lumped into the system cost efficiency. The parasitic losses are included in the roundtrip efficiency [113].

For the hydrogen case there is a 500 psia minimum for each intermediate transmission and the sub-transmission station. The lower heating value of hydrogen is used to quantify the amount of energy being delivered through each component in the pathway (i.e., component efficiencies) as we are considering electrical energy at the load. When considering energy at the load used for heating demands, a higher heating value would be more appropriate. Optimal sizing of additional pipelines requires needless complications for the analysis, so instead all parallel pipelines are considered to be the same size, resulting in a varying transmission utilization factor spanning 0 to 29 percent in the LCOE analysis. A separate case is analyzed where the transmission utilization factor is forced to be 18%. A secondary case is considered where this utilization factor is held constant and demand is varied instead. A slight discount is given for the generation site in the hydrogen case as the inverter can be omitted at the generation site and the buck converter cost is assumed to be similar to the generation transformer.

In 2017, Riverside County reportedly generated 3.5 TWh of electricity from a 1.4 GW capacity solar farm [114]. By dividing the annual energy generated by capacity approximately 2500 MWh per MW capacity is utilized to scale the annual electricity production for varying PV generation capacities. This is an optimistic value only possible in the best counties of California but also typical for importing from the desert or from states like Nevada and Arizona. NREL models the cost for PV generation systems and indicate the inverter for a 100 MW system accounts for 5.4% of the PV plant LCOE [20], a 5.4% discount is given for the PV cost in the hydrogen case. A summary of the major components and pathway is presented as a figure at the beginning of the next two sub-sections. Figure 26 presents the electric pathway leading Section 5.2 and Figure 28 presents the hydrogen pathway leading Section 5.3.

5.2. All Electric Pathway Assumptions

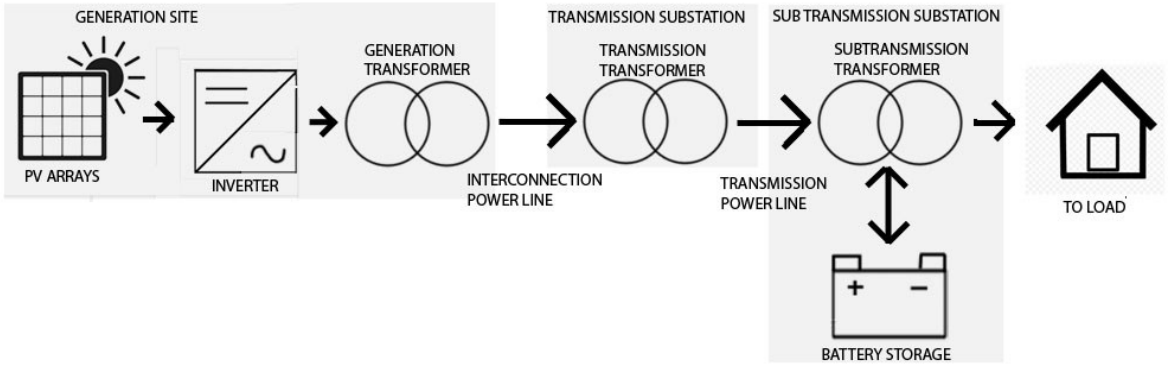

Figure 26 – Electric pathway considered. Battery energy storage is assumed to have the necessary power conditioning units. The battery system interconnection power line is assumed to have negligible costs and efficiency losses.

The CPUC has implemented Electric Rule 21 that requires IOUs to provide interconnection, operating, and metering cost estimates for typical generator facilities to

be connected to a transmission node. More recently, this rule has been extended to require a non-binding cost guide to provide further transparency for generators to make an interconnection [115]. The cost guide lists 230 and 500 kV as bulk transmission in the assumptions. The substation and transmission line costs are estimated according to Southern California Edison's (SCE) 2018 values [116]. The O&M costs for electrical lines is estimated by considering SCE's forecasted 2018 O&M costs for transmission lines and substations. Each of these costs are divided by their transmission circuit miles of respective power line or number of substations that SCE reports on their website [115], [117].

The SCE cost guide lists the total of new substation equipment with a breaker-and-a-half scheme and base site costs to be around 4.4 million for 66 kV and 115 kV stations. The cost increases significantly for a 230 kV substation. The breaker-and-a-half scheme allows two generation connections and two end-tie connections, but a backup transformer is not considered. Likewise, no backup transmission or storage compressors for the hydrogen case is assumed. Assumptions for the breaker configuration and operation buses are for typical stations recorded in the SCE cost guide [118].

One way the right-of-way (ROW) cost for transmission lines can be calculated by multiplying the typical ROW width by voltage class [119] by the Bureau of Land Management land rental rent/capital cost schedule [120]. This is difficult to pinpoint as the varying valued zones change and physically siting the transmission length is avoided. So, in addition to the yearly ROW rental cost being expected to be almost two orders of magnitude lower than the EAC from capital cost alone, it is reasonable to omit this

contribution for simplicity. This same reasoning stands for the pipeline case where exact geographical information is unavailable and for typical transmission pipeline sizes, the ROW typically makes up around 4 to 7% of the cost, or neglected altogether by repurposing or laying new lines in existing corridors or close to existing natural gas lines [121].

5.2.1. Power Lines

American Electric Power reports a 345 kV power line has a total energy loss of 4.2% (corona and resistive losses) over 100 miles at a throughput of 1000 MW [122]. The power losses over amount of power at the beginning of transmission be used to calculate the efficiency (η_{line}) of the transmission line seen by Equation 2. Power losses are dependent on the total current as well as the resistance of the wire calculated with the usage of Ohm's law listed as Equation 3 and Equation 4 below. The electrical resistance and ultimately power rating of the transmission line varies based on the size of the conductor. Many SCE 230 kV transmission upgrades [123] and new 230 kV power lines [124] use 1590 aluminum conductor steel-reinforced (ACSR) cables, which is one of largest in sizes listed in ACSR datasheets [125]. The total line resistance (R_{tot}) is calculated by the resistance per length (R_{1590}) of a certain conductor size—in this case 1590 ACSR which is assumed to have a constant resistance at 25 degrees Celsius corresponding to an electrical resistance of 0.0359 Ω/km.

$$\eta_{line} = 1 - \frac{P_{loss}}{P_{in}} \qquad Eq.(2)$$

$$P_{loss,i} = I^2 R_{tot} \qquad Eq.(3)$$

$$I = \frac{P_{in,i}}{V} \qquad Eq.(4)$$

$$R_{tot} = R_{1590} L \qquad Eq.(5)$$

The SCE cost guide lists a 1120 megavolt-ampere (MVA) as the highest rating for transformers, roughly the same value as when using Eq. 6 to calculate the power rating of 230 kV circuit using 1590 ACSR conductors. This is the assumed conductor size for all the transmission lines for this work. The throughput capacity of one of the three phases for transmission lines is calculated by the following equation which assumes a power factor (PF) of 0.85, the maximum ampacity (I_{max}) of 1590 American wire gauge ACSR is approximately 1354 Amperes, and the voltage (V) is the transmission voltage level. The maximum ampacity is typically only available for four hours due to the heating up of the conductor [124] but assuming it is not working at full capacity for extended periods of time and is sized to handle the annual peak. The power rating calculation is given by Equation 6 and the resulting capacities used for the considered electrical transmission wires are presented in Table 12.

$$P_{line,max} = \sqrt{3}\, cos(PF)\, I_{max} V \qquad Eq.(4)$$

The power capacity used for the considered electrical transmission wires are presented in Table 12.

Table 12 - Transmission line maximum power rating constraints used.

Transmission Line Actual Power Ratings (MW)	
230 kV single-circuit	1146
230 kV double-circuit	2292
500 kV single-circuit	2491
500 kV double-circuit	4983

The minimum necessary amount of power lines ($N_{powerline}$) is modeled in parallel to ensure there is sufficient transmission capacity, seen in Equation 9, and ensure the transmission voltage drop does not fall below the set minimum delivery voltage level of 66 kV, represented by Equation 8.

$$min\ N_{powerline} = f(V_{outlet}, P_{powerline,total}) \qquad Eq.(5)$$

$$s.t.\ V_{outlet} > V_{min} \qquad Eq.(6)$$

$$N_{powerline} = ROUNDUP\left(\frac{P_{elec,powerline}}{P_{line,max}}\right) \qquad Eq.(7)$$

Where the voltage drop can be calculated by Ohm's law given by:

$$V_{outlet} = V_{inlet} - \Delta V \qquad Eq.(8)$$

$$\Delta V = IR_{tot} \qquad Eq.(9)$$

Black & Veatch adapted transmission capital costs from the previous Western Renewable Energy Zones (WREZ) model to fit a recommendations report for WECC transmission expansion planning [119]. Here they establish a baseline transmission cost case that assumes ACSR conductor type, tubular structure type for 230 kV lines and lattice for the higher ones and a transmission length greater than 10 miles. From these baseline costs, transmission costs can be estimated with cost multipliers. Aluminum conductor steel supported (ACSS) wire type has a cost multiplier of 1.08 and high-temperature low-sag (HTLS) wire type has a cost multiplier of 3.60 for all voltage levels. 230 kV on a lattice structure's multiplier is 0.90 whereas 500 kV on lattice is 1. There is also a terrain multiplier with forested areas comprimising a multiplier of 3, but for simplicity sake a flat or farmland's multiplier of 1 is assumed. When assuming an HTLS conductor, the ending cost

is close to the SCE cost guide numbers. 5 million per mile versus SCE's 4.5 million for 230 kV and 11 million per mile versus SCE's 9.4 million.

5.2.2. Transformers

Industrial and Tertiary Product Testing and Application of Standards (INTAS) considers four types of losses in transformers: Load, no-load, auxiliary losses, and extra losses from harmonics and unbalance [126]. Transformer efficiency typically varies based upon whether the transformer is operating near its rated load. In cases where they operate near rated load higher efficiencies can be expected whereas at lower loads the efficiency drops. Accounting for transformer operational dynamics is avoided in this work due to the level of complexity that would be required to properly account for dynamic operation. For example, studies have been conducted that support that the losses from harmonics and unbalance could be significant. Sadati et al. [127] finds that due to harmonic loads, losses predicted by typical methods increase by 23 percent. A 2014 analysis regarding P2G complementing wind considers a minimum transformer efficiency of 80, maximum of 98, and base case of 95%. Balci et al. [128] design and analyze a medium frequency transformer with nanocrystalline core material, reporting an operational efficiency of 98%. Zini and Rosa [129] model and validate an Italian PV system and also use a 98% transformer average efficiency. Literature in general is only able to validate efficiencies for kVA-scale transformers, so not much can be confirmed about MVA-scale transformers via the literature. If serving PV loads, the transformer can be shut-off outside of the predictable generation times—reducing idle no-load losses, however one cannot be certain it will only serve PV sites upstream in which case the amount of time spent working at a near-rated

load efficiency is unknown. For these reasons it is assumed an average transformer efficiency. Similar to assumed efficiencies in literature, an average transformer efficiency of 97% is assumed.

Transformer costs are challenging to estimate as they can be specifically designed for certain applications and typically subject to a complex procurement process [130]. For example, Darras et al. [131] conduct a techno-economic analysis of PV and hydrogen systems, but assumptions for the transformer substation are obscure relative to the other components considered (i.e., fuel cell, inverter, electrolyzer, etc.). An older 1997 study by Dagle and Brown [132] find that transformer cost can be estimated as a function of size and higher-side voltage levels. In this study 230 kV transformers are modeled to be roughly \$6/kVA+\$550,000 and 500 kV transformers \$6/kVA+\$1,100,000 based on existing transformer datasets in the United States. Black & Veatch is an engineering firm that has evaluated capital costs for electricity transmission infrastructure for WECC [119]. In this report they find 115/230 kV transformers to be roughly \$7,250/MVA and \$11,400/MVA for 230/500 kV transformers. Another considered source is the SCE cost guide, as it is the most specifically tailored for the scenario. 280 MVA is the maximum size for a 230/66 kV transformer estimated at \$7.6 million [132]. This corresponds with roughly \$27/kVA. Similarly, a 500/230 kV transformer with 1120 MVA is estimated to be at \$28/kVA. It is reasonable to assume that 500 kV transmission levels is done in multiple steps from typical transformer ratings, so it may effectively double the transformer cost to represent two transformers in series and assume a \$55/kVA total transformer cost when the transmission

voltage level is 500 kV. These cost models are adjusted for inflation to 2017 USD and reported summarized in Figure 27. Ultimately, the average $/MVA of the three for a 230/500 kV is used and slightly more weight is given to the SCE estimate (1.5:1:1) due to geographical pertinence.

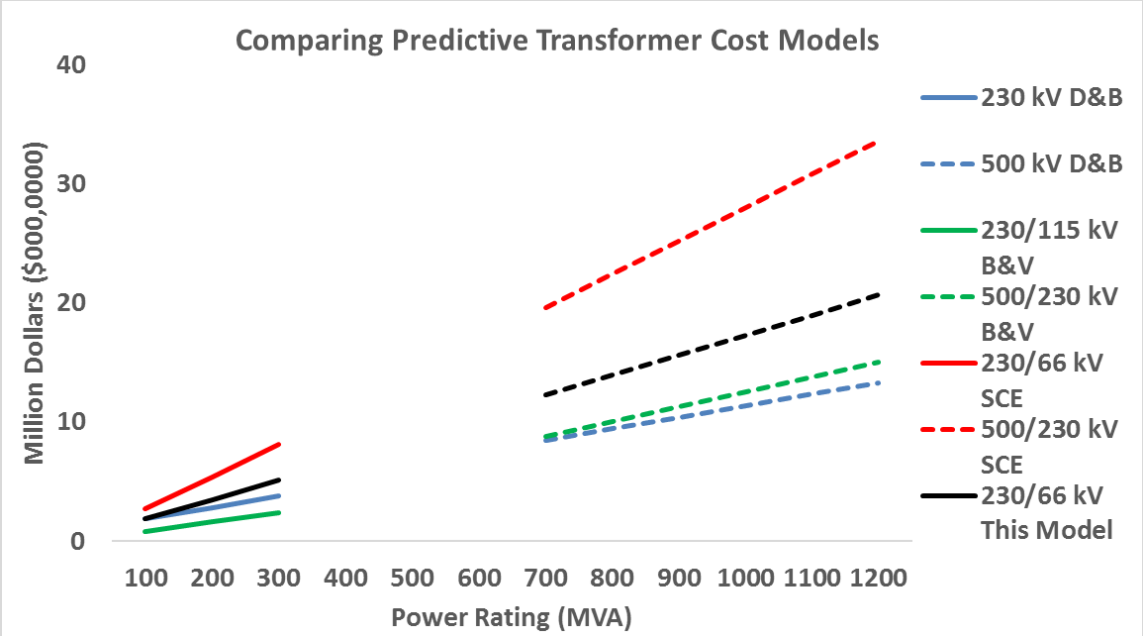

Figure 27 – Comparison of power transformer costs.

5.2.3. Battery

Lazard's levelized cost of storage provides valuable insights regarding the typical costs of different energy storage system types. A lithium ion battery system implemented to serve utility-scale solar has a price range of 265-295 $/kWh capital cost whereas when implemented in transmission and distribution 190-442 $/kWh. The price difference most likely occurs due to the higher cycling dynamics the battery must handle for ancillary services. A battery shifting solar without considering load results in mild ramping whereas a battery just upstream of the customer may deal with frequent fluctuations following

load, which may be another reason for the difference. In addition, a battery at a substation deferring transmission upgrades must be more reliable than at a generation node suggesting more maintenance to ensure reliability and maintain capacity. Model battery system costs are set to 350 $/kWh and the corresponding inverter costs are set to 80 $/kW [133]. Customer-Led Network Revolution implemented a 2,500 kVA 5,000 kWh Li-ion based energy storage system to support a primary transformer [113]. Its roundtrip efficiency of 69.0% when considering parasitic losses, which are primarily for HVAC for the space the battery system and inverter dwell is adopted. It is assumed the AC-DC power conditioning components are lumped into the modeled battery cost and efficiency. The operational voltage of the battery is proportional to the number of cells and consequently design capacity and rating. An additional transformer specifically designed to transform the sub-transmission voltage levels to the battery voltage and vice versa. It is assumed this transformer is rated like the BESS so that it may always work at near-rated load efficiency. An average efficiency of 99% for this transformer is used. Table 13 acts as a summary before moving on to the hydrogen pathway details.

Table 13 - Electric pathway major components summary

i	Component	η	Lifespan (years)	Component	Cost ($USD)
1	PV Panel	1	30	Fixed PV Generation Site w/ Inverter and Transformer ($/MW)	1,030,000 [20]
2	Inverter	0.95 [134]	30	230 kV Double Circuit Power Line ($/mi)	4,495,000 [118]
3	Generation Power Transformer	0.97 [117]- [121]	40	500 kV Double Circuit Power Line ($/mi)	9,382,000 [118]
4	Transmission Substation (w/ XFMR)	0.97 [117]- [121]	35	230 kV Substation Base Cost ($)	17,710,000 [118]
5	Transmission Power Line	Eq. 2	30	500 kV Substation Base Cost ($)	36,194,000 [118]
6	Sub-transmission Substation (w/ XFMR)	0.97 [117]- [121]	35	230/66 kV Power Transformer ($/MVA)	15,638 [118], [132], [135]
7	Lithium-Ion Energy Storage System	0.69 [113]	20	500/230 kV Power Transformer ($/MVA)	16,713 [118], [132], [135]
8				Li-Ion Energy Storage System ($/MWh)	350,000 [136]

5.3. Hydrogen Pathway Assumptions

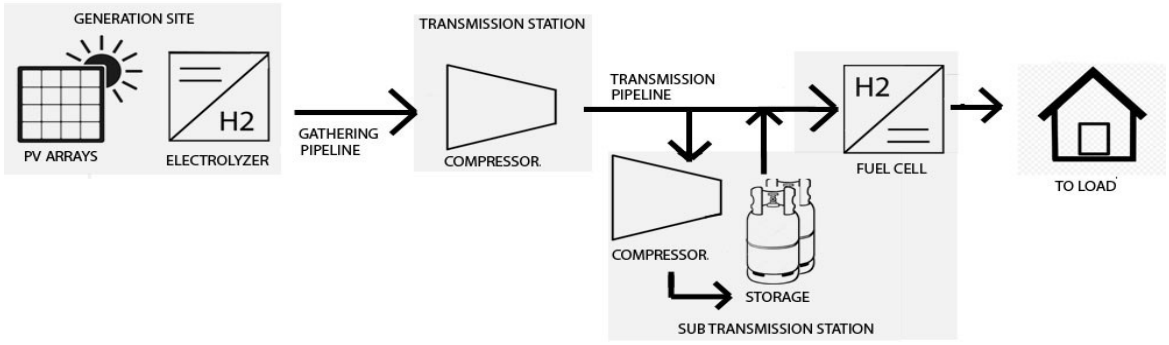

Figure 28 - Hydrogen pathway considered. Gathering pipeline is assumed to have negligible costs and efficiency losses.

We assume the hydrogen gas is produced at the PV site, delivered at the electrolyzer's outlet pressure (435 psia) to a transmission station where it is compressed to 1500 psia. It is assumed assume the pipeline between the PV plant and compressor

station is negligible relative to total pathway cost and efficiency (which is identical to the assumption regarding electrical equipment costs between the PV plant and the generation substation for the electrical case).

5.3.1. Transmission Pipeline

We assume that for each unit of hydrogen entering the pipeline, a unit can be withdrawn on the receiving end, making transport as instantaneous as electricity to meet loads. Compressor stations are set every 150 miles, so if the pressure drop is too great—an additional pipeline is added in parallel with its own compressor. A minimum of 500 psia is needed for each additional receiving transmission substation including the final sub-transmission substation. When an additional pipeline is necessary, the flow rate is split so that the capacity and utilization factor of each pipeline are equal. The same is done in the electric case.

We use the maximum pressure inlet (p_{inlet}) and minimum pressure outlet and other factors considered in the Darcy Weisbach equation to determine what some define as pipeline hydraulic capacity ($P_{d,max}$) [137]. Other relevant variables are pipeline length (L), pipeline diameter (D), hydrogen gas density (ρ), and peak gas velocity (v_{max}). The Colebrook-White correlation is used for determining the friction factor (f) used for determining pressure losses as follows.

$$P_{d,max} = p_{inlet} - \frac{fL}{2D}\rho {v_{max}}^2 \qquad Eq.(10)$$

$$v_{max} = \frac{4(\frac{\dot{m}_{max}}{3600})}{\pi D^2 N_{pipeline}} \qquad Eq.(11)$$

$$p_{outlet} = p_{inlet} - \Delta p \qquad Eq.(12)$$

$$\Delta p = \frac{fL}{2D}\rho v^2 \qquad Eq.(13)$$

Here $\dot{m}_{max}$ is the peak flow rate per hour throughout the year with the possibility of being split between several pipelines ($N_{pipeline}$) in parallel. In the gas case, the downstream substation also houses a fuel cell to allow a comparable analysis for serving electric loads where hydrogen could be fed at 500 psia. Pressure drop calculations are summarized in Table 14.

Table 14 - Pipeline pressure drop calculation assumptions

Hydrogen Pressure Drop Calculation Assumptions	
f, friction factor (36") [1]	0.00914
ρ, density @ 300 K [kg/m^3]	0.082
z, Compressibility [1]	1.03009
R, Universal Gas Constant [kJ/(K*kg*mol)]	8.3144
T_{in}, Inlet Temperature [K]	300
γ, Heat Capacity Ratio [1]	1.4
$\eta_{comp,isen}$, Isentropic Efficiency [%]	65
N_{stage}, # of Compression Stages	Calc.

A 2004 study takes into account the pipeline costs in the past 13 years and finds that the typical natural gas pipeline cost breakdown of material, labor, miscellaneous, and right of way costs are 30%, 42%, 23%, and 5% respectively [121]. To predict hydrogen pipeline costs each cost component is multiplied by a different multiplier. Parker [138] suggests a 1.5 multiplier for material costs to address hydrogen embrittlement and 1.25 for lack of skilled labor regarding these pipelines, and 1 for miscellaneous. However, these multipliers are arbitrarily determined in both Parker's work [121] and in the DOE's hydrogen pipeline delivery model which assumes 1.1 multiplier values for each factor

[139]. A 2015 work conducts a cost analyses to evaluate the pipeline thickness necessary to transport based on ASME hydrogen pipeline code to better understand the material cost [140]. In this work, Fekete et al. find that a technical based proposed adaption to the ASME code can reduce pipeline costs by as much as 31% relative to natural gas pipelines for a 24" diameter pipeline operating at 1500 psia. The price differential for the 1000 psia case increases inversely with size -2% for 12", -24% for 24", and -25% for 36". For 1500 psia there is a -19% decrease for 12" and -31% for 24". Though there is no comparison in the price change for 36" pipeline at 1500 psia because the older code did not allow 36" hydrogen pipelines at 1500 psia, a discount of 31% is also assumed for this work based on these results. It is assumed the developers for hydrogen pipelines will be the same owners as natural gas pipelines, so the ROW cost is negligible as also done in the electric case. The cost of pipeline is modeled with the follow equations where *d* represents diameter (in.), *L* is length (mi), and F is the multiplier for the respective component. The 31% discount corresponds with an F factor of 0.69 for all three components.

$$H2\ Materials\ (d,L) = F_{mat}([330.5d^2 + 687d + 26{,}960]L + 35{,}000) \quad Eq.(16)\ [121]$$

$$H2\ Labor\ (d,L) = F_{lab}([343d^2 + 2074d + 170{,}013]L + 185{,}000) \quad Eq.(17)\ [121]$$

$$H2\ Misc\ (d,L) = F_{misc}([8{,}417d + 7{,}324]L + 95{,}000) \quad Eq.(18)\ [121]$$

$$H2\ Pipeline\ Cost\ = H2\ Materials + H2\ Labor + H2\ Misc \quad Eq.(19)\ [121]$$

The pipeline O&M is extracted from SCG's direct testimony to have their proposed 2019 O&M expenses approved by the CPUC [141]. Dividing their 2016 value of $17.7 million for their 3,455 transmission pipeline miles for a value of roughly 5,100 $/mi-year.

This is an optimistic estimate as this figure is for natural gas pipelines and it is reasonable to expect additional expenses to account for hydrogen-specific issues

Arpino et al. [142] analyze unaccounted for gas in natural gas transmission networks and states that "losses and emissions are often wrongly included in unaccounted gas (UAG)." Arpino et al. define the uncertainty of UAG as a function of the uncertainty of volume at entry points, storage, delivery of gas, self-consumptions that drive the compressors, losses and line-pack rather than losses from leakage. Consequently, larger pipeline systems have higher uncertainty reflected by typical numbers in Table 15 corresponding with the coverage of gas companies. With this definition of UAG in mind, companies report losses with unaccounted for gas and NG compressors as a single figure in the California Gas Report 2016 [143]. This report serves as an outlook device compliant to the California Public Utilities Commission Decision D.95-01-039. Since company use, losses, and uncertainty are all lumped together this work suggests that a one percent pipeline loss be used, equivalent to a modest pipeline efficiency of 99% used in the model. This is a conservative an estimate, as Arpino et al. suggest emissions and losses only make up a tenth of the aggregated UAG figure seen in the last column of Table 15.

Table 15 – Reported throughput, lost and unaccounted for gas, and compressor gas usage numbers from the California Gas Report [143]. SDG&E appears to be zero due to rounding.

Company	Throughput (MMcf/day)	Company Use + UAG (MMcf/day)	"Losses" as Percentage of Throughput
SoCalGas Co.	2559	28	1.094%
SDG&E	327	0	0
Northern California (PG&E)	2833	56	1.977%

5.3.2. Transmission Compressor

A paper by Zhao and Rui [144] considers the construction cost of natural gas compressor stations based on historical costs between 1992 and 2008. It finds the average cost per horsepower capacity of compressor stations is $2,558 across the US, but only $2,100 (about 2800 $/kW) when considering the Western US region. After accounting for inflation with the United States' Consumer Price Index, this comes out to be about 3,300 $/kW for the entire compression station. DOE's HDSAM calculates the central compressor energy efficiency to be 97.6% and 96.6% for 400 psia to 1000 and 1500 psia outlet pressure [139]. This energy efficiency first requires the motor efficiency ($\eta_{motor,act}$) which is empirically approximated with the compressor's power rating ($P_{H2,Comp}$) seen by Equation 20.

$$\eta_{motor} = 0.00008 * \left(ln\left(P_{H2,Comp}\right)\right)^4 - 0.0015 * \left(ln\left(P_{H2,Comp}\right)\right)^3 + 0.0061 * \left(ln\left(P_{H2,Comp}\right)\right)^2 + 0.0311 * \left(ln\left(P_{H2,Comp}\right)\right) + 0.7617 \quad Eq.(20)$$ [139]

This motor efficiency is used in Equation 21 to calculate the additional electricity used by the compressor. Equation 21 involves some gas properties such as compressibility (z), temperature (T_{in}), heat capacity ratio (γ), specific gas constant (R),

as well as operational characteristics: inlet (p_{in}) and outlet pressure (p_{out}), isentropic compressor efficiency ($\eta_{comp,isen}$), and the number of compression stages (N_{stage}).

$$Compressor\ Elec\ Use\ [kWh/yr] = 8760\left(\frac{(\dot{m}_{avg,sec})zRT_{in}N_{stage}}{2.0158}\right)\left(\frac{\gamma}{\gamma-1}\right)\frac{\left(\frac{p_{out}}{p_{in}}\right)^{\left(\frac{\gamma-1}{\gamma N_{stage}}\right)}-1}{\eta_{motor}\eta_{comp,isen}} \quad Eq.(21)$$ [139]

$$N_{stage} = ROUNDUP\left[\frac{(\log(P_{out})-\log(P_{in}))}{\log(2.1)}\right] \quad Eq.(22)$$ [139]

After some unit conversion, the amount of energy per kilogram hydrogen throughput is calculated by the following equation as done in the Hydrogen Delivery Cost Model (HDSAM).

$$Compressor\ Energy\ Used\ \left[\frac{MJ(LHV)}{kg_{H2}}\right] = \frac{\frac{CompressorElecUse*3600}{8760*1000}}{\dot{m}_{max}} \quad Eq.(23)$$ [139]

The efficiency of the compressor is represented as the usable energy of hydrogen output divided by the input and amount of energy used to fuel the compressor. The EPA [145] utilizes industry data to report that across all natural gas segments 1.4 ± 0.5% of gross natural gas production is lost as emissions (whether fugitive or vented). Of this figure, about 37% come from the transmission and storage segments and the measured emissions from underground pipelines make up less than one thousandth of these emissions. This implies that the leakage in underground pipeline is negligible even when tripling the leakage rate to account for hydrogen's relatively higher volumetric leakage rate [146]. A recent study by Hormaza Mejia and Brouwer [147] even suggests in low enough pressure environments, hydrogen leaks at the same rate as natural gas, but we use the three times rate as a conservative assumption. Consequently, 1.55% (37% of 1.4% times factor of 3 for

hydrogen) leakage ($\eta_{station,leak}$) is modeled to represent the amount of emissions from compressor and storage facilities. Similarly, it is assumed the leakage in underground storage is very low at 0.1% [148]. Transmission calculation assumptions are summarized in Table 16.

$$\eta_{comp} = \frac{\dot{m}_{design} LHV_{H2}}{\dot{m}_{design} LHV_{H2} / \eta_{station,leak} + CompressEnergyUsed * \dot{m}_{design}} \quad Eq.(24) \text{ [139]}$$

Compressor power rating is calculated by the following equation to establish a capital cost.

$$P_{compressor} = \frac{Z \dot{m_{max}} RTn}{S_{motor} \eta_{motor,act}} \left(\frac{k}{k-1}\right) \left[\frac{P_{outlet}}{P_{inlet}}^{\left(\frac{k-1}{nk}\right)} - 1\right] \quad Eq.(25) \text{ [139]}$$

Table 16 – Transmission compressor calculation assumptions.

Transmission Compressor Power Calculation Assumptions	
Z, Mean Compressibility [1]	1.03009
R, Gas Constant [kJ/k*kg*mol]	8.3144
T, Temperature [K]	300
n, Number of Stages [1]	2
k, Cp/Cv Ratio [1]	1.4
S_{motor}, Motor Sizing Factor [1]	1.1
$\eta_{motor,act}$, Motor Efficiency [1]	Calc.

5.3.3. Underground Storage

Lord et al. [149] calculate the levelized cost of storying hydrogen in underground geological features and identifies that depleted oil & gas reservoirs are the most economical choice and geographically available in Southern California. In addition the characterization of oil & gas reservoirs in Lord et al. resembles those in Southern California according to EIA data derived from their monthly underground gas storage reports. This information is tabulated in Table 17.

Table 17 – Depleted natural gas storage facility characteristics in Southern California [150].

Southern California Underground Natural Gas Storage Facilities			
Storage Site	Playa Del Rey	Honor Rancho	Aliso
Type	Depleted Field	Depleted Field	Depleted Field
Working Gas Capacity (Mcf)	2,400,000	27,000,000	86,200,000
Cushion Gas Percentage of Total (%)	65.0	43.7	48.6
Reservoir Depths (ft)	6,200	10,000	9,000
Storable H2 (MWh)	205,388	2,310,614	7,376,849
Calculated Cost [w/o Compressor] ($)	28,738,660	112,155,537	270,393,833
$/MWh H2 Storage Capacity	139.92	48.54	36.65
$/kg H2 Storage Capacity	0.940	0.326	0.246

Our transmission lengths provide a large range where underground storage sites can be utilized further from the demand point, as a result it can be assumed only depleted field storage types are utilized. In evaluating multiple types geological storage types, [149] considers the site preparation, cushion gas, compressor, pipeline, and wells cost components. In the depleted case, there are no site preparations (i.e., mining, leaching plant, site characterization costs) so the total capital cost can be represented by the sum of compressor capital cost ($\$CCC$), cushion gas cost ($\$CG$), and well capital cost ($\$WCC$) as shown in [149].

$$Capex_{USG} = \$CCC + \$CG + \$WCC \qquad Eq.\,(26) \text{ [149]}$$

Furthermore, the compressor capital cost is the product of the power capacity of the compressors (cp) and the cost per power rating (cpc). The compressor power rating is calculated with equation 25 as shown in [149].

$$\$CCC = cp * cpc \qquad Eq.(27) \text{ [149]}$$

The cushion gas (cg) is simply the mass of hydrogen gas that must be present to preserve the integrity of the underground structure times the price per unit mass of hydrogen gas. This is assumed to be 50% of the cavern's volume and must be left in the facility at all times [149]. The amount of cushion gas is equal to the working gas capacity because of this assumption and can be calculated by the required P_{stor} value as shown in [149].

$$\$CG = \$H2 * cg \qquad Eq.(28) \text{ [149]}$$

The only drilling and wells necessary for the depleted field storage type are those used for the storage gas [149]. As a result the well fixed cost can be estimated by the summing the assumed fixed capital cost per well (ccw) and variable well cost (vcw), where the variable well cost is a function of the storage location well depth (wd) and pipeline size. This model assumes that the withdrawal occurs from the expansion of the gas and the compressor capacity constitutes the injection rate. The average well depth from the considered SCG sites is taken.

$$\$WCC = ccw + (vcw * wd) \qquad Eq.(29) \text{ [149]}$$

The operation and maintenance cost of underground storage $(O\&M_{USG})$ is the sum of the compressors' $(\$com)$ and wells' $(\$wom)$ with slightly adjusted equations from Lord et al. This cost is in addition to the assumed 4% hardware O&M.

$$O\&M_{USG} = \$com + \$wom \qquad Eq.(30) \text{ [149]}$$

$$\$com = \left[\frac{kWh_c * EC}{\frac{\dot{m}_{design}}{24} * \left(\frac{hr}{yr}\right) * CF_c}\right] + [(WC * WRCC) * nc] \qquad Eq.(31) \text{ [149]}$$

$$kWh_c = \dot{m}_{annual} * \left(\frac{kWh}{kg}\right) \qquad Eq.(32) \text{ [149]}$$

Where (kWh_c) is the annual electricity the compressor uses, (EC) is the cost of electricity, IR is injection rate (kg/hr), $(\frac{hr}{yr})$ is the number of hours the compressors work per year, and (CF_c) is the capacity factor for the compressor. Note the number of operating hours for the compressor does not significantly change the \$com (e.g., 8400 to 840 operating hours results in 1% change \$com), so even though the activity of a storage compressor can be difficult to predict, there should not be too much concern with the exact value and simply use 8400 as done in [149]. In addition, (WC) is the cost of water for cooling and $(WRCC)$ is the required water for cooling. Equation 31 is also used to calculate operating O&M for the transmission compressor as shown in Lord et al. [149].

The well O&M cost is given by the initial drilling variable cost times the capital recovery factor (CRF_w) in addition to an assumed O&M fraction of the well capital costs (drilling plus well) [149]. This latter term is normalized by total site hydrogen gas storage capacity (cushion and working).

$$\$wom = (vcw * CRF_w) + (\$WCC + vcw) * \frac{O\&M_{well}}{kg_{H2}} \qquad Eq.(33)$$ [149]

The annual compressor electricity use and total hydrogen gas storage are all calculated values based on the supply and demand dynamics. A complete list of other assumed constant values for prior calculations is provided in Table 18.

Table 18 – Underground storage compressor calculation assumptions.

Underground Storage Cost Assumptions	Value	Source
$H2, Hydrogen Cushion Gas ($/kg)	4.5	[151]
nc, Number of Compressors	2	[149]
cpc, Cost of Compressor ($/kW)	2481	[144]
% Cushion Gas Percent	50	[149]
ccw, Fixed Well Capital Cost ($)	260,000	[149]
vcw, Variable Well Capital Cost ($/km)	319,757	[149]
wd, Well Depth (km)	2.56	[152]
kWh/kg, Compressor Energy Per Unit Mass	0.82	[153]
EC, Electricity Cost ($/kWh)	0.05	[149]
WC, Cooling Water Cost ($/100L)	0.02	[149]
WRCC, Required Water Cooling (L/kg)	50	[149]
$O\&M_{well}$, Well O&M Percent of Capex (%)	4	[149]
CRF_{well}, Well Capital Recovery Factor (%)	11	[149]
CF_c, Compressor Capacity Factor	0.96	[149]
hr/yr, Operating Hours per Year	Calc.	

Amid et al. [154] report using injection pressure between 5 and 10 megapascals (MPa) to store hydrogen in a natural gas reservoir, so it is assumed the storage compressor outlet is an average of 7 MPa (1015 psia) injecting into the underground storage. Underground storage injection is driven by a compressor while the withdrawal is driven by high pressure expansion and managed by regulators which is assumed to be negligible regarding cost and energy efficiency.

5.3.4. Line-pack

Line-pack is the amount of extra gas that can be stored in pipelines without surpassing the maximum pressure of 1500 psi and maintaining a minimum pressure of 500 psi. It is assumed a wall thickness of 15 mm [155] and treat the hydrogen as an ideal gas. It is assumed a constant temperature of 298 Kelvin and allow a 1000 psi fluctuation. The constant demand case considers all parallel pipelines whereas the constant transmission utilization factor case only has one pipeline. Table 19 acts as a summary for the established hydrogen pathway before moving onto dynamics and cost calculations.

Table 19 – Hydrogen pathway major components summary.

i	Component	Cost ($USD)	Lifespan (years)	η
1	Fixed PV Generation Site w/ DC-DC Booster ($/MW)	1,030,000 [20]	30	0.95 [129]
2	Electrolyzer ($/$MW_{out}$)	1,200,000 [156]	12	0.71 [157]
3	Transmission Compressor + Substation ($/MW)	2,682,000 [144]	20	Eq. 24.
4	Transmission Pipeline ($/mi)	Eq. 19	30	0.99 [143]
5	Sub-transmission Storage Compressor ($/MW)	2,481,000 [149]	35	0.99 [143]
6	Underground Storage Site w/ Compressor ($/MWh)	Eq.26 + Eq.30 [149]	30	Eq. 24
7	Fuel Cell ($/$MW_{out}$)	3,500,000 [156]	10	0.60 [158]

5.4. Dynamics and Cost Calculations

In this portion of the analyses, the statewide solar generation profile and electrical load profile are assumed. A sample of the dynamics utilizing the previously established pathways is presented in Figure 29.

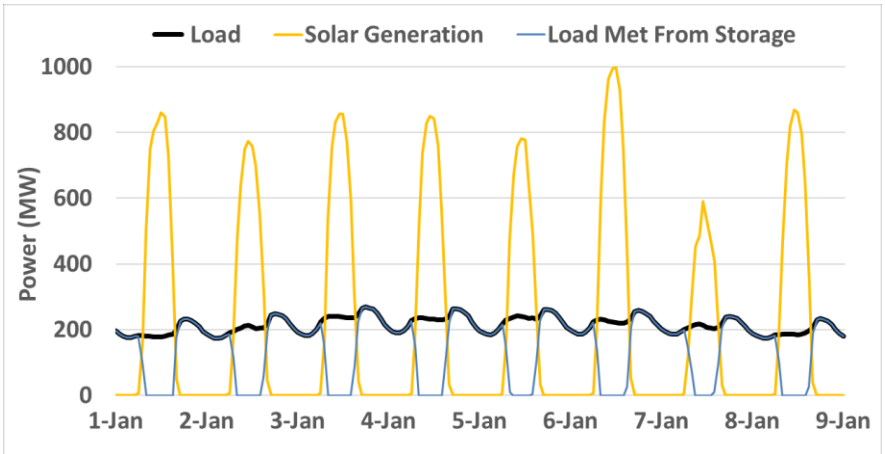

Figure 29 – Snapshot of the first week of the simulated year. Solar is sent through transmission to meet load when possible, otherwise sent to storage. Storage is dispatched when solar is insufficient to meet load. Solar shown here is downstream of the solar power plant as the grid would view it.

Each component in the pathway rating is determined after considering the upstream component efficiencies. The average annual flow rate for compressor ratings is used rather than peak throughput. The storage capacity needed to get through the year, corresponding to all of the storage required for hourly, daily, weekly and seasonal shifting, is identified and referred to as the seasonal shifting capacity. The energy amount required by the largest excess solar production day in the year is referred to as the daily shifting capacity. For the daily shifting case, there are many days in which there is not enough excess solar energy to shift to meet the nightly load and for the days with the most excess we assume the storage can entirely discharge before the next day so they can start at zero

state-of-charge. The daily shifting case is only valid if the demand being met is only a portion of the total system demand and other resources can be dispatched complement the solar and energy storage systems. The seasonal shifting case is more reflective if the total demand being modeled is the entire system's demand and other generation and storage resources are not available. There is zero curtailment in all cases.

The following components are assumed to have a hardware O&M cost assumed to be 4% of the capital cost: substations, transformers, compressors, electrolyzers. All other components' O&M costs are calculated. A 5% rate per year period is assumed for the annuity factor calculation. The EAC for each component is the sum of the capital cost divided by annuity factor plus the annual O&M cost. To calculate the LCOE, the sum of all EAC is then divided by the product DC power produced by the PV solar panels (E_{PV}) and the entire pathway efficiency ($\eta_{pathway}$) seen below.

$$LCOE = \frac{\sum EAC_{components}}{E_{PV} * \eta_{pathway}} \qquad Eq.(34)$$

5.5. Transmission Results

In order to understand the magnitude of capacity modeled in this analysis, note that the amount of solar installed in these cases span 1300 to 1800 MW of solar nameplate. Assuming all electricity produced from this amount of capacity can be used directly, this is roughly a 12-14% increase in solar generated in state or 1.5% of total state electric consumption for the year of 2018 [40]. However, if the solar generation is to meet a proportional unit reflecting system demand dynamics, it is found that 54% and 62% of

generated hydrogen and electricity, respectively, is sent to storage in order to be able to meet later loads throughout the year as seen in Figure 29.

Because storage is downstream of the delivery pathway, the amount of necessary storage for each transmission case at the same transmission level is roughly the same. If storage were modeled to be upstream, the necessary amount of storage would be forced to account for variations in the transmission losses.

5.5.1. Levelized Cost of Transmission

The annual utilization factor of the transmission medium spans from 0 to 0.29 corresponding with the capacity factor of solar in Southern California. In general, the hydrogen pipeline cases' show a levelized cost of transmission (LCOT) that increases at higher utilization due to compressor work and the electric pathway LCOT curves increase due to ohmic losses. If it is assumed that each transmission medium typically operates at around a 30% utilization factor on average, then all mediums have very comparable levelized cost of transmission for the 100-mile case. In a solar dominated scenario where local energy storage serves the majority of nighttime loads, transmission lines may operate at these lower levels too. As the distance grows, higher voltage transmission and larger pipelines are economically better for the accompanying higher throughput. In the 500-mile case, the 36" pipeline and 500 kV float at around 50 $/MWh. For the extreme 900-mile distance, the pipeline cases maintain a slight advantage in the higher utilization factor regime. Some curves are shorter than others due to the amount of solar that must be installed to vary the utilization factors in the same range. An attempt to increase utilization factor by adding more upstream solar results in the need to install parallel power lines or

pipelines to handle the additional peak power transmission. Because of this we, cannot extrapolate how the curves would behave at higher capacity factors without properly modeling the dynamics of other types of upstream generation. This is left to future work.

On a cost basis, the transmission line makes up two-thirds of the LCOT EAC at 100 miles and disproportionally more at longer distances (e.g., 88% at 500 miles, 500 kV and 90% 300 miles, 230 kV). On the other hand, compressor work consistently stays 73 to 84% of LCOT across the simulated distances. LCOT results are summarized in Figure 30.

a)

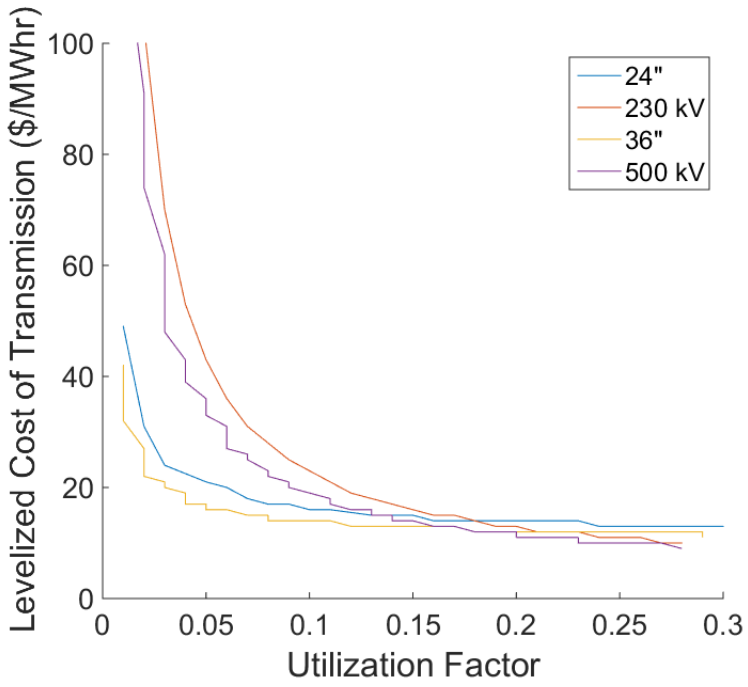

b)

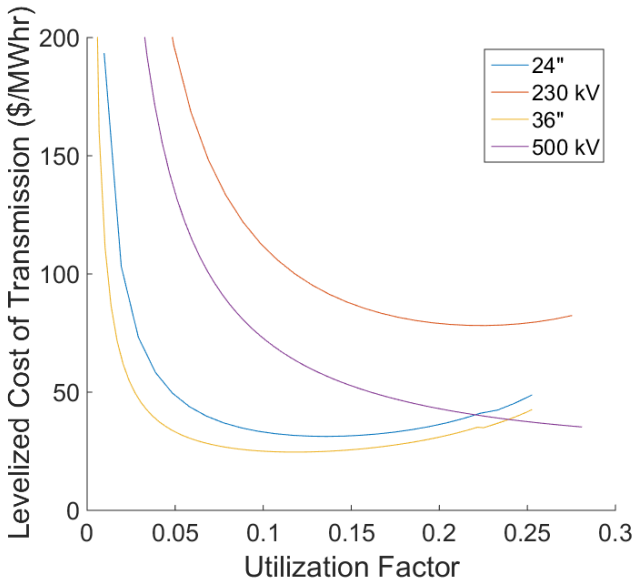

c)

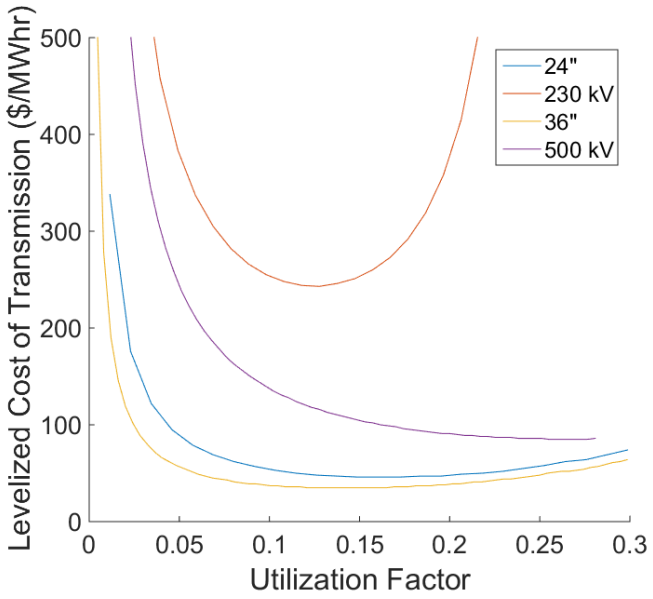

Figure 30 – Levelized cost of transmitting energy versus utilization factor for (a) 100 miles, (b) 500 miles, and (c) 900 miles.

5.5.2. Levelized Cost of Electricity

Though the amount of electricity consumed at the delivery point is the same, more solar is installed at the origin if total pathway efficiency is lower. The higher voltage level cases have enough reduction in ohmic losses to offset the additional losses from the extra voltage transformation steps and higher costs. At 100-mile transmission lengths, 230 kV appears slightly cheaper than the 500 kV case and break even at around 300 miles. The storage systems are sized to be able to handle the energy capacity needs as well as power rating needs. Both of these technical requirements are reflected in the battery system size in the electric case and represented by the compressor and underground geological storage capacity in the hydrogen case. Note that storage is majority of the total pathway's EAC and obscures the LCOT advantage that the 500 kV case has over 230 kV at longer distances (i.e., half at 500 miles) seen in Figure 30. The additional cost primarily arises from the cost of storage being 70 to 85% of EAC. If one were to ignore the cost of storage in the electric case, the LCOE is approximately 9 cents/kWh for 100 miles and 14 cents/kWh for 300 miles. As a reference, SCE's standard residential tiered rate plan is 19 cents/kWh for tier 1 usage allocation and 24 cents/kWh for tier 2 usage. In addition, their cost breakdown shows that generation and transmission on average make up half of the rate, suggesting roughly a 10 to 12 cents/kWh which is in the range of the calculated LCOE. The LCOE results for both scenarios and both medium are presented in Figure 31.

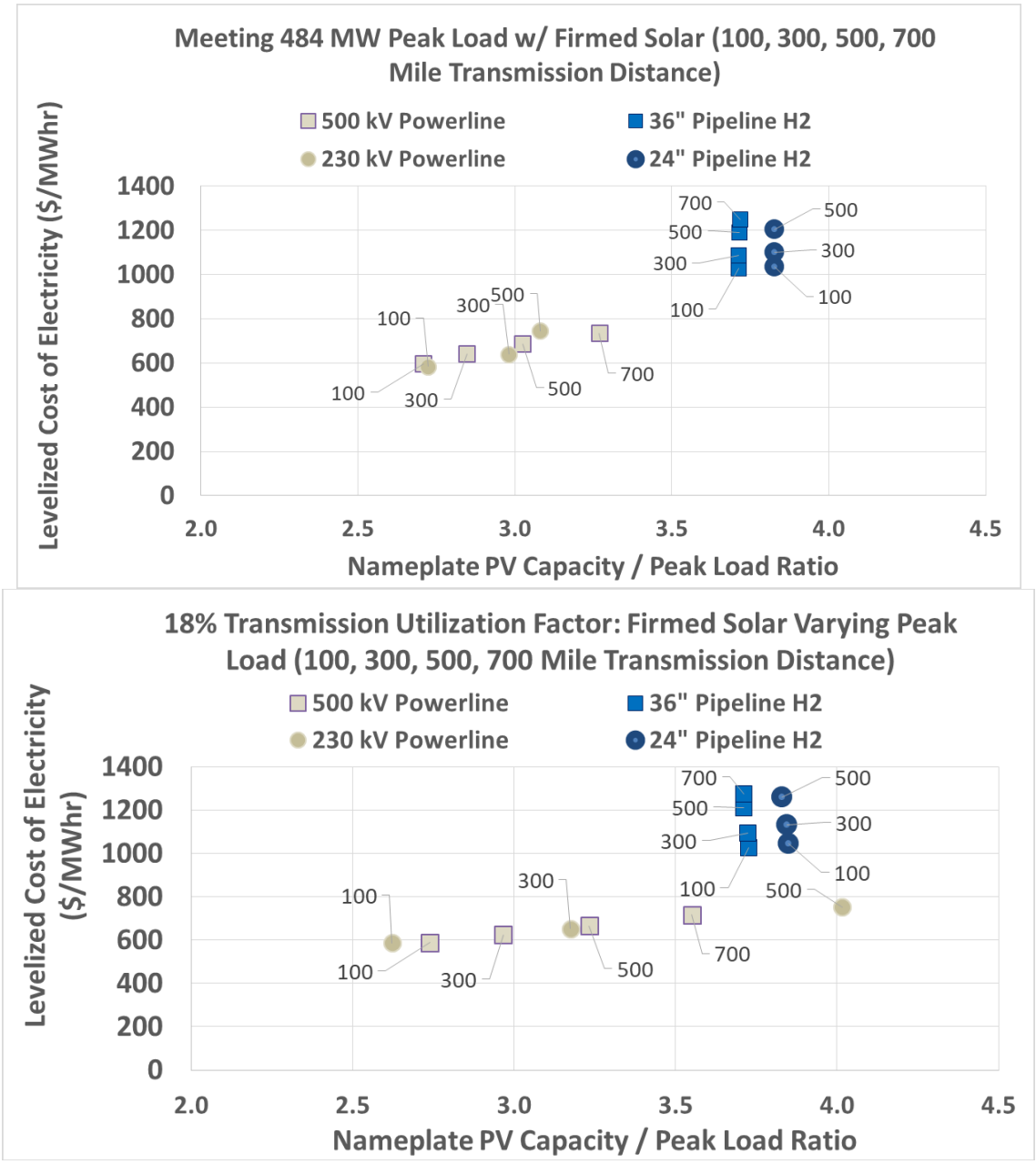

Figure 31 - Daily Shifting LCOE (a) constant demand scenario and (b) when transmission medium utilization factor is constant at 18%.

In the hydrogen case, similar costs between the 24- and 36-inch pipeline are seen. This is mostly due to EAC from the PV, fuel cell, and electrolyzer, which make up 78 to 86% of total EAC. The amount from pipeline is less than 1% different between the 24" case and 36". The difference in LCOE arises from the additional parallel pipelines needed to support

flowrate in the 24". Because the pipeline efficiency is an average percentage of volume rather than distance, a proportional amount is attributed to pipeline leakage. In other words, there is no change to transmission losses due to transmission distance. LCOE increases with distance due to compressor and pipeline costs for the hydrogen case and due primarily to power lines in the electric case. Electrical components costs increase primarily due to higher power ratings needed while only pipeline and compressor costs increase in the hydrogen case. At higher transmission distances the hydrogen pathway efficiency is higher due to more intermediate compressors working more efficiently. Regarding costs, Table 20 summarizes how each major component cost changes at different distances. As expected, many of the endpoint equipment do not change significantly with transmission distances. For the hydrogen case, the compressor work and associated cost is quite significant relative to pipeline cost itself.

Table 20 – Comparing change in component EAC when increasing transmission distance. Numbers are provided as a percentage of the shortest transmission distance for each transmission level for a) the electric pathways and b) the hydrogen pathways.

a)

Transmission Miles	PV	Substation & XFMR	Power Line	Battery
230 kV Power Line Case				
100	100%	100%	100%	100%
300	109%	103%	473%	100%
500	118%	120%	788%	98%
500 kV Power Line Case				
300	100%	100%	100%	100%
500	106%	102%	167%	100%
700	115%	105%	233%	100%

b)

Transmission Miles	PV	EC	Compressor	Pipeline	FC	UGS
24" Pipeline Case						
100	100%	100%	100%	100%	100%	100%
300	100%	100%	160%	299%	100%	96%
500	100%	100%	278%	499%	100%	92%
36" Pipeline Case						
300	100%	100%	100%	100%	100%	100%
500	98%	98%	172%	167%	98%	99%
700	98%	98%	205%	233%	98%	99%

The amount of necessary energy storage is higher in the hydrogen case than the electric case due to the lower discharge efficiency from storage. By modeling the fuel cell efficiency as 62 percent, the discharge efficiency of the battery is still higher at 87 percent. In this work self-discharge is not accounted for. If it had been, the energy storage capacity needed would grow larger, proportionally with the timeframe energy would be needed to be shifted. Le Duigou et al. explore the cost associated with implementing large scale underground hydrogen storage in France finds that in the most demanding scenario

(electrolysis driven by purely wind generation), the storage component only accounts for 2.9% of the cost to produce and meet projected transportation demand loads [159]. There is reasonable agreement with this result as it is found underground storage accounts for 2.1% of the pathway cost (4.1% if omitting the fuel cell system cost) in the 100-mile case compared to the 124-mile case considered by Le Duigou et al. Note the previous Figure 31 illustrated the amount of solar that would have to be overbuilt, whereas Figure 32 illustrates the amount of energy storage needed to complement the pathway but both y-axes are the same. Storage capacities are similar for case (a) because of the same demand and different discharging efficiencies. Case (b) storage capacities suggest the 230 kV serves a slightly larger load than 24" after accounting for discharge efficiencies whilst the higher transmission levels meet comparable loads.

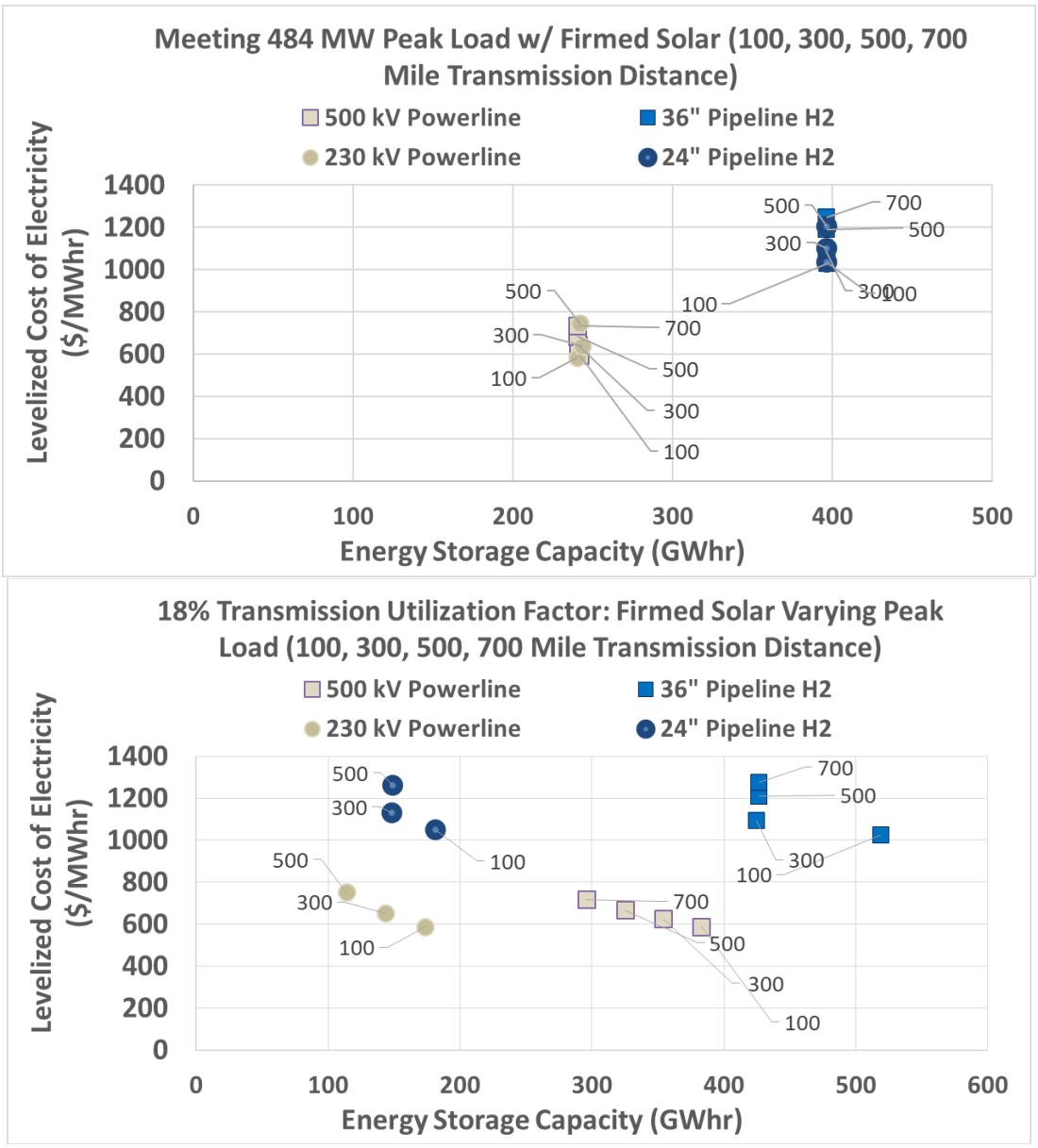

Figure 32 – Comparing necessary energy storage capacity for each case with levelized cost of electricity for (a) constant demand scenario and (b) when transmission medium utilization factor is constant at 18%.

The next step is to calculate the LCOE as done similarly in the previous chapter. We consider the EAC from the major components as well as the delivered electricity for each pathway. This is illustrated by Figure 33.

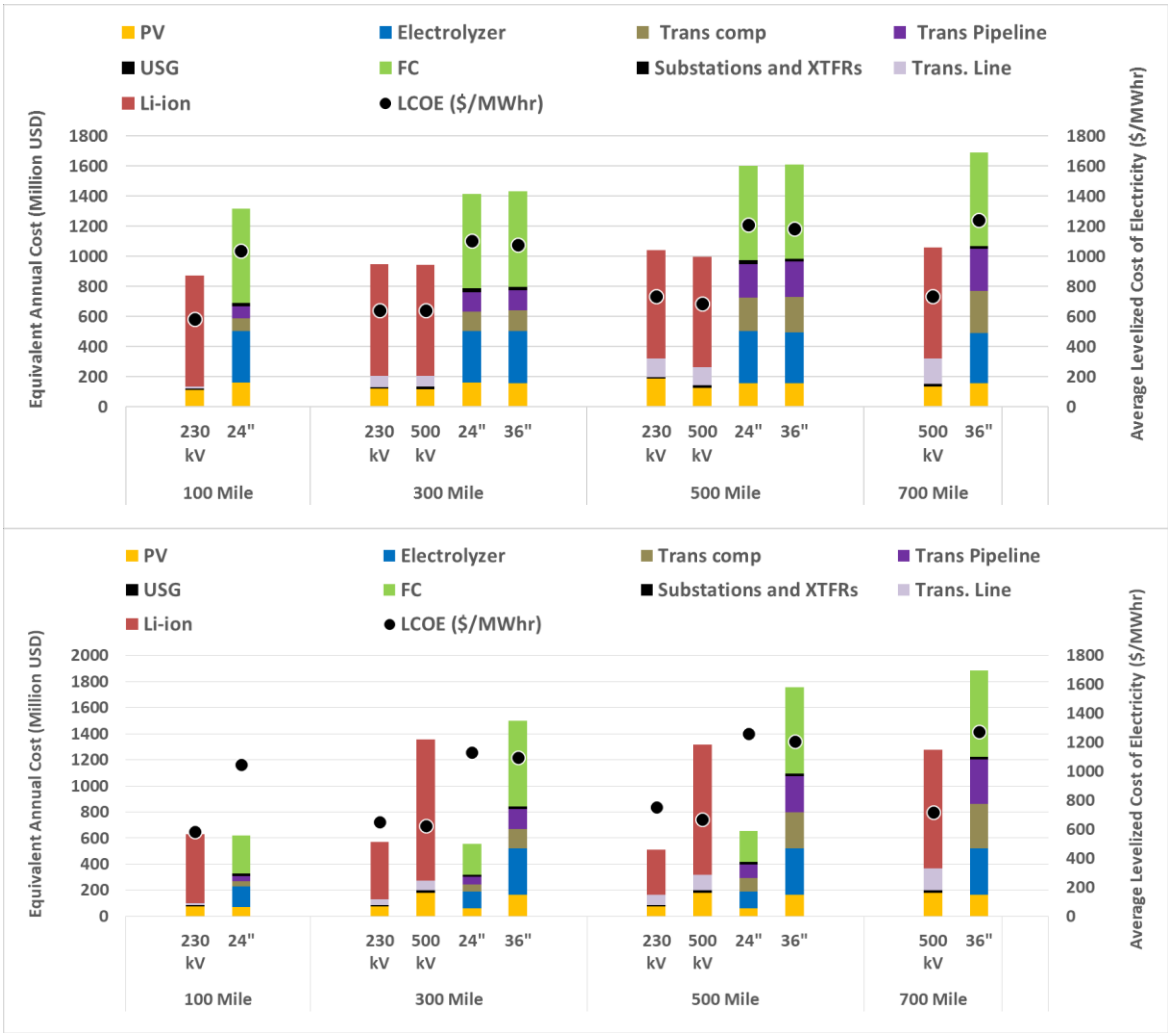

Figure 33 – Equivalent annual cost breakdown (primary axis) and levelized cost of electricity (secondary axis) for each delivery scenario for (a) constant demand scenario and (b) when transmission medium utilization factor is constant at 18%.

If one were to consider seasonal storage, the hydrogen cases need 38 times the storage capacity while the electric cases need 60 times the storage capacity. Despite a higher discharge efficiency, the daily to yearly storage capacity increases more in the electric case since due to the modestly modeled 4% self-discharge per month for the battery energy storage system. The increase of battery energy storage capacity needed translates into a two orders of magnitude increase in levelized cost— from roughly 0.65 to

30 $/kWh. Note even if battery costs were to decrease by 50%, from 350 $/kWh to 175 $/kWh, the resulting LCOE would decrease at most by 50%. In the hydrogen case, storage capacity costs are primarily associated with underground storage, which on a dollar per energy storage capacity basis is two orders of magnitude cheaper than battery energy storage systems. The LCOE in the hydrogen case increases about 1%, remaining around 1.2 $/kWh when seasonal storage is needed. Note that this minor increase is solely associated with the increased cost of the larger underground storage medium required for seasonal storage. The compressor costs remain largely the same and do not significantly add to the injection costs. This is before accounting for the innate storage value of pipelines.

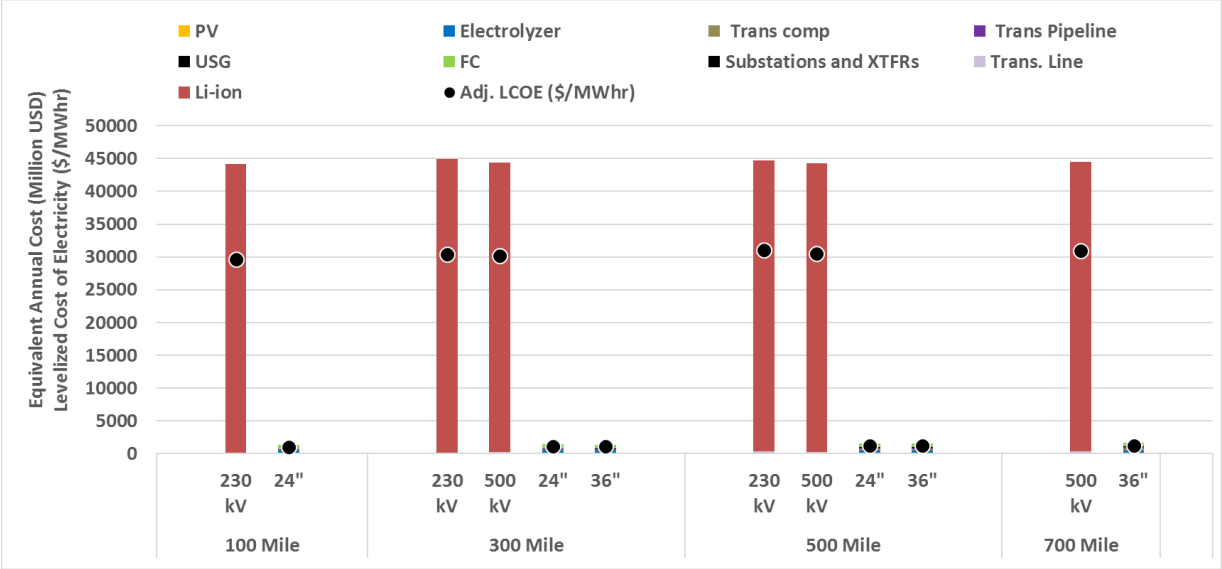

Figure 34 – Equivalent annual cost breakdown and levelized cost of electricity when seasonal storage is necessary. Case is for constant demand case.

5.5.3. Line-pack Versus Daily Shifting

Many critique the need for such expansive seasonal storage, so a further analysis is conducted assuming only daily energy shifting is necessary. Let me note that the transmission power line or pipeline considered should be thought to be the backbone for

moving power to and from regions. Many smaller generators and loads will make interconnections, especially as candidate PV sites and renewable projects are located remotely from major loads. Independent power producers who would like to connect to the California grid today finance the development of interconnections to the CAISO network. If one were to imagine an equivalent case in a hydrogen future, new power producers would be responsible for producing hydrogen on site and the spur pipeline to be implemented to the greater gas grid. Storage systems that are implemented into the grid can act as transmission deferral vehicles but also as energy shifting systems.

Suppose an independent PV farm exports power onto the grid and grid operators are responsible for ensuring available infrastructure to manage this marginal power. In an all-electric scenario, batteries would be responsible for these tasks. Assuming both types, electrical and gas network existed, batteries or pipelines could be contracted to act as a storage medium. The amount of energy stored in the pipeline and put through a fuel cell can be thought as the amount of electrical energy and considered as the avoided EAC from procuring batteries. At distances greater than the breakeven distance, the value of line-pack helps bring the LCOE of the hydrogen pathway lower than the electric case. A negative LCOE reflects a profitable project if storage alternative can be realized by avoiding battery installations and being contracted to store energy. Figure 35 illustrates the actualization of this value in our considered cases.

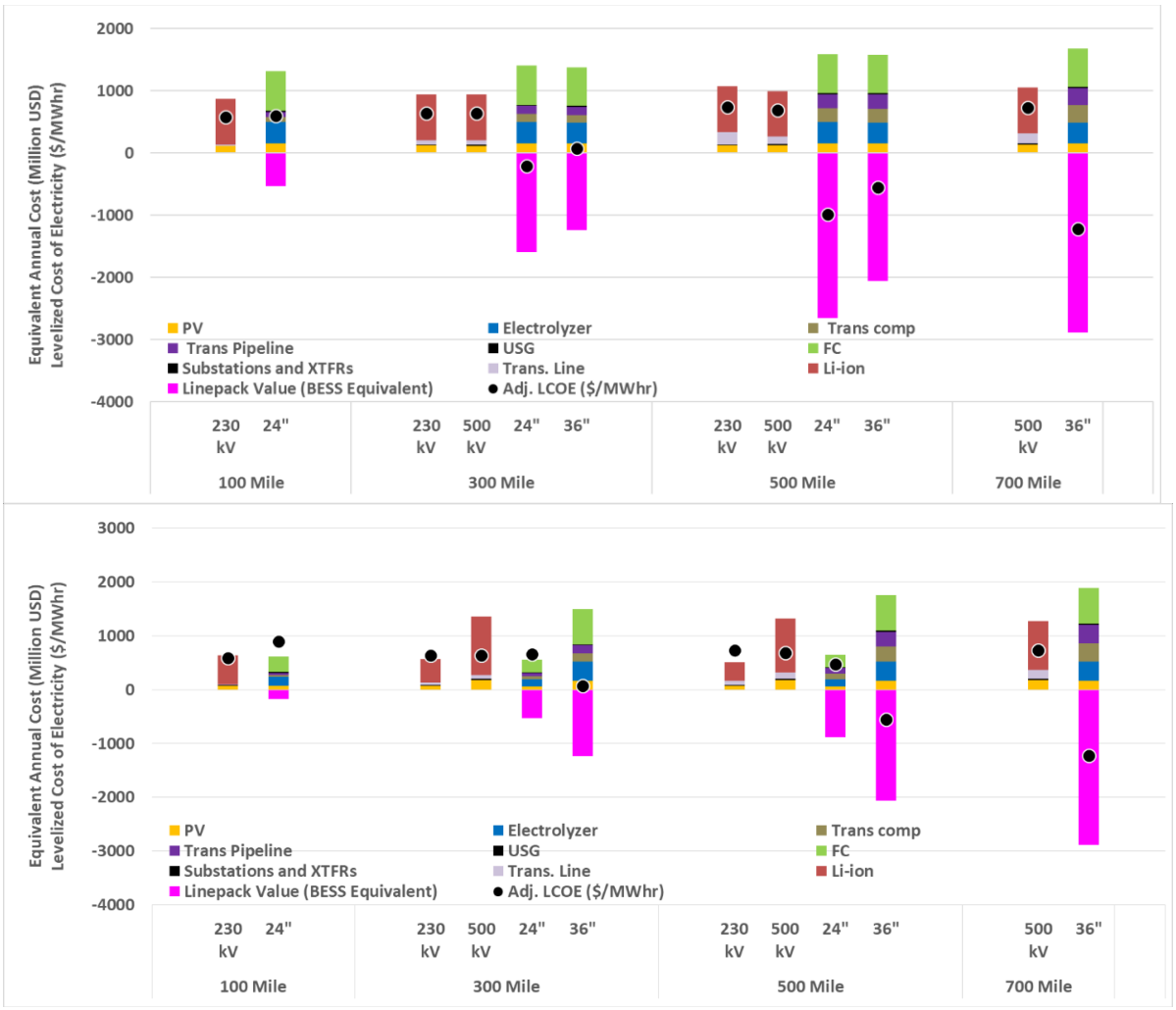

Figure 35 – Equivalent annual cost breakdown and levelized cost of electricity for each delivery scenario when line-pack value is accounted for in the daily shifting (a) constant demand scenario and (b) transmission medium utilization factor is constant at 18%.

Three 24" pipelines in parallel were necessary for the considered generation and demand levels. Table 21 reflects the line-pack available from all three 24" pipelines in parallel at all transmission distances which is greater than the single 36" pipeline. Although it may seem unintuitive to have three pipelines alongside one another, the model does not physically site the transmission distance. As a result, the three-pipeline case is as fair a representation of transmitting solar from three different directions as the case with PV

capacity in a single location. One should not mistake the multiple 24" pipeline case to be better than the single 36" pipeline because the two are operating at different capacity factors. If one were to increase the demand, causing additional solar installation, the 24" pipeline would suffice with three pipelines before a second line is necessary in the 36" case. The amount of line-pack would therefore double and demonstrate a case where the LCOE adjusted for line-pack value would be more attractive in the 36" case. This was the primary motivation for conducting a constant utilization factor analysis.

Referring to Figure 35, a pipeline in Fresno, California which is already a candidate region for PV, could strongly benefit from a hydrogen pipeline. A pipeline to deliver gas to major loads in Los Angeles or towards the major cities in the north already exist would allow for many parties along the central valley to be able to inject hydrogen produced excess renewables (i.e., increasingly abundant residential rooftop PV or other utility-scale power plants) or and withdraw hydrogen at a later time to meet night loads. This would be a practical manifestation of line-pack storage value being realized. Transmission distances with even greater lengths, such as between states have even greater potential line-pack value, such as El Paso Corporation's Ruby Pipeline—a 680-mile 42" pipeline spanning Wyoming, Utah, Nevada, Oregon, and California. Some other generalized breakeven distances are presented in Table 21.

Table 21 – Summary of levelized cost of electricity for constant demand scenario. Results shown consider the three parallel pipeline case. Electric case levelized costs are similar in the constant utilization factor case due to majority of costs being due to storage so breakeven mile is similar. The only difference is in the constant utilization scenario, only one 24" pipeline is considered thus the breakeven distance is three times the amount shown here.

Transmission Distance	Electric Case Voltage Level (kV)	Electric Case LCOE ($/MWh)	24" Line-pack Breakeven Distance (mil)	36" Line-pack Breakeven Distance (mil)
100	230	584	103	127
300	230	640	106	147
300	500	641	106	147
500	230	736	108	138
500	500	687	119	152
700	500	734	N/A	152

The amount of energy that could be stored in pipelines is presented in Figure 36. They are compared to the daily and yearly shifting needed in our considered constant demand cases. Note that a relatively short segment could fulfill the daily shifting needs for the PV capacity we have modeled. A network of pipelines is implied to be able to fulfill the yearly shifting needs.

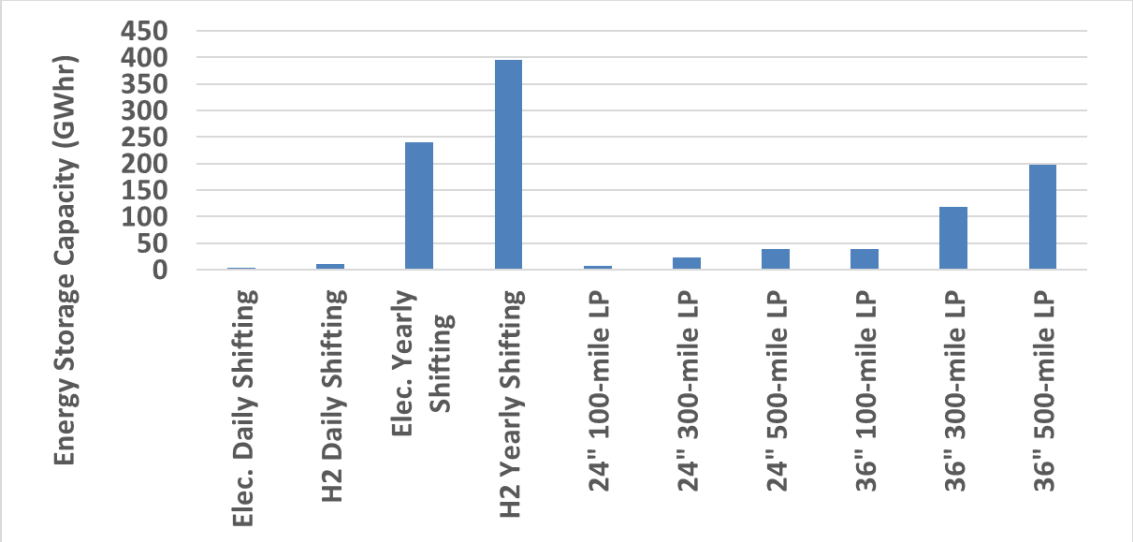

Figure 36 – Comparison of shifting energy storage capacity needed for constant demand cases and the amount of storage found in pipeline line-pack.

5.6. Discussion

5.6.1. Pathway Efficiency versus System Needs

California IOU utilities report their transmission and distribution losses to the CPUC. As of 2014, the total estimated losses for delivering electricity from generation to end use from major utilities in California is 6.58%. Constituents for this figure are PG&E's 8.66%, SCE's 4.26%, and SDG&E's 4.66% [160]. These figures are much lower than the pathway efficiency in many of the cases considered in this effort. Though the IOU losses consider distribution losses, they typical meters delivered power downstream of power plants and therefore not capturing the losses of power conditioning done at the generation sites. In addition, these IOUs presumably have many generation resources within a 100-mile radius and thus minimal transmission losses. The idea of a renewable future supposes major project developments further from loads in areas with less geographical constraints. Along the same lines is the idea of regionalization, or exchange of renewables between states, requires long distance analyses that require a scope greater than just intrastate utility companies.

A review of building electric transmission lines by Eto [161] addresses the challenges of citing and evaluating the value of large transmission projects involving various agencies and stakeholders. An evaluation of what is the "most efficient" method of delivering electricity from a point A to point B does not capture the potential needs of stakeholders. The idea of line pack for renewable gases such as substitute natural gas or renewable hydrogen has inherent value that is not often quantified. Doing so fairly would need to account for renewable goals and renewable generation dynamics of other states,

benefits of other sectors outside of power generation (e.g., transportation), public opinion, safety, and reliability of transmission infrastructure.

The CEC has mandated solar installations for new homes built in California to be sized for to produce as much electricity as annual consumption [34]. Doing so has major implications on the energy system as a whole. This will most likely exacerbate the duck curve, a symbolic representation of net load for a day due to solar generation coming online in the middle of the day. This will increase the need for controllable resources, presumably an increasing amount coming from energy storage. Community batteries and distribution natural gas pipelines can be analyzed similarly to the transmission case. In addition, fewer central level power plants will be needed—reducing the midday utilization factor of transmission lines.

On a local level, even a slight 5% blend of hydrogen in Southern California provides 650 GWh of energy storage equivalent to 130 billion in battery costs [162] potentially alleviating transmission constraints arising from solar project-populated Central California and enabling further solar deployment.

5.6.2. Availability of ROW and environmental impact

Some compare HVDC to HVAC similar to the comparison considered in this analysis. A major positive point in HVDC is the lesser environmental impact and necessary right-of-way for such technology. Bahrman [163] states that transmission options considered for the first stage of the Three Gorges Project in China would have been five circuit lines compared to two lines in the HVDC case minimizing effect on environmentally-sensitive

areas. When considering a renewable future, the existing natural gas infrastructure's, which spans the contiguous United States, conversion to support hydrogen is an interesting concept that may even have comparable implications to the HVDC case. Doing so would reduce the need to allot new land to expand electrical infrastructure supporting remote renewable projects [164].

5.6.3. Reliability and safety

Overhead power lines have proven to be a hazard in California due to the amount of earthquakes and severe weather that the state experiences. 2019 has been a challenging year for PG&E due to multiple incidents regarding their power lines causing fires leading them to declare bankruptcy. Underground power lines are an option that would have the advantage of having some protection from severe weather but the cost can be an order of magnitude higher [165]. In this analysis it is found that the LCOT is similar for the traditional overhead HVAC to hydrogen pipelines, so an increase in electric pathway costs for the underground reliability and safety would increase appeal for the hydrogen pathway. LCOE which has been dominated by storage costs in the electric pathway will most likely see significant changes for longer transmission paths. The 500-mile 500 kV transmission line accounts for 12% of the EAC and an order of magnitude increase could put its contribution to over 50% and double the LCOE. This would put it on par with the hydrogen LCOE (when not accounting for line-pack value) at around 1500-1600 $/MWh for this transmission distance.

5.6.4. Scalability

In this analysis a case with a peak load of 483 MW met by a range of 1317 MW (100 mile, 230 kV case) to 1851 MW (500 mile, 24" case) solar capacity is considered. If one were to scale both generation and demand by a factor of 100, the amount of PV installation is similar to the 154 to 169 GW PV in the high solar case in Colbertaldo et al. [100] which analyzes a 100% renewable California. The resulting peak demand is also similar to the historical state peak of 50.3 GW in 2006 [106]. Maintaining the same dynamics of this analysis, one would also need roughly 100 times the amount of energy storage. In the electric case this would correspond with roughly 0.4 TWh of batteries or 1 TWh of hydrogen storage for daily shifting need. If one were make the same assumptions of existing pipelines as in this analysis, the collection of pipelines with 19-inch and above diameters in California [166] represents 930 GWhr of line-pack storage. What this suggests is that though there may be a proliferation of solar PV plants with batteries, at some point the system will require long-term storage if most generation assets are solar. The opportunity to utilize the existing gas infrastructure poses an interesting value proposition—being able to shift away from natural gas usage whilst enabling more PV generation with line-pack storage.

5.6.5. Transmission Analysis, Summary, and Conclusions

An analysis has been conducted which investigates delivering utility-scale solar PV as electricity or hydrogen for a dynamic load in California. The levelized cost of transmitting the same amount of renewable electric energy via electric and hydrogen infrastructures is comparable at short distances and slightly lower for the hydrogen cases

at longer distances due to the minor gas leakage in pipelines versus the ohmic losses that scale linearly with distance. We further analyzed the levelized cost of delivering electricity (i.e., putting delivered hydrogen through a fuel cell) and comparing the two pathways. With more and more PV solar being deployed at the central and distributed levels, energy storage is increasingly necessary due to the duck-shaped demand profile in California.

The amount of innate energy storage in pipelines poses an interesting value proposition as it could mitigate the amount of batteries needed for energy storage. When daily energy shifting is necessary, the cost of batteries increases the average LCOE to three to four times the average residential retail rate but pathway still maintains an economic advantage over the hydrogen pathway for lower transmission distances. At certain transmission distances, the amount of line-pack can provide energy storage comparable to necessary daily shifting capacities. The value quantified as avoided battery installations puts the hydrogen pathway LCOE on par with the electric case at transmission distances under 200 miles.

When seasonal storage is necessary, the LCOE of the electric pathway increases several orders of magnitude becoming impractical whilst the hydrogen pathway only marginally increases with the benefit of cheaper underground hydrogen storage and pipeline line-pack when more storage capacity is necessary. Majority of the costs in the hydrogen pathway are from the electrolyzer and fuel cell, but the advantage is their capacity does not change significantly with transmission distances. Consequently, the lower pipeline losses and necessary compressor work has efficiency benefits over the

ohmic losses in the power line case. Corona losses that also typically occur in high voltage transmission lines are not considered in this work.

6. Conclusions

The major findings of this research lead to the conclusions and summary statements as follows:

1. **If can solar PV electricity can be directly used, it is cheaper than using biogas in an existing cogeneration plant to achieve higher renewable electricity supply levels.**

In this analysis only cost of the biogas fuel itself for producing electricity in existing gas turbines is considered. At 6 $/MMBtu this translates to roughly 64 $/MWh electricity. If considering the variable O&M costs for necessary hardware this figure will increase. At the assumed distributed lifespan and PV prices (which are expected to continue to improve) the LCOE of these are in the 65-70 $/MWh range. In addition, even though both could be considered renewable electricity, the biogas case will still have on-site emissions which would arguably require additional carbon offsets. PV solar prices are also expected to be much less volatile than biogas prices

The decision to implementing storage and even higher levels of distributed PV will depend on the average price achievable from each campus. For every campus, the average LCOE for the BESS only case falls below 150 $/MWh. In some cases this value is falls under 100 $/MWh when most of the PV is used directly, being quite competitive with electricity rates that campuses already pay for.

2. **Near maximum technical on-campus PV amounts with storage alone are insufficient for meeting electrical loads in the research university campus setting.**

The simulated storage scenarios for UCM are above 88% RES, UCSB roughly above 68% (excludes renewable portion of imports). Urban campuses, UCB, UCLA, and UCSF

struggle to reach 50% with on-campus resources. Though the UC campuses may have higher energy usage buildings for research usages, the remaining spaces are mostly offices and residential settings—providing a reference for the limitations of distributed resources in urban and suburban settings. Even more rural campuses UCD, UCR, and UCSB only reach 48%, 58%, 75% RES with distributed solar and storage. If the 40% fraction of natural gas usage replaced by renewable biogas increases to 100% an argument for 100% clean electricity could be made but additional resources would still be needed to justify a carbon neutral claim.

3. **UCSC and UCSD achieve slightly higher RES% in scenarios with P2G storage than the battery only scenario at comparable costs.**

These two campuses satisfy a majority of campus load with existing gas turbines. In the battery only case, some PV generated electricity is curtailed while in the P2G only case, hydrogen can be generated and injected into the cogeneration fuel stream. This would technically increase the gas turbine electricity renewable attribute from 40% to 41.7%. Utilization of hydrogen in this way allows larger installations of electrolyzers by mitigating a decreasing capacity factor. Similarly, because UCSD has cogeneration assets to meet most of the electric load, it must operate at minimum loads to accommodate a greater amount of PV installations. This results in less residual load that must be meet from storage during the night. Consequently, the battery does not cycle as often as when implemented in no-cogeneration campuses, decreasing throughput, and increasing the LCOE for the battery only case.

4. No-cogeneration campuses benefit the most by deploying an only battery system. The exception is UCM which achieves RES over 90% in all cases in which the hybrid scenarios and P2G only cases achieve notably higher RES%.

Battery only storage systems excel in settings in which it can be cycled daily. If both storage technologies had the opportunity to cycle daily, the higher roundtrip efficiency technology would likely be favored at current modeled costs. At higher RES% levels, seasonal peaks in demand and lower PV generation levels require some seasonal shifting in which large amounts of batteries at low capacity factors become expensive. P2G achieves higher RES% at more reasonable costs due to ability to decouple power and energy capacity and the storage capacity cost being orders of magnitude lower than batteries. Though having a lower roundtrip efficiency, it is still found for the same amount of generation resources a P2G only case results in higher RES% than battery only case. Economically speaking, taking advantage of both technologies achieves an even higher RES% for resulting in a LCOE 8% higher than the battery only LCOE (at hydrogen storage capacity of 0.8 $/kWh).

5. A 4 $/kWh hydrogen storage capacity cost in the distributed setting would result in comparable levelized cost of storage to the battery pathway.

This is best communicated by Figure 17. At 4 $/kWh majority of points for both BESS only and P2G only cases fall between 150 and 250 $/MWh LCOS. As the hydrogen storage component, electrolyzer, or fuel cell cost decreases, the cost to store electricity could reach parity with the BESS system. This is partly due to degradation modeled by

operation hours for electrolyzers and fuel cells and the advantage this has at lower capacity factors. Utilization of the existing gas grid is an option that needs to be explored to confirm these low costs.

6. **Delivering renewable centrally-generated PV electricity directly to load through the traditional electric pathway is cheaper than the hydrogen pathway that needs to be re-electrified.**

We have considered a scenario in which a fixed amount generation must be delivered and another scenario in which the average utilization factor of the transmission medium are kept constant. In both cases, the LCOE of the electric pathway is about 600 $/MWh whereas the LCOE for the hydrogen pathway is between 1000 and 1200 $/MWh. Note that these values are higher than distributed PV generation due to transmission losses and the cost of additional transmission components.

7. **At low transmission utilization factors, moving energy around as hydrogen in a pipeline is cheaper than moving electricity through power lines. As utilization factor increases past 30 percent, the cost associated with powering compressors begins to outweigh the capital expenditures of the electrical pathways. (This does not account for the inherent benefit of a cheaper distribution system and innate storage for the gas pathway.)**

In high renewable energy penetration future, many remote sites will probably be utilized to install massive amounts of central PV and wind. The highest voltage power lines and largest pipelines run North and South through California. These assets are highly utilized and serve as a highway for electrons. On the other hand, spur-lines which connect

renewable generation projects to this highway typically have much lower utilization factors. This suggests the idea of connecting utility-scale generation projects to the backbone via pipeline and subsequently re-electrified for longer distance transmission. Similarly, if interstate energy transfer occurs only a quarter of the time, this may suggest that energy transmission is cheaper as hydrogen gas than electricity. One should also consider that despite higher cost, the gas transmission system has advantages such as storage addressed in the next point.

8. **Hydrogen pipelines may double as a storage asset rather than simply a transmission asset. When accounting for avoided costs from utilizing modest lengths of pipeline storage, centralized hydrogen pipeline energy delivery to re-electrified sub-transmission achieves lower levelized system costs than the traditional electric pathway that needs battery energy storage systems.**

In the analyses, the entirety of the pipeline line-pack storage value is not realized. By considering the storage capacity of line-pack one would be able to suggest an avoided cost of installing battery energy storage and results in a much lower LCOE—in some cases below zero. This suggests that when centrally generated renewables can meet load, the preferred pathway is electric. However, once the system requires more and more storage for higher renewable penetration levels, utilizing the gas grid system has enormous economic value. This suggests that the future of 100% renewable electricity in California would require the orchestration of a storage electricity and gas grid storage assets to achieve lower total system costs. Figure 36 shows that a 100-mile 36" pipeline could

provide enough energy storage to shift energy for as much as 10 times the simulated PV capacity.

7. References

[1] S. J. Davis, L. Cao, K. Caldeira, and M. I. Hoffert, "Rethinking wedges," *Environmental Research Letters*, vol. 8, no. 1. Institute of Physics Publishing, 2013.

[2] "Renewable capacity highlights," 2019.

[3] "Electric Generation Capacity & Energy." [Online]. Available: http://www.energy.ca.gov/almanac/electricity_data/electric_generation_capacity.html. [Accessed: 05-May-2018].

[4] "Energy storage." [Online]. Available: https://www.iea.org/tcep/energyintegration/energystorage/. [Accessed: 24-Oct-2019].

[5] A. Evans, V. Strezov, and T. J. Evans, "Assessment of utility energy storage options for increased renewable energy penetration," *Renewable and Sustainable Energy Reviews*, vol. 16, no. 6. pp. 4141–4147, Aug-2012.

[6] A. Pina, C. A. Silva, and P. Ferrão, "High-resolution modeling framework for planning electricity systems with high penetration of renewables," *Appl. Energy*, vol. 112, pp. 215–223, 2013.

[7] M. I. Alizadeh, M. Parsa Moghaddam, N. Amjady, P. Siano, and M. K. Sheikh-El-Eslami, "Flexibility in future power systems with high renewable penetration: A review," *Renewable and Sustainable Energy Reviews*, vol. 57. Elsevier Ltd, pp. 1186–1193, 01-May-2016.

[8] P. Denholm and M. Hand, "Grid flexibility and storage required to achieve very high penetration of variable renewable electricity," *Energy Policy*, vol. 39, no. 3, pp. 1817–1830, Mar. 2011.

[9] J. Dong, F. Gao, X. Guan, Q. Zhai, and J. Wu, "Storage-Reserve Sizing with Qualified Reliability for Connected High Renewable Penetration Micro-Grid," *IEEE Trans. Sustain. Energy*, vol. 7, no. 2, pp. 732–743, Apr. 2016.

[10] "California ISO - Managing Oversupply." [Online]. Available: http://www.caiso.com/informed/Pages/ManagingOversupply.aspx#dailyCurtailment. [Accessed: 30-May-2019].

[11] T. T. Mai *et al.*, "Electrification Futures Study: Scenarios of Electric Technology Adoption and Power Consumption for the United States," Golden, CO (United States), Jun. 2018.

[12] S. Ebrahimi, M. Mac Kinnon, and J. Brouwer, "California end-use electrification impacts on carbon neutrality and clean air," *Appl. Energy*, vol. 213, pp. 435–449, Mar. 2018.

[13] A. Mahone, C. Li, Z. Subin, M. Sontag, G. Mantegna, and A. Karolides, "Residential Building Electrification in California Consumer economics, greenhouse gases and grid impacts," 2019.

[14] CEC, "California Energy Commission – Tracking Progress- Renewable Energy Overview," vol. 1078, no. August, pp. 1–30, 2017.

[15] "Bill Text - SB-350 Clean Energy and Pollution Reduction Act of 2015." [Online]. Available: https://leginfo.legislature.ca.gov/faces/billNavClient.xhtml?bill_id=201520160SB350. [Accessed: 23-Aug-2018].

[16] K. Watson, *Senate Bill No. 969*, no. 969. 2017.

[17] "Google And Apple Lead The Corporate Charge Toward 100% Renewable Energy." [Online]. Available: https://www.forbes.com/sites/energyinnovation/2018/04/12/google-and-apple-lead-the-corporate-charge-toward-100-renewable-energy/#57e439bb1b23. [Accessed: 25-Oct-2019].

[18] "Companies - RE100." [Online]. Available: http://there100.org/companies. [Accessed: 25-Oct-2019].

[19] "Data and Statistics - IRENA REsource." [Online]. Available: http://resourceirena.irena.org/gateway/dashboard/?topic=4&subTopic=18. [Accessed: 23-Aug-2018].

[20] R. Fu *et al.*, "U . S . Solar Photovoltaic System Cost Benchmark : Q1 2017 U . S . Solar Photovoltaic System Cost Benchmark : Q1 2017," no. September, 2017.

[21] "How much does it cost to generate electricity with different types of power plants? - FAQ - U.S. Energy Information Administration (EIA)." [Online]. Available: https://www.eia.gov/tools/faqs/faq.php?id=19&t=3. [Accessed: 24-Aug-2018].

[22] "Energy - United Nations Sustainable Development." [Online]. Available: https://www.un.org/sustainabledevelopment/energy/. [Accessed: 23-Aug-2018].

[23] "Ergebnisse der Sondierungsgespräche von CDU, CSU und SPD Finale Fassung," 2018.

[24] "IEA - China." [Online]. Available: https://www.iea.org/policiesandmeasures/pams/china/name-161254-en.php?s=dHlwZT1yZSZzdGF0dXM9T2s,&return=PG5hdiBpZD0iYnJlYWRjcnVtYiI-PGEgaHJlZj0iLyI-SG9tZTwvYT4gJnJhcXVvOyA8YSBocmVmPSIvcG9saWNpZXNhbmRtZWFzdXJlcy8iPlBvbGljaWVzIGFuZCBNZWFzdXJlczwvYT4gJnJhcXV. [Accessed: 23-Aug-2018].

[25] "China steps up green energy push with revised renewable target of 35 per cent by 2030 | South China Morning Post." [Online]. Available: https://www.scmp.com/news/china/politics/article/2165831/china-steps-green-energy-push-revised-renewable-target-35-2030. [Accessed: 25-Oct-2019].

[26] A. Ozarslan, "Large-scale hydrogen energy storage in salt caverns," *Int. J. Hydrogen Energy*, vol. 37, no. 19, pp. 14265–14277, Oct. 2012.

[27] Sandia, "Doe Global Energy Storage Database," *Database*, p. 1464 projects, 2016.

[28] M. R. Shaner, S. J. Davis, N. S. Lewis, and K. Caldeira, "Geophysical constraints on the reliability of solar and wind power in the United States," *Energy Environ. Sci.*, pp. 914–925, 2018.

[29] IEC, "Electrical Energy Storage - White Paper," *Int. Electrotech. Comm.*, pp. 1–78, 2011.

[30] J. Gustavsson, "Energy Storage Technology Comparison," 2016.

[31] J. P. Maton, L. Zhao, and J. Brouwer, "Dynamic modeling of compressed gas energy storage to complement renewable wind power intermittency," *Int. J. Hydrogen Energy*, vol. 38, no. 19, pp. 7867–7880, 2013.

[32] California Distributed Generation Statistics, "Distributed Generation Interconnection Program Data." [Online]. Available: https://www.californiadgstats.ca.gov/downloads/. [Accessed: 02-Jun-2019].

[33] "California ISO - Clean, green grid." [Online]. Available: http://www.caiso.com/informed/Pages/CleanGrid/default.aspx. [Accessed: 24-Oct-2019].

[34] R. B. C. Weisenmiller *et al.*, "BUILDING ENERGY EFFICIENCY STANDARDS FOR RESIDENTIAL AND NONRESIDENTIAL BUILDINGS."

[35] A. Ramdas, K. Mccabe, P. Das, and B. Sigrin, "California Time-of-Use (TOU) Transition: Effects on Distributed Wind and Solar Economic Potential," 2019.

[36] "Powerwall | The Tesla Home Battery." [Online]. Available: https://www.tesla.com/powerwall. [Accessed: 24-Oct-2019].

[37] C. Schaber, P. Mazza, and R. Hammerschlag, "Utility-scale storage of renewable energy," *Electr. J.*, vol. 17, no. 6, pp. 21–29, Jul. 2004.

[38] A. Poullikkas, "A comparative overview of large-scale battery systems for electricity storage," *Renew. Sustain. Energy Rev.*, vol. 27, pp. 778–788, Nov. 2013.

[39] B. Dunn, B. Dunn, H. Kamath, and J. Tarascon, "Electrical energy storage for the gridfor the Grid : A Battery of choices," *Sci. Mag.*, vol. 334, no. 6058, pp. 928–936, 2011.

[40] "Total System Electric Generation." [Online]. Available: http://www.energy.ca.gov/almanac/electricity_data/total_system_power.html. [Accessed: 23-Aug-2018].

[41] P. Denholm, M. O'connell, G. Brinkman, and J. Jorgenson, "Overgeneration from Solar Energy in California: A Field Guide to the Duck Chart," 2013.

[42] "Energy and environmental goals drive change," 2016.

[43] "California ISO - Regulatory." [Online]. Available: http://www.caiso.com/rules/Pages/Regulatory/Default.aspx. [Accessed: 30-Aug-2018].

[44] CAISO, "2018 Summer Loads & Resources Assessment," 2018.

[45] G. Guandalini, M. Robinius, T. Grube, S. Campanari, and D. Stolten, "Long-term power-to-gas potential from wind and solar power: A country analysis for Italy," *Int. J. Hydrogen Energy*, vol. 42, no. 19, pp. 13389–13406, May 2017.

[46] M. Jentsch, T. Trost, and M. Sterner, "Optimal Use of Power-to-Gas Energy Storage Systems in an 85% Renewable Energy Scenario," *Energy Procedia*, vol. 46, pp. 254–261, Jan. 2014.

[47] B. P. Heard, B. W. Brook, T. M. L. Wigley, and C. J. A. Bradshaw, "Burden of proof : A comprehensive review of the feasibility of 100 % renewable-electricity systems," *Renew. Sustain. Energy Rev.*, vol. 76, no. April, pp. 1122–1133, 2017.

[48] B. Tarroja, L. Zhang, V. Wifvat, B. Shaffer, and S. Samuelsen, "Assessing the stationary energy storage equivalency of vehicle-to-grid charging battery electric vehicles," *Energy*, vol. 106, pp. 673–690, 2016.

[49] M. Muratori and G. Rizzoni, "Residential Demand Response: Dynamic Energy Management and Time-Varying Electricity Pricing," *IEEE Trans. Power Syst.*, vol. 31, no. 2, pp. 1108–1117, 2016.

[50] D. Wang, M. Muratori, J. Eichman, M. Wei, S. Saxena, and C. Zhang, "Quantifying the flexibility of hydrogen production systems to support large-scale renewable energy integration," *J. Power Sources*, vol. 399, no. July, pp. 383–391, 2018.

[51] G. Guandalini, S. Campanari, and M. C. Romano, "Power-to-gas plants and gas turbines for improved wind energy dispatchability: Energy and economic assessment," *Appl. Energy*, vol. 147, pp. 117–130, Jun. 2015.

[52] M. Doroshenko and C. Rosenberg, "Poster : Flattening the Duck Curve Using Grid-friendly Solar Panel Orientation," pp. 375–377.

[53] H. O. R. Howlader, M. Furukakoi, H. Matayoshi, and T. Senjyu, "Duck curve problem solving strategies with thermal unit commitment by introducing pumped storage hydroelectricity & renewable energy," *Proc. Int. Conf. Power Electron. Drive Syst.*, vol. 2017-Decem, no. December, pp. 502–506, 2018.

[54] "CAISO Business Practice Manual Change Management: Definitions and Acronyms BPM." [Online]. Available: https://bpmcm.caiso.com/Pages/BPMDetails.aspx?BPM=Definitions and Acronyms. [Accessed: 23-Oct-2019].

[55] V. N. Ave and S. Francisco, "CPUC SETS ENERGY STORAGE GOALS FOR UTILITIES," pp. 1–2, 2014.

[56] K. Bradbury, L. Pratson, and D. Patiño-Echeverri, "Economic viability of energy storage systems based on price arbitrage potential in real-time U.S. electricity markets," *Appl. Energy*, vol. 114, pp. 512–519, 2014.

[57] U. Energy Information Administration, "U.S. Battery Storage Market Trends," 2018.

[58] X. Luo, J. Wang, M. Dooner, and J. Clarke, "Overview of current development in electrical energy storage technologies and the application potential in power system operation," *Appl. Energy*, vol. 137, pp. 511–536, 2015.

[59] B. Zakeri and S. Syri, "Electrical energy storage systems: A comparative life cycle cost analysis," *Renew. Sustain. Energy Rev.*, vol. 42, pp. 569–596, 2015.

[60] D. Pelzer, D. Ciechanowicz, and A. Knoll, "Energy arbitrage through smart scheduling of battery energy storage considering battery degradation and electricity price forecasts," *IEEE PES Innov. Smart Grid Technol. Conf. Eur.*, pp. 472–477, 2016.

[61] R. Walawalkar, J. Apt, and R. Mancini, "Economics of electric energy storage for energy arbitrage and regulation in New York," *Energy Policy*, vol. 35, no. 4, pp. 2558–2568, 2007.

[62] G. Mulder, D. Six, B. Claessens, T. Broes, N. Omar, and J. Van Mierlo, "The dimensioning of PV-battery systems depending on the incentive and selling price conditions," *Appl. Energy*, vol. 111, pp. 1126–1135, 2013.

[63] E. McKenna, M. McManus, S. Cooper, and M. Thomson, "Economic and environmental impact of lead-acid batteries in grid-connected domestic PV systems," *Appl. Energy*, vol. 104, pp. 239–249, 2013.

[64] G. Graditi, M. G. Ippolito, E. Telaretti, and G. Zizzo, "Technical and economical assessment of distributed electrochemical storages for load shifting applications: An Italian case study," *Renew. Sustain. Energy Rev.*, vol. 57, pp. 515–523, 2016.

[65] H. T. Le, S. Santoso, and T. Q. Nguyen, "Augmenting wind power penetration and grid voltage stability limits using ESS: Application design, sizing, and a case study," *IEEE Trans. Power Syst.*, vol. 27, no. 1, pp. 161–171, 2012.

[66] T. Kamal and S. Z. Hassan, "Energy Management and Simulation of

Photovoltaic/Hydrogen/Battery Hybrid Power System," *Adv. Sci. Technol. Eng. Syst. J.*, vol. 1, no. 2, pp. 11–18, 2016.

[67] H. Tebibel and S. Labed, "Design and sizing of stand-alone photovoltaic hydrogen system for HCNG production," *Int. J. Hydrogen Energy*, vol. 39, no. 8, pp. 3625–3636, 2014.

[68] L. Dusonchet, M. G. Ippolito, E. Telaretti, G. Zizzo, and G. Graditi, "An optimal operating strategy for combined RES-based generators and electric storage systems for load shifting applications," *Int. Conf. Power Eng. Energy Electr. Drives*, vol. 5, pp. 552–557, 2013.

[69] A. Shcherbakova, A. Kleit, and J. Cho, "The value of energy storage in South Korea's electricity market: A Hotelling approach," *Appl. Energy*, vol. 125, pp. 93–102, 2014.

[70] A. Zucker and T. Hinchliffe, "Optimum sizing of PV-attached electricity storage according to power market signals - A case study for Germany and Italy," *Appl. Energy*, vol. 127, pp. 141–155, 2014.

[71] R. Sioshansi, P. Denholm, T. Jenkin, and J. Weiss, "Estimating the value of electricity storage in PJM: Arbitrage and some welfare effects," *Energy Econ.*, vol. 31, no. 2, pp. 269–277, 2009.

[72] R. Dufo-López, J. L. Bernal-Agustín, and J. A. Domínguez-Navarro, "Generation management using batteries in wind farms: Economical and technical analysis for Spain," *Energy Policy*, vol. 37, no. 1, pp. 126–139, 2009.

[73] D. Parra and M. K. Patel, "Techno-economic implications of the electrolyser technology and size for power-to-gas systems," *Int. J. Hydrogen Energy*, vol. 41, no. 6, pp. 3748–3761, Feb. 2016.

[74] U. Mukherjee, S. Walker, M. Fowler, and A. Elkamel, "Power-to-gas in a demand-response market," *Int. J. Environ. Stud.*, vol. 73, no. 3, pp. 390–401, 2016.

[75] A. Zucker, T. Hinchliffe, and A. Spisto, *Assessing storage value in electricity markets a literature review*. 2013.

[76] M. L. Awad *et al.*, "Economic Assessment of Transmission Upgrades: Application of the California ISO Approach," *Restructured Electr. Power Syst. Anal. Electr. Mark. with Equilib. Model.*, no. Section II, pp. 241–270, 2010.

[77] M. Naumann, R. C. Karl, C. N. Truong, A. Jossen, and H. C. Hesse, "Lithium-ion battery cost analysis in PV-household application," *Energy Procedia*, vol. 73, pp. 37–47, 2015.

[78] J. Z. J. Zhu, G. Jordan, and S. Ihara, "The market for spinning reserve and its impacts on energy prices," *2000 IEEE Power Eng. Soc. Winter Meet. Conf. Proc. (Cat. No.00CH37077)*, vol. 2, no. c, pp. 1202–1207, 2000.

[79] B. F. Hobbs and F. A. M. Rijkers, "Price responses in a mixed transmission pricing system - part I : Formulation," *IEEE Trans. Power Syst.*, vol. 19, no. 2, pp. 707–717, 2004.

[80] J. Eyer and G. Corey, "Energy Storage for the Electricity Grid : Benefits and Market Potential Assessment Guide," *Contract*, vol. 321, no. February, p. 232, 2010.

[81] D. Rastler, "Electricity Energy Storage Technology Options," p. 170, 2010.

[82] D. Feldman, R. Margolis, P. Denholm, and J. Stekli, "Exploring the Potential Competitiveness of Utility-Scale Photovoltaics plus Batteries with Concentrating Solar Power, 2015-2030," 2016.

[83] T. M. Gür, "Review of electrical energy storage technologies, materials and systems: Challenges and prospects for large-scale grid storage," *Energy and Environmental Science*, vol. 11, no. 10. Royal Society of Chemistry, pp. 2696–2767, 01-Oct-2018.

[84] J. W. Choi and D. Aurbach, "Promise and reality of post-lithium-ion batteries with high energy densities," *Nature Reviews Materials*, vol. 1. Nature Publishing Group, 31-Mar-2016.

[85] M. Sufyan, N. A. Rahim, M. M. Aman, C. K. Tan, and S. R. S. Raihan, "Sizing and applications of battery energy storage technologies in smart grid system: A review," *J. Renew. Sustain. Energy*, vol. 11, no. 1, Jan. 2019.

[86] S. Bahramirad, W. Reder, and A. Khodaei, "Reliability-constrained optimal sizing of energy storage system in a microgrid," *IEEE Trans. Smart Grid*, vol. 3, no. 4, pp. 2056–2062, 2012.

[87] G. Carpinelli, F. Mottola, and D. Proto, "Probabilistic sizing of battery energy storage when time-of-use pricing is applied," *Electr. Power Syst. Res.*, vol. 141, pp. 73–83, Dec. 2016.

[88] C. Ju and P. Wang, "Energy management system for microgrids including batteries with degradation costs," in *2016 IEEE International Conference on Power System Technology, POWERCON 2016*, 2016.

[89] E. Zarezadeh, H. Fakharzadegan, A. Ghorbani, and H. Fathabadi, "A probabilistic approach to determine PV array size and battery capacity used in grid-connected PV systems," in *ICEE 2015 - Proceedings of the 23rd Iranian Conference on Electrical Engineering*, 2015, vol. 10, pp. 1533–1538.

[90] "OASIS - OASIS Prod - PUBLIC - 0." [Online]. Available: http://oasis.caiso.com/mrioasis/logon.do. [Accessed: 30-May-2019].

[91] C. Lu, H. Xu, X. Pan, and J. Song, "Optimal sizing and control of battery energy storage system for peak load shaving," *Energies*, vol. 7, no. 12, pp. 8396–8410, 2014.

[92] B. Mohammadi-Ivatloo and F. Jabari, "Operation, Planning, and Analysis of Energy Storage Systems in Smart Energy Hubs," *Operation, Planning, and Analysis of Energy Storage Systems in Smart Energy Hubs*. pp. v–vii, 2018.

[93] A. Lewandowska-Bernat and U. Desideri, "Opportunities of Power-to-Gas technology," in *Energy Procedia*, 2017, vol. 105, pp. 4569–4574.

[94] J. Ma, Q. Li, M. Kühn, and N. Nakaten, "Power-to-gas based subsurface energy storage: A review," *Renewable and Sustainable Energy Reviews*, vol. 97. Elsevier Ltd, pp. 478–496, 01-Dec-2018.

[95] J. Vandewalle, K. Bruninx, and W. D'Haeseleer, "Effects of large-scale power to gas conversion on the power, gas and carbon sectors and their interactions," *Energy Convers. Manag.*, vol. 94, pp. 28–39, 2015.

[96] O. S. Buchholz, A. G. J. Van Der Ham, R. Veneman, D. W. F. Brilman, and S. R. A. Kersten, "Power-to-Gas: Storing surplus electrical energy a design study," in *Energy Procedia*, 2014, vol. 63, pp. 7993–8009.

[97] E. Frank, J. Gorre, F. Ruoss, and M. J. Friedl, "Calculation and analysis of efficiencies and annual performances of Power-to-Gas systems," *Appl. Energy*, vol. 218, pp. 217–231, May 2018.

[98] M. De Saint Jean, P. Baurens, and C. Bouallou, "Parametric study of an efficient renewable

power-to-substitute-natural-gas process including high-temperature steam electrolysis," *Int. J. Hydrogen Energy*, vol. 39, no. 30, pp. 17024–17039, Oct. 2014.

[99] G. J. May, A. Davidson, and B. Monahov, "Lead batteries for utility energy storage: A review," *Journal of Energy Storage*, vol. 15. Elsevier Ltd, pp. 145–157, 01-Feb-2018.

[100] P. Colbertaldo, S. B. Agustin, S. Campanari, and J. Brouwer, "Impact of hydrogen energy storage on California electric power system: Towards 100% renewable electricity," *Int. J. Hydrogen Energy*, vol. 44, no. 19, pp. 9558–9576, 2019.

[101] "Solar Maps | Geospatial Data Science | NREL." [Online]. Available: https://www.nrel.gov/gis/solar.html. [Accessed: 01-Dec-2019].

[102] "Facilities Inventory System at UCI." [Online]. Available: https://fdx.cap.uci.edu/UCIFDX/cfapps/FDXStart.cfm?auth=ucinet&auth=ucinet. [Accessed: 01-Dec-2019].

[103] "Assessing UC and CSU Enrollment and Capacity." [Online]. Available: https://lao.ca.gov/Publications/Report/3532. [Accessed: 01-Dec-2019].

[104] I. Penn, "PG&E Begins Power Shut-Off to 179,000 California Customers - The New York Times," *New York Times*, 2019. [Online]. Available: https://www.nytimes.com/2019/10/23/business/energy-environment/california-power.html. [Accessed: 14-Nov-2019].

[105] California Energy Commission, "Status of all Projects," *Webpage*, 2016. [Online]. Available: http://www.energy.ca.gov/sitingcases/all_projects.html. [Accessed: 04-May-2018].

[106] "California ISO - Todays Outlook." [Online]. Available: http://www.caiso.com/TodaysOutlook/Pages/default.aspx. [Accessed: 05-Sep-2019].

[107] M. R. Islam, Y. Guo, and J. Zhu, "Power converters for small- to large-scale photovoltaic power plants," *Green Energy Technol.*, vol. 182, pp. 17–49, 2014.

[108] B. Shiva Kumar and K. Sudhakar, "Performance evaluation of 10 MW grid connected solar photovoltaic power plant in India," *Energy Reports*, vol. 1, pp. 184–192, Nov. 2015.

[109] Y. Aldali, D. Henderson, and T. Muneer, "A 50 MW very large-scale photovoltaic power plant for Al-Kufra, Libya: Energetic, economic and environmental impact analysis," *Int. J. Low-Carbon Technol.*, vol. 6, no. 4, pp. 277–293, Dec. 2011.

[110] "California Electric Transmission Line." [Online]. Available: https://cecgis-caenergy.opendata.arcgis.com/datasets/california-electric-substation/data. [Accessed: 11-May-2018].

[111] "California Electric Transmission Line." [Online]. Available: https://cecgis-caenergy.opendata.arcgis.com/datasets/california-electric-transmission-line?geometry=-124.776%2C34.753%2C-114.482%2C37.851. [Accessed: 11-May-2018].

[112] L. C. Area, "Local Capacity Area Substation List," no. 4, 2011.

[113] J. Baker, J. Cross, and I. Lloyd, "CLNR: Lessons Learned Report: Electrical Energy Storage," *Cust. Netw. Revolut. - North. Powergrid*, no. December, 2014.

[114] C. E. Commission, "California Solar Energy Statistics & Data," 2015. [Online]. Available: http://www.energy.ca.gov/almanac/renewables_data/solar/. [Accessed: 04-May-2018].

[115] Southern California Edison, "Publication of SCE's Initial Unit Cost Guide Pursuant to D.16-06-052," 2016.

[116] CPUC, "Rule 21 Interconnection," 2018. [Online]. Available: http://www.cpuc.ca.gov/Rule21/. [Accessed: 18-Sep-2018].

[117] "Who We Are | About Us | Home - SCE." [Online]. Available: https://www.sce.com/wps/portal/home/about-us/who-we-are/!ut/p/b1/hc89D4IwEAbg3-LASk8LiG4lEiiDSiABuhgwWEiAklLl7wuGxcSP297L8yZ3iKEUsS5_1DxXtejyZs7Muqxtj_g0AurFhgnU2Wyx51Acu-YEsgnAlyHwr58g9oscDGMBOw9cPzjNIMRAcQjHiBAMYC3gxw0BYrwRxeufjHQFtjlisryVspT6XU7rSql-2G. [Accessed: 11-May-2018].

[118] "SCE2017PerUnitCostGuide." .

[119] R. Pletka, J. Khangura, A. Rawlines, E. Waldren, and D. Wilson, "Capital Costs for Transmission and Substations," *West. Electr. Coord. Counc.*, no. February, p. 35, 2014.

[120] "Calendar Years 2016 – 2025 Per-Acre Rent Schedule," p. 2025, 2018.

[121] N. Parker, "Using Natural Gas Transmission Pipeline Costs to Estimate Hydrogen Pipeline Costs," p. 86, 2004.

[122] American Electric Power, "American Electric Power Transmission Facts," 2008.

[123] "SCE CONCEPTUAL TRANSMISSION REQUIREMENTS AND COSTS FOR INTEGRATING RENEWABLE RESOURCES Southern California Edison Company," 2007.

[124] "RIVERSIDE TRANSMISSION RELIABILITY PROJECT (RTRP) 230 KV UNDERGROUND ALTERNATIVES DESKTOP STUDY JULY 2015."

[125] "CONDUCTOR DATA SHEET ALUMINUM CONDUCTORS STEEL REINFORCED (ACSR)."

[126] A. Baggini, "Power transformers – Introduction to measurement of losses," 2016.

[127] S. B. Sadati, A. Tahani, B. Darvishi, M. Dargahi, and H. Yousefi, "Comparison of distribution transformer losses and capacity under linear and harmonic loads," *PECon 2008 - 2008 IEEE 2nd Int. Power Energy Conf.*, no. PECon 08, pp. 1265–1269, 2008.

[128] S. Balci, I. Sefa, and N. Altin, "Design and analysis of a 35 kVA medium frequency power transformer with the nanocrystalline core material," *Int. J. Hydrogen Energy*, vol. 42, no. 28, pp. 17895–17909, Jul. 2017.

[129] G. Zini and A. Dalla Rosa, "Hydrogen systems for large-scale photovoltaic plants: Simulation with forecast and real production data," *Int. J. Hydrogen Energy*, vol. 39, no. 1, pp. 107–118, Jan. 2014.

[130] DOE, "Large Power Transformers and the U.S. Electric Grid."

[131] C. Darras, G. Bastien, M. Muselli, P. Poggi, B. Champel, and P. Serre-Combe, "Techno-economic analysis of PV/H2 systems," *Int. J. Hydrogen Energy*, vol. 40, no. 30, pp. 9049–9060, Aug. 2015.

[132] J. E. Dagle and D. R. Brown, "Electric power substation capital costs," Richland, WA, Dec. 1997.

[133] Lazard, "Lazard's levelized cost of storage analysis -- version 4.0," 2018.

[134] "PV Performance Modeling Collaborative | CEC Inverter Test Protocol." [Online]. Available: https://pvpmc.sandia.gov/modeling-steps/dc-to-ac-conversion/cec-inverter-test-protocol/. [Accessed: 28-Oct-2019].

[135] R. Pletka, J. Khangura, A. Rawlines, E. Waldren, and D. Wilson, "Capital Costs for Transmission and Substations," 2014.

[136] Lazard, "Lazard's levelized cost of storage analysis — version 3.0," 2017.

[137] L. I. Langelandsvik, W. Postvoll, B. Aarhus, and K. K. Kaste, "Accurate Calculation of Pipeline Transport Capacity," *Proc. to 24th World Gas Conf.*, 2005.

[138] N. Parker, "Using Natural Gas Transmission Pipeline Costs to Estimate Hydrogen Pipeline Costs," 2004.

[139] "DOE Hydrogen and Fuel Cells Program: DOE H2A Delivery Analysis." [Online]. Available: https://www.hydrogen.energy.gov/h2a_delivery.html. [Accessed: 18-Sep-2018].

[140] J. R. Fekete, J. W. Sowards, and R. L. Amaro, "Economic impact of applying high strength steels in hydrogen gas pipelines," *Int. J. Hydrogen Energy*, vol. 40, no. 33, pp. 10547–10558, Sep. 2015.

[141] "SOCALGAS DIRECT TESTIMONY OF BETH MUSICH (GAS TRANSMISSION OPERATION) October 6, 2017," 2017.

[142] F. Arpino, M. Dell'Isola, G. Ficco, and P. Vigo, "Unaccounted for gas in natural gas transmission networks: Prediction model and analysis of the solutions," *J. Nat. Gas Sci. Eng.*, vol. 17, pp. 58–70, Mar. 2014.

[143] S. C. E. Southern California Gas Company, Pacific Gas & Electric Company, San Diego Gas & Electric Company, Southwest Gas Corporation, City of Long Beach Gas & Oil Department, "2016 CALIFORNIA GAS REPORT Prepared by the California Gas and Electric Utilities," 2014.

[144] Y. Zhao and Z. Rui, "Pipeline compressor station construction cost analysis," *Int. J. Oil, Gas Coal Technol.*, vol. 8, no. 1, p. 41, 2014.

[145] EPA, "Methane Emissions from the Natural Gas Industry, Volume 9: Underground Pipelines," vol. 9, 1996.

[146] M. W. Melaina, O. Antonia, and M. Penev, "Blending Hydrogen into Natural Gas Pipeline Networks: A Review of Key Issues," 2013.

[147] N. A. Hormaza Mejia and J. Brouwer, "Gaseous fuel leakage from natural gas infrastructure," pp. 1–6, 2018.

[148] K. Hedegaard and P. Meibom, "Wind power impacts and electricity storage – A time scale perspective," *Renew. Energy*, vol. 37, no. 1, pp. 318–324, Jan. 2012.

[149] A. S. Lord, P. H. Kobos, and D. J. Borns, "Geologic storage of hydrogen: Scaling up to meet city transportation demands," *Int. J. Hydrogen Energy*, vol. 39, no. 28, pp. 15570–15582, Sep. 2014.

[150] "United States - Maps - U.S. Energy Information Administration (EIA)." [Online]. Available: https://www.eia.gov/state/maps.php?v=Natural Gas. [Accessed: 03-Sep-2019].

[151] G. Saur and C. Ainscough, "U.S. Geographic Analysis of the Cost of Hydrogen from Electrolysis," 2011.

[152] M. L. Jerrett, N. Meshkati, S. A. Perfect, S. J. Traina, M. W. Wara, and C. M. Elder, "Long-Term Viability of Underground Natural Gas Storage in California Non-Voting Ex Officio Steering Committee Members," 2018.

[153] "Fuel Cell Technologies Office Multi-Year Research, Development, and Demonstration Plan - Section 3.2 Hydrogen Delivery," 2015.

[154] A. Amid, D. Mignard, and M. Wilkinson, "Seasonal storage of hydrogen in a depleted natural gas reservoir," *Int. J. Hydrogen Energy*, vol. 41, no. 12, pp. 5549–5558, Apr. 2016.

[155] B. Meng *et al.*, "HYDROGEN EFFECTS ON X80 PIPELINE STEEL UNDER HIGH-PRESSURE NATURAL GAS/HYDROGEN MIXTURES."

[156] A. Körner, "Technology Roadmap - Hydrogen and Fuel Cells," 2015.

[157] L. Bertuccioli, A. Chan, D. Hart, F. Lehner, B. Madden, and E. Standen, "Study on development of water electrolysis in the EU," *LC-GC North*, no. February, 2014.

[158] DOE, "FUEL CELL TECHNOLOGIES OFFICE: Fuel Cells." [Online]. Available: https://www.energy.gov/sites/prod/files/2015/11/f27/fcto_fuel_cells_fact_sheet.pdf. [Accessed: 28-Oct-2019].

[159] A. Le Duigou, A.-G. Bader, J.-C. Lanoix, and L. Nadau, "Relevance and costs of large scale underground hydrogen storage in France," *Int. J. Hydrogen Energy*, vol. 42, no. 36, pp. 22987–23003, Sep. 2017.

[160] C. P. U. Commission, "Report : System Efficiency of California ' s Electric Grid," 2017.

[161] J. H. Eto, "Building Electric Transmission Lines: A Review of Recent Transmission Projects," 2016.

[162] J. Brouwer and A. Director, "Realizing a Renewable Energy Future through Power-to-Gas California Fuel Cell Partnership," 2017.

[163] M. P. Bahrman, "Overview of HVDC transmission," *2006 IEEE PES Power Syst. Conf. Expo. PSCE 2006 - Proc.*, pp. 18–23, 2006.

[164] The University of Texas at Austin Energy Institute, "The Full Cost of Electricity (FCe-): Estimation of Transmission Costs for New Generation."

[165] P. S. C. of Wisconsin, "Underground Electric Transmission Lines," pp. 1–22, 2011.

[166] CEC, "California Natural Gas Pipeline," 2018. [Online]. Available: https://cecgis-caenergy.opendata.arcgis.com/datasets/california-natural-gas-pipeline/data?geometry=-124.289%2C32.276%2C-110.413%2C35.468. [Accessed: 11-May-2018].

Appendix A: Campus PV Numerical Results

Case 1: Building and Parking Lot PV Potential

	Case 1: Maximum Potential				
(MW)	Pessimistic	Lower Bound	Average	Upper Bound	Optimistic
UCB	27.4	30.9	31.6	32.2	35.7
UCLA	40.6	46.1	47.1	48.1	53.6
UCSD	66.1	72.2	73.4	74.5	80.6
UCR	58.4	61.7	62.3	62.9	66.2
UCI	37.9	41.3	42.0	42.6	46.1
UCSB	46.6	51.0	51.8	52.6	57.0
UCSC	24.8	27.2	27.6	28.1	30.4
UCM	29.6	30.4	30.5	30.7	31.5
UCD	68.3	75.8	77.2	78.7	86.2

Case 2: Building and Parking Lot PV Potential with Future Constructions

	Case 2: 50% Parking for New Developments				
(MW)	Pessimistic	Lower Bound	Average	Upper Bound	Optimistic
UCB	21.4	24.8	25.5	26.1	29.6
UCLA	32.4	37.9	38.9	39.9	45.4
UCSD	46.5	52.6	53.7	54.9	61.0
UCR	36.5	39.8	40.4	41.0	44.4
UCI	26.6	30.1	30.7	31.4	34.9
UCSB	33.0	37.4	38.2	39.0	43.4
UCSC	17.6	19.9	20.4	20.8	23.2
UCM	16.5	17.3	17.5	17.6	18.4
UCD	50.8	58.3	59.7	61.2	68.7

Parking Lot Areas for each Campus

Parking Lot Area (ft2)	
UCB	911271
UCLA	1229077
UCSD	2944129
UCR	3282806
UCI	1687316
UCSB	2040886
UCSC	1087954
UCM	1959753
UCD	2624031

Building Rooftop and Parking Lot Total Number of Modules

MPP	0.390	0.478	0.495	0.512	0.600
	Pessimistic	**Lower Bound**	**Average**	**Upper Bound**	**Optimistic**
UCB	61,170	75,048	77,638	80,228	94,107
UCLA	96,785	118,744	122,842	126,940	148,900
UCSD	107,441	131,818	136,367	140,916	165,293
UCR	58,389	71,637	74,109	76,582	89,830
UCI	61,391	75,320	77,919	80,518	94,447
UCSB	77,405	94,968	98,245	101,522	119,085
UCSC	41,334	50,712	52,462	54,212	63,590
UCM	13,877	17,026	17,613	18,201	21,349
UCD	133,148	163,357	168,995	174,632	204,842

Appendix B: Images

Campus Image Used for Rooftop Analysis

UCB

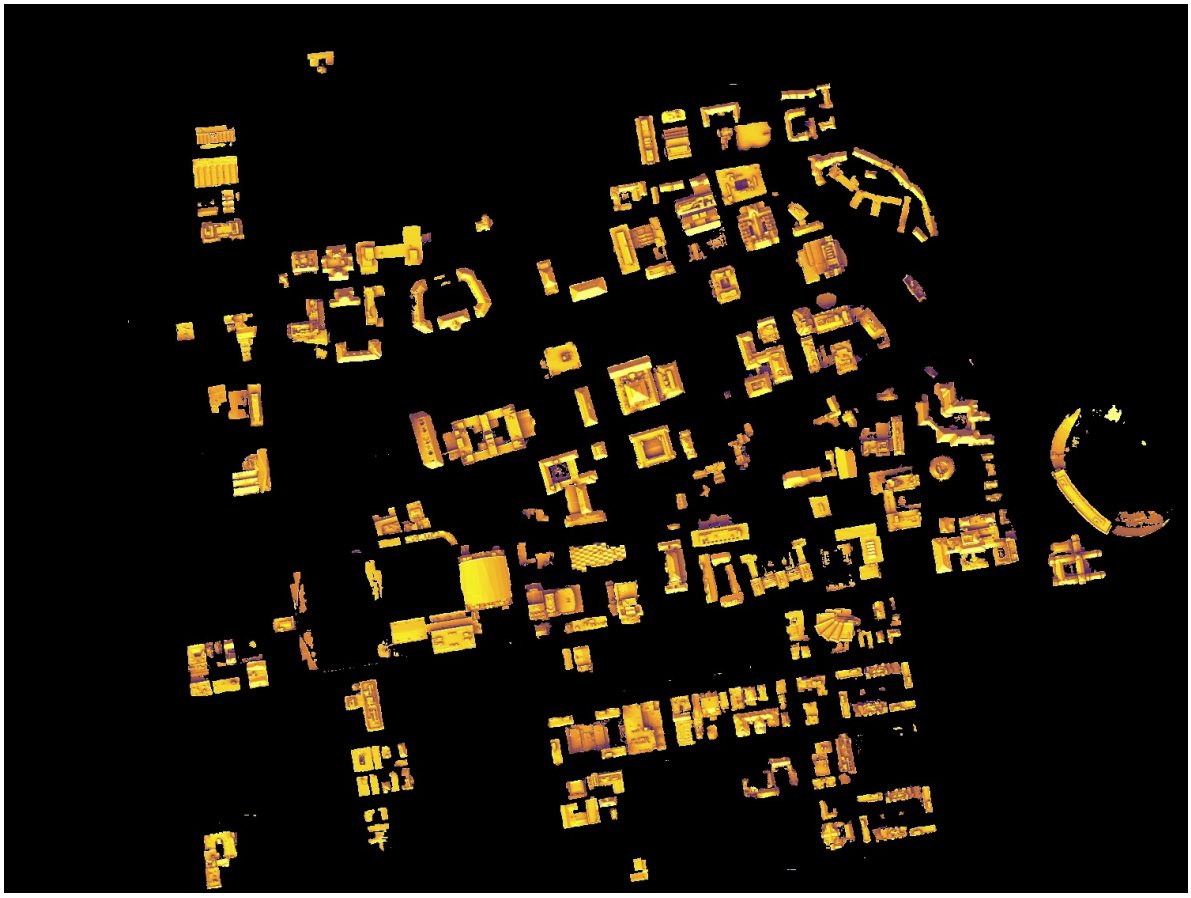

UCD

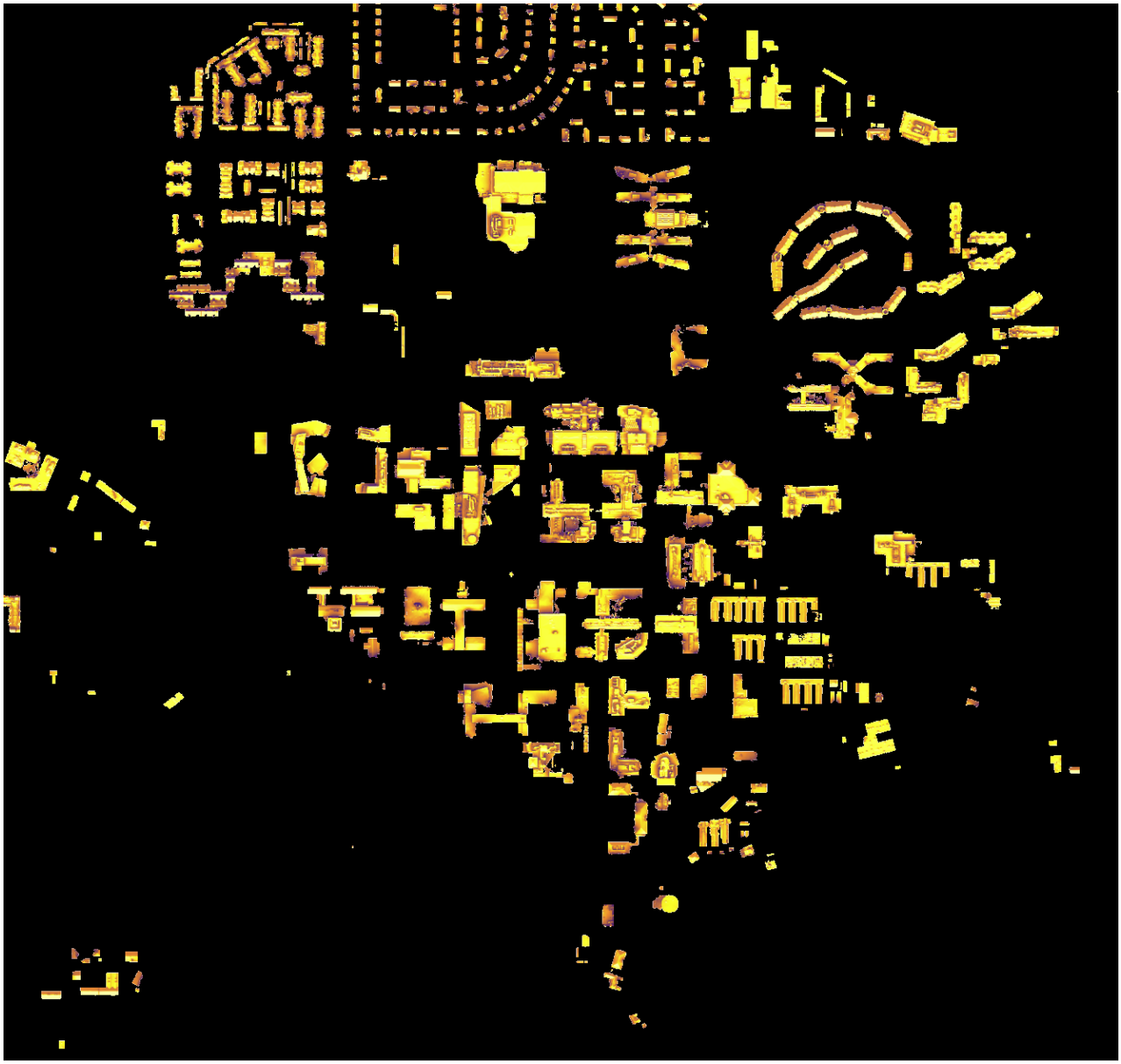

UCI

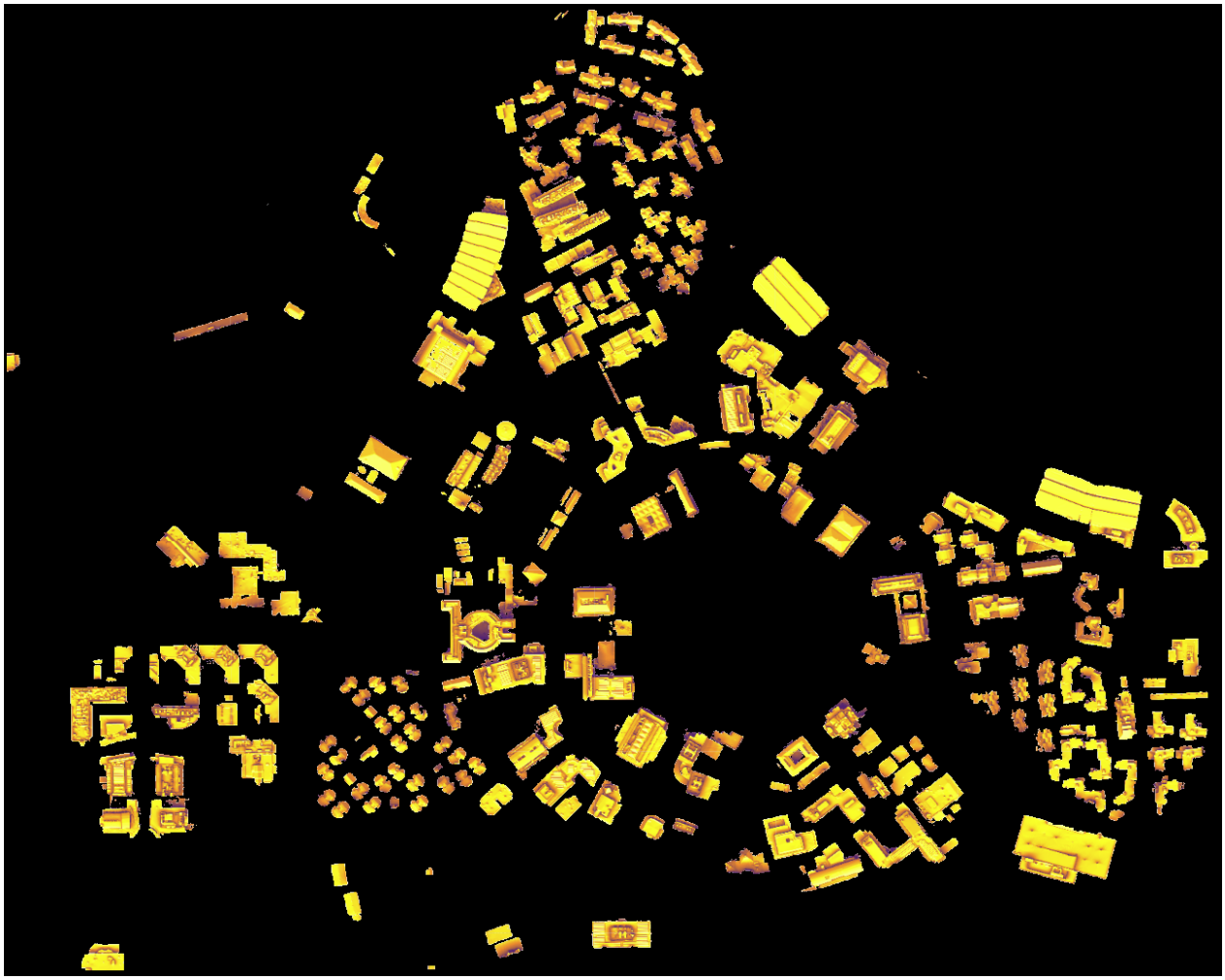

UCLA

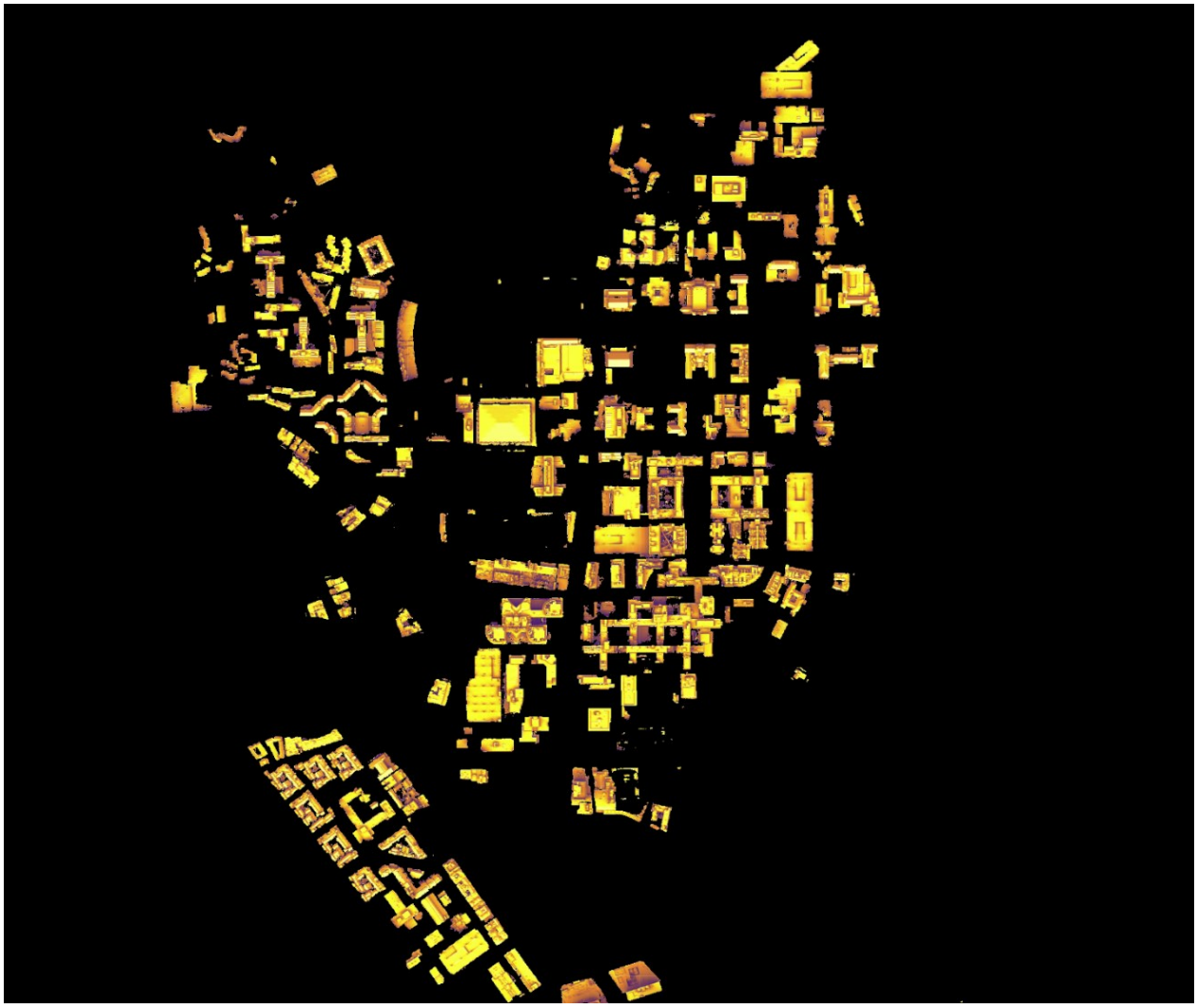

UCM

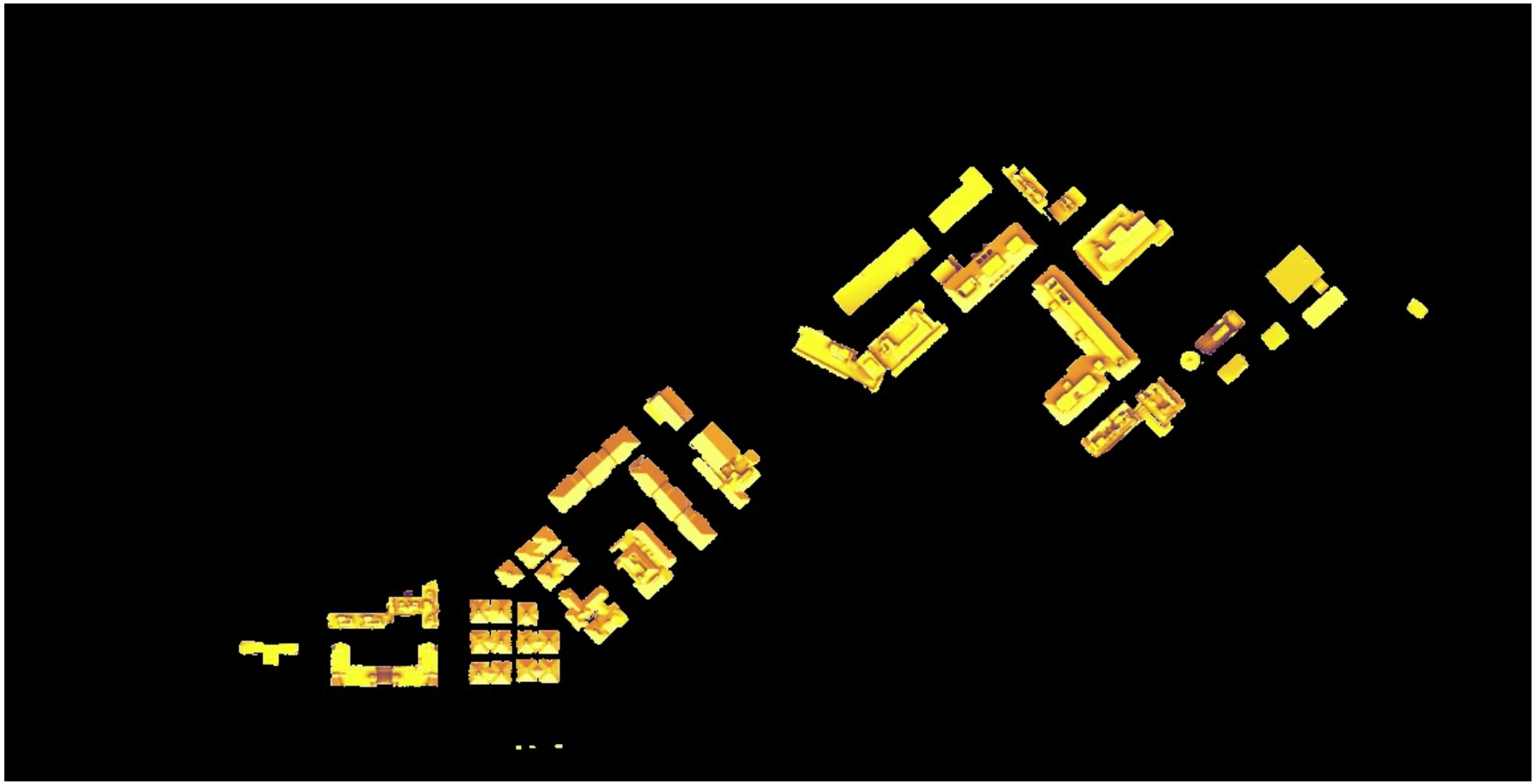

UCR

UCSD

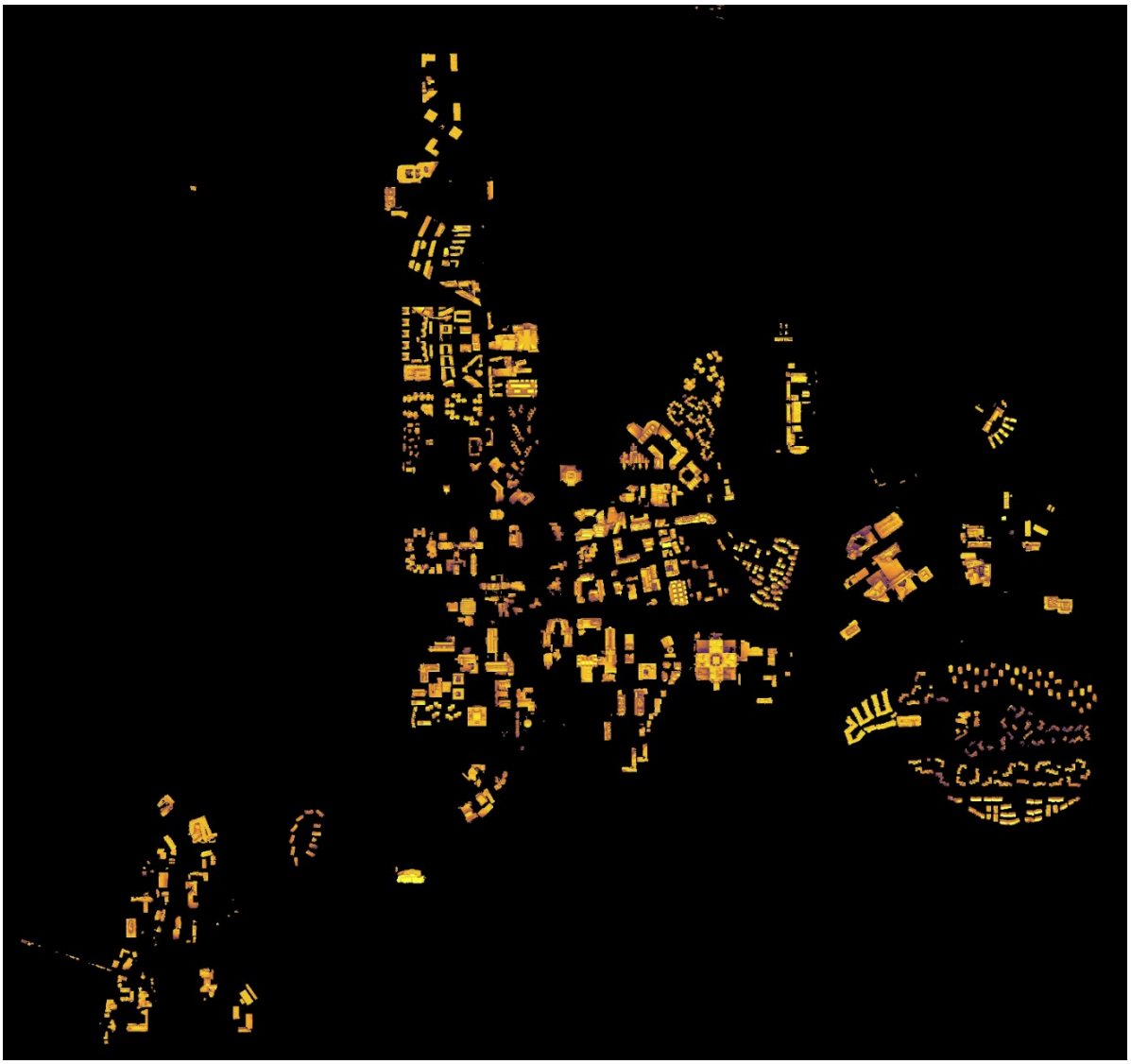

UCSB

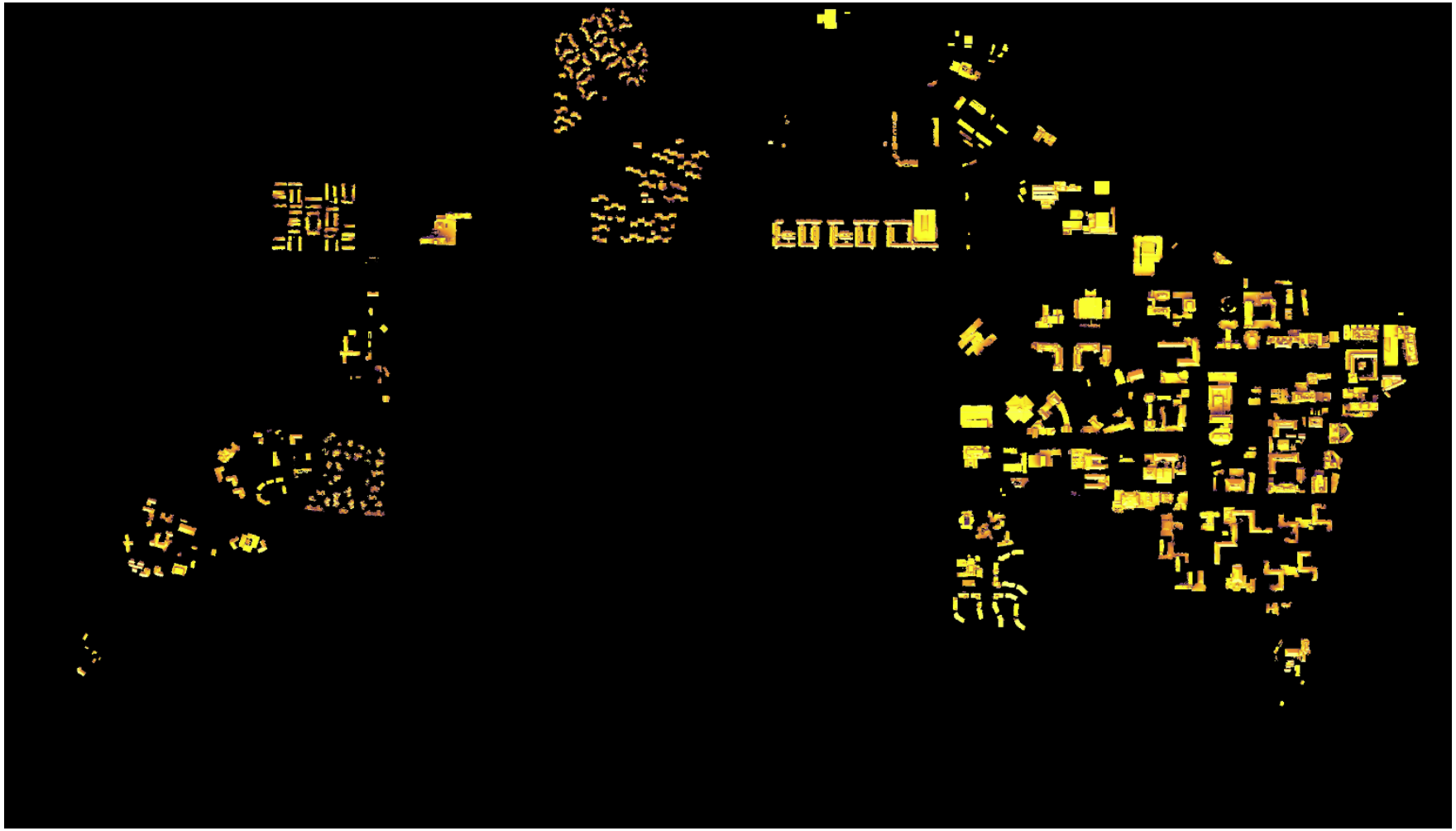

UCSC

Select Buildings for Main Campus Building MPP Analysis

*Entirety of UCM was used

UCB

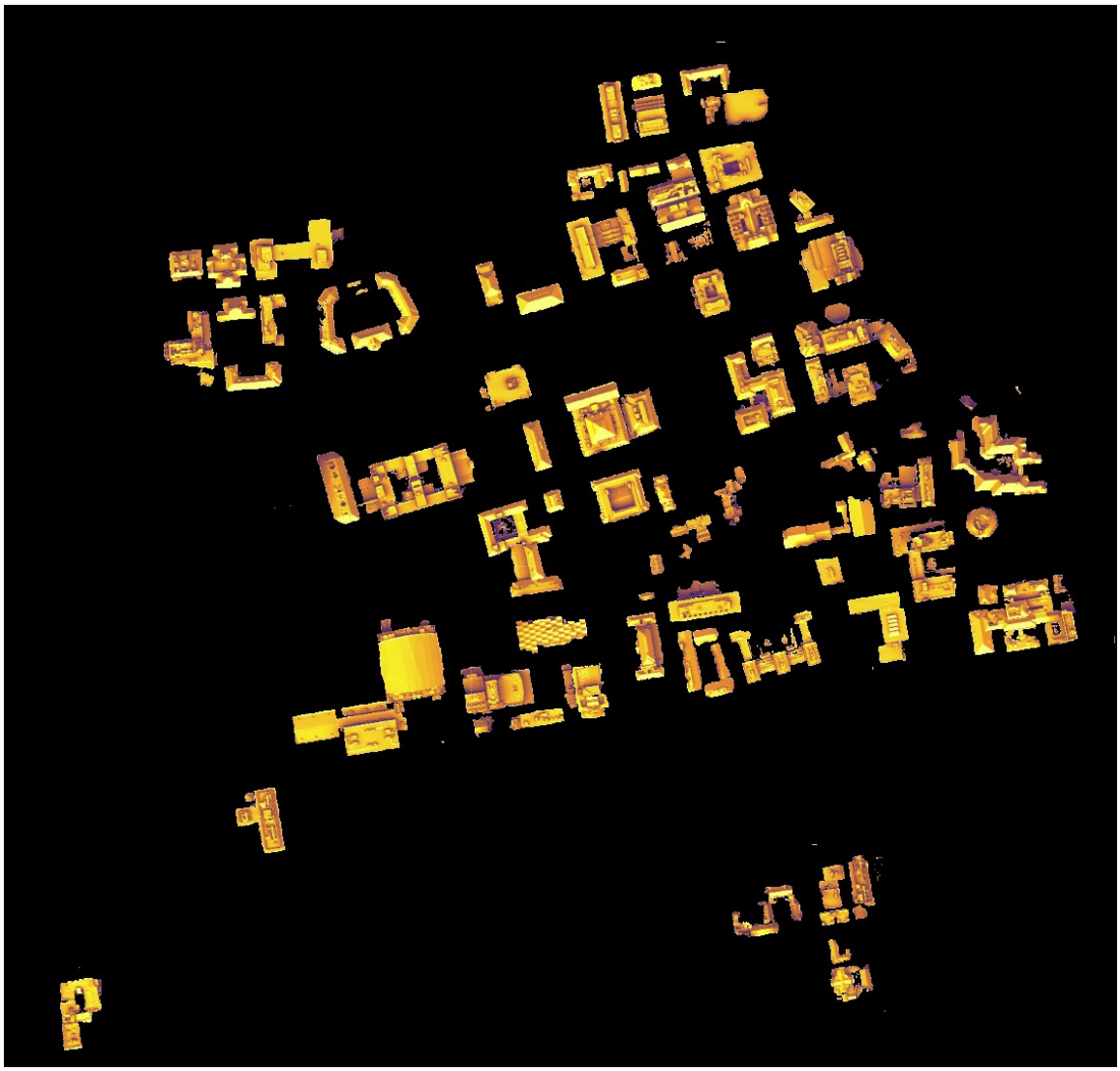

UCD

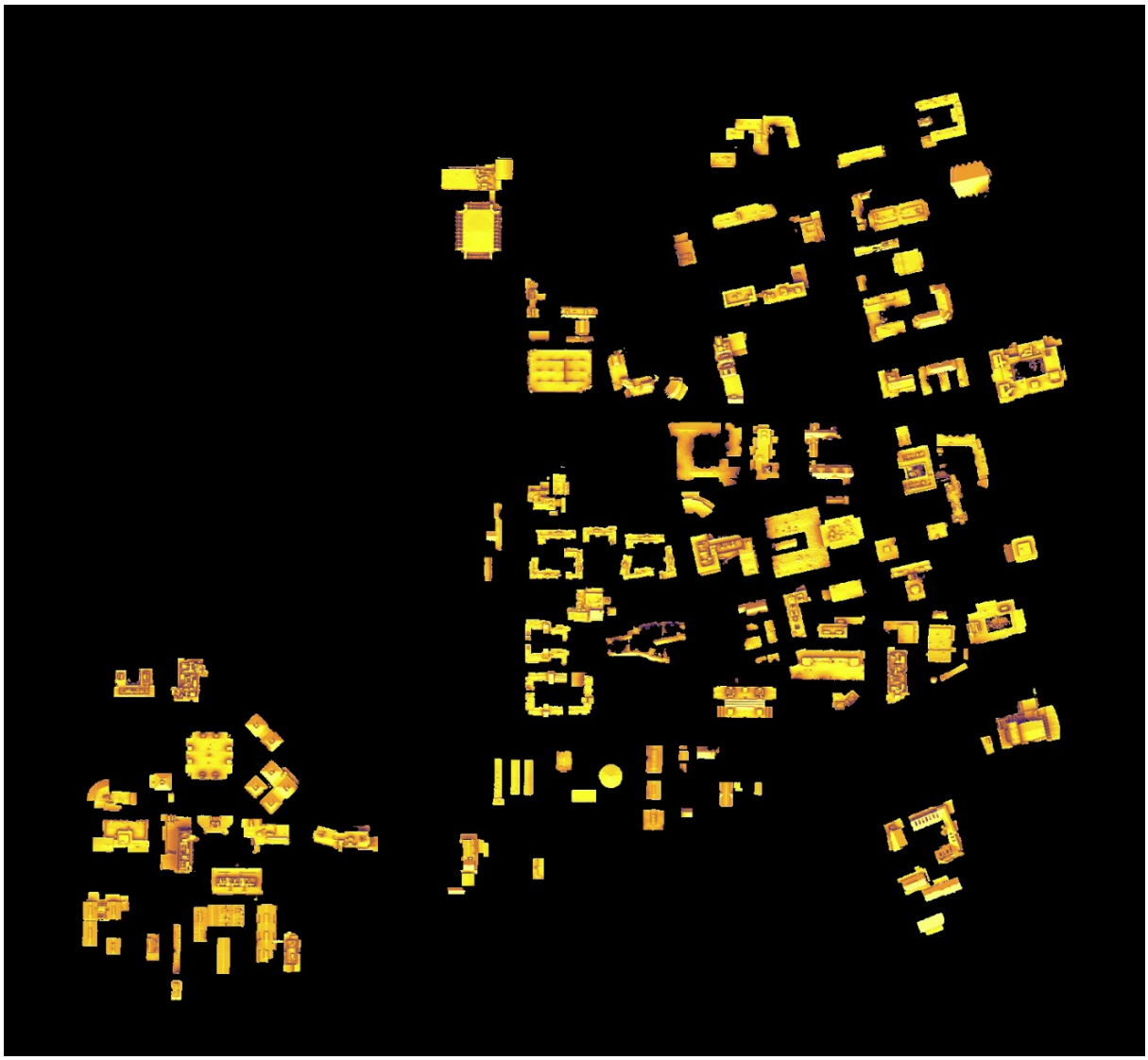

UCI

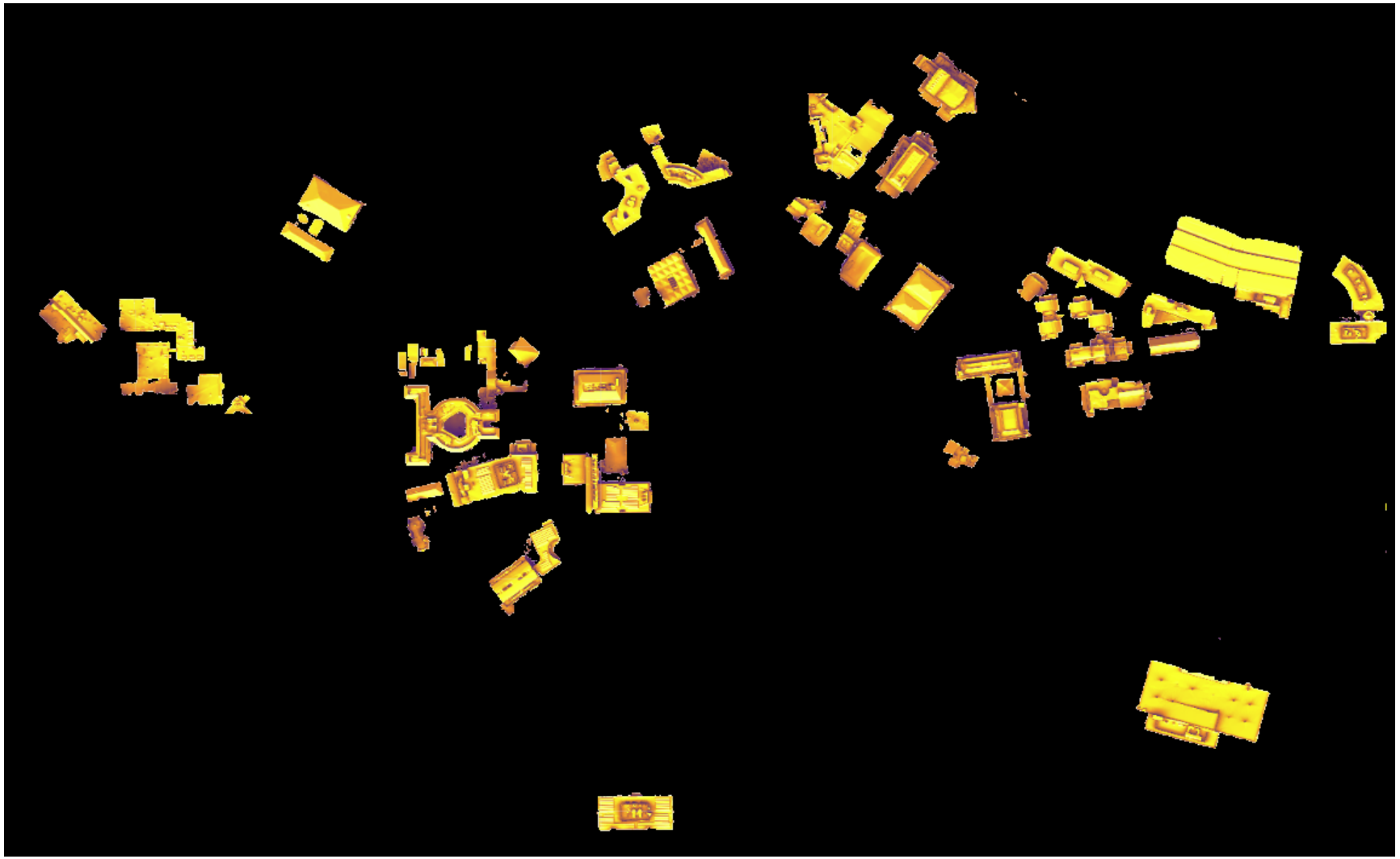

UCLA

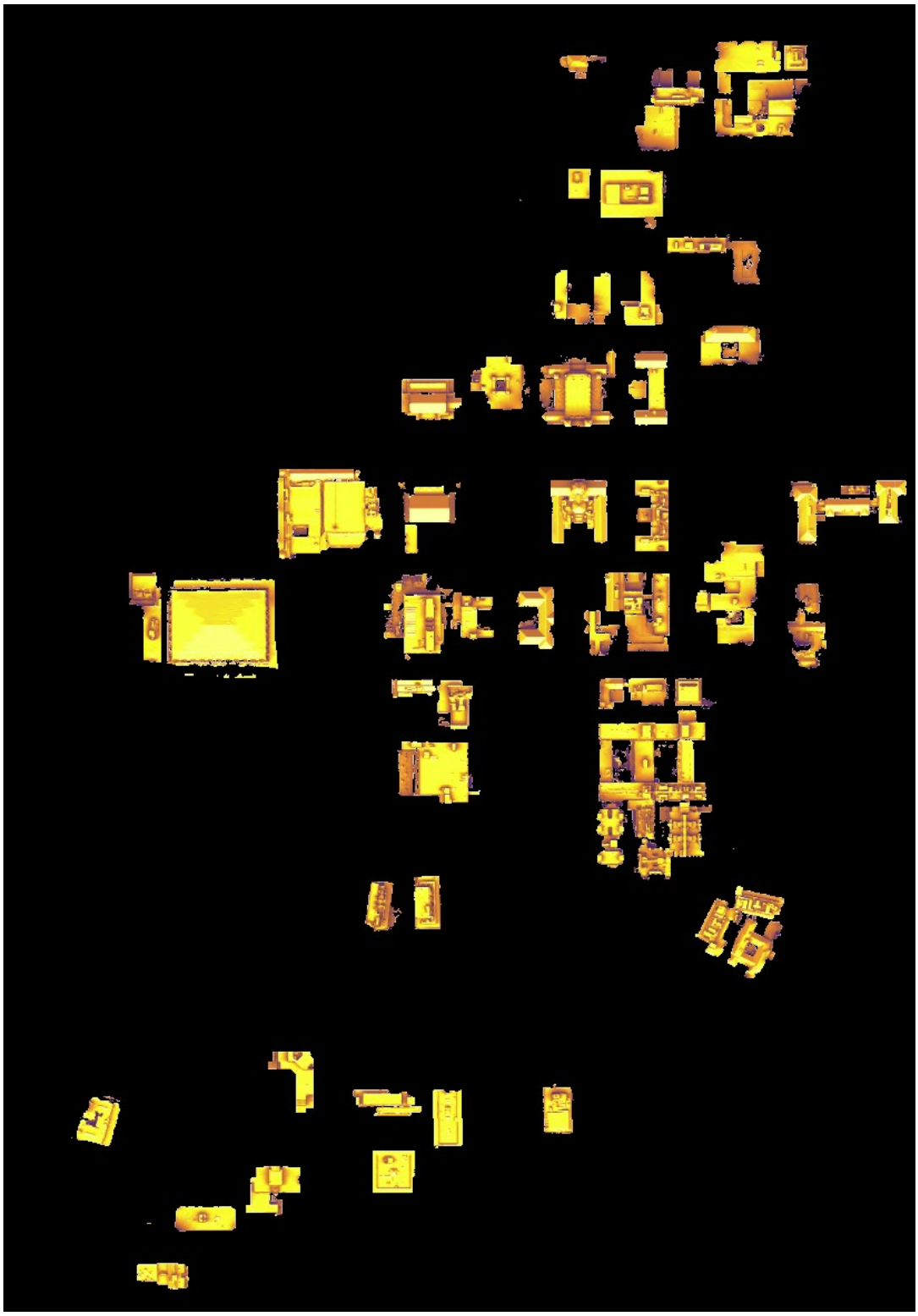

UCR

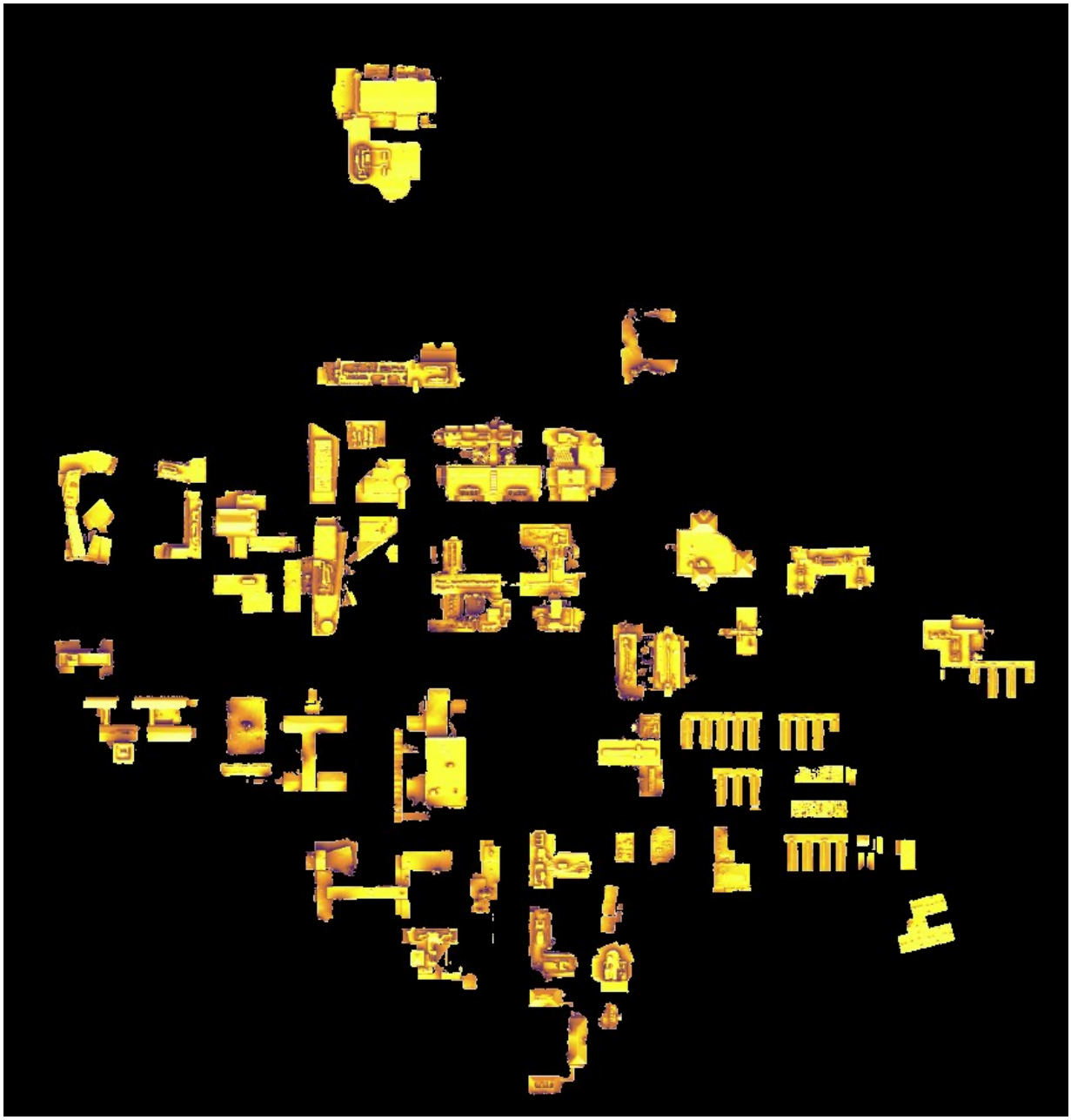

UCSD

UCSB

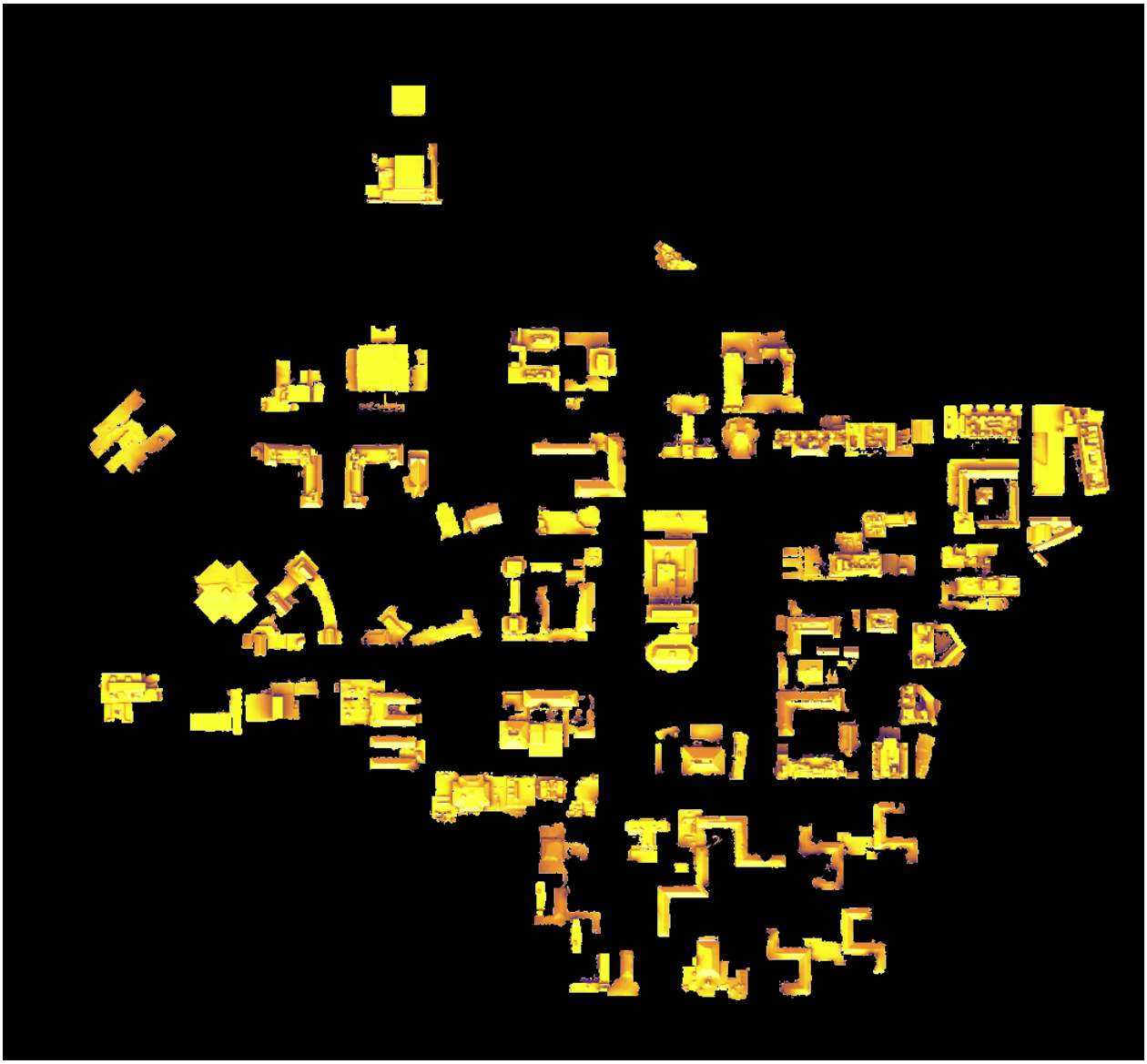

UCSC

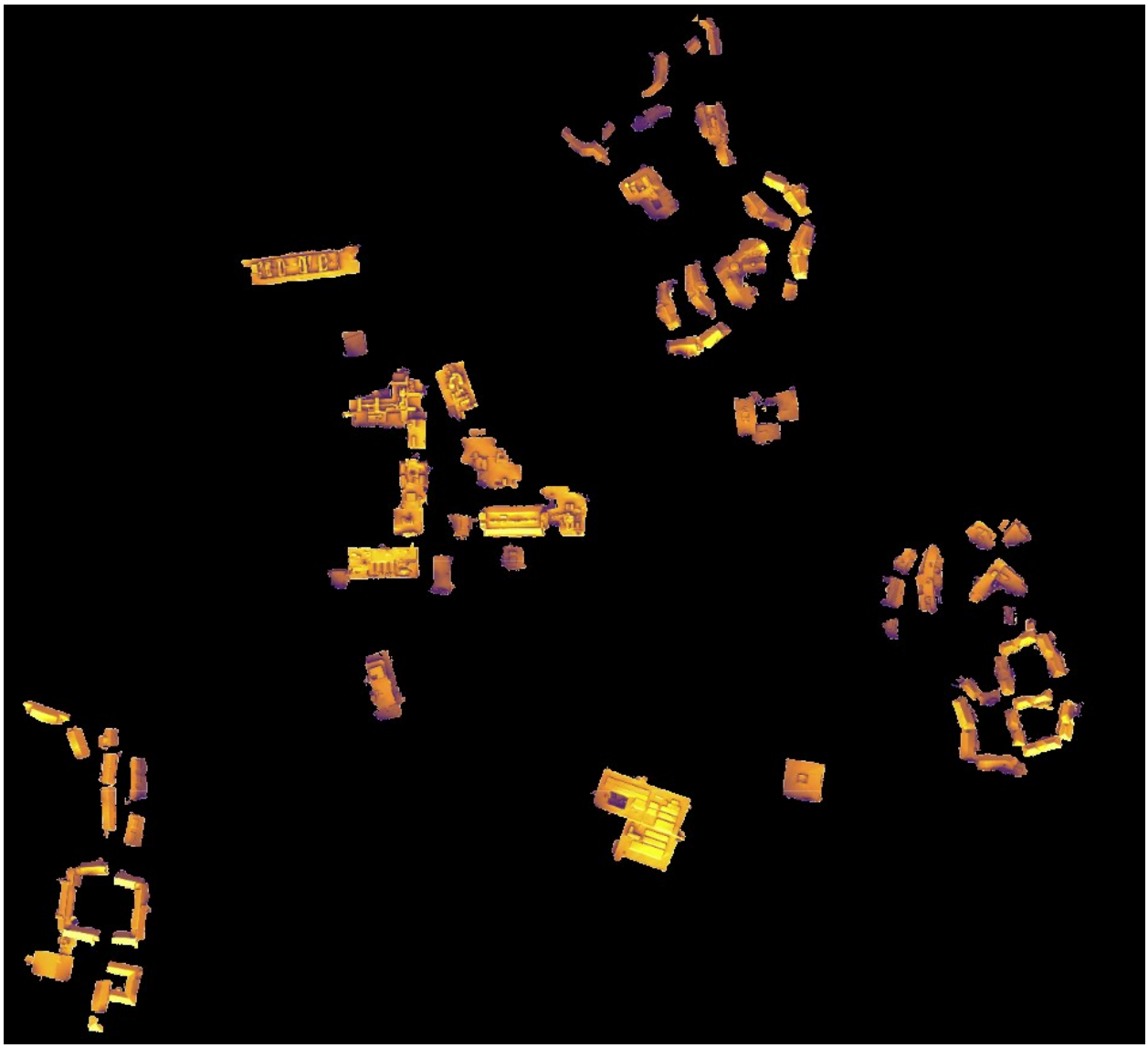

UCSF Parnassus

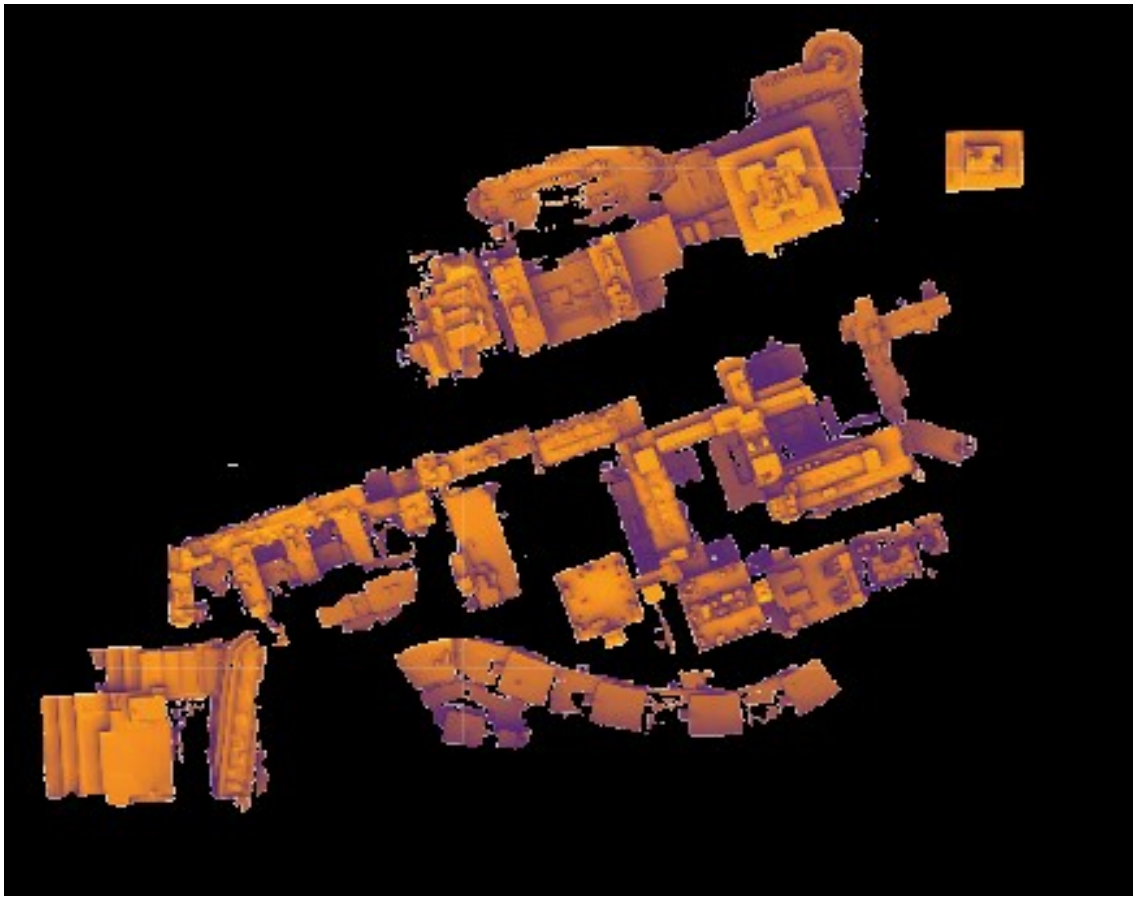

UCSF Mission Bay

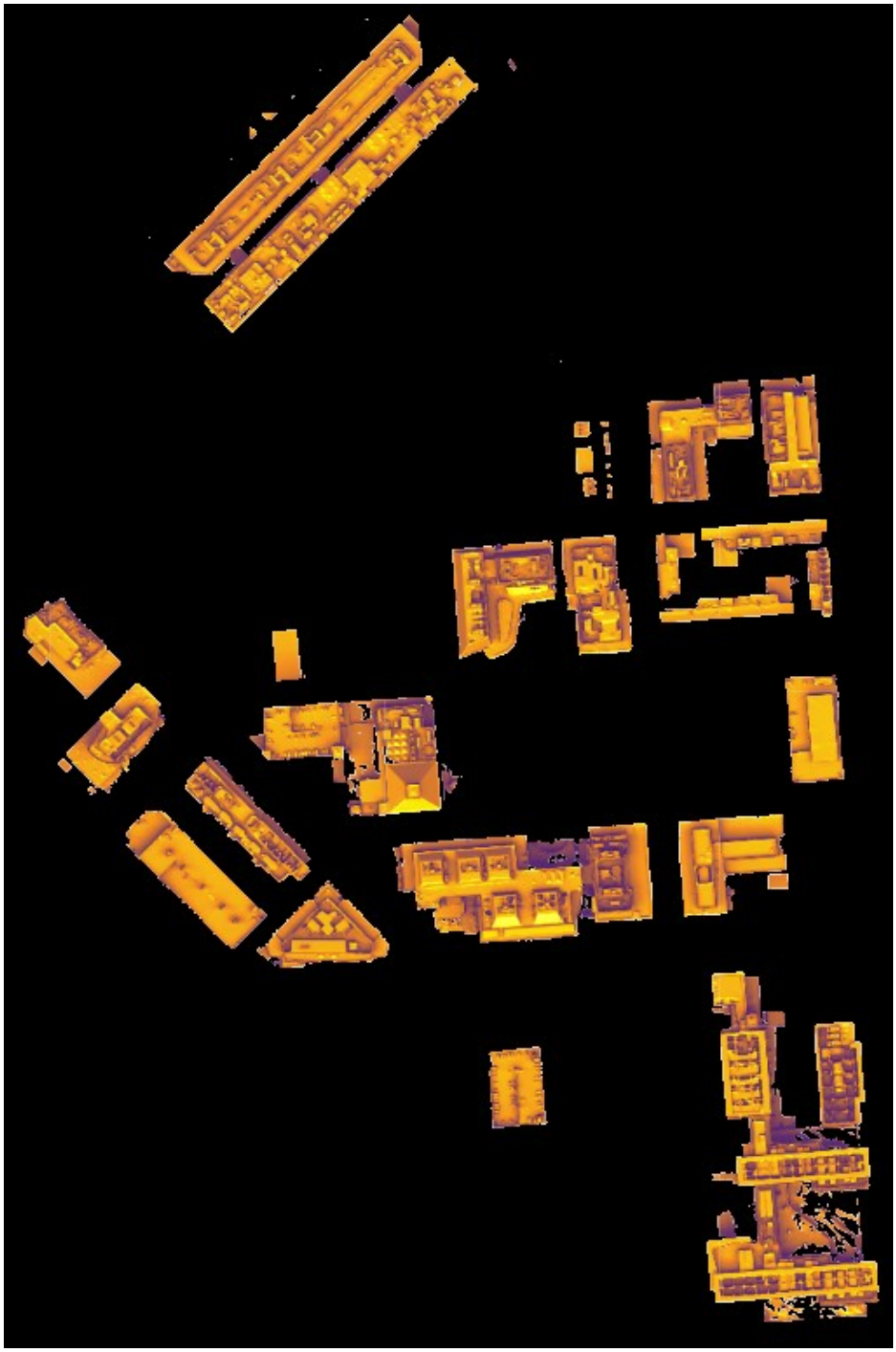

UCIMC

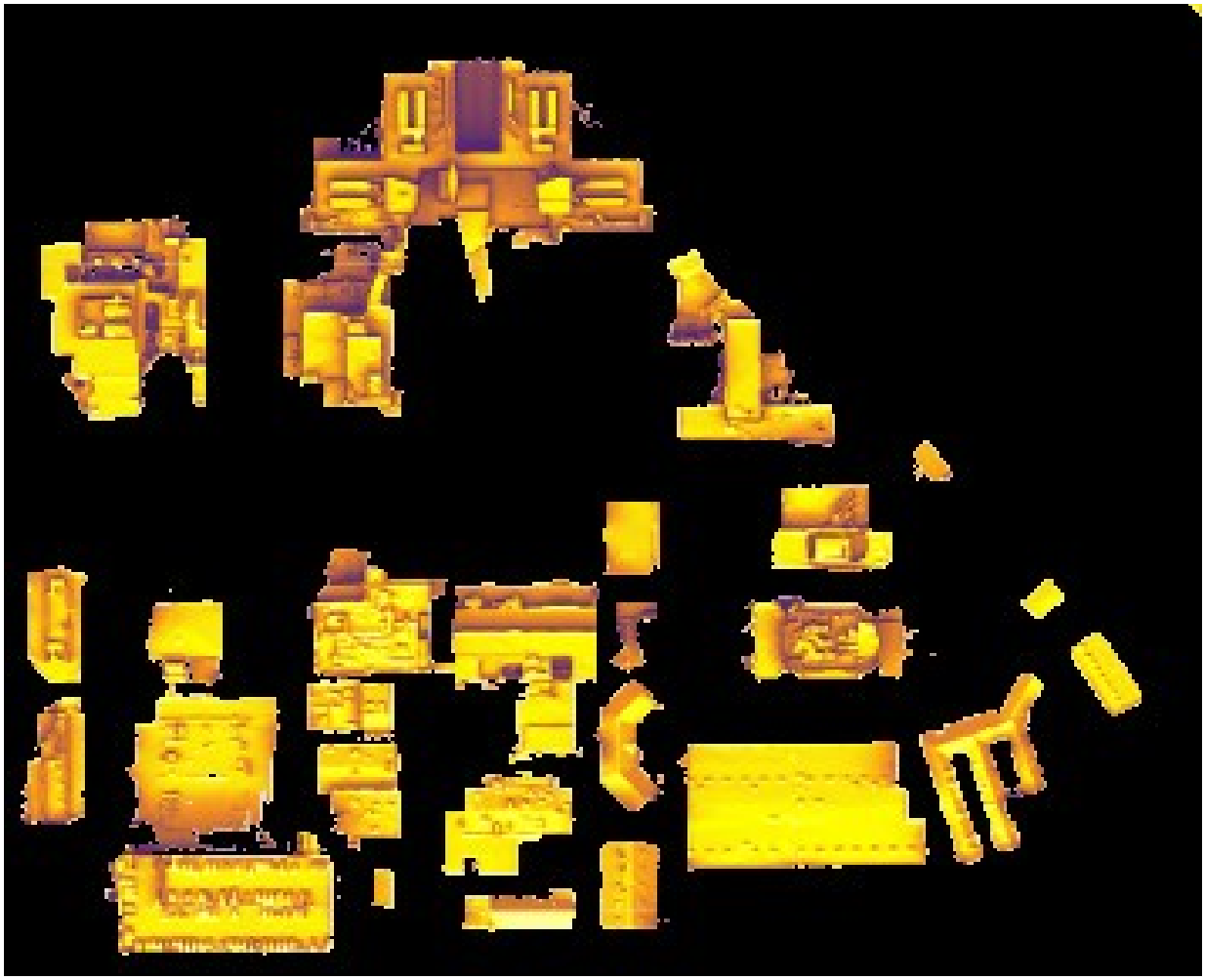

UCDMC

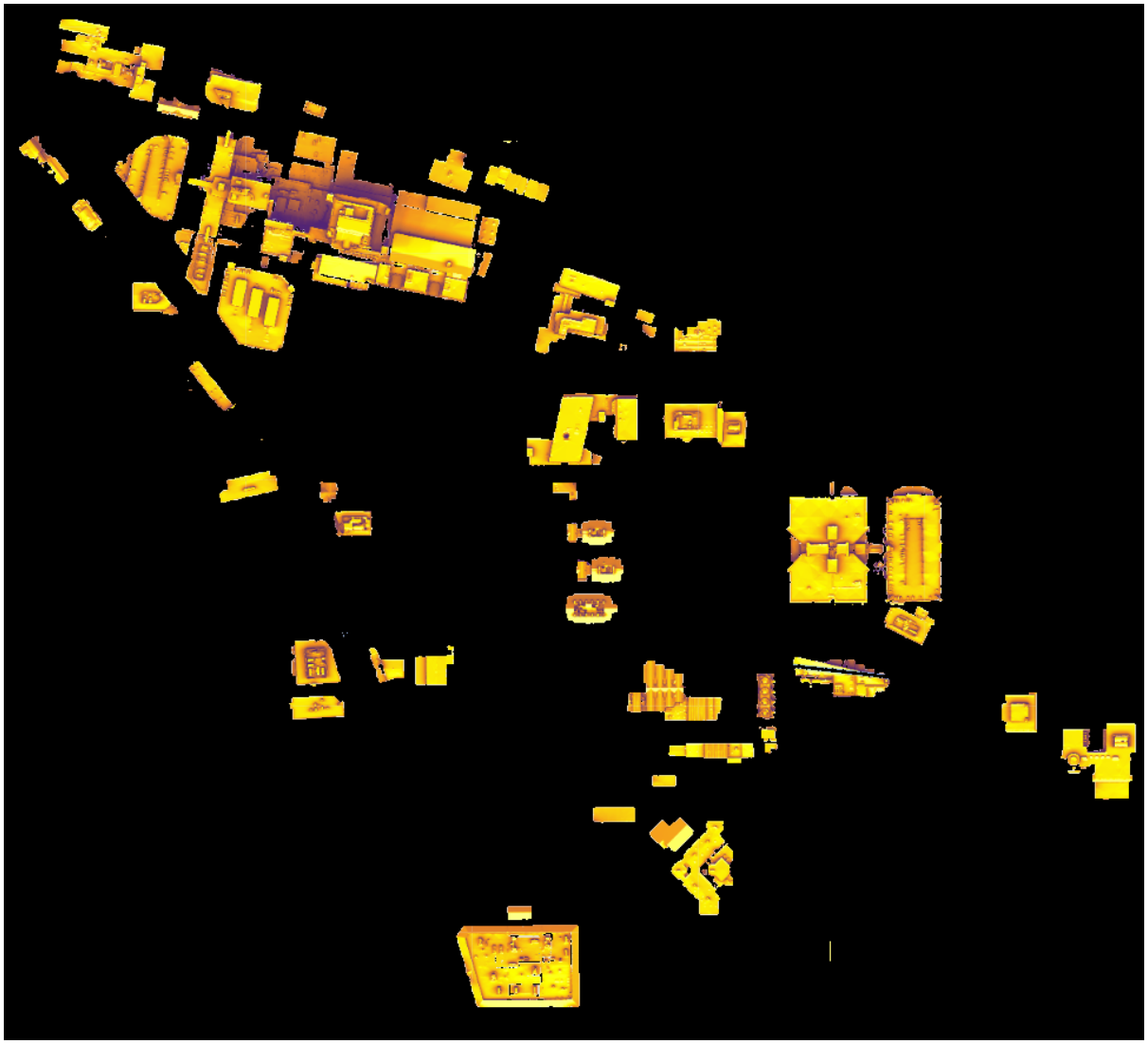

Parking Lots

UCB

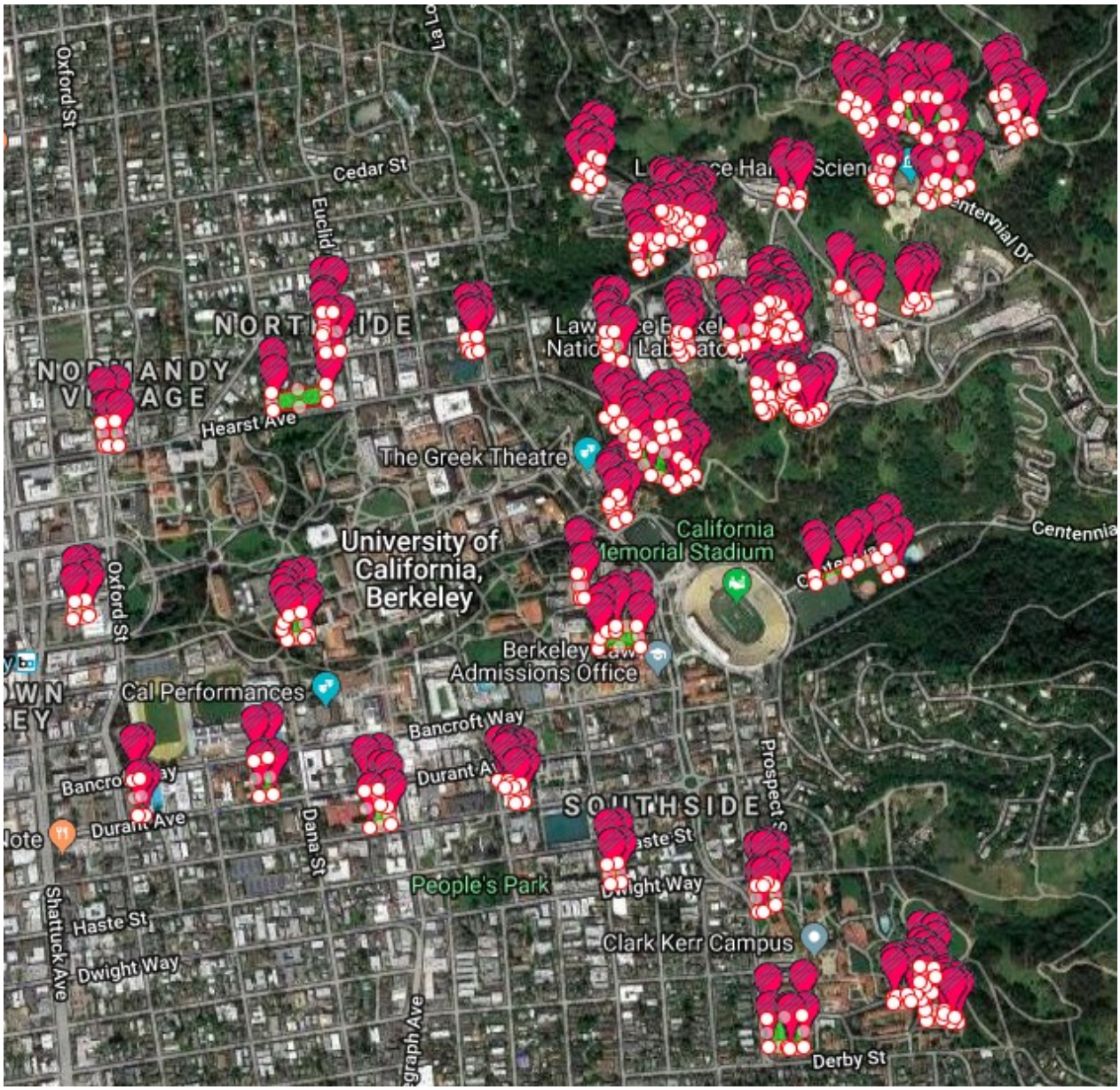

UCD

UCI

UCLA

UCM


Lake Rd
Fairfield Canal
Academic Office Annex Lot
North Bowl 2
Services Lane
Sierra Terraces
Muir Pass Road
Joseph E. Gallo Recreation & Wellness...
Zipcar
Visitor Center
University of California, Merced
The Marketplace
Yosemite Lateral
Bellevue Rd
Map data ©2019 Google Imagery ©2019 , DigitalGlobe, USDA Farm Service Age

UCR

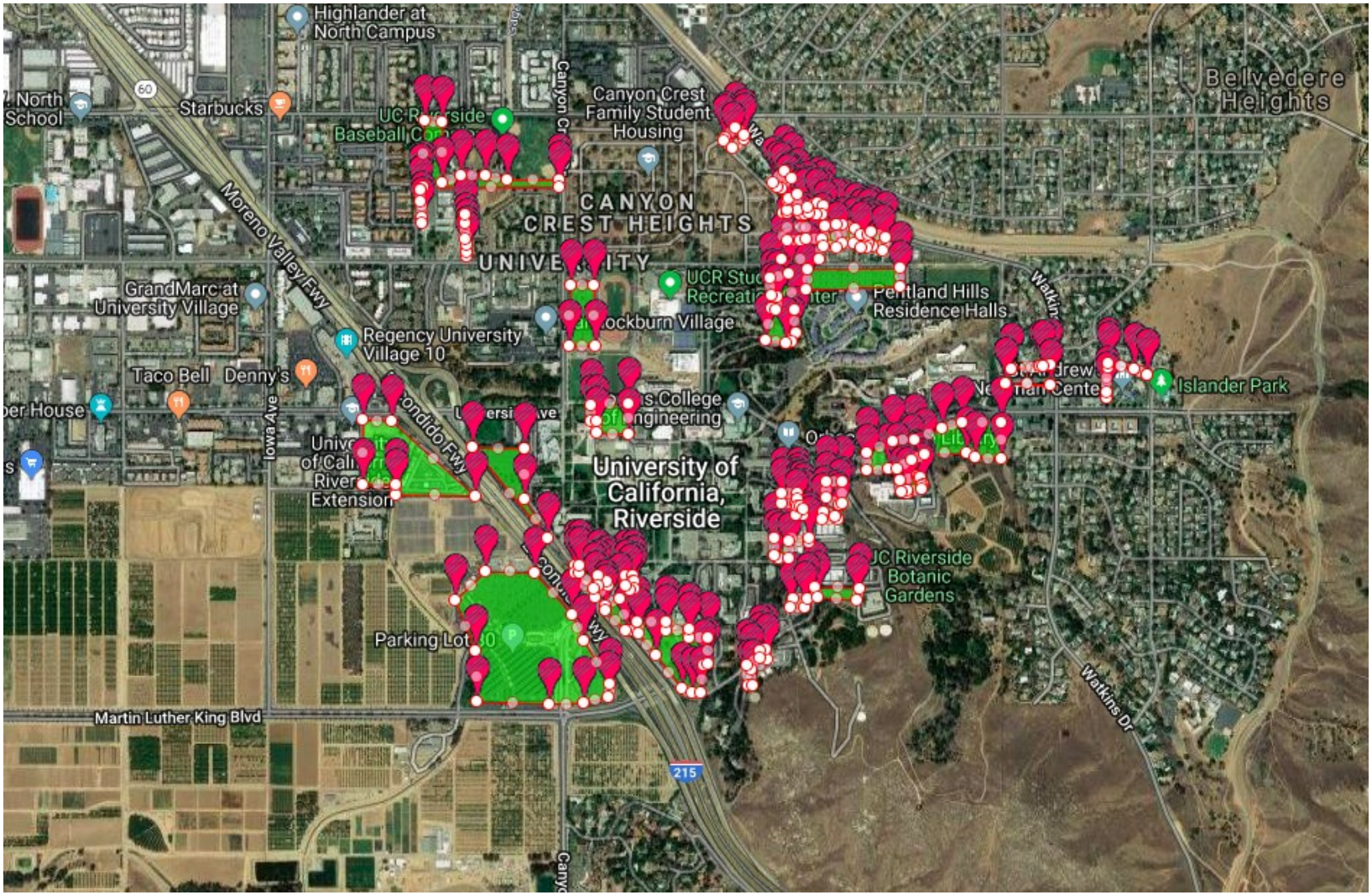
Highlander at North Campus
North School
Starbucks
Canyon Crest Family Student Housing
Belvedere Heights
CANYON CREST HEIGHTS
Moreno Valley Fwy
GrandMarc at University Village
Regency University Village 10
Taco Bell
Denny's
Pentland Hills Residence Halls
Islander Park
Iowa Ave
Riverside Extension
University of California, Riverside
UC Riverside Botanic Gardens
Parking Lot
Martin Luther King Blvd
Watkins Dr
215

UCSD

UCSB

UCSC

UCIMC

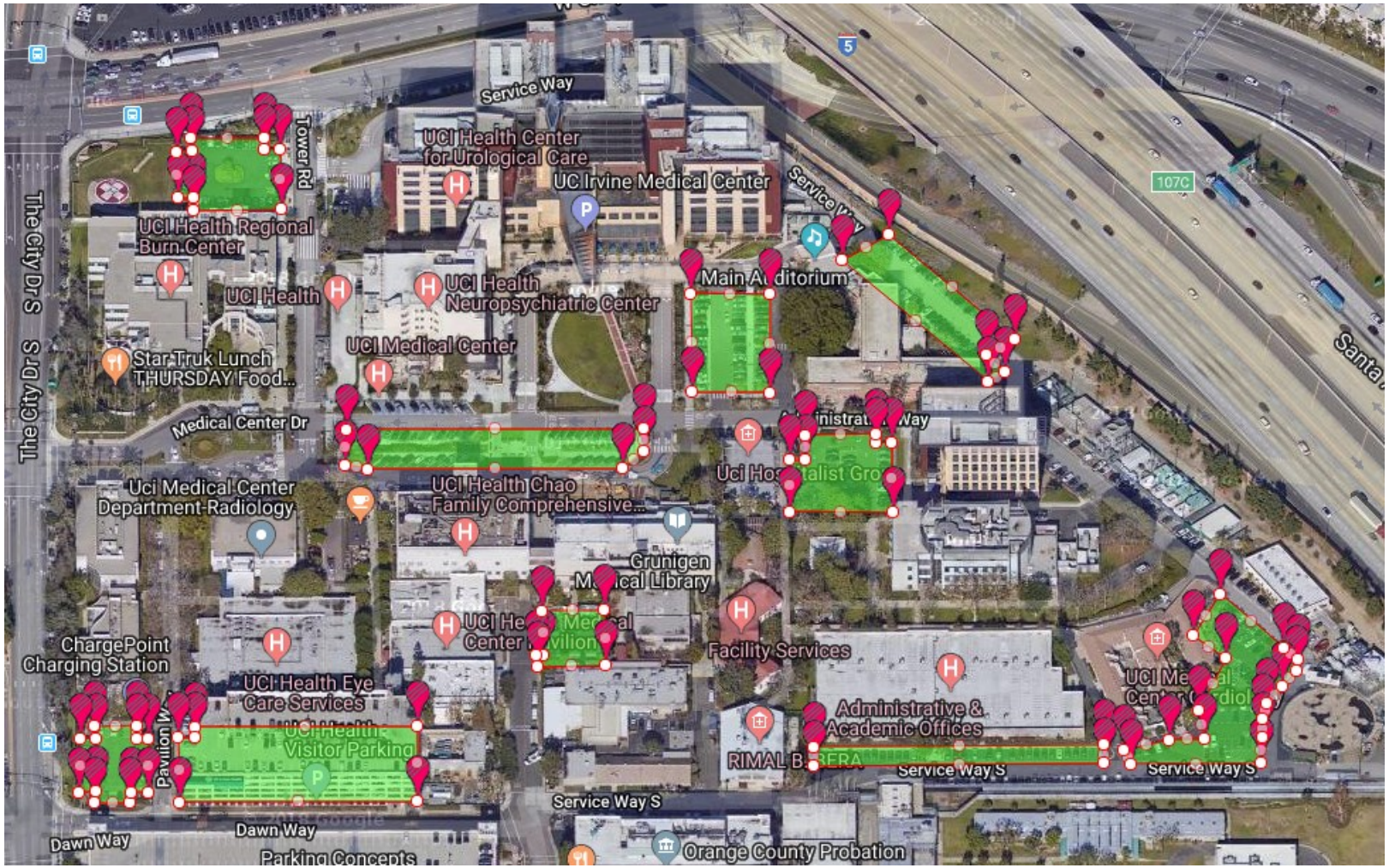
Service Way
UCI Health Center for Urological Care
UC Irvine Medical Center
Tower Rd
UCI Health Regional Burn Center
UCI Health
UCI Health Neuropsychiatric Center
Main Auditorium
The City Dr S
Star Truk Lunch THURSDAY Food...
UCI Medical Center
Medical Center Dr
Uci Medical Center Department-Radiology
UCI Health Chao Family Comprehensive...
Grunigen Medical Library
ChargePoint Charging Station
UCI Health Eye Care Services
UCI Health Visitor Parking
Facility Services
Administrative & Academic Offices
Service Way S
Dawn Way
Parking Concepts
Orange County Probation
107C

UCSF: Parnassus (left) and Mission Bay (right)

UCDMC

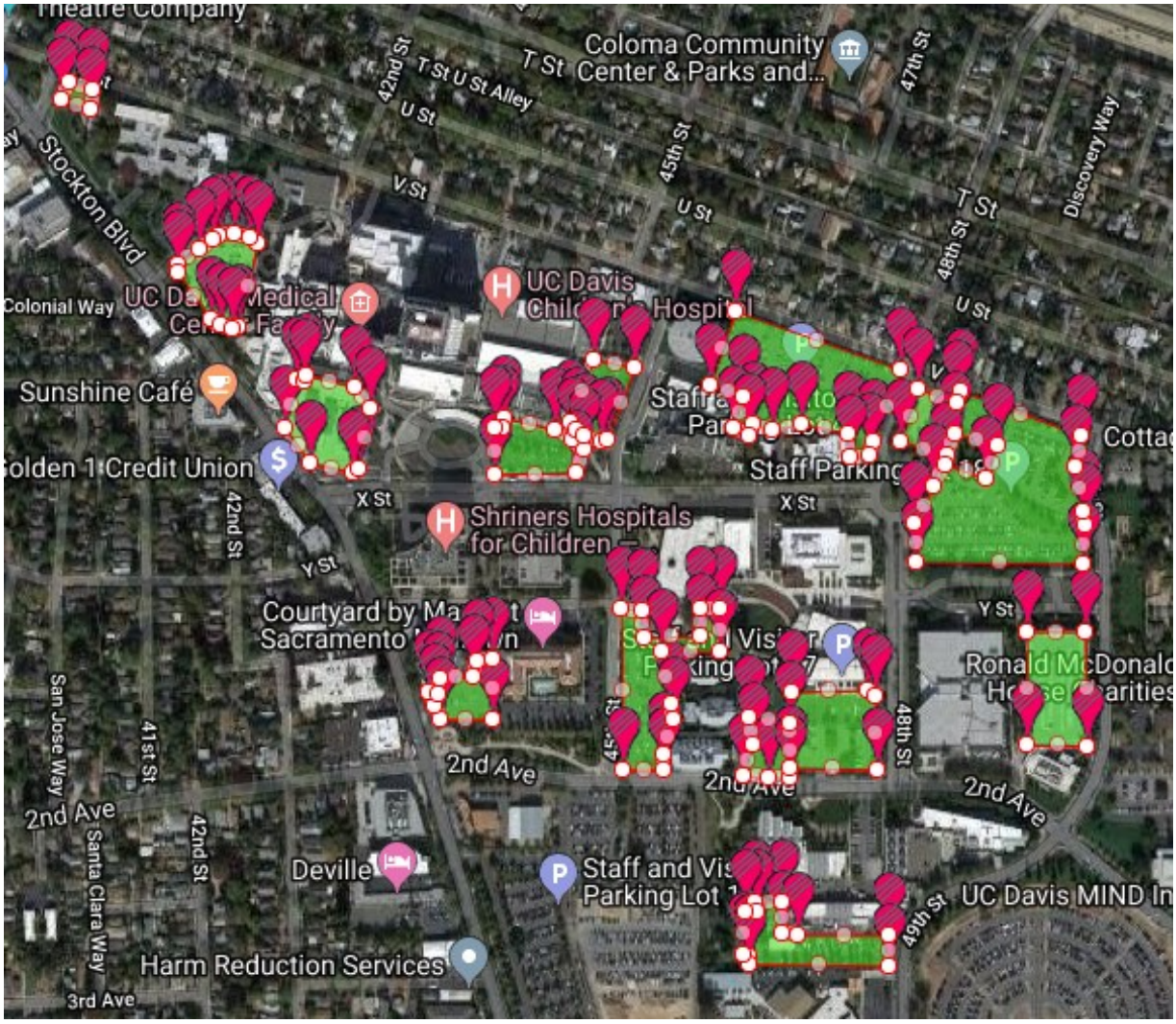
Coloma Community Center & Parks and...
T St
U St
V St
X St
Y St
Stockton Blvd
Colonial Way
Sunshine Café
Golden 1 Credit Union
UC Davis Children's Hospital
Staff Parking
Shriners Hospitals for Children
Courtyard by Marriott Sacramento
Ronald McDonald House Charities
2nd Ave
Deville
Harm Reduction Services
UC Davis MIND In
42nd St
45th St
47th St
48th St
49th St
41st St
San Jose Way
Santa Clara Way
3rd Ave
Discovery Way

Reference Zip Code Images

*UCSC campus aligns with 95064 zip code. The campus image is used as a reference zip code.

94704 (UCB)

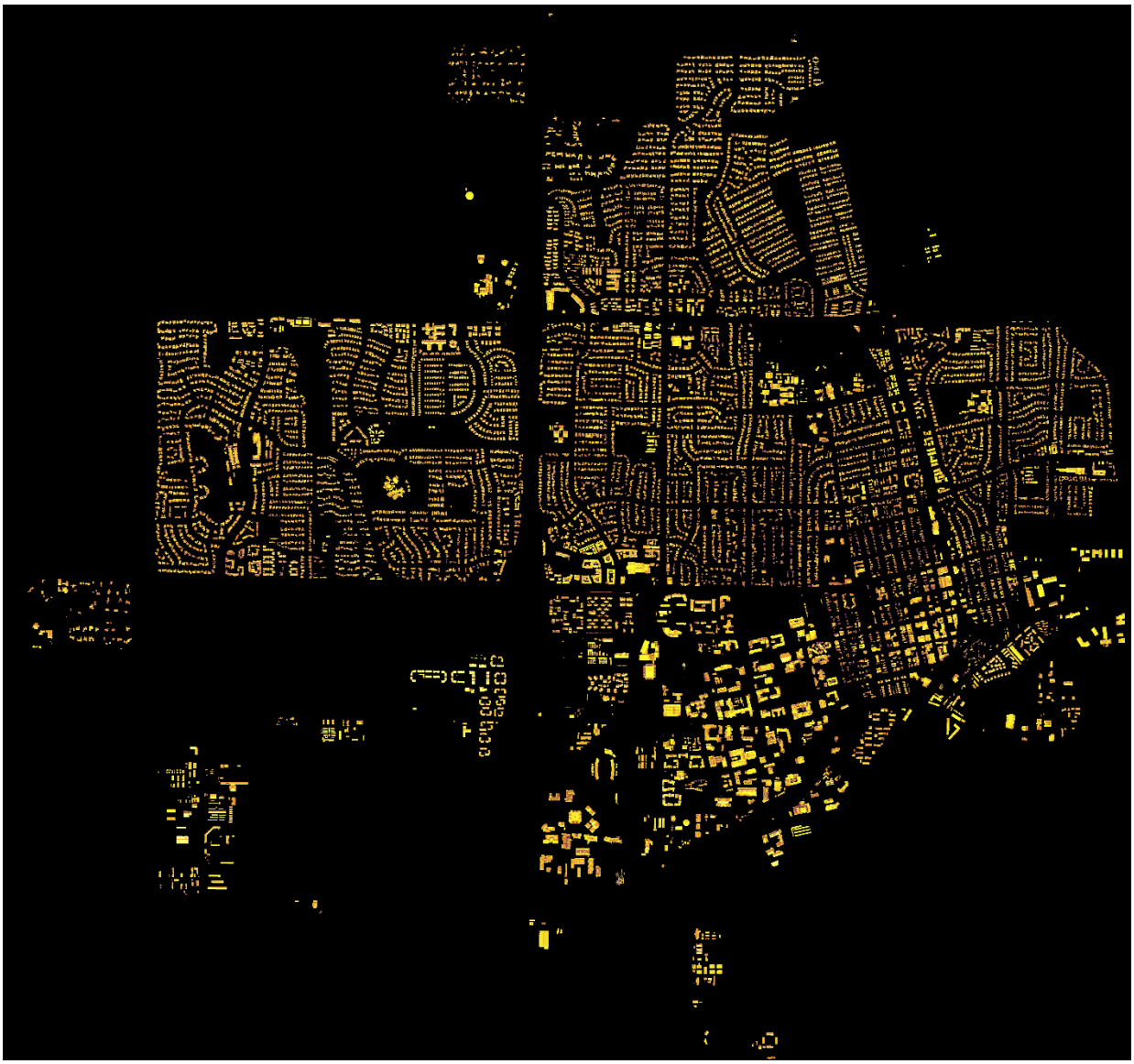

95616 (UCD)

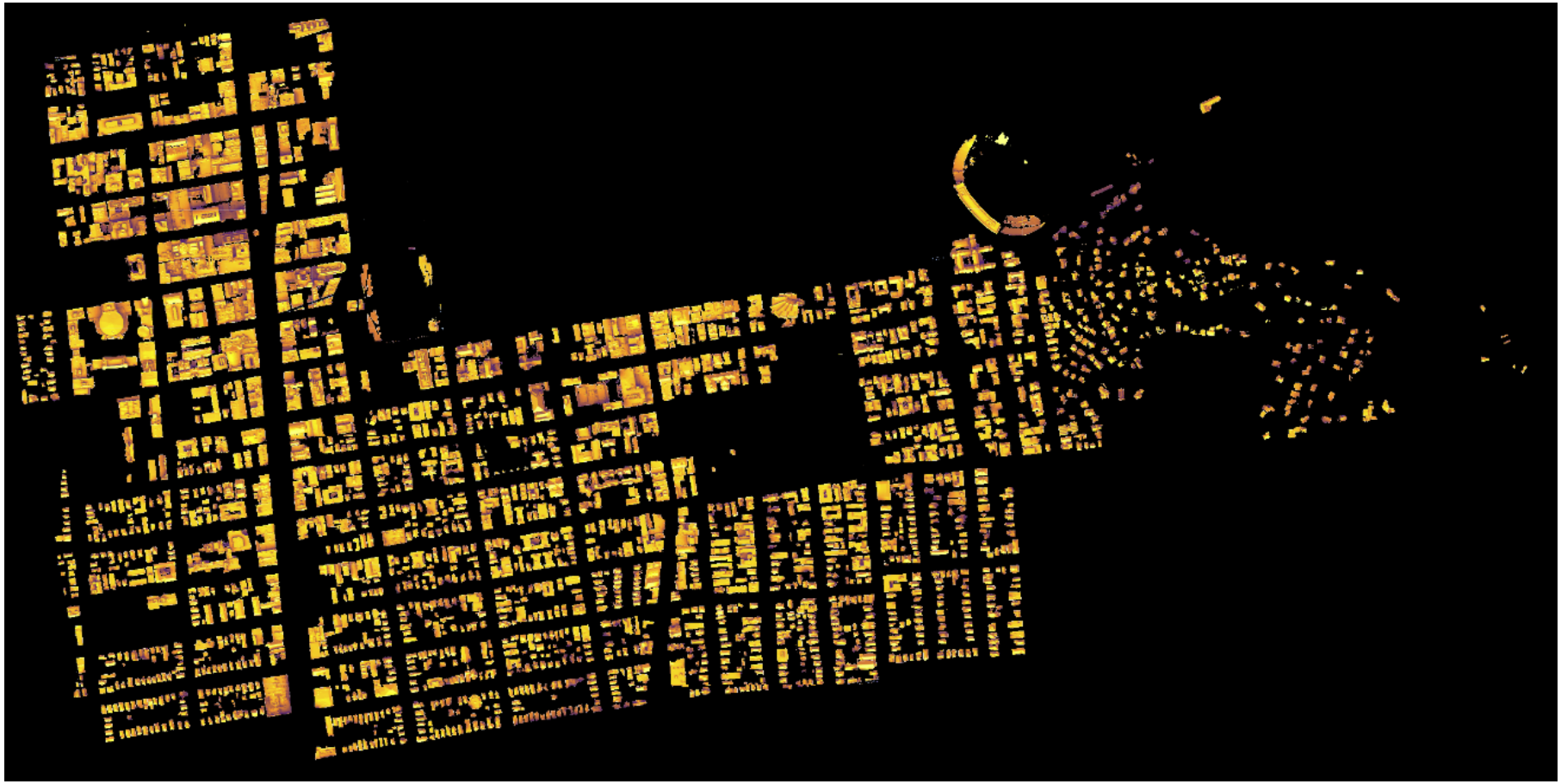

92617 (UCI)

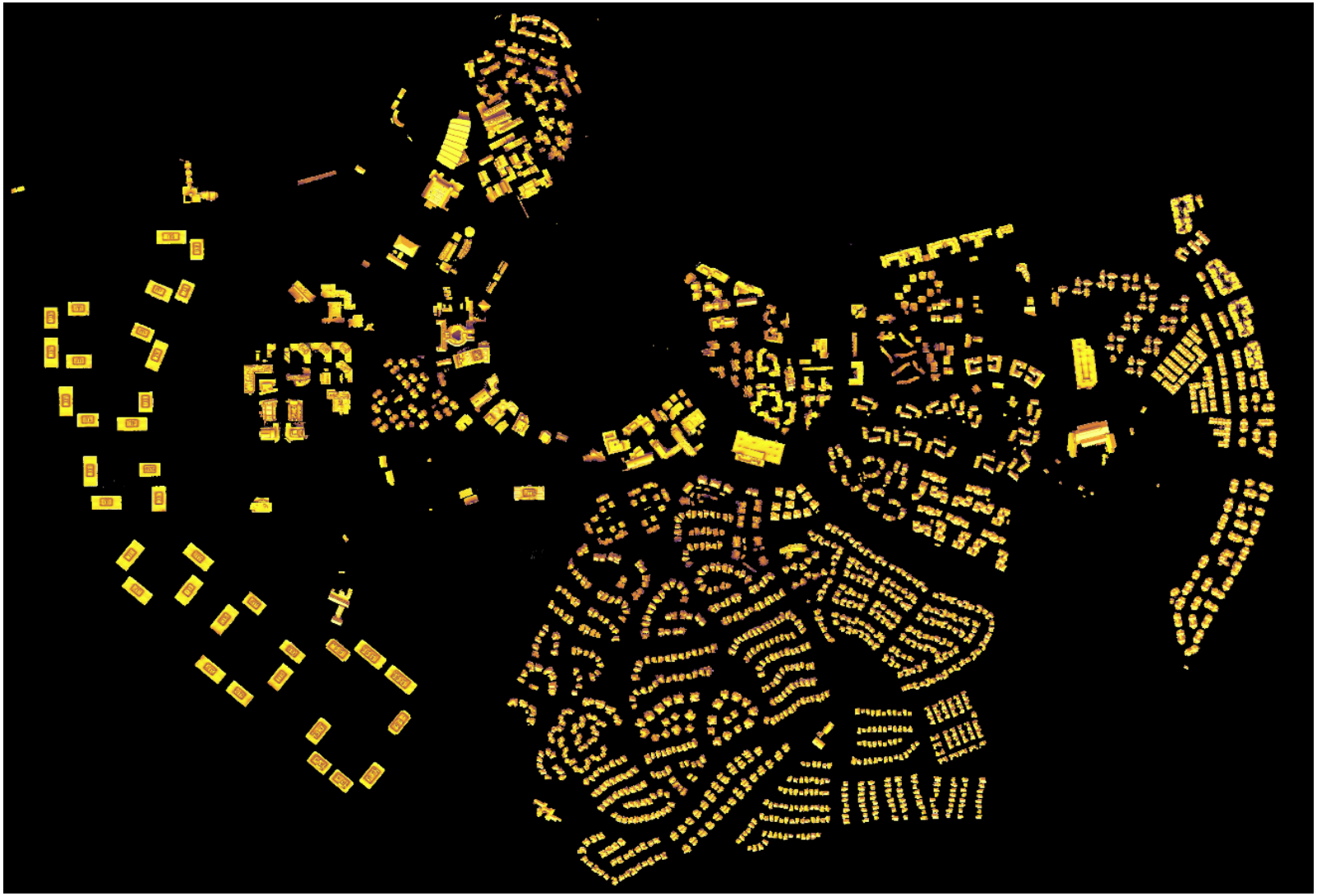

90025 (UCLA)

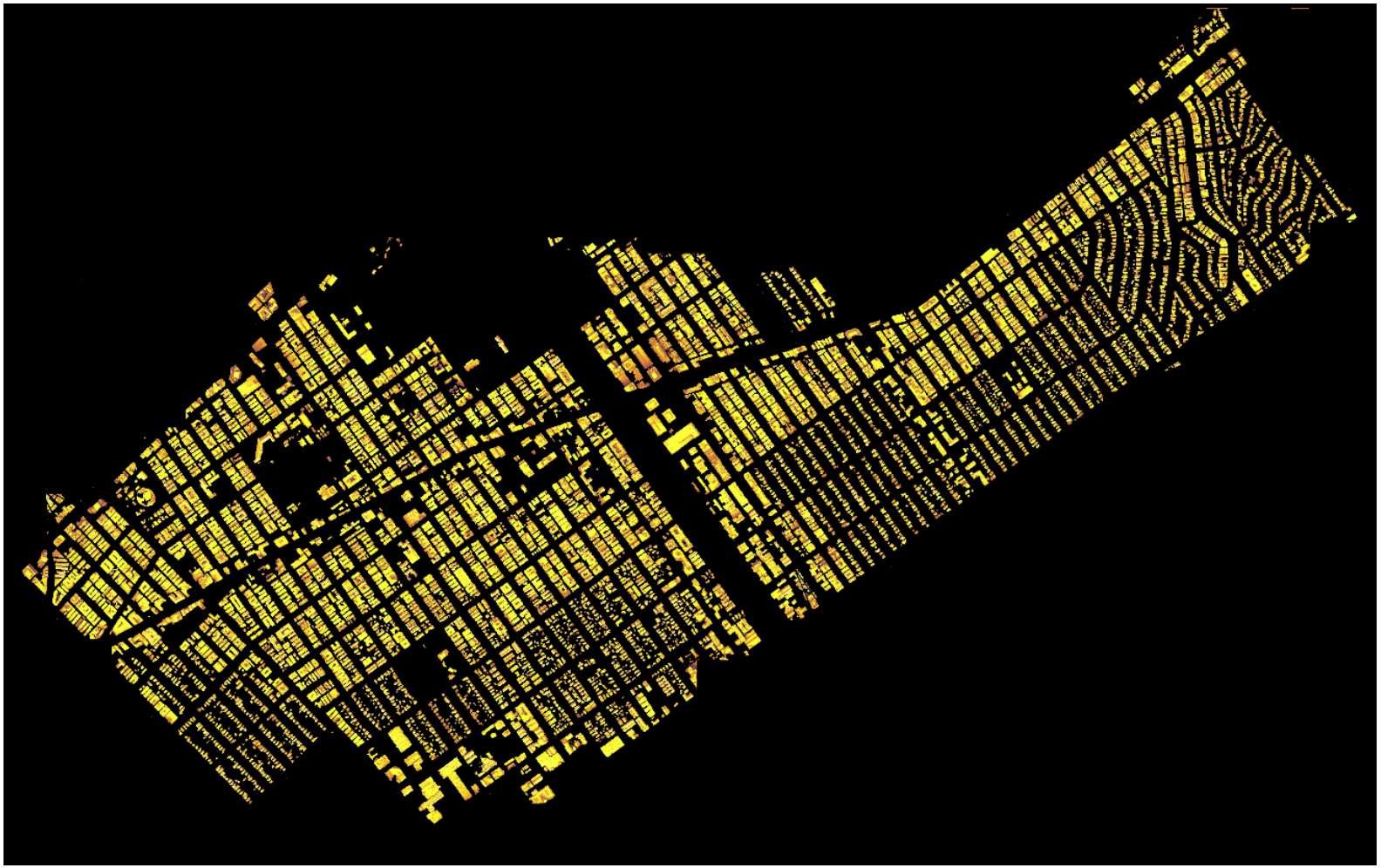

95348 (UCM)

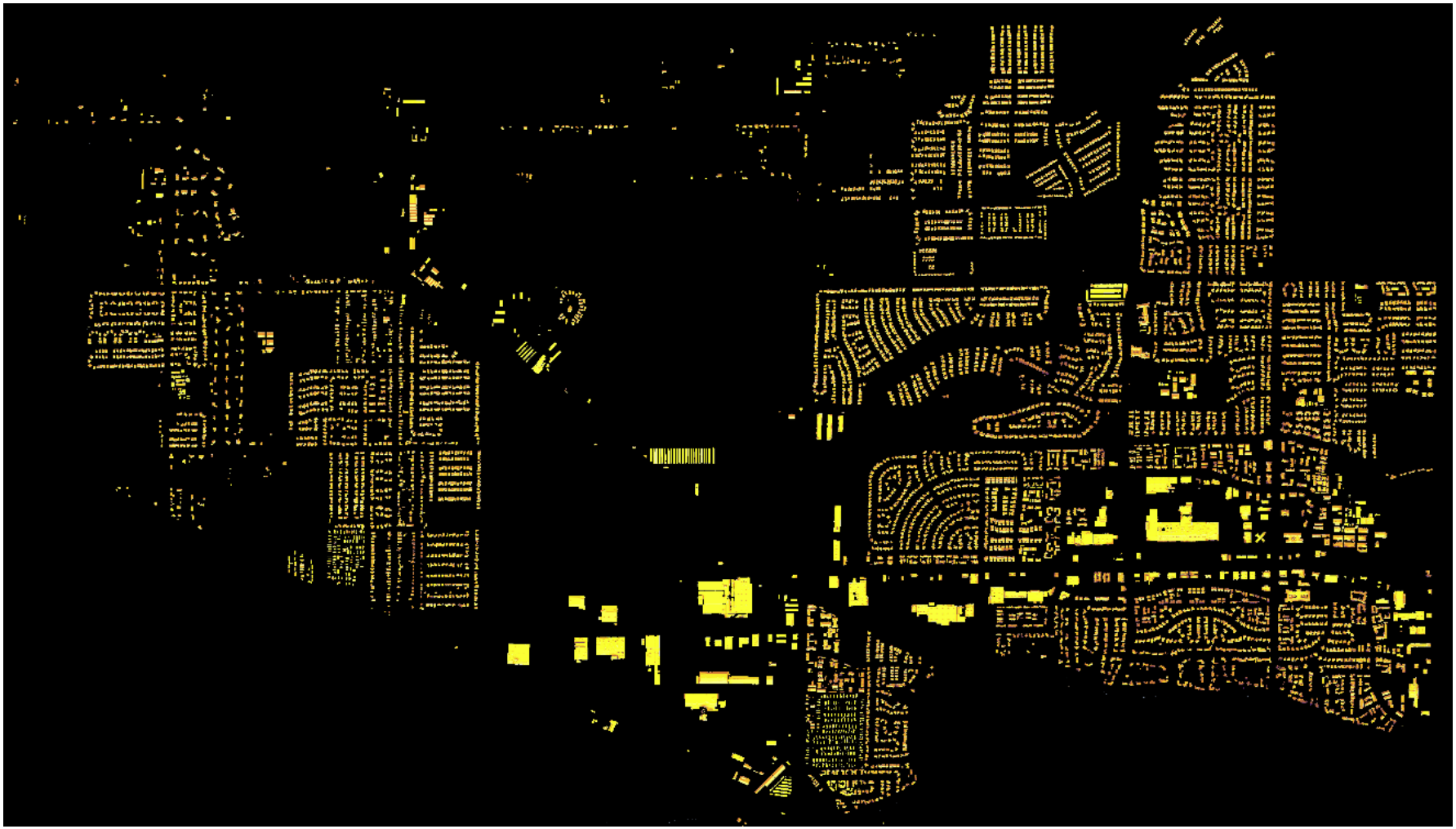

92507 (UCR)

92122 (UCSD)

93117 (UCSB)

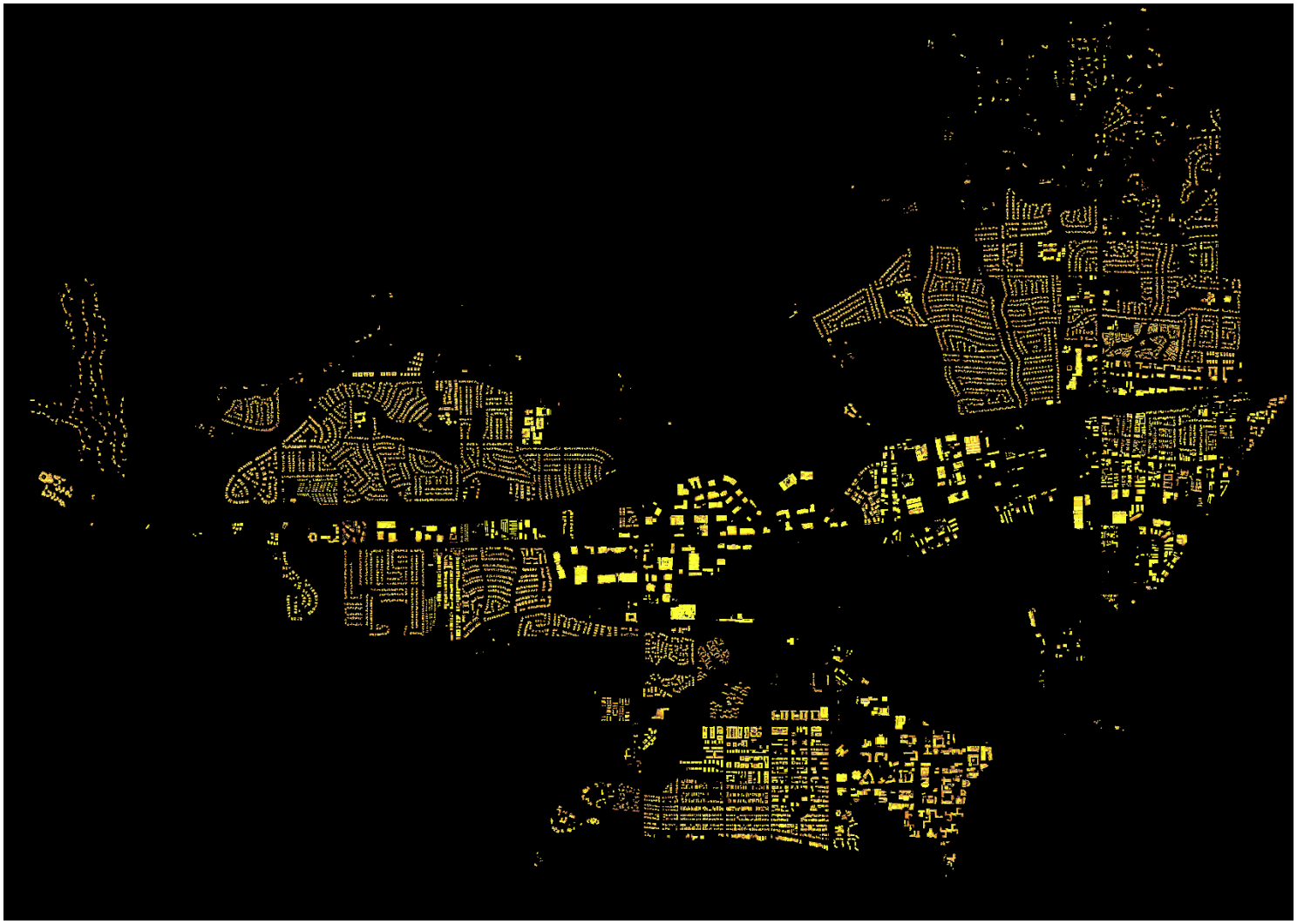

Validation Zip Codes

94720 (UCB)

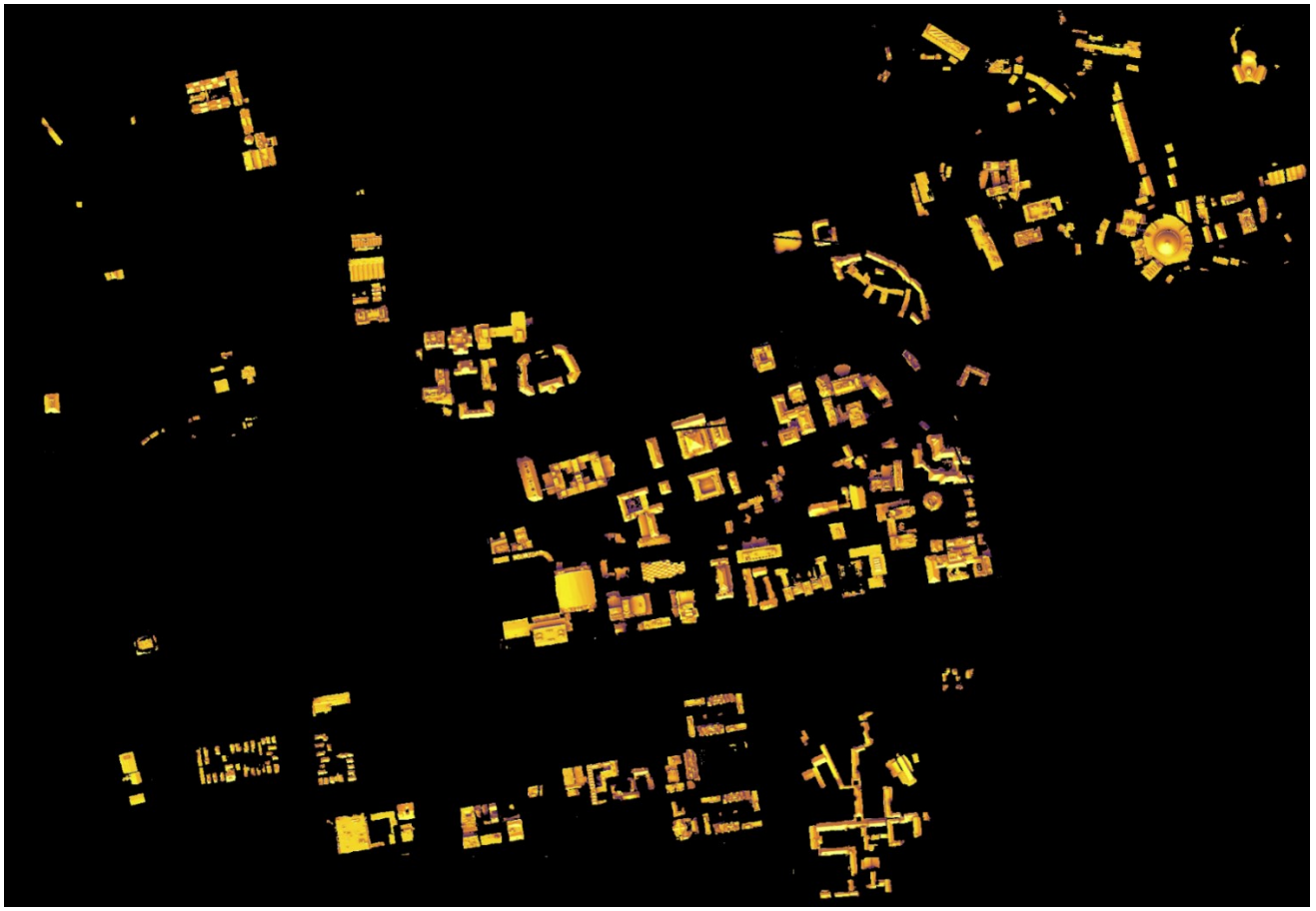

95618 (UCD)

92612 (UCI)

95341 (UCM)

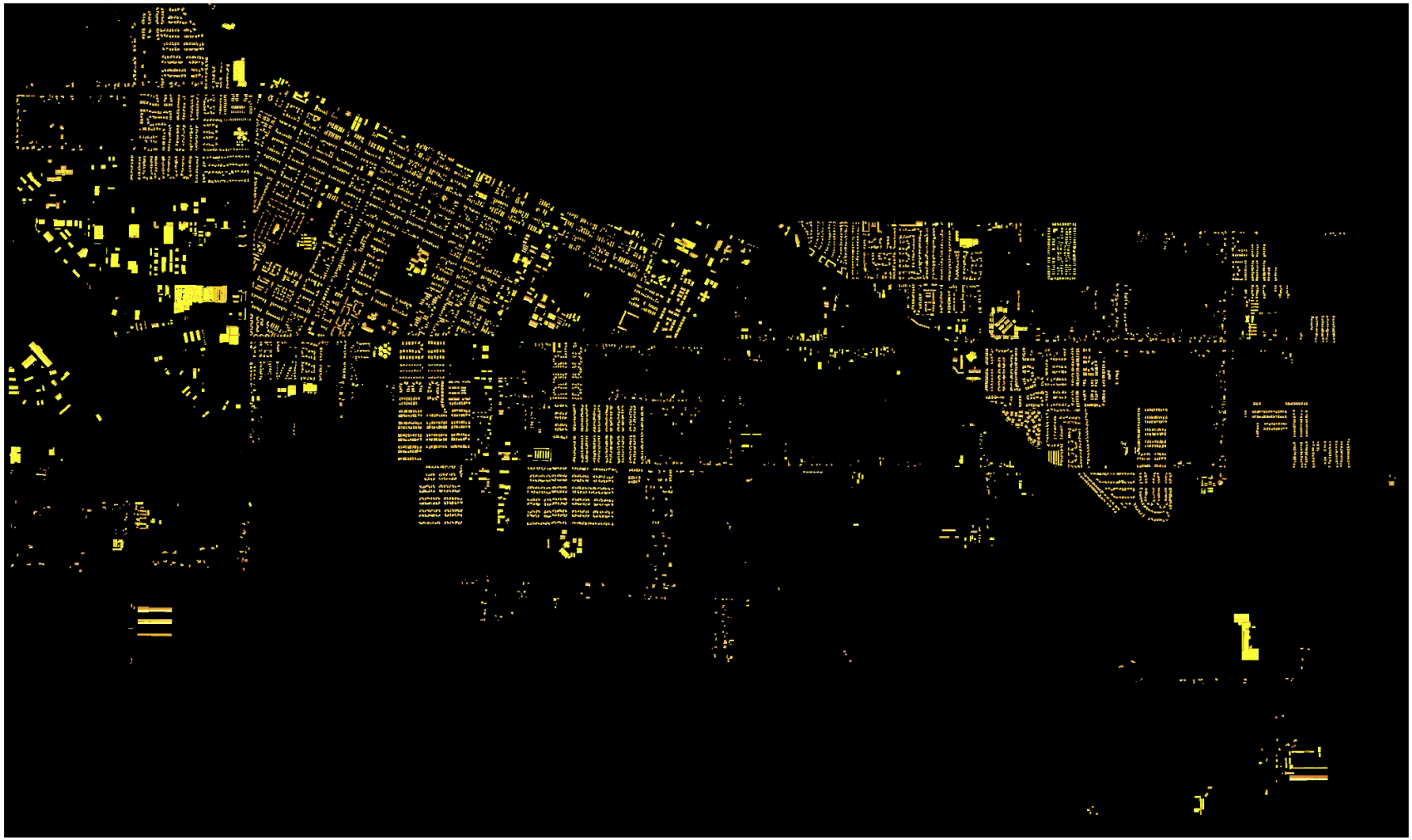

92553 (UCR)

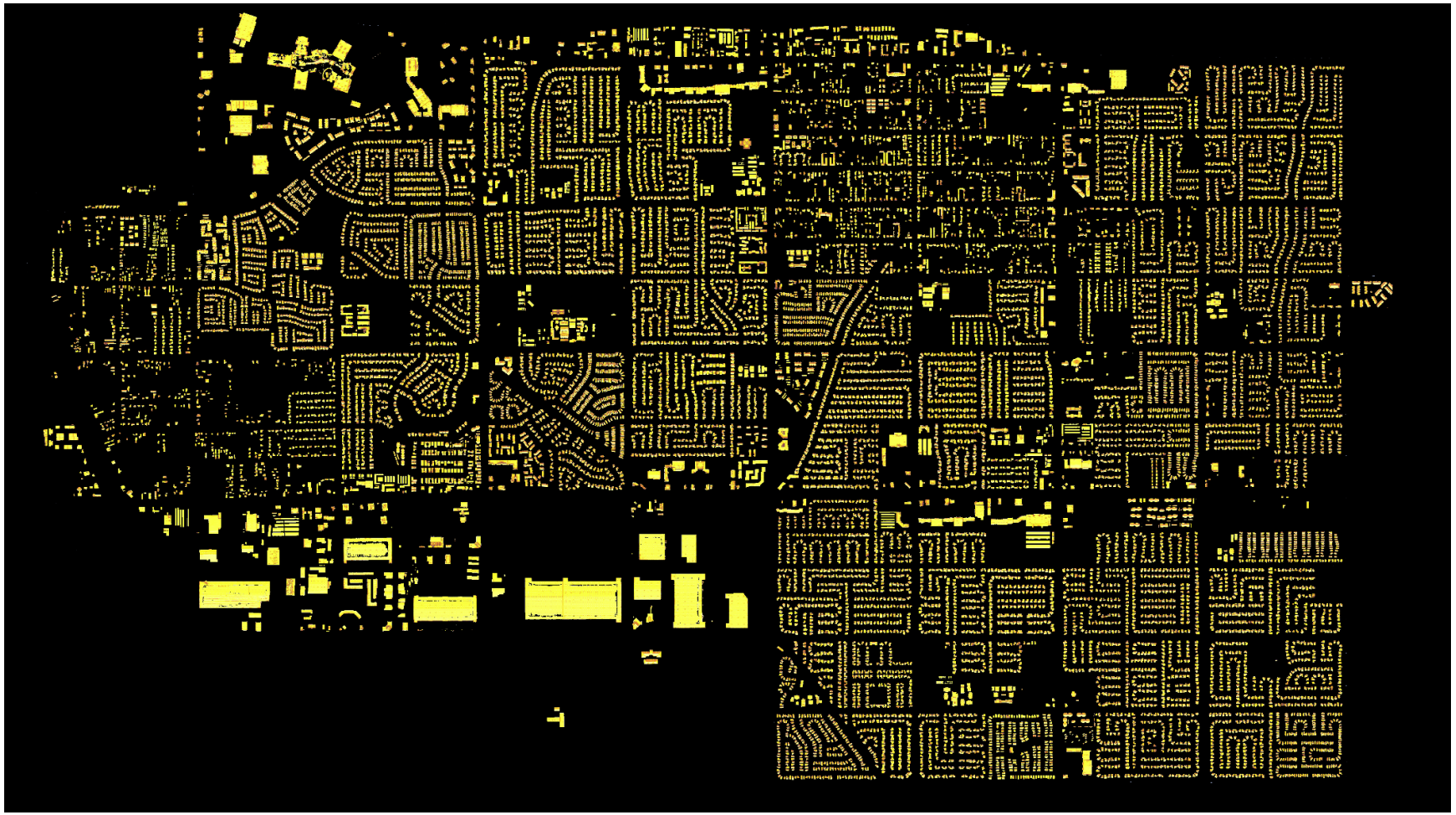

90024 (UCLA)

93111 (UCSB)

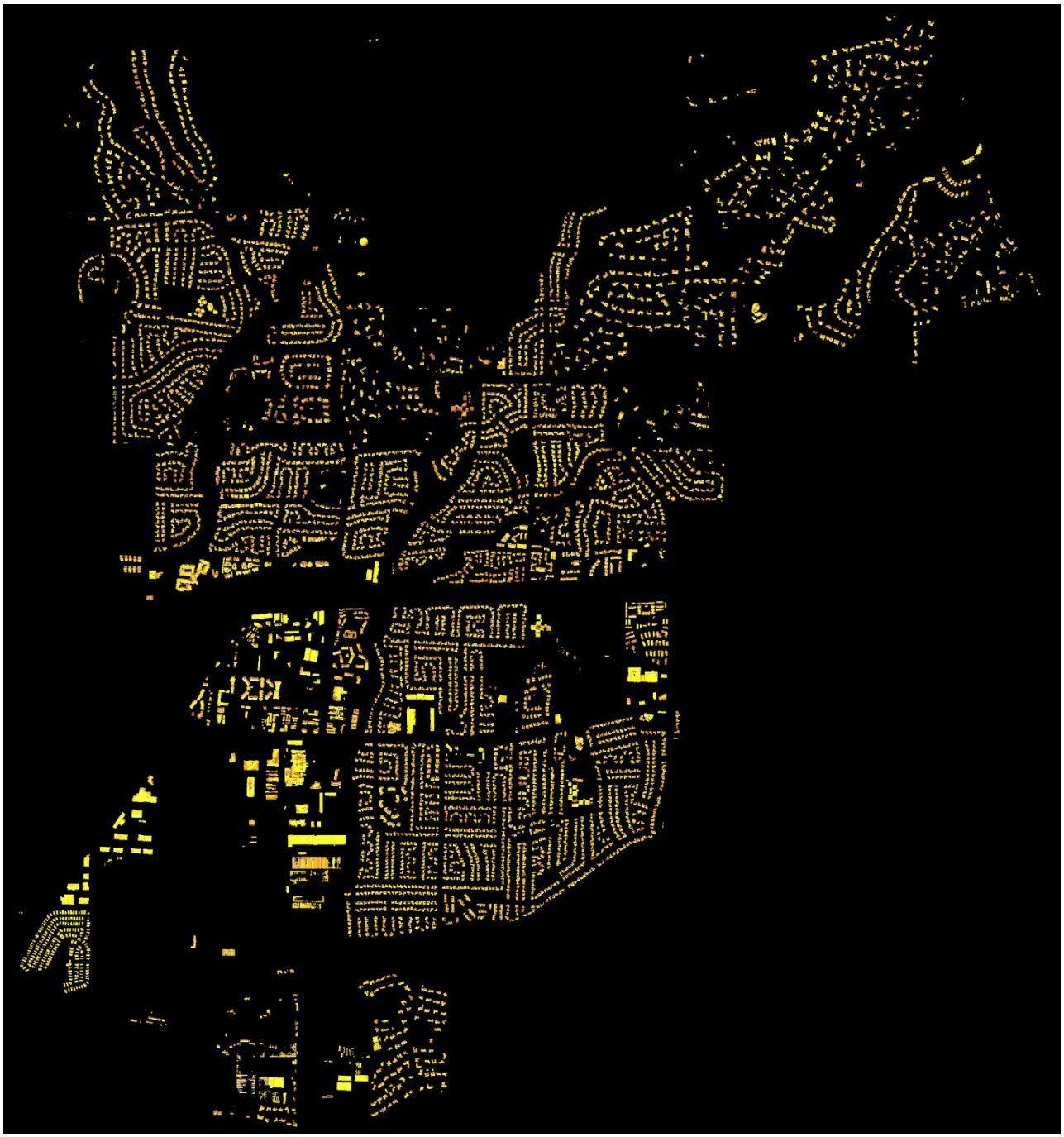

95060 (UCSC)

92161 (UCSD)